

Physical Mechanisms of Generation and Deactivation of Singlet Oxygen

Claude Schweitzer and Reinhard Schmidt*

Institut für Physikalische und Theoretische Chemie, Johann Wolfgang Goethe-Universität,
Marie-Curie-Strasse 11, D60439 Frankfurt am Main, Germany

Received September 6, 2002

Contents

I. Introduction	1685	5. Zeolite Systems	1750
II. Electronic States of the O ₂ Molecule	1686	D. Estimation of $a \rightarrow X$ Emission Quantum Yields	1750
III. Deactivation of Singlet Oxygen	1687	E. e–v Deactivation of Isoelectronic Molecules	1750
A. The Unperturbed Molecule	1687	F. Optimization of Singlet Oxygen Sensitizers	1750
1. Results from Experimental Studies	1687	G. Estimation of Singlet Oxygen Diffusion Lengths	1752
2. Results from Theoretical Studies	1689	VII. Conclusion	1752
B. The Perturbed Molecule	1690	VIII. Acknowledgment	1752
1. Radiative Deactivation	1690	IX. References	1752
2. Radiationless Deactivation	1700		
3. Radiationless Deactivation: Electronic-to-Vibrational Energy Transfer	1700		
4. Radiationless Deactivation: Charge-Transfer Deactivation	1710		
5. Radiationless Deactivation: Electronic Energy Transfer	1719		
IV. Photosensitized Production of Singlet Oxygen	1721		
A. Oxygen Quenching of Excited Triplet States	1725		
1. Parameters Influencing the Generation of Singlet Oxygen	1725		
2. Mechanism of Oxygen Quenching of $\pi\pi^*$ Triplet States	1731		
3. Mechanism of Oxygen Quenching of $n\pi^*$ Triplet States	1736		
B. Oxygen Quenching of Excited Singlet States	1737		
1. Rate Constants of S ₁ -State Quenching	1737		
2. Products of S ₁ -State Quenching	1739		
3. Mechanism of Oxygen Quenching of Excited Singlet States	1742		
V. Detection of Singlet Oxygen	1745		
VI. Applications	1746		
A. Estimation of the $a \rightarrow X$ Radiative Rate Constant in Different Environments	1746		
1. Liquid Phase	1747		
2. Gas Phase	1747		
3. Microheterogeneous Systems	1747		
B. Estimation of the Contribution of e–v, CT, EET, and Chemical Pathways to O ₂ (¹ Δ _g) and O ₂ (¹ Σ _g ⁺) Deactivation	1748		
C. Estimation of O ₂ (¹ Δ _g) and O ₂ (¹ Σ _g ⁺) Lifetimes in Different Environments	1749		
1. Liquid Phase	1749		
2. Polymers	1749		
3. Gas Phase	1749		
4. Microheterogeneous Systems	1749		

I. Introduction

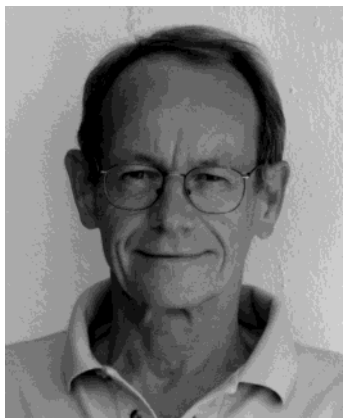
For more than 70 years, researchers in several areas of science have been intrigued by the physical and chemical properties of the lowest excited states of molecular oxygen. With two singlet states lying close above its triplet ground state, the O₂ molecule possesses a very unique configuration, which gives rise to a very rich and easily accessible chemistry, and also to a number of important photophysical interactions. In particular, photosensitized reactions of the first excited state, O₂(¹Δ_g), play a key role in many natural photochemical and photobiological processes, such as photodegradation and aging processes including even photocarcinogenesis. Reactions of O₂(¹Δ_g) are associated with significant applications in several fields, including organic synthesis, bleaching processes, and, most importantly, the photodynamic therapy of cancer, which has now obtained regulatory approval in most countries for the treatment of several types of tumors. The development of both applications and novel observation techniques has strongly accelerated during the past few years. Significant recent advances include, for example, the development of novel luminescent singlet oxygen probes,^{1–4} the time-resolved detection of O₂(¹Δ_g) in a transmission microscope,⁵ the first time-resolved measurements of singlet oxygen luminescence in vivo,⁶ and the observation of oxygen quenching of triplet-excited single molecules.⁷

Experimental and theoretical studies on the mechanisms of photosensitized formation of excited O₂ states and of their deactivation have been performed for almost 40 years. While most early liquid-phase studies were exclusively concerned with O₂(¹Δ_g), recent technological advances also made possible time-resolved investigations of the second excited state, O₂(¹Σ_g⁺), which can be formed in competition with O₂(¹Δ_g) in many cases. A significant number of

* Corresponding author. Tel.: ++49 69 79829448. Fax: ++49 69 79829445. E-mail: R.Schmidt@chemie.uni-frankfurt.de.



Claude Schweitzer was born in Luxembourg in 1975. He studied chemistry in Luxembourg and in Strasbourg, where he graduated from the Ecole Européenne de Chimie Polymères et Matériaux in 1999, working with Charles Tanielian on photochemistry of free radicals and singlet oxygen. After receiving his Ph.D. degree with Reinhard Schmidt from the Johann Wolfgang Goethe-Universität in 2001, for mechanistic research on singlet oxygen photophysics, Claude joined Tito Scaiano's group at the University of Ottawa to do postdoctoral research on fluorescent probes for DNA damage detection.



Reinhard Schmidt was born 1944 in Reichenberg/Sudeten. He studied chemistry at the J. W. Goethe-Universität in Frankfurt/M, where he received the Dr. Phil. Nat. degree in 1972 with Prof. H.-D. Brauer for investigating the magnetic properties and the association behavior of some biradicaloids. Afterward, he joined the group of Prof. H. Kelm at the same institute, doing research in high-pressure kinetics and kinetic investigations of chemiluminescent systems based on dioxetanes. He later moved with H.-D. Brauer into the field of photochemistry. His habilitation occurred in 1989, with a thesis on the deactivation of singlet oxygen by solvent molecules. In 1995, he was appointed as professor at the J. W. Goethe-Universität. He was visiting professor at the University of Grenoble in 1987, and at the ECPM, University of Strasbourg, in 1993. His present research interests are photochemistry and photophysics, particularly of singlet oxygen.

studies have been carried out during the past 10 years, and it has become clear that a full discussion of all photophysical processes involving $O_2(^1\Sigma_g^+)$, $O_2(^1\Delta_g)$, and ground-state oxygen, $O_2(^3\Sigma_g^-)$, is required to achieve a complete understanding of photosensitized reactions of molecular oxygen.

Starting with a short presentation of the most important features of the $O_2(^1\Sigma_g^+)$, $O_2(^1\Delta_g)$, and $O_2(^3\Sigma_g^-)$ states, we propose here an overview of experimental and theoretical studies on the mechanisms of physical deactivation of $O_2(^1\Sigma_g^+)$ and $O_2(^1\Delta_g)$ to $O_2(^1\Delta_g)$ and/or $O_2(^3\Sigma_g^-)$ in the gas and liquid phases, and in the absence and presence of physical and/or chemical quenchers. This includes radiative,

electronic-to-vibrational, charge transfer, and electronic energy-transfer processes, which all may compete in a given chemical system. We also cover the physical mechanisms of generation of $O_2(^1\Sigma_g^+)$ and $O_2(^1\Delta_g)$, focusing mainly on the quenching of excited singlet and triplet states by $O_2(^3\Sigma_g^-)$. Both processes can proceed via energy-transfer and charge-transfer pathways, and we explain here how the physical properties of the quencher and of the medium influence the mechanisms, rate constants, efficiencies, and products of the individual deactivation processes.

Our review will conclude with a short presentation of the most recent advances in the field of singlet oxygen detection, and with a guide to the utilization of the mechanistic knowledge presented here, showing, for example, how to evaluate the contribution of individual physical and/or chemical mechanisms to the generation or deactivation of $O_2(^1\Sigma_g^+)$ and $O_2(^1\Delta_g)$ in a given situation, or how to design molecules in order to maximize or minimize their $O_2(^1\Sigma_g^+)$ and/or $O_2(^1\Delta_g)$ photosensitization ability in a given medium.

The review is strictly limited to physical mechanisms of generation and deactivation of singlet oxygen. Chemical processes are discussed only in those cases where they compete with the physical processes and/or proceed via common intermediates. It should be noted that most chemical reactions of singlet oxygen are well understood, and only a few fundamentally new aspects have been revealed since the publication of previous reviews.^{8–11} The only significant exception seems to be the antibody-catalyzed singlet oxygenation of water, which was suggested in 2001.^{12,13} An introduction to applications of photosensitized reactions of singlet oxygen was also published very recently.¹⁴

The solvent dependence of singlet oxygen formation and deactivation parameters is discussed to the extent to which it provides relevant mechanistic information; a more detailed review of the solvent dependence of singlet oxygen deactivation can be found elsewhere.¹⁵ Also, extensive data collections of quantum yields of $O_2(^1\Delta_g)$ generation¹⁶ and of rate constants for its deactivation¹⁷ were published in 1993 and 1995, respectively, and are freely accessible on the Internet.¹⁸ A recent (1999) update of singlet oxygen yields from biologically relevant molecules is also available.¹⁹ The present review considers the literature published through the end of November 2002.

II. Electronic States of the O_2 Molecule

Despite its apparent simplicity, the O_2 molecule exhibits a number of rather unusual properties with respect to magnetic behavior, spectroscopy, energy-transfer processes, and chemical reactivity. These peculiarities are a consequence of the open-shell electronic structure of the molecule. Two oxygen atoms, each with six outer electrons, are bound, leading to the initial electronic configuration $(K)(K)-(2\sigma_g)^2(2\sigma_u)^2(3\sigma_g)^2(1\pi_u)^4(1\pi_g)^2$. With the exception of the first two degenerate antibonding $\pi_{g,x}$ and $\pi_{g,y}$ orbitals, all molecular orbitals (MOs) are doubly occupied. It was Mullikan who predicted that this special electronic configuration should give rise to three ener-

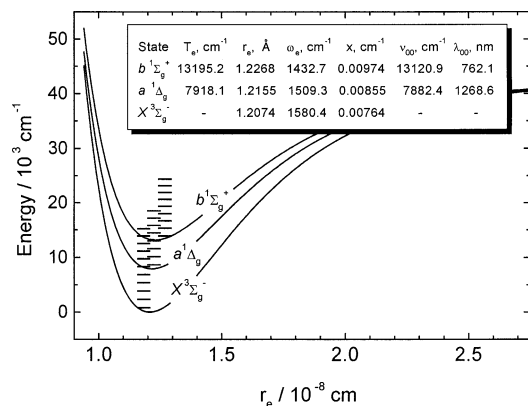


Figure 1. Potential energy curves of the three lowest electronic states of O_2 . Adapted from ref 24, with permission. Copyright 1950 Van Nostrand Reinhold. Reprint Ed. Copyright 1989 Krieger Publishing. See text for details.

getically closely lying electronic states, the Σ triplet ground state, and the excited Σ and Δ singlet states.²⁰ Childs and Mecke demonstrated a little later, by measuring the intensity of the weak absorption band of gaseous O_2 at 762 nm, that this band originates from the spin-forbidden transition to the Σ singlet state.²¹ This result allowed Mullikan to further specify the electronic states as $^3\Sigma_g^-$ ground state and $^1\Delta_g$ and $^1\Sigma_g^+$ excited singlet states.²² Finally, Ellis and Kneser discovered the optical transition $^1\Delta_g \leftarrow ^3\Sigma_g^-$ in absorption experiments with liquid O_2 at ~ 1261 nm,²³ identifying $\text{O}_2(^1\Delta_g)$ as the metastable O_2 species, which is now commonly called singlet oxygen. Further detailed gas-phase spectroscopic studies corroborated these early assignments and led to the potential energy curves and the precise data given in Figure 1.²⁴

Figure 1 lists values of the electronic term T_e , i.e., the energy of the respective potential minimum relative to the $^3\Sigma_g^-$ ground-state minimum, the nuclear equilibrium distance r_e between the O atoms, the vibrational constant ω_e , the first anharmonicity constant x , and the wavenumber ν_{00} and the wavelength λ_{00} of the 0–0 electronic transition from the ground state. These and further data listed by Herzberg are very useful for the calculation of vibrational and vibronic transition energies of the unperturbed O_2 molecule.²⁴ The designation of the different electronic states in Figure 1 includes also the leading symbols X , a , and b , which are often used for short reference to the ground state and to the next two excited states of different multiplicity. It should be noted that the value of r_e increases by only 0.7 and 1.6%, respectively, on going from the ground state to the excited singlet states. This very small graduation indicates the same bond order of 2 for these three states, as a consequence of their identical initial electronic configuration. The distribution of the two electrons on the $\pi_{g,x}$ and $\pi_{g,y}$ MOs is described by six wave functions, where one corresponds to $^1\Sigma_g^+$, two to $^1\Delta_g$, and three to $^3\Sigma_g^-$. This result is consistent with the twofold degeneracy of $^1\Delta_g$, due to its nonzero orbital quantum number $\Lambda = 2$, and the threefold degeneracy of the $^3\Sigma_g^-$ ground state, with its triplet multiplicity.

The open-shell electronic structure of the O_2 molecule represents a particular challenge for ab initio calculations. The experimental values of T_e , r_e , ω_e , and x are sometimes used as a benchmark for the validity of the method used. Very recently, Pittner and co-workers demonstrated that these values can be calculated with rather high accuracy by applying the eight-reference state-specific Brillouin–Wigner coupled-cluster method.²⁵ The deviations of the calculated T_e , r_e , ω_e , and x data amounted to less than 4%, 0.5%, 5%, and 15%, respectively, for the excited $^1\Delta_g$ and $^1\Sigma_g^+$ singlet states, and even better results have been reported for the $^3\Sigma_g^-$ ground state, demonstrating the progress of theoretical methods suited for the treatment of O_2 .

III. Deactivation of Singlet Oxygen

A. The Unperturbed Molecule

1. Results from Experimental Studies

If the excitation energy is smaller than the ground-state dissociation energy D_0 , then any isolated and thus unperturbed molecule can lose its excitation energy only by radiative deactivation. This is observed for both the $^1\Delta_g$ and the $^1\Sigma_g^+$ states of O_2 , with $D_0 = 41\,236 \text{ cm}^{-1}$ ($493.6 \text{ kJ mol}^{-1}$). Three different optical transitions are possible between the $X^3\Sigma_g^-$ ground state and the $a^1\Delta_g$ and $b^1\Sigma_g^+$ singlet states, and all of them are forbidden as electric-dipole transitions, due to the even (g) parity of the electronic states. Further restrictions exist for singlet \leftrightarrow triplet and $\Sigma \leftrightarrow \Delta$ transitions.²⁴

Two radiative deactivation paths exist for the O_2 molecule in the upper excited $b^1\Sigma_g^+$ state. From measurements of the strength of the $b \leftarrow X$ absorption of O_2 in air around 762 nm, Childs and Mecke derived a corresponding Einstein coefficient of spontaneous emission of $A_{b-X} = 0.13 \text{ s}^{-1}$.²¹ Later experiments in other laboratories resulted in slightly smaller values.²⁶ Ritter and Wilkerson obtained, by ultrahigh-resolution laser absorption for pressures up to 1 bar, $A_{b-X} = 0.0887 \text{ s}^{-1}$, corresponding to the radiative lifetime $\tau_{b-X} = 1/A_{b-X}$ of 11.3 s with respect to deactivation of $\text{O}_2(^1\Sigma_g^+)$ to the ground state.²⁶ (Symbols used frequently in this paper are summarized in Table 1.)

The competing $b \rightarrow a$ radiative transition occurs between two excited singlet states at 1908 nm. Comparative measurements of the $b \rightarrow X$ and $b \rightarrow a$ emissions of O_2 induced by a microwave discharge in an O_2 –He mixture at 0.2 bar allowed Noxon to determine $A_{b-a} = 2.5 \times 10^{-3} \text{ s}^{-1}$ with reference to $A_{b-X} = 0.13 \text{ s}^{-1}$.²⁷ $A_{b-a} = 1.7 \times 10^{-3} \text{ s}^{-1}$ is obtained with the more accurate A_{b-X} value reported by Ritter and Wilkerson. However, the uncertainty in A_{b-a} is large and amounts to a factor of 2.²⁷

The $a^1\Delta_g \rightarrow X^3\Sigma_g^-$ transition is, according to Kasha, quite possibly the molecular electronic transition that is most forbidden in nature.²⁸ Badger et al. found in the absorption spectrum of pure gaseous O_2 very weak, discrete-line bands centered at 1269 nm.²⁹ The integral molecular absorption coefficients of the lines were found to be independent of gas pressure,

Table 1. List of Frequently Used Symbols

a	efficiency of direct $O_2(^1\Sigma_g^+)$ generation during O_2 quenching of T_1
$A_{b-X}, A_{b-a}, A_{a-X}$	Einstein coefficients of spontaneous emissions $b-X$, $b-a$, and $a-X$
b	efficiency of direct $O_2(^1\Delta_g)$ generation during O_2 quenching of T_1
e	elementary charge
E_{ox}	oxidation potential
E_{red}	reduction potential
E_S	singlet-state energy
E_T	triplet-state energy
E_Δ	state energy of $O_2(^1\Delta_g)$
E_Σ	state energy of $O_2(^1\Sigma_g^+)$
F	Faraday constant
f_S^T	efficiency of T_1 -state formation during O_2 quenching of S_1
f_S^A	efficiency of singlet oxygen production during O_2 quenching of S_1
h	Planck constant
IP	ionization potential
k_D	rate constant for deactivation of triplet-state O_2 encounter complexes
k_B	Boltzmann constant
$k_{b-X}, k_{b-a}, k_{a-X}$	radiative rate constants of transitions $b-X$, $b-a$, and $a-X$
$K_{b-X}, K_{b-a}, K_{a-X}$	relative radiative rate constants of transitions $b-X$, $b-a$, and $a-X$
k_c	rate constant of chemical $O_2(^1\Delta_g)$ deactivation
$k_{b-X}^c, k_{b-a}^c, k_{a-X}^c$	second-order rate constants of radiative transitions $b-X$, $b-a$, and $a-X$
$k_{CT}^{1\Sigma}, k_{CT}^{1\Delta}, k_{CT}^{3\Sigma}$	rate constants for charge-transfer-induced triplet-sensitized formation of $O_2(^1\Sigma_g^+)$, $O_2(^1\Delta_g)$, and $O_2(^3\Sigma_g^-)$
k_{diff}, k_{-diff}	diffusion-controlled rate constants of encounter complex formation and dissociation
k_p	rate constant of physical $O_2(^1\Delta_g)$ deactivation
$k_S^{1\Delta}, k_S^{3\Sigma}$	rate constants for formation of $O_2(^1\Delta_g)$ and $O_2(^3\Sigma_g^-)$ during O_2 quenching of S_1
k_S^Q	rate constant for O_2 quenching of an excited singlet state
k_{SS}	rate constant for formation of S_0 and $O_2(^3\Sigma_g^-)$ during O_2 quenching of S_1
k_{ST}	rate constant for formation of T_1 and $O_2(^3\Sigma_g^-)$ during O_2 quenching of S_1
k_{SD}	rate constant for formation of T_1 and $O_2(^1\Delta_g)$ during O_2 quenching of S_1
$k_T^{1\Sigma}, k_T^{1\Delta}, k_T^{3\Sigma}$	overall rate constants for triplet-sensitized formation of $O_2(^1\Sigma_g^+)$, $O_2(^1\Delta_g)$, and $O_2(^3\Sigma_g^-)$
k_T^Q	rate constant for O_2 quenching of triplet states
k_{TS}	rate constant for formation of S_0 and $O_2(^3\Sigma_g^-)$ during O_2 quenching of S_1
k_{TD}	rate constant for formation of S_0 and $O_2(^1\Delta_g)$ during O_2 quenching of S_1
$k_{AE}^{1\Sigma}, k_{AE}^{1\Delta}, k_{AE}^{3\Sigma}$	rate constants for non-charge-transfer-induced triplet-sensitized formation of $O_2(^1\Sigma_g^+)$, $O_2(^1\Delta_g)$, and $O_2(^3\Sigma_g^-)$
k_Q^O	rate constant of $O_2(^1\Delta_g)$ quenching
k_{XY}^A	rate constant of $O_2(^1\Delta_g)$ quenching by a single terminal bond X-Y
k_Q^Σ	rate constant of $O_2(^1\Sigma_g^+)$ quenching
k_{XY}^Σ	rate constant of $O_2(^1\Sigma_g^+)$ quenching by a single terminal bond X-Y
n	refractive index
N_A	Avogadro's number
P	pressure
\mathcal{P}	bulk polarizability
$\rho_S^{O_2}$	fractions of singlet states quenched by oxygen
$\rho_T^{O_2}$	fractions of triplet states quenched by oxygen
Q_F	fluorescence quantum yield
Q_L	luminescence quantum yield
Q_T	triplet yield
Q_T^0	triplet yield in the absence of O_2
Q_Δ	quantum yield of $O_2(^1\Delta_g)$ sensitization
R	molar refraction
S_Δ	overall efficiency of singlet oxygen sensitization during O_2 quenching of T_1
V_m	molar volume
V_{vdW}	van der Waals volume
ΔE	excess energy
ΔE_{ST}	S_1-T_1 energy gap
ΔG_{CET}	free energy change of complete electron transfer
ΔH^\ddagger	activation enthalpy
ΔS^\ddagger	activation entropy
ΔV_C	volume of contact complex formation
ΔV_{exc}	excess volume
ΔV_{obs}^\ddagger	activation volume
ϵ_s	static dielectric constant
η	viscosity
η'	packing fraction
κ_T	isothermal compressibility
ρ	density
$\tau_{b-X}, \tau_{b-a}, \tau_{a-X}$	radiative lifetimes for transitions $b-X$, $b-a$, and $a-X$
τ_S	excited singlet-state lifetime
τ_T	sensitizer triplet-state lifetime
τ_Δ	lifetime of $O_2(^1\Delta_g)$
τ_Σ	lifetime of $O_2(^1\Sigma_g^+)$

and it was therefore concluded that the intensity of the line spectrum is related to the probability of the $a \leftarrow X$ transition in isolated molecules. The Einstein coefficient of spontaneous emission of the isolated $O_2(^1\Delta_g)$ was calculated to be $A_{a-X} = 2.58 \times 10^{-4} \text{ s}^{-1}$.²⁹ More recent investigations using electron paramagnetic resonance and emission spectroscopy,³⁰ cavity ringdown spectroscopy,^{31,32} and absorption spectroscopy³² led consistently to the slightly smaller value of $A_{a-X} = 2.3 \times 10^{-4} \text{ s}^{-1}$, which corresponds to the extremely long radiative lifetime of the unperturbed $O_2(^1\Delta_g)$ of $\tau_{a-X} = 72 \text{ min}$! It should be noted that the given Einstein coefficients all refer to transitions between the vibrational ground states (0–0 transitions). The corresponding transition energies are listed in Figure 1.

2. Results from Theoretical Studies

Theoretical calculations provide further information on these strongly forbidden radiative transitions. Different mechanisms contribute to the radiative processes (see Figure 2). Both the $b \rightarrow X,1$ and $a \rightarrow X,1$ transitions 1 and 2 occur as spin-forbidden magnetic dipole transitions to the $M_s = \pm 1$ spin sublevels of the ground state X . The $b \rightarrow a$ transition 3 is a spin-allowed electric quadrupole transition.^{33,34} Transition 1 is about 400 times stronger than transition 2, although both are of the same magnetic nature. For the explanation of this strange behavior, it is very important to consider the magnetic dipole transition $X,1 \rightarrow X,0$ between the spin sublevels $M_s = \pm 1$ and 0 of the triplet ground state.³⁵ This microwave transition 6 is observed in ESR spectra of solid oxygen at zero field.³⁶ According to Minaev,³⁵ there is a strong spin-orbit coupling (SOC) between $b^1\Sigma_g^+$ and the lowest spin substate $X^3\Sigma_{g,0}^-$ ($M_s = 0$) of the ground state, introducing appreciable admixture of triplet $X,0$ character into the singlet b state, and singlet b character into the triplet $X,0$ state. The corresponding SOC-perturbed wave functions Ψ_b and $\Psi_{X,0}$ are given by eqs 1 and 2. Perturbation theory yields the admixture coefficient C (eq 3).

$$|\Psi_b\rangle = |b^1\Sigma_g^+\rangle + C|X^3\Sigma_{g,0}^-\rangle \quad (1)$$

$$|\Psi_{X,0}\rangle = |X^3\Sigma_{g,0}^-\rangle - C^*|b^1\Sigma_g^+\rangle \quad (2)$$

$$C = \frac{\langle X^3\Sigma_{g,0}^- | H_{SO} | b^1\Sigma_g^+ \rangle}{E_b - E_X} \quad (3)$$

In an effective one-electron approximation of SOC, the matrix element in the numerator of eq 3 is equal to $-\zeta_0$, where $\zeta_0 = 153 \text{ cm}^{-1}$ is the SOC constant for the $O(^3P)$ atom. Accounting for the energy difference between the b and X states of $13\,121 \text{ cm}^{-1}$ in the denominator of eq 3, the admixture coefficient is obtained as $C = 0.0117i$.³⁵ Use of the improved value $\zeta_0 = 176 \text{ cm}^{-1}$, obtained by Klotz et al.³⁴ in ab initio calculations, results in $C = 0.0134i$. This coefficient plays a crucial role in the explanation of radiative properties of the unperturbed but also of the perturbed O_2 molecule.³⁷

Transition 1, $b \rightarrow X,1$, can borrow intensity from the magnetic dipole transition 6, $X,1 \rightarrow X,0$, be-

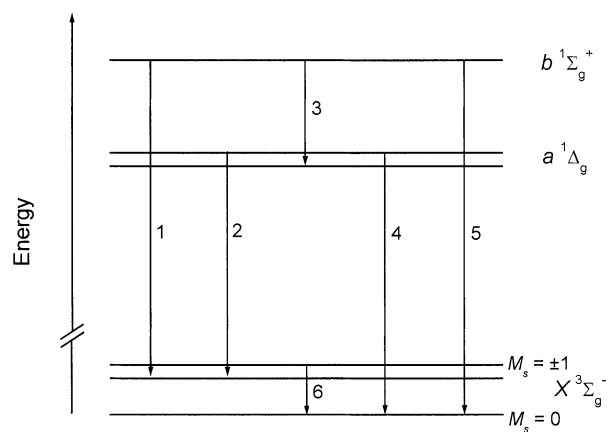


Figure 2. Numbering of possible radiative transitions in O_2 . Adapted from ref 33. Reprinted with permission from the The Royal Society of Chemistry.

tween the spin sublevels of the triplet ground state X , since the singlet b state has partial triplet $X,0$ character due to SOC (see eq 1). The magnetic dipole transition moment \mathbf{M}_{b-X} is given by eq 4.

$$\mathbf{M}_{b-X} = \langle \Psi_b | M | X^3\Sigma_{g,\pm 1}^- \rangle = \langle b^1\Sigma_g^+ | M | X^3\Sigma_{g,\pm 1}^- \rangle + C \langle X^3\Sigma_{g,0}^- | M | X^3\Sigma_{g,\pm 1}^- \rangle \quad (4)$$

In eq 4, $M = \beta(L + 2S)$ is the magnetic dipole operator, with L and S being the orbital and spin angular momenta, and $\beta = eh/(4\pi mc)$. The first term of eq 4 vanishes because of the orthogonality of the singlet and triplet wave functions. It was shown by Minaev and Klotz et al. that the L contribution to \mathbf{M}_{b-X} is much smaller than the S contribution.^{33–35} Thus, the simplified eq 5 is obtained. This result gives

$$\mathbf{M}_{b-X} = C \langle X^3\Sigma_{g,0}^- | 2\beta S | X^3\Sigma_{g,\pm 1}^- \rangle = 0.0268i\beta \quad (5)$$

$A_{b-X} = 0.086 \text{ s}^{-1}$ for the 0,0 band of transition 1, which is in excellent agreement with the experiment (vide supra).³⁴

The magnetic dipole transition 2, $a \rightarrow X,1$, has only orbital angular momentum contributions, induced by SOC mixing with Π_g states. However, these contributions are very small because of the huge energy difference between the $^1,3\Pi_g$, X , and a states at $O-O$ equilibrium distance.^{33,35} Since the a state acquires no partial triplet character by SOC with the $X,0$ state, no intensity borrowing from the allowed transition 6 takes place, explaining the big difference between the probabilities of transitions 1 and 2 in the unperturbed O_2 molecule. Ab initio calculations resulted in $A_{a-X} = 1.9 \times 10^{-4} \text{ s}^{-1}$, again in very good agreement with the experiment.³⁴

The Noxon transition 3, $b \rightarrow a$, is an electric quadrupole transition with transition quadrupole moment $\mathbf{Q}_{a-b} = 1.005 \text{ au}$ and, as such, is only weak. Ab initio calculations yield $A_{b-a} = 1.4 \times 10^{-3} \text{ s}^{-1}$, in agreement with experiment.³⁴

Two further radiative mechanisms profiting from intensity borrowing are possible, as indicated in Figure 2. Transition 4, $a \rightarrow X,0$, can borrow intensity from the electric quadrupole transition 3, $b \rightarrow a$, because of the partial singlet b character of the triplet

$X,0$ state. The corresponding induced transition quadrupole moment is $Q_{a-X,0}$ is given by eq 6, where Q is the electric quadrupole operator.

$$Q_{a-X,0} = \langle a^1\Delta_g | Q | \Psi_{X,0} \rangle = \langle a^1\Delta_g | Q | X^3\Sigma_{g,0}^- \rangle - C^* \langle a^1\Delta_g | Q | b^1\Sigma_g^+ \rangle \quad (6)$$

Again, the first term of eq 6 vanishes.³³ The second factor of the perturbation term of eq 6 is identical with the transition quadrupole moment $Q_{a-b} = 1.005$ au of transition 3, $b \rightarrow a$. Thus, the induced transition quadrupole moment is simply given by eq 7.

$$Q_{a-X,0} = -C^* Q_{a-b} = 0.0135i \quad (7)$$

The electric quadrupolar contribution of the $a \rightarrow X,0$ transition is very small and amounts only to $2 \times 10^{-6} \text{ s}^{-1}$, following the ab initio results of Klotz et al.³⁴ Consequently, the $a \rightarrow X$ emission band for the unperturbed O_2 consists principally of magnetic contributions (transition 2).

Finally, transition 5, $b \rightarrow X,0$, borrows a transition multipole moment from the difference between permanent multipoles of the b and X states. In the free O_2 molecule, both states have only electric quadrupole moments as the lowest multipoles. Minaev derived eq 8 for the induced transition quadrupole moment $Q_{b-X,0}$.³³

$$Q_{b-X,0} = C^*(Q_b - Q_X) \quad (8)$$

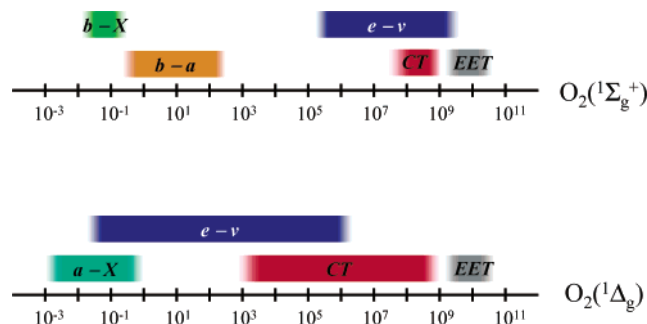
With $Q_b - Q_X = 0.278$ au, the electric quadrupolar contribution of $1.5 \times 10^{-7} \text{ s}^{-1}$ is calculated from eq 8,³⁴ which is almost 6 orders of magnitude smaller than the magnetic dipolar contribution to $b \rightarrow X$ (transition 1).

Thus, the electric quadrupole transitions 4 and 5 are without importance for the radiative decay of the isolated O_2 molecule. However, this situation changes dramatically in the presence of intermolecular perturbations (see section III.B.1.a-2).

B. The Perturbed Molecule

Collisions with other atoms or molecules induce perturbations of the electronic structure, which weaken the strong forbiddenness of the radiative processes of the O_2 molecule. The radiative transitions acquire partially allowed character, leading to a strongly graduated enhancement of the different transitions in absorption as well as in emission. Furthermore, changes from discrete-line spectra to band spectra and small spectral shifts are observed. However, the most important effect of perturbations is the opening of the door to very effective radiationless deactivation processes, such as electronical-to-vibrational ($e-v$) energy transfer and, if the respective prerequisites are fulfilled, also charge-transfer-induced quenching (CT) and electronic energy transfer (EET). These mechanisms will be discussed in detail in sections III.B.3–5. The range of variation of the corresponding second-order rate constants (in $M^{-1} \text{ s}^{-1}$) covers almost 13 orders of magnitude and is shown in Scheme 1.

Scheme 1. Range of Bimolecular Rate Constants ($M^{-1} \text{ s}^{-1}$) for Deactivation of $O_2(^1\Sigma_g^+)$ and $O_2(^1\Delta_g)$ by Radiative ($b-X$, $b-a$, $a-X$), Electronic-to-Vibrational ($e-v$), Charge Transfer (CT), and Electronic Energy Transfer (EET) Mechanisms



1. Radiative Deactivation

a. Enhancement of Radiative Transitions. (1) Results from Experimental Studies. The $b \rightarrow X$ Transition. The transition moment of the $b \rightarrow X$ transition increases relatively little upon perturbation. Few studies have been performed. Long and Kearns found that, in pure O_2 gas in the range below 100 bar, the integrated $b \leftarrow X$ absorption band increases linearly with pressure, indicating no change in A_{b-X} .³⁸ The rate constant of the radiative transition, k_{b-X} ($= A_{b-X}$), increases relatively little on going from the gas to the condensed phase. Long and Kearns determined the corresponding radiative lifetime, $\tau_{b-X} = 1/k_{b-X}$, by absorption measurements to be 2 s in liquid O_2 at 90 K, and 6 s in perhalogenated solvents at room temperature.³⁸ A heavy-atom effect was noticed, reducing τ_{b-X} in iodoperfluoropropane to 0.53 s. Schmidt and Bodesheim measured the quantum yield of the very weak $b \rightarrow X$ phosphorescence in CCl_4 at room temperature to be $Q_{b-X} = 5.2 \times 10^{-8}$.³⁹ Combined with the measured actual lifetime τ_Σ of $O_2(\Sigma_g^+)$, they obtained $\tau_{b-X} = 2.5$ s. Chou et al. also determined Q_{b-X} and τ_Σ in CCl_4 at room temperature and arrived at $\tau_{b-X} = 0.65$ s.⁴⁰ Despite the scatter of these results, one notes a significant but only moderate increase of the probability of the $b \rightarrow X$ transition by at least a factor of 2–4 on going from the diluted gas phase to O_2 dissolved in liquids, and a strong heavy-atom effect further increasing the probability of the radiative transition by a factor of ~ 10 .

The lifetime of $O_2(\Sigma_g^+)$ has also been measured in the solid phase. Becker et al. determined $\tau_\Sigma = 24.5$ ms in Ar at 5 K.⁴¹ Only radiative transitions contribute to the decay of $O_2(\Sigma_g^+)$ under these conditions. Since both radiative processes $b \rightarrow a$ and $b \rightarrow X$ compete, the lifetime is determined by the faster transition. By comparison with results obtained in emission experiments on matrix-isolated isoelectronic species NF ,⁴² it was deduced that the short decay time of 24.5 ms corresponds to the radiative lifetime of the $b \rightarrow a$ transition of O_2 under these particular conditions (vide infra).

The $b \rightarrow a$ Transition. Few investigations deal with the intensity of the perturbed $b \rightarrow a$ radiative transition. Chou and Frei discovered the correspond-

Table 2. Rate Constants k_{b-a}^c of Collision-Induced $b \rightarrow a$ Radiative Deactivation of O_2^a

collider	k_{b-a}^c , $M^{-1} s^{-1}$	R , $mL mol^{-1}$
He	≤ 0.6	
Ne	≈ 0.6	1.00
N ₂	7.8	4.34
O ₂	9.0	4.00
Ar	10.2	4.13
Kr	21.6	6.22
SF ₆	26.4	11.34
SO ₂	31.8	9.71
Xe	46.8	10.10
PCl ₃	252	25.0

^a Data from Fink et al.⁴⁴ Molar refractions R given for means of comparison.³⁹

ing emission in the condensed phase as a narrow-band emission centered at ~ 1930 nm in CCl₄ at room temperature.⁴³ $O_2(\Sigma_g^+)$ was produced by photosensitization using benzophenone as triplet sensitizer. Considering that the emission originates from the second excited singlet state, for which a very short lifetime had to be assumed, this result already qualitatively indicated a strong enhancement of the $b \rightarrow a$ transition in solution compared with that in the gas phase. Using the $a \rightarrow X$ emission in benzene as a reference, Schmidt and Bodesheim measured the quantum yield of the emission in room-temperature CCl₄ to be $Q_{b-a} = 4.5 \times 10^{-4}$.³⁹ From the experimental value for τ_Σ , the radiative lifetime was calculated to be $\tau_{b-a} = 290 \mu s$. It follows that the probability of the $b \rightarrow a$ transition is 6 orders of magnitude larger in CCl₄ solution than that for the isolated O_2 molecule! The comparison with the result reported by Becker and Schurath, $\tau_{b-a} = 24.5$ ms, obtained in an Ar matrix at 5 K (vide supra), indicates that differences in the surroundings of the O_2 molecule and/or the temperature could also strongly influence the transition probability.

Similar conclusions can be drawn from the results of Fink et al., who investigated the influence of different gases on the intensity of the $b \rightarrow a$ emission in gas mixtures.⁴⁴ $O_2(\Sigma_g^+)$ was produced by microwave discharge under reduced pressures up to 0.02 bar, and the emission was observed by Fourier transform infrared (FTIR) spectroscopy. It was found that, with increasing pressure, a strong continuum appears under the discrete lines of the electric quadrupole branches. The position of the continuum spectrum was independent of the added gas. It was concluded that the line spectra correspond to the emission of unperturbed $O_2(\Sigma_g^+)$, whereas the band spectra result from the emission of collision complexes. The quantitative treatment of the data allowed the calculation of second-order rate constants k_{b-a}^c of collision-induced $b \rightarrow a$ emission, which are calibrated with the value of $k_{b-a} = 1.4 \times 10^{-3} s^{-1}$, theoretically derived by Klotz et al.³⁴ for the radiative $b \rightarrow a$ decay of the isolated $O_2(\Sigma_g^+)$. Table 2 lists the results of this important study.⁴⁴ The values of k_{b-a}^c are strongly dependent on the nature of the collider and increase by a factor of 400 on going from Ne to PCl₃.

Weldon and Ogilby first identified the $b \leftarrow a$ transition in absorption.⁴⁵ The use of a very sensitive step-scan FTIR spectrometer⁴⁶ allowed these authors

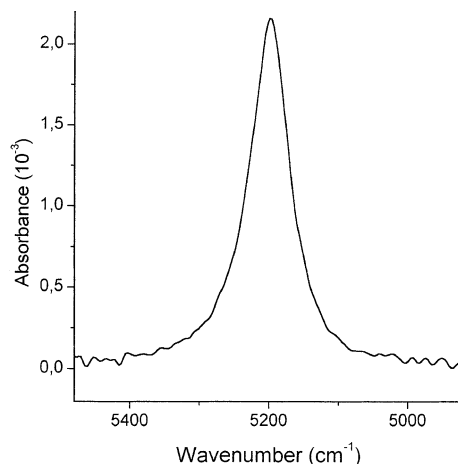


Figure 3. Absorption spectrum of $O_2(^1\Delta_g)$ in air-saturated n -hexane. Reprinted with permission from ref 47. Copyright 2002 American Chemical Society.

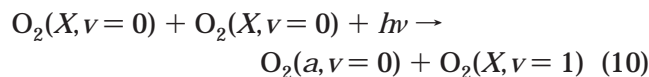
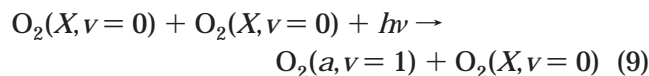
to make time-resolved and quantitative measurements of the absorption of $O_2(^1\Delta_g)$ being formed in liquid solution by laser-pulsed photosensitization.^{45,47,48} The kinetics of the transient absorption corresponds to the $a \rightarrow X$ phosphorescence kinetics. Figure 3 displays the $b \leftarrow a$ absorption spectrum recorded recently in air-saturated n -hexane.⁴⁷

The signal-to-noise ratio of the spectrum is very good if the small absorbance is taken into account. The bandwidth of the spectrum, centered at 5199 cm^{-1} , amounts to only 69 cm^{-1} ; the extinction coefficient at the maximum of absorption was determined to be $39.7 \text{ M}^{-1} \text{ cm}^{-1}$ in n -hexane.⁴⁵ Integration of the absorption band yields the rate constants k_{b-a} of the $b \rightarrow a$ radiative transition in n -hexane (1280 s^{-1}), toluene (2260 s^{-1}), and CS₂ (3000 s^{-1}).⁴⁸ Again, differences in the surroundings of the O_2 molecule strongly influence the transition probability. Bachilo et al. also investigated the $b \leftarrow a$ absorption in solution.⁴⁹ They, too, found that the absorption intensity is solvent dependent and decreases in the series toluene, hexane, methanol- d_4 from 1 to 0.6 and 0.4, respectively. Insofar as the solvents overlap, these results agree.

The $a \rightarrow X$ Transition. By far, the most experimental studies have been performed on the $a \rightarrow X$ transition. Badger et al. observed the formation of a continuous absorption band underlying the discrete-line spectrum in the spectrum of pure gaseous O_2 with increasing pressure.²⁹ The molecular absorption coefficient of the continuous absorption increases linearly with pressure and was therefore assigned to the absorption of O_2 in collision complexes. The rate constant of collision-induced $a \leftarrow X$ absorption, k_{a-X}^c was calculated, for O_2 as collision partner, to be $2.4 \times 10^{-2} \text{ M}^{-1} \text{ s}^{-1}$. It was also noted that the strength of perturbation is different when CO₂ or N₂ is the collision partner. Long and Kearns investigated various near-infrared (NIR) absorption bands of O_2 in the gas phase and in liquid solution over a wide range of pressures up to 150 bar.³⁸ It was found that the absorption coefficient of the vibronic $a \leftarrow X(1 \leftarrow 0)$ transition at 1070 nm increases linearly with O_2 pressure in pure O_2 gas and in solution, whereas the absorption coefficient of the $a \leftarrow X(0 \leftarrow 0)$ transition

band at 1270 nm is proportional to O₂ pressure only in the gas phase. In perhalogenated solvents, no dependence of that transition on O₂ pressure was observed. The surprising suppression of the oxygen-induced enhancement of the $a \leftarrow X(0 \leftarrow 0)$ transition could be explained by the quantitative data, which demonstrate that the average radiative lifetime, $\tau_{a-X} = 5$ s, in perhalogenated solvents is more than 3 orders of magnitude smaller than that in the highly diluted gas phase. Thus, the enormous enhancement of the $0 \leftarrow 0$ transition exerted by the solvent apparently hides the O₂ concentration-dependent perturbation. However, it remained unclear why this explanation fails for the $a \leftarrow X(1 \leftarrow 0)$ transition. Interestingly, only little variation of τ_{a-X} was observed in the series of nine perhalogenated solvents. However, in perfluoroacetic acid, the 4-fold longer radiative lifetime, $\tau_{a-X} = 19$ s, was found.³⁸

Quantitative studies on the enhancement of the $(0 \rightarrow 0)$ and $(0 \rightarrow 1)$ $a \rightarrow X$ emissions by O₂ were performed by Fink and co-workers in the gas phase.^{50,51} The second-order rate constant, $k_{a-X}^c(0 \rightarrow 0) = 2.0 \times 10^{-2} \text{ M}^{-1} \text{ s}^{-1}$, was determined, in agreement with the previous results obtained by Badger et al. in absorption experiments.²⁹ The collision-induced enhancement of the $(0 \rightarrow 1)$ emission is a little weaker, i.e., $k_{a-X}^c(0 \rightarrow 1) = 0.84 \times 10^{-2} \text{ M}^{-1} \text{ s}^{-1}$. Interestingly, the $(0 \rightarrow 1)$ band is, in absorption as well as in emission, a superposition of two distinct vibronic transitions of an O₂·O₂ collision complex with slightly different energies (see eqs 9 and 10).^{52,53}



These first quantitative studies clearly indicate that the enhancement of the $a \rightarrow X$ transition in the gas phase at higher pressures is caused by the weakening of the forbiddenness of the radiative transition in binary collision complexes. The very strong reduction of the radiative lifetime τ_{a-X} in solution by more than 3 orders of magnitude is the consequence of the much larger concentration of perturbing molecules, compared with their concentration in the gas phase.

Krasnovsky first observed the $(0 \rightarrow 0)$ $a \rightarrow X$ emission in solution in photosensitization experiments.⁵⁴ O₂(¹Δ_g) was formed by energy transfer from triplet-excited sensitizers to O₂. Using a phosphoroscope equipped with an NIR-sensitive photomultiplier, he observed the weak emission at ~1270 nm. These early investigations were restricted to very weakly O₂(¹Δ_g)-deactivating solvents, such as CCl₄, CS₂, and Freon, and suffered from the photobleaching of the sensitizers caused by the necessary high excitation powers. Khan and Kasha recorded $(0 \rightarrow 0)$ $a \rightarrow X$ emission spectra in C₆F₁₄, CCl₄, and even in H₂O using different photosensitizers.⁵⁵ Time-resolved measurements of the $(0 \rightarrow 0)$ and $(0 \rightarrow 1)$ $a \rightarrow X$ emissions in solution became possible with the development of sensitive Ge diode detectors. Salokhid-

inov et al. located both transitions in CCl₄ at 1272 and 1588 nm, respectively, where the intensity, I_{01} , of the $(0 \rightarrow 1)$ band was found to be 60 times weaker than I_{00} .⁵⁶ Schmidt and Afshari measured a solvent-independent ratio of $I_{00}/I_{01} = 64 \pm 5$ in CCl₄, CS₂, and C₆F₁₄.⁵⁷ Macpherson et al. determined a much larger solvent-independent ratio of $I_{00}/I_{01} = 103 \pm 7$ in 14 solvents.⁵⁸ The results of Salokhiddinov et al.⁵⁶ and Schmidt and Afshari⁵⁷ were confirmed by Chou et al.,⁵⁹ who determined that, independent of the solvent, $I_{00}/I_{01} = 66 \pm 5$. Thus, also in solution, the $(0 \rightarrow 0)$ transition contains almost the entire intensity of the $a \rightarrow X$ radiative transition.

The accurate determination of the rate constant k_{a-X} from photosensitized emission experiments in solution proved to be a difficult task. Suitable reference compounds for use in measurements of the luminescence quantum yield Q_L of the $a \rightarrow X$ emission in the NIR are lacking, and the quantum yield Q_Δ of O₂(¹Δ_g) sensitization has to be known for each solvent. k_{a-X} is obtained by using eq 11, where τ_Δ is the actual solvent-dependent O₂(¹Δ_g) lifetime.

$$k_{a-X} = \frac{Q_L}{\tau_\Delta Q_\Delta} \quad (11)$$

Substituting Q_L in eq 11 by the $a \rightarrow X$ emission intensity, I_L , in stationary experiments, or substituting Q_L/τ_Δ by the intensity, I_L^0 , of the $a \rightarrow X$ emission extrapolated to the time of laser pulse excitation in time-resolved experiments, leads to the more easily obtainable relative rate constants K_{a-X} . First determinations of K_{a-X} resulted in an apparently negligible solvent dependence.⁶⁰ However, Hurst et al. noticed that K_{a-X} increases with solvent polarizability in aromatic solvents.⁶¹ Scurlock and Ogilby demonstrated, in an investigation involving 15 different solvents, that a surprisingly large effect of the solvent on the radiative rate constant exists.⁶² Values of K_{a-X} increase by a factor of 25 on going from trifluoroethanol to CS₂. The solvent effect was almost simultaneously confirmed by Gorman et al., who found a strong variation of K_{a-X} in six solvents.⁶³ In contrast with these results from time-resolved studies, Schmidt et al. measured, in steady-state experiments, K_{a-X} data for six different solvents which were interpreted to indicate a solvent-independent radiative rate constant.⁶⁴ However, later Schmidt and Afshari also used the more reliable time-resolved technique and extended their investigation to 27 solvents, obtaining data which clearly confirmed the solvent dependence of K_{a-X} .⁶⁵

Several attempts have been made to determine absolute values of k_{a-X} . Krasnovsky measured $k_{a-X} = 0.25 \text{ s}^{-1}$ in CCl₄, using the fluorescence of tetraphenylporphine as a luminescence standard.⁶⁰ His result is in accordance with $k_{a-X} = 0.19 \text{ s}^{-1}$, obtained by Long and Kearns in absorption measurements in CCl₄.³⁸ However, Losev et al. determined the much larger value, $k_{a-X} = 0.8 \text{ s}^{-1}$, in CCl₄ by means of a Li-Nd phosphate glass luminescence standard.⁶⁶ In a later study, Losev et al. compared k_{a-X} values determined in emission and absorption experiments.⁶⁷ They found agreement with $k_{a-X} = 0.2 \text{ s}^{-1}$

only for D₂O. For the rest of the solvents studied, absorption experiments yielded in part significantly smaller values than emission measurements; e.g., for CCl₄, the absorption method yielded $k_{a-X} = 0.5 \text{ s}^{-1}$. The discrepancy is even larger for benzene, where they obtained $k_{a-X} = 4.5 \text{ s}^{-1}$ using the emission technique but only 0.9 s^{-1} with the absorption technique. The difference between the k_{a-X} values obtained with the two techniques was attributed, in a more speculative interpretation, to the fact that O₂ forms different kinds of complexes with solvent in both the ground and excited states. Schmidt determined with the emission method that $k_{a-X} = 1.5 \text{ s}^{-1}$ in benzene, using three different sensitizers and their corresponding fluorescence as luminescence standards.⁶⁸ With this result and the relative values of $K_{a-X} = 0.2$ (D₂O) and 0.62 (CCl₄) reported by Schmidt and Afshari,⁶⁵ which are normalized to $K_{a-X} = 1$ for benzene, absolute rate constants $k_{a-X} = 0.3 \text{ s}^{-1}$ (D₂O) and 0.9 s^{-1} (CCl₄) are calculated, which agree rather well with the emission results of Losev's group.⁶⁷ However, the k_{a-X} emission value reported by Losev for benzene is still 3-fold larger than the value reported by Schmidt. Finally, Shimizu et al. determined the absolute value of $k_{a-X} = 0.039 \text{ s}^{-1}$ with phenalene as sensitizer in CCl₄, using the fluorescence of quinine bisulfate as the standard.⁶⁹

The scatter of these data is, unfortunately, large. The value reported by Shimizu et al. is 15 times smaller than the average value, $k_{a-X} = 0.6 \text{ s}^{-1}$, calculated from the results obtained in CCl₄ in emission studies by the other workers. The investigations conducted by Losev et al. question the compatibility of results from absorption and emission measurements. Since, by far, most of the K_{a-X} data originate from emission measurements, absolute rate constants k_{a-X} should be calculated using a k_{a-X} reference value determined with this technique. In the recent literature, the value of $k_{a-X} = 1.5 \text{ s}^{-1}$ measured in benzene^{65,68} is generally used for that purpose.^{39,45,48}

A large number of literature K_{a-X} data and new results were compiled by Scurlock et al.⁷⁰ The relative rate constants correlate very smoothly with the solvent refractive index n of the 29 solvents investigated,⁷⁰ or with functions of n such as the bulk polarizability P (see Figure 4).⁶² These empirical correlations strongly indicate that the polarizability of the solvent plays an important role in the enhancement of the $a \rightarrow X$ radiative transition.

Different attempts at interpretation of the solvent effect have been made, most of them assuming the formation of collision complexes S·O₂ between a solvent molecule S and oxygen. Long and Kearns developed a perturbation model in which strongly allowed optical transitions of S contribute, by intensity-borrowing, to the enhancement of the S·O₂(¹Δ_g) → S·O₂(³Σ_g⁻) radiative transitions of collision complexes.³⁸ Schmidt and Afshari showed that, on the basis of this model, a linear correlation of K_{a-X} with the molar refraction, $R = V_m(n^2 - 1)/(n^2 + 2)$, could be expected, where V_m is the solvent molar volume. Actually, the data correlate roughly linearly with R .⁶⁵ Darmanyan assumed CT interactions in exciplexes

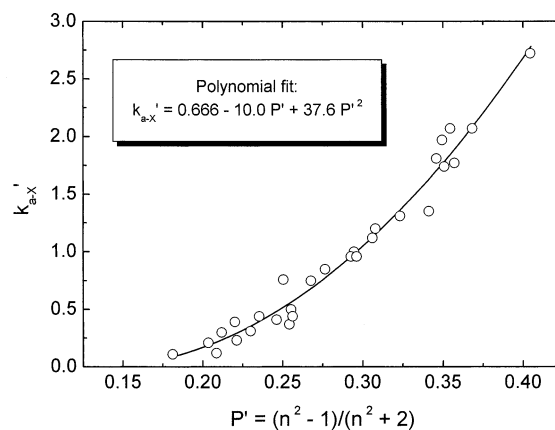


Figure 4. Plot of the relative $a \rightarrow X$ radiative rate constants, $k_{a-X}' = k_{a-X}/k_{a-X}(\text{benzene})$ versus solvent bulk polarizability P . Data compiled by Scurlock et al.⁷⁰

S·O₂(¹Δ_g) to be responsible for the S·O₂(¹Δ_g) → S·O₂(³Σ_g⁻) enhancement and correlated $\log(K_{a-X}/n^2)$ with the gas-phase ionization potential, IP, of S.⁷¹ However, these correlations are weaker than those similar to the one shown in Figure 4, as was shown by Scurlock et al.⁷⁰ Alternatively, Ogilby and co-workers proposed describing the solvent effect by a Kirkwood/Onsager reaction field model.^{70,72} Dispersive interactions between an isolated O₂ existing in a cavity and the solvent, which is considered as a homogeneous and isotropic medium, have to be taken into account. However, a quantitative formulation of this model, allowing the correlation of experimental data, has not been given.

At this point, it is interesting to note that, despite the findings from the gas-phase studies, which clearly demonstrate the bimolecular character of the perturbation process, only first-order rate constants have been correlated with solvent parameters, but not the really more appropriate second-order rate constants. This indicates a surprising information barrier between physicists and chemists working in the field of singlet oxygen, which has prevented more rapid scientific progress.

(2) Results from Theoretical Studies. Short-lived collision complexes S·O₂ are formed in binary collisions of oxygen and collider S. The intermolecular interaction between S and O₂ in these complexes leads to the loss of symmetry of the O₂ moiety and, hence, to a very graduated lifting of radiative selection rules. According to Minaev, the SOC in O₂ and the character of the electronic states of O₂ are not changed much upon collision.³³ Thus, the application of eqs 1 and 2 should easily rationalize the most prominent trends of the collision-induced intensity changes for the O₂ molecule. There are no sources of intensity enhancement of the magnetic dipole transitions 1, $b \rightarrow X, 1$, and 2, $a \rightarrow X, 1$, on intermolecular interaction. Thus, it is sufficient to discuss the changes in transitions 3, 4, and 5 (see Figure 2).

The $b \rightarrow X$ Transition. Transition 5, $b \rightarrow X, 0$, contributes, along with transition 1, to the overall $b \rightarrow X$ transition. Transition 5 is very weak for the isolated O₂ molecule (eq 8) but acquires electric-dipole-allowed character in collision complexes M·O₂, since it borrows intensity from the difference of the

collision-induced electric-dipole moments \mathbf{D}_b and \mathbf{D}_X in the b and X states. Minaev derives eq 12 for the electric-dipole transition moment $\mathbf{D}_{b-X,0}$.³³

$$\mathbf{D}_{b-X,0} = -C^*(\mathbf{D}_X - \mathbf{D}_b) \quad (12)$$

Depending on the colliding molecule, different values of $\mathbf{D}_{b-X,0}$ are obtained from eq 12. For example, $A_{b-X,0} = 0.017 \text{ s}^{-1}$ is calculated for the collision complex $\text{H}_2 \cdot \text{O}_2$. This corresponds to an overall enhancement of the $b \rightarrow X$ transition by only 20%, if compared with the experimental value $A_{b-X} = 0.0887 \text{ s}^{-1}$ reported by Ritter and Wilkerson.²⁶ For butadiene as the collider, an enhancement by a factor of 2.6 is calculated by means of ab initio methods.³³ However, the enhancement is smaller than 1 order of magnitude, even in this case. Semiempirical calculations, which consider intermolecular CT interactions, giving electric-dipole-allowed character to the microwave transition 6, $X,1 \rightarrow X,0$, between the spin sublevels of the triplet ground state, were also performed by Minaev and explain the external heavy-atom effect on the $b \rightarrow X$ transition.³⁵ Thus, theory and experiments agree in the finding that the $b \rightarrow X$ transition is only weakly influenced by intermolecular perturbations.^{33,35,38-40}

The $b \rightarrow a$ Transition. Transition 3 acquires a relatively strong electric-dipole transition moment in collisions, as was pointed out by Minaev.⁷³⁻⁷⁵ Because of the particular open-shell electronic structure of the O_2 molecule, with its degenerate antibonding $\pi_{g,x}$ and $\pi_{g,y}$ MOs, an asymmetric charge transfer occurs in the collision complex $\text{S} \cdot \text{O}_2$. For example, in a trapezium-like complex $\text{H}_2 \cdot \text{O}_2$, where the z axis is parallel to the O-O and H-H bonds and zx is a plane of the trapezium, the $\pi_{g,x}$ MO has an admixture of the MOs of H_2 , but not the $\pi_{g,y}$ MO. This leads to different permanent dipole moments \mathbf{D}_x and \mathbf{D}_y of the $\pi_{g,x}$ and $\pi_{g,y}$ MOs in complexes $\text{S} \cdot \text{O}_2$. The difference between the dipole moments is inherent to O_2 collisions with any collider. The main contribution to the collision-induced electric-dipole transition moment is given by eq 13, where D is the electric-dipole operator.³⁷

$$\mathbf{D}_{b-a} = \langle b^1 \Sigma_g^+ | D | a^1 \Delta_g \rangle = 0.5(\mathbf{D}_x - \mathbf{D}_y) \quad (13)$$

Semiempirical calculations lead to an enhancement of the $b \rightarrow a$ transition in the $\text{H}_2 \cdot \text{O}_2$ complex by a factor of 4400.⁷⁴ Ab initio calculations even predict a 10^5 -fold enhancement.⁷⁵

The $a \rightarrow X$ Transition. As realized by Minaev,^{73,74} transition 4, $a \rightarrow X,0$, borrows intensity from transition 3, $b \rightarrow a$, because of the partial singlet b character of the triplet $X,0$ state, which is the consequence of SOC. Since the $b \rightarrow a$ transition acquires partially allowed dipole character in collisions, a corresponding electric-dipole transition moment $\mathbf{D}_{a-X,0}$, given by eq 14, is induced in the $a \rightarrow X,0$ transition.

$$\mathbf{D}_{a-X,0} = \langle a^1 \Delta_g | D | \Psi_{X,0} \rangle = \langle a^1 \Delta_g | D | X^3 \Sigma_{g,0}^- \rangle - C^* \langle a^1 \Delta_g | D | b^1 \Sigma_g^+ \rangle \quad (14)$$

Again, the second term in eq 14, the perturbation term, dominates. In a treatment analogous to eq 7, the expression can be further simplified to eq 15.^{33,37}

$$\mathbf{D}_{a-X,0} = -C^* \langle a^1 \Delta_g | D | b^1 \Sigma_g^+ \rangle = -C^* \mathbf{D}_{a-b} \quad (15)$$

Thus, the strong enhancement of the $b \rightarrow a$ transition in collisions induces the enhancement of the $a \rightarrow X$ transition. Equation 15 directly relates the electric-dipole transition moments $\mathbf{D}_{a-X,0}$ and \mathbf{D}_{a-b} of both collision-induced transitions. The ratio k_{a-X}^c/k_{b-a}^c of the rate constants of the corresponding collision-induced radiative transitions is given by eq 16.³⁷

$$k_{a-X}^c/k_{b-a}^c = \frac{(\nu_{a-X})^3 (\mathbf{D}_{a-X,0})^2}{(\nu_{b-a})^3 (\mathbf{D}_{b-a})^2} = \frac{(\nu_{a-X})^3 |C|^2}{(\nu_{b-a})^3} \quad (16)$$

Using $C = 0.0134i$, $\nu_{a-X} = 7882 \text{ cm}^{-1}$, and $\nu_{b-a} = 5239 \text{ cm}^{-1}$ in eq 16 results in $k_{a-X}^c/k_{b-a}^c = 6.1 \times 10^{-4}$. It is most remarkable that, in this simplifying treatment, the ratio k_{a-X}^c/k_{b-a}^c should be constant for any diamagnetic collider.³⁷ In an extension of the theory, Minaev also considered charge-transfer interactions between S and O_2 in the collision complex and expected a minor but selective enhancement of the $a \rightarrow X$ transition, which should lead to an increase of k_{a-X}^c/k_{b-a}^c with decreasing ionization potential of S.³⁷

(3) Mechanism of the Collision-Induced $b \rightarrow a$ and $a \rightarrow X$ Transitions. The $b \rightarrow a$ and $a \rightarrow X$ transitions are closely related. Actually, eq 16 allows Minaev's theory to be tested experimentally. Schmidt and Bodesheim first investigated the solvent dependence of the $a \rightarrow X$ transition in this connection. They determined the radiative rate constants of $k_{a-X} = 1.1 \text{ s}^{-1}$ and $k_{b-a} = 3.4 \times 10^3 \text{ s}^{-1}$ in liquid CCl_4 at room temperature.³⁹ Earlier, and under very different conditions, Becker et al. measured the values of $k_{a-X} = 1.3 \times 10^{-2} \text{ s}^{-1}$ and $k_{b-a} = 41 \text{ s}^{-1}$ at 5 K in solid Ar.⁴¹ The results indicate the strong influence of the surrounding matrix on both radiative processes. As shown by Schmidt and Bodesheim, the ratios k_{a-X}/k_{b-a} are the same, i.e., 3.2×10^{-4} in liquid CCl_4 and 3.1×10^{-4} in solid Ar, despite the large variation of rate constants, in agreement with Minaev's prediction of a constant ratio.³⁹ Moreover, the absolute value of the experimental ratio is close to the predicted value.³⁷

The molecular properties of the collider, determining the enhancement of these transitions, were still unknown. According to Minaev, the degenerate antibonding $\pi_{g,x}$ and $\pi_{g,y}$ MOs of O_2 acquire different dipole moments in collisions due to an admixture of the MOs of the collider. On the basis of this fundamental concept, Schmidt and Bodesheim concluded that the asymmetrical charge transfer should depend on the collider's molecular polarizability, which can be expressed by the molar refraction R . If the perturbation is caused in the liquid phase, too, by bimolecular interactions, then some correlation between the second-order rate constants $k_{a-X}^c = k_{a-X}/[S]$, where $[S]$ is the solvent molarity, and R should exist. Actually, a linear correlation of $\log(k_{a-X}^c)$ with $\log(R)$, with slope $s_{a-X} = 1.71 \pm 0.08$ and intercept

$i_{a-X} = -3.37 \pm 0.12$, was found.³⁹ Moreover, correlation of the gas-phase k_{b-a}^c data reported by Fink et al.⁴⁴ (Table 2) and the CCl_4 value of $k_{b-a}^c = 330 \text{ M}^{-1} \text{ s}^{-1}$ versus $\log(R)$ also yielded a linear plot. The slope and intercept of this correlation are $s_{b-a} = 1.84 \pm 0.11$ and $i_{b-a} = -0.22 \pm 0.13$.³⁹ These two correlations are parallel in the limits of experimental uncertainty. This finding emphasizes the common origin of the collision-induced $b \rightarrow a$ and $a \rightarrow X$ radiative transitions.

From the result that both slopes s_{a-X} and s_{b-a} are only slightly little smaller than 2, it was concluded that a pure quadratic dependence of $\log(k_{a-X}^c)$ and $\log(k_{b-a}^c)$ on R should exist for a hypothetical set of colliders of the same molecular weight, shape, and size but different molecular polarizability. The normalized collision frequency and the collision distance would then be constant, and the transition moment induced by intermolecular interactions in collisions would be directly proportional to the molar refraction. Thus, the enhancement of the two collision-induced transitions was, for the first time, directly related with a molecular property of the collider, i.e., its molecular polarizability.³⁹

In contrast with these conclusions, however, several subsequent studies analyzed the solvent effect on the $a \rightarrow X$ radiative transition on the basis of first-order rate constants k_{a-X} , and it was discussed whether correlations with the ionization potential or with the refractive index of the solvent would be more appropriate.^{76,77} Shimizu et al. published absolute k_{a-X} data determined in 20 solvents.⁷⁸ These values were calibrated with $k_{a-X} = 0.039 \text{ s}^{-1}$, determined in CCl_4 ,⁶⁹ which is much smaller than the value found by other investigators. However, relative values K_{a-X} , normalized to the reference solvent benzene, agree with the data collected by Scurlock et al.,⁷⁰ where overlap occurs.

A very interesting study on the variation of K_{a-X} in a number of homogeneous binary solvent mixtures was published by Bilski et al.⁷⁹ Values of K_{a-X} have been shown to correlate best with the bulk polarizability P . The prevailing trend was that K_{a-X} increases with increasing P of the solvent medium. However, a generally valid correlation, similar to the one shown in Figure 4, was not found. The increase of K_{a-X} with P is almost linear in D_2O /dioxane mixtures. However, in $\text{D}_2\text{O}/\text{CH}_3\text{CN}$, P and K_{a-X} increase with increasing CH_3CN content until a maximum of P is reached. Then, P begins to decrease, while the increase of K_{a-X} continues. This anomalous behavior was explained by more specific interactions between $\text{O}_2(^1\Delta_g)$ and solvent, such as exciplex formation. These specific interactions were also assumed to be probably responsible for considerable scattering in plots of K_{a-X} with bulk polarizability (see Figure 4).⁷⁹

However, anomalous correlations of k_{a-X} with P are not a consequence of specific interactions between $\text{O}_2(^1\Delta_g)$ and some component of the solvent mixture, but between the mixture components itself, as was demonstrated by Schmidt et al.⁸⁰ Figure 5 plots their values of k_{a-X} , determined for three different homogeneous solvent mixtures, versus P .

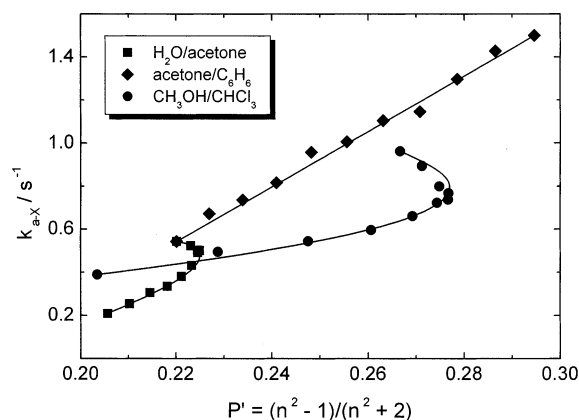


Figure 5. Plot of absolute $a \rightarrow X$ radiative rate constants, k_{a-X} , versus solvent bulk polarizability P for three different solvent mixtures. Reprinted with permission from ref 80. Copyright 1999 American Chemical Society.

In agreement with the results reported by Bilski et al.,⁷⁹ it was found that no general form of the correlation of k_{a-X} with P exists. In contrast to the slightly upward-curved correlation for the pure liquids of Figure 4, Figure 5 displays different forms of correlations of k_{a-X} with P : a linear variation of k_{a-X} for acetone/ C_6H_6 , and two strongly bent anomalous curves for H_2O /acetone and $\text{CH}_3\text{OH}/\text{CHCl}_3$, both passing through a maximum of P . It was shown that these different dependences can be described quantitatively on the basis of a bimolecular perturbation process.⁸⁰ If collisions of $\text{O}_2(^1\Delta_g)$ with molecules A and B contribute independently to the overall probability k_{a-X} of the radiative transition in mixtures of solvents A and B, then eq 17 should hold true, where $k_{a-X,A}^c$ and $k_{a-X,B}^c$ are the rate constants of the $a \rightarrow X$ radiative transition in binary collisions with A and B, respectively.

$$k_{a-X} = k_{a-X,A}^c[A] + k_{a-X,B}^c[B] \quad (17)$$

The bulk polarizability P can be calculated, even for mixtures with strongly anomalous behavior, with high accuracy by using eq 18 from the molar refractions R_A and R_B and the molar concentrations of both components, as shown, for example, for the mixture of H_2O /acetone.⁸⁰

$$P_{\text{calc}} = R_A[A] + R_B[B] \quad (18)$$

In this example, the deviation of P_{calc} from P amounts, at maximum, to only 0.0009, or 0.4%. Similar accuracy was obtained for other investigated solvent mixtures, demonstrating that the calculation of bulk polarizabilities leads to reliable results, if it is based on the molar refractions of the components and on the respective concentration-dependent excess volumes ΔV_{exc} .

The two curves and the straight line connecting the k_{a-X} data from the pure mixture components drawn in Figure 5 match the experimental rate constants k_{a-X} very well. It should be noted that they were simply calculated by eqs 17 and 18 using the corresponding values of k_{a-X}^c , R , and ΔV_{exc} . Thus, anomalous as well as almost ideal behavior could be reproduced without referring to specific interactions

of $O_2(^1\Delta_g)$ with some component of the mixture. The anomalous dependences of k_{a-X} on P in H_2O /acetone and $CH_3OH/CHCl_3$ are the consequences of strongly attractive interactions between the respective mixture components, which lead to distinctly negative excess volumes ΔV_{exc} , whereas the mixture acetone/ C_6H_6 behaves almost ideally, due to a negligible ΔV_{exc} . Specific interactions of $O_2(^1\Delta_g)$ with the colliders, inducing the $a \rightarrow X$ radiative transition, are already accounted for in the corresponding bimolecular rate constant k_{a-X}^c . Thus, the quantitative treatment of the data for the homogeneous solvent mixtures definitely proved the bimolecularity of the emission process also in the liquid phase.⁸⁰

A further step in complexity was taken by Martinez et al.,⁸¹ who investigated the $a \rightarrow X$ radiative transition in microheterogeneous systems such as micellar solutions and microemulsions. Experimental $k_{a-X,m}$ data could not be reproduced by application of eq 17, which is valid only for homogeneous systems. In micellar solutions there exist $O_2(^1\Delta_g)$ concentration differences between the interior organic and the exterior aqueous phases, which can be quantified by the equilibrium constant $K_{eq} = [O_2(^1\Delta_g)]_{int}/[O_2(^1\Delta_g)]_{ext}$, which is equal to the ratio of the corresponding O_2 solubilities, as was shown by Lee and Rodgers.⁸² This pseudophase model also considers the volume fractions f_m and $1 - f_m$ of the micellar and the aqueous phases in which deactivation occurs with rate constant $k_{d,int}$ and $k_{d,ext}$. The observable overall rate constant k_d is then given by eq 19.⁸²

$$k_d = \frac{K_{eq} f_m k_{d,int} + (1 - f_m) k_{d,ext}}{K_{eq} f_m + (1 - f_m)} \quad (19)$$

Equation 19 quantitatively reproduces the experimental $k_{a-X,m}$ data if the values of k_d are replaced by the corresponding k_{a-X} data, as shown by Martinez et al.⁸¹

Rate constants k_{a-X}^c were determined with rather high accuracy for 12 pure solvents by Schmidt et al.,⁸⁰ using the universal $O_2(^1\Delta_g)$ reference sensitizer phenalene.⁸³ Values of $\log(k_{a-X}^c)$ correlate roughly with the square of the molar refraction R of the solvent. However, a closer look at the data revealed significant graduations, depending on the size of the collider. The data for small colliders (such as H_2O , D_2O , CH_3OH , and CS_2) are all above the correlation found for medium size colliders, whereas those for large colliders (e.g., C_4Cl_6) are below this correlation. This observation was also confirmed by Martinez et al.⁸¹ Obviously, other factors besides the molecular polarizability also influence the values of k_{a-X}^c : (i) the solvent refractive index n , (ii) the normalized collision frequency Z , and (iii) the van der Waals volume V_{vdw} of the collider.⁸⁰

(i) The investigations were performed in liquids of strongly varying refractive index: $1.290 \leq n \leq 1.743$. However, radiative rate constants are proportional to the square of the refractive index of the surroundings of the emitter.⁸⁴ Thus, the proportionality $k_{a-X}^c \sim n^2$ has to be taken into account.

(ii) Since a collision-induced process was analyzed, the relation $k_{a-X}^c \sim Z$ was assumed. Real colliders

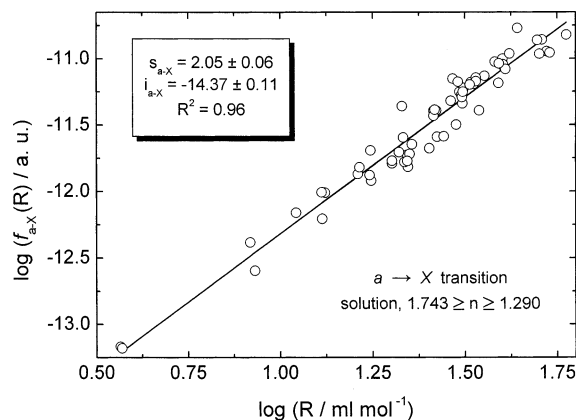


Figure 6. Dependence of bimolecular $a \rightarrow X$ radiative rate constants, $k_{a-X}^c = k_{a-X}/[S]$, on normalized collision frequency Z , solvent refractive index n , van der Waals volume V_{vdw} , and molar refraction R , as demonstrated by a double-logarithmic plot of solution-phase values of $f_{a-X}(R) = k_{a-X}^c/(Zn^2 V_{vdw}^{-2/3})$ versus R . Reprinted with permission from ref 85. Copyright 1999 American Chemical Society.

differ in size, shape, and mass, leading to different collision frequencies with O_2 . The variations of Z were considered, approximating both the collider and O_2 as spheres and calculating gas-phase values of the normalized collision frequency Z .

(iii) The remarkable effect of the molecular size of the collider on k_{a-X}^c could be understood when the molecular mechanism of the collision-induced transition was considered. Only those MOs of the colliding molecule which overlap with the $\pi_{g,x}$ and $\pi_{g,y}$ MOs of O_2 in the collision can strongly contribute to the enhancement of the $a \rightarrow X$ radiative transition by a transient shift of electron density. A size correction function could be derived, assuming the colliders are simply spheres of uniform polarizability. The overall surface of the collider is then proportional to $V_{vdw}^{2/3}$. The transient shift of electron density into the $\pi_{g,x}$ and $\pi_{g,y}$ MOs of O_2 can take place only in the small contact region of O_2 and the collider, where the MOs mutually overlap. As long as the area of the contact region is constant in the series of colliders, its relative magnitude varies with the collider size, proportionally to $V_{vdw}^{-2/3}$. Therefore, $V_{vdw}^{-2/3}$ should be proportional to that part of the collider polarizability which becomes effective in the collision-induced $a \rightarrow X$ radiative transition. Thus, the function $f_{a-X}(R) = k_{a-X}^c/(Zn^2 V_{vdw}^{-2/3})$, which represents relative rate constants normalized to the same refractive index, collision frequency, and size, should reveal the dependence of the collision-induced radiative probability on R .⁸⁰ Actually, a very good linear correlation of $\log(f_{a-X}(R))$ versus $\log(R)$ with slope $s_{a-X} = 2.06 \pm 0.08$ resulted from the original data reported in that paper.⁸⁰ This analysis still rested only on a small data basis. However, since in the meantime a large body of reliable k_{a-X} data had been compiled,^{62,65,70,76,77,80} Hild and Schmidt used an extended data set from 63 pure solvents to test the validity of the above-presented evaluation.⁸⁵ The corresponding plot of $\log(f_{a-X}(R))$ versus $\log(R)$ is given in Figure 6.

Again, a rather smooth linear correlation with slope $s_{a-X} = 2.05 \pm 0.06$ was found. Both the linearity

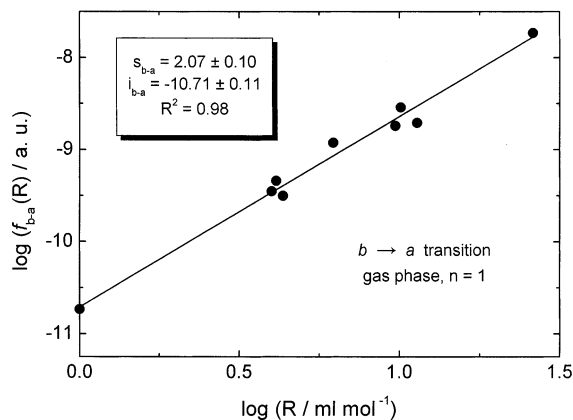


Figure 7. Experimental confirmation of Minaev's theory of spin-orbit coupling mediated intensity borrowing between the $a \rightarrow X$ and $b \rightarrow a$ radiative transitions, by a double-logarithmic plot of gas-phase values of $f_{b-a}(R) = k_{b-a}^c / (Zl^2 V_{\text{vdW}}^{-2/3})$ versus molar refraction R of collider. Data from Fink et al.⁴⁴ Reprinted with permission from ref 85. Copyright 1999 American Chemical Society.

of the correlation and its slope of 2 show that a correlation of $f_{a-X}(R) \sim R^2$ with negligible intercept exists. Thus, it was found that the probability of the collision-induced $a \rightarrow X$ radiative transition is directly proportional to the square of the molecular polarizability of the collider, if the effects of changes in refractive index, collision frequency, and collider size are removed,^{80,85} confirming the earlier conclusions.³⁹ Since radiative rate constants are proportional to the square of the transition moment (see eq 16), the simple direct proportionality $\mathbf{D}_{a-X} \sim R$ exists for $a \rightarrow X$ radiative transitions of binary collision complexes $S \cdot O_2$.

According to Minaev's simplified theoretical treatment, $\mathbf{D}_{a-X,0} \sim \mathbf{D}_{b-a}$ should be valid (see eq 15). Thus, a corresponding plot of $\log(f_{b-a}(R))$ versus $\log(R)$, derived from the k_{b-a}^c data reported by Fink et al.,⁴⁴ determined in the gas phase, where $n = 1$, should also be linear with a slope of 2. This is actually true (see Figure 7).⁸⁵ The slope $s_{b-a} = 2.07 \pm 0.10$ of the linear fit almost coincides with s_{a-X} , confirming Minaev's theory of the SOC-mediated intensity borrowing. The experimental results $\mathbf{D}_{a-X,0} \sim R$ and $\mathbf{D}_{b-a} \sim R$ demonstrate that the difference $\mathbf{D}_x - \mathbf{D}_y$ of the dipole moments induced in the only partially filled $\pi_{g,x}$ and $\pi_{g,y}$ MOs of O_2 in binary collisions complexes $S \cdot O_2$ linearly depends on the molecular polarizability of the collider S .^{80,85} Actually, induced dipole moments are known to be directly proportional to R in the range of optical frequencies.

Very recently, Andersen and Ogilby reported k_{b-a} values determined by $b \leftarrow a$ absorption spectroscopy in the solvents D_2O , n -hexane, toluene, benzene, and CS_2 .⁴⁸ These data were used to calculate liquid-phase values of $f_{b-a}(R) = k_{b-a}^c / (Zl^2 V_{\text{vdW}}^{-2/3})$. A linear fit of $\log(f_{b-a}(R))$ versus $\log(R)$ resulted in slope $s_{b-a} = 2.3 \pm 0.3$, confirming the conclusions derived by Schmidt and co-workers in the application of Minaev's theory.

Ratios of k_{a-X}/k_{b-a} for individual colliders were determined in the meantime by several groups. Tyczkowski et al. measured the radiative lifetimes τ_{b-a} and τ_{a-X} at very low temperature in matrices of Ne, Ar, Kr, and Xe by directly monitoring the $O_2(^1\Sigma_g^+)$

and $O_2(^1\Delta_g)$ decays, and they obtained k_{a-X}/k_{b-a} ratios of 3.2×10^{-4} , 3.7×10^{-4} , 4.2×10^{-4} , and 8.3×10^{-4} , respectively.⁸⁶ Anderson and Ogilby determined the respective ratios of 9.0×10^{-4} , 4.7×10^{-4} , 6.5×10^{-4} , 6.5×10^{-4} , and 10.5×10^{-4} in D_2O , n -hexane, toluene, benzene, and CS_2 by means of $b \leftarrow a$ absorption and $a \rightarrow X$ emission techniques,⁴⁸ and Schmidt et al. obtained the ratios of 4.4×10^{-4} , 6.0×10^{-4} , and 7.8×10^{-4} in $b \rightarrow a$ and $a \rightarrow X$ emission measurements in CCl_4 , C_2Cl_4 , and C_4Cl_6 .⁸⁰ The ratios k_{a-X}/k_{b-a} increase in each series of solvents with decreasing ionization potential, if the D_2O ratio is neglected. This is in line with the calculations of Minaev, who expects, in his more refined treatment, that CT interactions between the collider and O_2 should lead to an additional but minor enhancement of the $a \rightarrow X$ radiative transition (vide supra).³⁷ However, the D_2O ratio contradicts this interpretation. The uncertainties of these experimental data are considerable. Because of the different techniques used, different systematic errors could result. However, if only average values of each group are considered, then the ratios 5×10^{-4} , 7×10^{-4} , and 6×10^{-4} , calculated from the data reported by Tyczkowski et al., Anderson and Ogilby, and Schmidt et al., show a surprising similarity with the theoretically derived $k_{a-X}/k_{b-a} = 6.1 \times 10^{-4}$.³⁷ Actually, the excellent linearities of the correlations of Figures 6 and 7 exclude a strong additional source of intensity borrowing for the collision-induced $a \rightarrow X$ radiative transition by charge-transfer interactions, i.e., in the region of large polarizabilities. A further determination by Losev et al. yielded $k_{a-X}/k_{b-a} = 3 \times 10^{-3}$ in CS_2 ,⁸⁷ which, however, deviates significantly from the other experimental results and the theoretically expected ratio.

Thus, a rather high level of understanding of the complex mechanisms of the collision-induced $b \rightarrow a$ and $a \rightarrow X$ radiative transitions has been achieved by a fortunate interplay between theoretical and experimental work. This holds true for diamagnetic colliders.

Very few paramagnetic compounds have been investigated with respect to emission enhancement, and these only with respect to the $a \rightarrow X$ emission. Wildt et al. determined the rate constants of the ($0 \rightarrow 0$) $a \rightarrow X$ emissions induced by collisions with the triplet O_2 molecule and the NO radical to be $k_{a-X}^c = 2.04 \times 10^{-2}$ and $1.02 \text{ M}^{-1} \text{ s}^{-1}$, respectively.⁵¹ If these rate constants are used to calculate, via $f_{a-X}(R) = k_{a-X}^c / (Zl^2 V_{\text{vdW}}^{-2/3})$, the corresponding values of $\log(f_{a-X}(R))$, then -12.10 and -10.40 are obtained for O_2 and NO. These numbers are significantly larger than the $\log(f_{a-X}(R))$ values of -13.14 and -13.05 , obtained using the molar refractions of 4.00 and 4.40 mL mol^{-1} for O_2 and NO and the linear fit of $\log(f_{a-X}(R))$ versus $\log(R)$ shown in Figure 6. Consequently, the probability of the collision-induced $a \rightarrow X$ radiative transition is, for O_2 and NO, factors of 10 and 440 larger than expected for diamagnetic colliders of the same size, collision frequency, and molecular polarizability.

The only study concerned with the enhancement of the $a \rightarrow X$ emission by paramagnetic solutes was

performed by Belford et al.⁸⁸ Initial luminescence intensities were determined by time-resolved measurements in the absence, L^0 , and in the presence, $L(N)$, of stable nitroxyl (N) radicals. Tetramethylpiperidine-*N*-oxyl (TEMPO), two TEMPO derivatives, and the diamagnetic control agent tetramethylpiperidine (TEMP) were investigated in this interesting work. A linear increase of $L(N)/L^0$ was observed with increasing $[N]$, already qualitatively indicating a significant emission enhancement.⁸⁸ The data can be quantitatively evaluated if the contributions of the solvent, $k_{a-X,S}^c[S]$, and of the nitroxyl, $k_{a-X,N}^c[N]$, to the collision-induced radiative transition are considered. Thereby, eq 20 is derived.

$$L(N)/L^0 = 1 + \frac{k_{a-X,N}^c[N]}{k_{a-X,S}^c[S]} \quad (20)$$

The solvent used was CCl_4 , for which $k_{a-X,S}^c[S] = 1.17 \text{ s}^{-1}$ had been determined.⁸⁰ With the slope $s = 11 \text{ M}^{-1}$ determined by Belford et al. for TEMPO, $k_{a-X,N}^c = 13 \text{ M}^{-1} \text{ s}^{-1}$ is obtained from eq 20. Very similar slopes had been found for the two TEMPO derivatives, whereas the diamagnetic TEMP apparently did not enhance the emission.⁸⁸ The TEMPO rate constant $13 \text{ M}^{-1} \text{ s}^{-1}$ corresponds to $\log(f_{a-X}(R)) = -9.26$. Using $R = 46.6 \text{ mL mol}^{-1}$, the linear fit of Figure 6 leads to $\log(f_{a-X}(R)) = -10.95$. Consequently, the probability of the collision-induced $a \rightarrow X$ radiative transition is a factor of 50 larger for TEMPO than for a diamagnetic collider of the same size, collision frequency, and molecular polarizability, such as TEMP.

These few investigations clearly demonstrate the existence of a much stronger enhancement of the collision-induced $a \rightarrow X$ radiative transition by paramagnetic colliders, which most probably is caused by a partial lifting of the intersystem crossing (isc) restrictions, since spin-allowed transitions exist in collision complexes with colliders of triplet and doublet multiplicity (see eqs 21 and 22).



The difference in the enhancement between the nitroxyl radicals and NO, by 1 order of magnitude, can be explained in part by the space-filling methyl substituents partially shielding the radical center. It is, however, not known why O_2 is much less effective than NO.⁵¹

b. Spectral Shifts of Radiative Transitions. Interestingly, the effects of intermolecular perturbation on both the probabilities of the radiative transitions of singlet oxygen and the corresponding transition energies differ by orders of magnitude. While the enhancement of the transition probabilities is tremendous, the spectral shifts observed in the liquid phase are only small. Obviously, weak interactions in collisions are already sufficient to produce severe perturbations for strongly forbidden transitions; however, they have only a small effect on the energies of

the ground and excited states of the nonpolar O_2 molecule. Solvent-dependent spectral shifts were discussed by Ogilby and co-workers in two reviews in 1999.^{89,90} Few articles dealing with this subject have been published since then. Therefore, the spectral shifts of the different possible emissions will be treated here only briefly for reasons of completeness.

(1) Results from Experimental Studies. *The $b \rightarrow X$ Transition.* The lifetime τ_Σ of the upper excited singlet oxygen $\text{O}_2(\Sigma_g^+)$ is drastically shortened in solution compared with that in the gas phase, due to very effective spin-allowed radiationless deactivation processes. Maximum lifetimes of 130–200 ns are observed only in perhalogenated liquids such as CCl_4 and C_2Cl_4 .^{80,91,92} In contrast, the probability of the $b \rightarrow X$ radiative transition increases only moderately in solution. This leads to a very small emission quantum yield Q_{b-X} , which was determined to be about 1×10^{-7} in CCl_4 .^{39,40} Thus, it not surprising that studies concerning the spectral shift of the $b \rightarrow X$ emission in different solvents are lacking. The emission spectrum was measured in CCl_4 by Chou et al., who found the maximum at 765 nm.⁴⁰ Wild et al. observed the maximum in liquid O_2 , at 77 K, also at 765 nm.⁹³ Thus, the $b \rightarrow X$ emission is red-shifted only slightly, by 3 nm or approximately -50 cm^{-1} , on going from the gas phase to these liquid media.

The $a \rightarrow X$ Transition. The spectral shift of this emission is well investigated. Bromberg and Foote first reported the small but significant solvent dependence of the $a \rightarrow X$ emission band to range from 1273 (acetone- d_6) to 1279 nm (anisole).⁹⁴ Losev and co-workers studied both the $(0 \rightarrow 0)$ and $(0 \rightarrow 1)$ transitions of this emission in 11 solvents.⁹⁵ Schmidt and Afshari recorded the $(0 \rightarrow 0)$ and $(0 \rightarrow 1)$ emission bands of ${}^{16}\text{O}_2({}^1\Delta_g)$ and ${}^{18}\text{O}_2({}^1\Delta_g)$ in four perhalogenated solvents, in CDCl_3 , and in CS_2 .⁵⁷ The $(0 \rightarrow 0)$ and $(0 \rightarrow 1)$ transitions of both isotopomers occurred in C_6F_{14} at the wavelengths calculated for the gas phase. Compared with these values, all transitions are red-shifted in CCl_4 by the same value, -30 cm^{-1} . A higher spectral resolution can be obtained with FTIR spectrometers than with dispersive instruments. Using this technique, Macpherson et al. determined the $(0 \rightarrow 0)$ and $(0 \rightarrow 1)$ transition energies ν_{00} and ν_{01} for $\text{O}_2({}^1\Delta_g)$ in 25 perdeuterated and perhalogenated solvents and in CS_2 .⁵⁸ An extension of the data basis was achieved when Wessels and Rodgers investigated the $(0 \rightarrow 0)$ transition of $\text{O}_2({}^1\Delta_g)$ by FTIR emission spectroscopy in 50 solvents, comprising the whole possible refractive index variation in liquids.⁹⁶ Furthermore, Dam et al. very recently complemented the data set with emission maxima and bandwidths of the $(0 \rightarrow 0)$ transition of the $\text{O}_2({}^1\Delta_g)$ phosphorescence, determined by the Fourier technique in toluene, pyridine, poly(methyl methacrylate), and polystyrene.⁴⁷

The data from the different studies yield altogether a consistent picture. The variation of ν_{00} is small but significant: only 0.63% variation between 7873.2 (CF_3COOH) and 7823.9 cm^{-1} (CH_2I_2). A strong linear correlation of ν_{00} with the bulk polarizability P was observed, from which only the data for the “anoma-

lous" solvents acetone, tetrahydrofuran, dioxane, CH₃CN, CH₃OH, and H₂O deviate significantly.⁹⁶ Thus, it seemed as if dispersion interactions between the solvent and O₂(¹Δ_g) would be the main reason for the observed red-shift. However, the extrapolation of the linear fit of ν_{00} versus P to the value for $P = 0$, corresponding to the gas phase, resulted in 7916.7 cm⁻¹, which is significantly larger than the actual gas-phase (0 → 0) transition energy, $\nu_{00}^g = 7882.4$ cm⁻¹.^{24,97} Therefore, the extrapolated value for ν_{00} either contradicts the assumption of a linear correlation between ν_{00} and P or indicates that, besides attractive, also repulsive interactions contribute to the solvent dependence of ν_{00} .

The $b \rightarrow a$ Transition. Chou and Frei published the first spectrum of the (0 → 0) transition of this emission in solution. They observed in CCl₄ a narrow-band emission centered at ~1930 nm.⁴³ Ogilby and co-workers investigated the influence of the variation of the refractive index of the solvent on this emission.⁹⁸ Using a dispersive instrument, they determined the transition energy ν_{00} in four perhalogenated solvents, in CS₂, and in mixtures of CCl₄ and CS₂, which are all nonpolar solvents. Red-shifts $\Delta\nu_{00} = \nu_{00} - \nu_{00}^g$ with respect to the gas-phase transition energy, $\nu_{00}^g = 5241$ cm⁻¹, were calculated and compared in a common plot versus the bulk polarizability P with the corresponding red-shifts of the $a \rightarrow X$ emission, calculated with $\nu_{00}^g = 7882.4$ cm⁻¹ from the data reported by Wessels and Rodgers, discarding the "anomalous" solvents.⁹⁶ Strong linear correlations were found. It was noted that the red-shift is slightly but significantly stronger for the $b \rightarrow a$ emission. This can also be inferred by comparing the $\Delta\nu_{00}$ values measured in CCl₄, which amount to -31.3 and -46.5 cm⁻¹ for the $a \rightarrow X$ and $b \rightarrow a$ emissions, respectively.^{24,96,98} It should be noted that the red-shift $\Delta\nu_{00} \approx -50$ cm⁻¹ of the $b \rightarrow X$ emission in CCl₄ is of similar magnitude (vide supra). Interestingly, extrapolation of the linear correlations to $P = 0$ leads, for both emissions, to the similar blue-shifts compared with the respective actual gas-phase transition energies of about 35 cm⁻¹.

A little later, Ogilby and co-workers used a step-scan FTIR spectrometer to obtain a precise measurement of the spectra of both the $b \rightarrow a$ emission and $b \leftarrow a$ absorption in CS₂, CCl₄, and Freon-113.^{45,99} Only negligibly small Stokes shifts were observed, indicating that the difference between the equilibrium and nonequilibrium solvation energies for the ¹Δ_g and ¹Σ_g⁺ states of O₂ is small in these nonpolar solvents.⁹⁹ Dam et al. continued the investigations of the $b \leftarrow a$ transition and recently reported the energies ν_{00} and the bandwidths $\Delta\nu$ of the absorption band for 19 solvents of very different refractive index n and dielectric constant ϵ , including the four "anomalous" solvents tetrahydrofuran, dioxane, CH₃CN, and CH₃OH.⁴⁷ For the analysis, these data were complemented with corresponding literature data for ν_{00} and $\Delta\nu$ on the $a \rightarrow X$ emission. The authors demonstrated that, with this solvent selection, only roughly linear correlations of ν_{00} with n —and thus also with P —are obtained for both optical transitions. In their interpretation of the role of the solvent, they emphasize

that it is important to recognize that solvent polarization is composed of the very fast optical polarization \mathbf{P}_{op} and the much slower inertial polarization \mathbf{P}_{in} . \mathbf{P}_{op} represents the response from the solvent electronic degrees of freedom, which is assumed to be in permanent equilibrium with the charge distribution of the solute. The inertial polarization vector \mathbf{P}_{in} represents the response from the solvent nuclear degrees of freedom (i.e., vibrational, rotational, and translational motion) and remains fixed during an electronic transition. Functions describing \mathbf{P}_{op} and \mathbf{P}_{in} depend on n and ϵ , respectively. Both the $b \leftarrow a$ and $a \rightarrow X$ transitions originate from O₂(¹Δ_g) (which is in equilibrium with the surrounding solvent and is stabilized as a consequence of both the inertial and optical polarization vectors) and lead to Franck–Condon states (which are not in equilibrium with the surrounding solvent), since the inertial vectors \mathbf{P}_{in} have not yet had the chance to respond to the new solute charge distribution. Therefore, it was argued that the corresponding transition energies ν_{00} may not correlate well with functions that depend only on n . However, much better correlations of the transition energy with functions that depend only on n were expected for the hypothetical transition from a nonequilibrated state of O₂ to another nonequilibrated state. Such a hypothetical transition was modeled by taking the sum of the $b \leftarrow a$ and $a \rightarrow X$ spectral shifts. Actually, Dam et al. showed that this sum correlates remarkably well with n . This is probably also the consequence of a similar charge distribution of the solutes O₂(¹Σ_g⁺) and O₂(³Σ_g⁻). It was suggested that this clearly demonstrates the importance of considering the effects of equilibrium and nonequilibrium solvation when interpreting the effect of solvent on the different optical transitions of oxygen. The analysis of the $\Delta\nu$ data led to the conclusion that the bandwidths of the $b \leftarrow a$ and $a \rightarrow X$ transitions, however, principally reflect only the effects of equilibrium solvation.

(2) Results from Theoretical Studies. Early attempts to explain the solvent dependence of $\Delta\nu_{00}$ were based on the assumption that dispersion interactions may be mainly responsible for the observed spectral shift of the $a \rightarrow X$ emission.^{58,94,96–98} Schmidt interpreted the solvent dependence of $\Delta\nu_{00}$ by means of a simple model based on the dispersion interactions between solvent molecules and O₂(¹Δ_g) and O₂(³Σ_g⁻), respectively. It was shown that the application of the London equation leads, in this particular case, to a linear correlation of $\Delta\nu_{00}$ with P with negative slope if the molecular polarizability of O₂ is larger in the ¹Δ_g state than in the ³Σ_g⁻ ground state.⁹⁷ However, Poulsen et al. demonstrated by ab initio calculations that this assumption does not hold true, neither for the isolated nor for the solvated O₂ molecule, thus withdrawing the basis of the dispersion model.¹⁰⁰ In fact, for most molecules, excited-state polarizabilities are larger than those for the ground state. However, O₂ differs from these molecules with respect to its degenerate antibonding $\pi_{g,x}$ and $\pi_{g,y}$ orbitals filled with two electrons. According to Poulsen et al., one electron is in each of the $\pi_{g,x}$ and $\pi_{g,y}$ MOs in the ³Σ_g⁻ ground state, whereas both

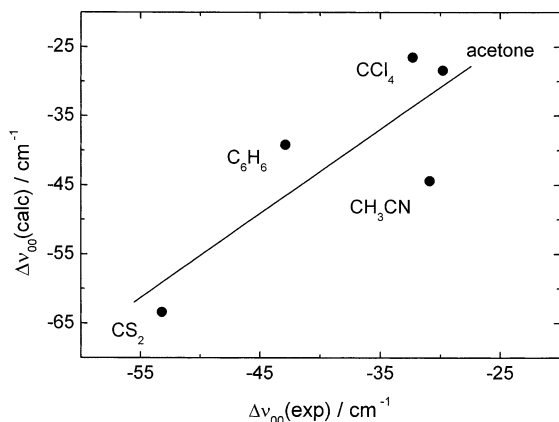


Figure 8. Plot of calculated versus experimental differences $\Delta\nu_{00} = \nu_{00} - \nu_{00}^g$ for the $a \rightarrow X$ emission in different solvents. Data from Poulsen et al.¹⁰¹

electrons are in the same orbital (either $\pi_{g,x}$ or $\pi_{g,y}$) in the ${}^1\Delta_g$ state, causing the larger polarizability of the ground state.¹⁰⁰

Extending their theoretical work, Poulsen et al. used ab initio methods to investigate the effect of solvent on the $a \rightarrow X$ transition energy.¹⁰¹ Energies had been calculated for binary complexes of oxygen and solvent molecule $S \cdot O_2({}^1\Delta_g)$, being in equilibrium with its surrounding outer solvent, and $S \cdot O_2({}^3\Sigma_g^-)$, being out of equilibrium with the outer solvent (i.e., the Franck–Condon state populated in the $a \rightarrow X$ transition). Values of ν_{00} had been calculated considering $S \cdot O_2$ complexes of different structures. This was achieved by taking weighted averages for a variety of $S \cdot O_2$ orientations. The calculated phosphorescence rate, which depends on the respective $S \cdot O_2$ complex structure, served hereby as the weighting factor. To model the solvation of $S \cdot O_2$ complexes, the solvent was regarded as a homogeneous dielectric medium which surrounds a spherical cavity containing the solute, and which is characterized by its static and optical dielectric constants ϵ , and n^2 . It was shown that the complex energies depend principally on the quadrupolar and higher order coupling terms between the complex and the outer solvent, and only minimally on the dipolar coupling term and on dispersion interactions. Figure 8 shows the good correlation of calculated and experimental red-shifts obtained.

It was concluded that the empirical correlations between experimental $a \rightarrow X$ spectral shifts and the solvent polarizability cannot be ascribed solely to a dispersion interaction, but rather they simply reflect the general importance of the solvent's electronic response in the oxygen–solvent interaction.¹⁰¹ Thus, a rather high level of understanding of the collision-induced radiative transitions of O_2 has been achieved also with respect to the small spectral shifts.

2. Radiationless Deactivation

The most important effect of perturbations of the singlet-excited O_2 molecule is the opening of the door to very effective radiationless deactivation processes. Hereby, different mechanisms compete. These are, in the order of increasing rate, a rather strange and almost unique electronic-to-vibrational energy trans-

fer (which is independent of charge-transfer interactions), charge-transfer induced quenching, and common electronic energy transfer.

3. Radiationless Deactivation: Electronic-to-Vibrational Energy Transfer

Electronic-to-vibrational (e–v) energy transfer is a general deactivation process of $O_2({}^1\Sigma_g^+)$ and $O_2({}^1\Delta_g)$, which converts electronic excitation energy of the O_2 molecule into vibration of O_2 and quencher and occurs with any di- or polyatomic collider in the gas or liquid phase. e–v deactivation is observed in its pure form with quenchers of high oxidation potential and sufficiently high triplet-state energy, for which charge-transfer (CT)-induced quenching or electronic energy transfer is impossible. In most liquids, the lifetimes of $O_2({}^1\Sigma_g^+)$ and $O_2({}^1\Delta_g)$ are limited by e–v deactivation. This is why the mechanism of this particular deactivation process has been explored during systematic studies of the $O_2({}^1\Delta_g)$ lifetime τ_Δ in solution.

a. Variation of the $O_2({}^1\Delta_g)$ Lifetime. Early investigations of the deactivation of $O_2({}^1\Delta_g)$ were performed in the gas phase. The experimental methods, results, and interpretations were discussed in detail in a comprehensive review by Wayne.¹⁰² It was found that $O_2({}^1\Delta_g)$ is quenched in bimolecular collisions with very small rate constants k_Q^Δ . In fact, the values of k_Q^Δ were often found to be at the lower limit of the experimental technique used, leading partially to strongly scattering results.

Two factors contribute to the relative inefficiency of the deactivation processes. (i) The $O_2({}^1\Delta_g)$ excitation energy has to be converted into vibrational, rotational, and translational energy of the quenching products. This explains why rare gas colliders such as Ar, Kr, and Xe, with second-order rate constants $k_Q^\Delta = 5\text{--}20 \text{ M}^{-1} \text{ s}^{-1}$, are the weakest quenchers of $O_2({}^1\Delta_g)$.¹⁰³ (ii) The $O_2({}^1\Delta_g) \rightarrow O_2({}^3\Sigma_g^-)$ deactivation is spin-forbidden for quenchers with singlet multiplicity. Actually, quenchers with doublet (NO, NO₂) or triplet (O_2) multiplicity seem to have larger rate constants than comparable singlet molecules.¹⁰² H_2 ($k_Q^\Delta = 2800 \text{ M}^{-1} \text{ s}^{-1}$), H_2O (~ 4900), NH_3 (2600), and C_6H_6 (3200) are the most efficient singlet-state quenchers, and this is related with the fact that all are hydrides with high vibrational frequencies which can act as good accepting modes. Thus, an e–v deactivation of $O_2({}^1\Delta_g)$ was assumed to take place. However, a quantitative model describing the graduations of k_Q^Δ found with different colliders has not been developed on the small basis of gas-phase data.

First determinations of singlet oxygen lifetimes τ_Δ in solution were performed by indirect chemical methods, since detectors that were sufficiently sensitive to monitor the very weak $a \rightarrow X$ phosphorescence were still lacking. The techniques and the underlying chemical kinetics are described in a review by Wilkinson and Brummer.¹⁰⁴ Young et al. used the stationary photo-oxygenation of 1,3-diphenylisobenzofuran in the presence of varying amounts of the physical $O_2({}^1\Delta_g)$ quencher β -carotene to obtain the product $\tau_\Delta k_Q^\Delta$.¹⁰⁵ Assuming k_Q^Δ for β -carotene to be

diffusion-controlled, as was suggested by Foote (see section III.B.5).¹⁰⁶ they estimated $\tau_{\Delta} = 5.5 \mu\text{s}$ in methanol, which is not far from the actual value, $9.5 \mu\text{s}$.⁵⁷ With the advent of pulsed lasers, the chemical method was improved mainly by Adams and Wilkinson,¹⁰⁷ Young et al.,¹⁰⁸ and Merkel and Kearns.¹⁰⁹ Merkel and Kearns discovered a large variation of τ_{Δ} with solvent which—according to their results—extends from $2 \mu\text{s}$ in H_2O to $700 \mu\text{s}$ in CCl_4 .¹¹⁰ In D_2O , $\tau_{\Delta} = 20 \mu\text{s}$ was determined. Thus, a strong H–D isotope effect ($\tau_{\Delta,\text{D}}/\tau_{\Delta,\text{H}} = 10$) on τ_{Δ} was observed with water but, surprisingly, not with acetone. The authors explained the solvent effect on τ_{Δ} by a Förster-type dipole–dipole energy transfer from $\text{O}_2(^1\Delta_{\text{g}})$ into appropriate overtones of solvent vibrations involving the hydrogen and deuterium atoms. This theoretical treatment leads to a correlation of τ_{Δ} with the solvent optical densities (ODs) at the wavelengths of the $(0 \rightarrow 0)$ and $(0 \rightarrow 1)$ $a \rightarrow X$ transitions, 1269 and 1592 nm, according to eq 23, where the higher terms were neglected in the first approximation. The OD factors in eq 23 are related to the Franck–Condon factors of the $(0 \rightarrow 0)$ and $(0 \rightarrow 1)$ vibronic transitions of O_2 .

$$1/\tau_{\Delta} \approx 0.5(\text{OD}_{1269}) + 0.05(\text{OD}_{1592}) + \text{higher terms} \quad (23)$$

This rather successful approach, which described the isotope effect in water and the apparently missing isotope effect in acetone, was adopted by others and expanded in attempts to improve the correlation by substituting the terms of eq 23 by the integrated overlap of the $(0 \rightarrow 0)$ and $(0 \rightarrow 1)$ $a \rightarrow X$ emission bands and the corresponding solvent absorption bands.¹¹¹ However, Ogilby and Foote soon found that a large H–D isotope effect ($\tau_{\Delta,\text{D}}/\tau_{\Delta,\text{H}} = 16$) exists also in acetone, thus throwing doubt on the theory put forth by Kearns.¹¹²

In the late 1970s and early 1980s, the direct spectroscopic detection of $\text{O}_2(^1\Delta_{\text{g}})$ became possible due to the development of NIR-sensitive photomultipliers and Ge diodes, first in Russia and then in the United States, enabling the easier and more accurate determination of τ_{Δ} by time-resolved^{54–56,60,61,113–116} and stationary studies.¹¹⁷ Much longer lifetimes^{54,56,60,117} and strong H–D isotope effects $\tau_{\Delta,\text{D}}/\tau_{\Delta,\text{H}}$ were observed in CHCl_3 (3.61×22^{117}), CH_3CN ($7.61 \times 11.116 \times 22^{117}$), acetone ($13.61,115 \times 15.116 \times 20^{117}$), and C_6H_6 ($21.61,116 \times 27^{117}$), thus finally invalidating the model proposed by Kearns. Ogilby and Foote discussed the failure of the theory and tried different correlations of $1/\tau_{\Delta}$ with linear combinations of solvent OD values at the wavelengths of the $(0 \rightarrow 0)$, $(0 \rightarrow 1)$, and $(0 \rightarrow 2)$ $a \rightarrow X$ transitions, similar to eq 23, but a quantitative description of the data was not possible.¹¹⁸ They concluded that Kearns's attempt to correlate transition probabilities with NIR optical densities was, in fact, a pioneering effort but still an oversimplification of a very complex problem.

A further step on the way to understanding the solvent effect on the $\text{O}_2(^1\Delta_{\text{g}})$ lifetime was taken by Rodgers, who determined values of τ_{Δ} in nine n -alkanes, ten n -alcohols, and in H_2O , CH_3CN , CH_3OH , C_6H_6 , and their perdeuterated derivatives, as well as in 15 different alkanes, alcohols, ethers, and chloro-

Table 3. Incremental Rate Constants for Bond Groupings^a

group	$k, \text{M}^{-1} \text{s}^{-1}$	group	$k, \text{M}^{-1} \text{s}^{-1}$
CH_3	550	OH	2290
CD_3	15	OD	165
CH_2	813	C=O	100
CH^b	90	CN	65

^a Data from Rodgers.¹¹⁹ ^b Aliphatic.

hydrocarbons as reference solvents.¹¹⁹ Second-order rate constants $k_{\text{Q}}^{\Delta} = 1/\tau_{\Delta}[\text{S}]$ of $\text{O}_2(^1\Delta_{\text{g}})$ quenching by solvent molecules S were calculated. Experiments with binary solvent mixtures of components A and B demonstrated that the variation of τ_{Δ} with mixture composition could actually be calculated with high accuracy from these data by using eq 24.

$$1/\tau_{\Delta} = k_{\text{Q,A}}^{\Delta}[\text{A}] + k_{\text{Q,B}}^{\Delta}[\text{B}] \quad (24)$$

It was found that the $1/\tau_{\Delta}$ values for both homologous series of n -alkanes and n -alcohols display a parallel dependence on the number of methylene groups. The systematic evaluation of the extensive data set yielded the incremental rate constants of $\text{O}_2(^1\Delta_{\text{g}})$ quenching by molecular groupings listed in Table 3, which can be used to calculate lifetimes τ_{Δ} in pure liquids with high accuracy.¹¹⁹ The study reported by Rodgers was very fruitful, not only because of its practical utility, but also because it was shown that the deactivation of $\text{O}_2(^1\Delta_{\text{g}})$ is a bimolecular process also in the liquid phase.

The next important step toward the understanding of the deactivation of $\text{O}_2(^1\Delta_{\text{g}})$ was achieved by Hurst and Schuster.¹²⁰ These authors determined τ_{Δ} in a variety of carefully selected solvents, e.g., in the series $\text{C}_6\text{H}_5\text{X}$ and $\text{C}_6\text{D}_5\text{X}$ ($\text{X} = \text{F}, \text{Cl}, \text{Br}, \text{I}$), in $\text{C}_6\text{H}_n\text{F}_{6-n}$ ($0 \leq n \leq 6$), in C_6D_6 , $\text{C}_2\text{D}_5\text{OD}$, CD_3OD , D_2O , CD_3CN , and CDCl_3 , and in acetone- d_6 . Hereby, they observed that, in halogenated solvents, the values of τ_{Δ} decrease with increasing power of the excitation pulse. Similar observations had been reported earlier with weakly $\text{O}_2(^1\Delta_{\text{g}})$ deactivating solvents.^{61,116,118} This effect was assumed to be caused by photochemically produced quenchers of $\text{O}_2(^1\Delta_{\text{g}})$ and sets upper experimental limits for τ_{Δ} values to be determined with accuracy in laser pulse experiments. The complications due to the power dependence could be reduced if values of τ_{Δ} are extrapolated to the limit of zero laser power.¹²⁰

In the series $\text{C}_6\text{H}_n\text{F}_{6-n}$, Hurst and Schuster found a linear increase of $1/\tau_{\Delta}$ with the molar concentration of hydrogen atoms, which is consistent with a constant incremental second-order rate constant k_{CH}^{Δ} of $\text{O}_2(^1\Delta_{\text{g}})$ quenching by a single C–H bond, irrespective of the number of fluorine atoms per benzene. Thus, it appeared that it is some specific property of the C–H bonds that determines the quenching ability of these solvents, and that donor–acceptor interactions of the solvent with $\text{O}_2(^1\Delta_{\text{g}})$ play little or no role. A similar evaluation yielded the rate constant k_{CD}^{Δ} of quenching by a single C–D bond. The ratio $k_{\text{CH}}^{\Delta}/k_{\text{CD}}^{\Delta} = 25$ was obtained as a H–D isotope effect.

Efforts have been made to investigate whether the absence or presence of atoms with nuclear spin in

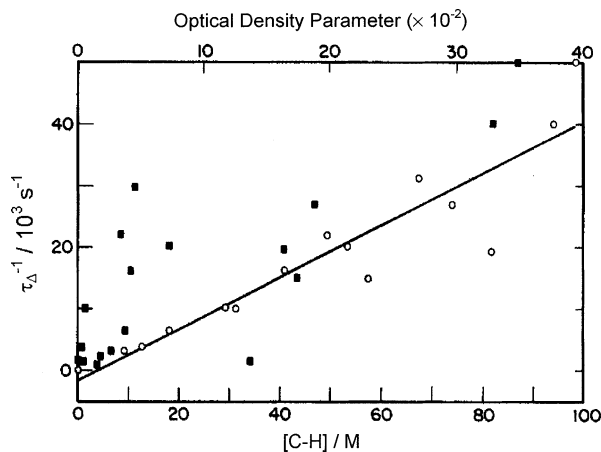


Figure 9. Plot of inverse $O_2(^1\Delta_g)$ lifetimes, $1/\tau_\Delta$, versus molar concentration of solvent C–H bonds (○, lower scale), and versus the Kearns OD parameter, see eq 23 (■, upper scale). Reprinted with permission from ref 120. Copyright 1983 American Chemical Society.

the solvent or oxygen molecules influences the radiationless deactivation of $O_2(^1\Delta_g)$. However, no effects have been found, neither in experiments with $^{17}O_2$ - or $^{18}O_2$ -enriched $O_2(^1\Delta_g)$, nor by applying external magnetic fields as high as 4800 G during lifetime measurements.¹²⁰ It was suggested that these observations eliminate the nuclear spin difference between hydrogen and deuterium atoms as the cause of their different quenching efficiencies. Furthermore, the temperature dependence of τ_Δ was examined in several solvents. Only weak effects were observed, in agreement with earlier findings reported by Ogilby and Foote.¹¹⁸ Finally, a small but significant heavy-atom effect was found to promote the spin-forbidden deactivation of $O_2(^1\Delta_g)$. The values of τ_Δ decreased for C_6D_5X in the series $X = Cl, Br, \text{ and } I$ from 1.2 to 0.81 and 0.28 ms.¹²⁰

Hurst and Schuster found strong linear correlations between $1/\tau_\Delta$ and the molar concentrations of C–H bonds or C–D bonds, respectively.¹²⁰ They interpreted the general H–D isotope effect on $1/\tau_\Delta$, in agreement with others, as a consequence of an e–v energy-transfer mechanism.^{110,118} But, in contrast to Merkel and Kearns, they proposed an e–v energy transfer which is independent of the optical transition moments of the solvent.¹²⁰ A similar idea was already proposed but not consequently followed by Ogilby and Foote, who considered that perhaps Raman- and IR-active vibrational modes together may correlate better with the observed lifetimes than IR optical densities alone.¹¹⁸

Hurst and Schuster plotted the values of $1/\tau_\Delta$ versus [C–H] (○, lower scale), and versus Kearns's OD parameter (■, upper scale, see Figure 9).¹²⁰ The line is the least-squares fit to [C–H]. Neither parameter predicts the observed lifetime with absolute certainty. However, it is clear that the correlation with [C–H] is the superior of the two. Of course, both parameters are related. The higher the concentration of carbon–hydrogen bonds, the greater the OD of the C–H overtone frequencies at 1269 and 1592 nm. The OD parameters, however, also include a factor derived from the magnitude of the transition dipole

moment, and it is the inclusion of this part that appears to weaken the observed correlation.¹²⁰

This result was in direct conflict with the predictions based on the dipole–dipole energy-transfer model. Exchange energy transfer depends, similarly to dipole–dipole energy transfer, on the overlap of vibronic wave functions of donor and acceptor molecules but not on the optical transition moments. Therefore, Hurst and Schuster assumed that $O_2(^1\Delta_g)$ deactivation takes place via an e–v deactivation mechanism which, similarly to an exchange energy-transfer mechanism, should be initiated by the repulsive interaction of $O_2(^1\Delta_g)$ and solvent molecules, coupling the highest frequency mode of the solvent with a vibronic transition of $O_2(^1\Delta_g)$. They derived eq 25, where k_{XY}^Δ is the second-order rate constant of

$$k_{XY}^\Delta = C_\Delta \sum_{mn} F_m F'_n R_{mn} \quad (25)$$

$O_2(^1\Delta_g)$ deactivation by bond X–Y, C_Δ is a solvent-independent term containing the electronic coupling matrix elements, F_m and F'_n are the Franck–Condon factors for the coupled $^1\Delta_g$, $v = 0 \rightarrow ^3\Sigma_g^-, v = m$ vibronic transition of O_2 and the $v = 0 \rightarrow v = n$ vibrational transition of bond X–Y, and R_{mn} is the off-resonance factor related to the energy mismatch E_{mn} between the two transitions. R_{mn} should be large for resonant transitions but small for large off-resonance energies.

For several X–Y bonds with differing energies E_{XY} of the highest frequency mode, the following rate constants k_{XY}^Δ for $O_2(^1\Delta_g)$ deactivation have been evaluated: for O–H, 3500 cm^{-1} , 2000 $M^{-1} s^{-1}$; for C–H, 3050 cm^{-1} , 420 $M^{-1} s^{-1}$; for O–D, 2550 cm^{-1} , 150 $M^{-1} s^{-1}$; and for C–D, 2240 cm^{-1} , 17 $M^{-1} s^{-1}$.¹²⁰ A strong monotonic but not linear decrease of k_{XY}^Δ with decreasing E_{XY} was found.

Using the model outlined above, and neglecting overtone excitations ($v = 0 \rightarrow v' = n$, with $n > 1$) of the energy-accepting mode of X–Y, Hurst and Schuster qualitatively explained the strong graduation of k_{XY}^Δ for $O_2(^1\Delta_g)$. The predictions from their model could be summarized in a simple way: the greater the energy of the highest frequency vibrational mode of the solvent, the nearer to resonance is a $O_2(^1\Delta_g)$ vibronic transition with a large Franck–Condon factor.¹²⁰ This work proved to be a milestone in the development of a quantitative and general e–v deactivation model.

However, the extension of the work of Hurst and Schuster required accurate values of τ_Δ in weakly $O_2(^1\Delta_g)$ deactivating solvents, which were not accessible with high-power laser excitation. A reduction of the energy and power of the excitation pulses by factors of 10^3 and 10^9 compared with the previous experiments was achieved by Schmidt and Brauer, who used the radiation of a mercury arc lamp which was spectrally resolved and chopped to 10-ms pulses.¹²¹ Lifetimes up to about 100 ms were determined in perhalogenated solvents. Further values of k_{XY}^Δ were derived by using eq 26, with N_{XY} being the number of times a particular terminal bond X–Y

occurs per solvent molecule, considering also the radiative deactivation path by $k_Q^\Delta = (1/\tau_\Delta - k_{a-x})/[S]$.

$$k_Q^\Delta = \sum_{XY} N_{XY} k_{XY}^\Delta \quad (26)$$

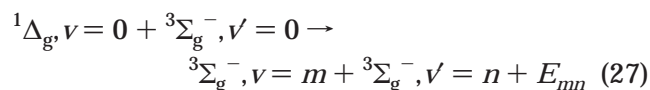
A strong linear correlation was found between $\log(k_{XY}^\Delta)$ and the energy E_{XY} of the highest frequency vibrational mode, i.e., the stretching vibration of terminal bond X–Y. The value of k_{XY}^Δ increases by about 4 orders of magnitude on going from C–Cl to O–H.¹²¹ The validity of these results was confirmed by Aubry et al.,¹²² who showed that the values $k_{ND}^\Delta = 84 \text{ M}^{-1} \text{ s}^{-1}$ and $k_{NH}^\Delta = 1530 \text{ M}^{-1} \text{ s}^{-1}$, determined from $\tau_\Delta = 212 \mu\text{s}$ (formamide-*d*₃) and $11.5 \mu\text{s}$ (formamide), excellently fit to the correlation of $\log(k_{XY}^\Delta)$ with E_{XY} .

Schmidt used sensitive equipment to study the effect of heavy-atom colliders on the spin-forbidden e–v deactivation of $\text{O}_2(^1\Delta_g)$ in greater detail.¹²³ It was supposed that, in the previous investigation with $\text{C}_6\text{D}_5\text{X}$ (X = Cl, Br, or I), the heavy-atom effect was eventually damped by the still rather strong deactivation by C–D bonds. Therefore, the study concerned mainly perhalogenated solvents with chlorine, bromine, and iodine substituents, for which particularly long lifetimes $25 \text{ ms} \leq \tau_\Delta \leq 110 \text{ ms}$ could actually be determined. It was found that the linear decrease of $\log(k_{XY}^\Delta)$ with decreasing E_{XY} holds true only for light-atom bonds in the series O–H to C–F. However, for aliphatic bonds C–F ($E_{XY} = 1250 \text{ cm}^{-1}$), C–Cl (800), C–Br (660), and C–I (560), the values of k_{XY}^Δ increase from 0.13 to 0.23 to 0.87 and $3.93 \text{ M}^{-1} \text{ s}^{-1}$, despite the further decrease of E_{XY} . Obviously, two opposite effects on k_{XY}^Δ are superposed in this series with increasing atomic weight of terminal atom: the frequency dependence, which causes k_{XY}^Δ to decrease, and the heavy-atom effect, which leads to larger isc probabilities and thus to larger values of k_{XY}^Δ . After removal of the masking frequency effect by use of the empirical correlation $\log(k_{XY}^\Delta)$ with E_{XY} , a very strong graduation of the isc probability of 1:16:130:950 resulted for the series C–F, C–Cl, C–Br, and C–I, which is typical for an internal heavy-atom effect. This finding indicates that e–v deactivation occurs in a collision complex of $\text{O}_2(^1\Delta_g)$ and the terminal atom of bond X–Y, under partial penetration of the electron clouds.¹²³

Krasnovsky and co-workers first applied the single-photon-counting technique to detect the $a \rightarrow X$ phosphorescence in H_2O .¹²⁴ The sensitizer was excited by a copper vapor laser with a 10-kHz repetition rate. About 10^7 laser shots were required to accumulate the extremely weak emission. However, this was a rewarding effort, since the biexponential rise and decay curve of $\text{O}_2(^1\Delta_g)$ with time constants τ_Δ and sensitizer triplet-state lifetime τ_T could be accurately evaluated. Measurements were performed varying the O_2 partial pressure from 1 to 15 bar, and $1/\tau_T$ was found to be proportional to $[\text{O}_2]$, whereas $\tau_\Delta = 3.1 \mu\text{s}$ remained constant. This number sets the lower limit of τ_Δ in neat solvents.¹²⁴

Pure, natural O_2 (99.8% $^{16}\text{O}_2$) acts, in the gas phase and in the liquid phase, as a rather strong quencher

of $^{16}\text{O}_2(^1\Delta_g)$, with rate constants $^{16}k_Q^\Delta = 1020 \text{ M}^{-1} \text{ s}^{-1}$ (gaseous O_2 , 295 K)⁹³ and $640 \text{ M}^{-1} \text{ s}^{-1}$ (liquid O_2 , 77 K).¹²⁵ Deactivation of $^{18}\text{O}_2(^1\Delta_g)$ by ground-state $^{18}\text{O}_2$, however, proceeds at 295 K with the much slower rate constant $^{18}k_Q^\Delta = 6 \text{ M}^{-1} \text{ s}^{-1}$, as was shown by Maier and co-workers.⁹³ The surprisingly large isotope effect on the collisional deactivation of $\text{O}_2(^1\Delta_g)$ in pure O_2 was quantitatively described by a model which considers the six possible coupled transitions, $0 \leq m \leq 5$, of eq 27, with $n = 5 - m$, and the corresponding changes in the off-resonance energies E_{mn} if one switches from pure $^{16}\text{O}_2$ to pure $^{18}\text{O}_2$.



Due to the slightly smaller frequency of the fundamental vibrational mode of $^{18}\text{O}_2$ (1467 versus 1556 cm^{-1} for $^{16}\text{O}_2$), values of E_{mn} are $\sim 400 \text{ cm}^{-1}$ larger for each of the coupled transitions of $^{18}\text{O}_2$. Since E_{mn} has to be transformed into rotational and translational energy for the diatomic quencher O_2 , the small changes in E_{mn} are sufficient to cause the very strong isotope effect, $^{16}k_Q^\Delta/^{18}k_Q^\Delta = 170$.^{93,125} The quantitative evaluation further demonstrated that the coupled transitions $m = 3, n = 2$ and $m = 2, n = 3$ of eq 27 have the highest probability. These interesting investigations show that overtone excitations of accepting modes are very important for the e–v deactivation of $\text{O}_2(^1\Delta_g)$ by diatomic molecules.

If quenching of $\text{O}_2(^1\Delta_g)$ by O_2 occurs in solvents consisting of polyatomic molecules, the picture could be quite different. Collision complexes of O_2 and a solvent molecule could provide suitable accepting modes for the off-resonance energy, leading to significantly larger rate constants $^{16}k_Q^\Delta$ and $^{18}k_Q^\Delta$ and a much smaller oxygen isotope effect. This question was studied by Afshari and Schmidt, who investigated the quenching of $\text{O}_2(^1\Delta_g)$ by O_2 for both $^{16}\text{O}_2$ and $^{18}\text{O}_2$ in a series of perhalogenated solvents at room temperature.¹²⁶ The strong isotope effect of $^{16}k_Q^\Delta/^{18}k_Q^\Delta = 70$ was determined in perfluorodecalin and was interpreted to be in accordance with the e–v deactivation model proposed by Meier.⁹³ Thus, solvent molecules were not assumed to support quenching by O_2 . The investigation also showed that the presence of O_2 in air-saturated perhalogenated solvents leads to in part strongly reduced singlet oxygen lifetimes.¹²⁶ This is illustrated by the data shown in Table 4, comparing lifetimes $^{16}\tau_\Delta$ determined in air-saturated solvents with values of $^{16}\tau_\Delta$ and $^{18}\tau_\Delta$ obtained at $[\text{O}_2] \leq 10^{-5} \text{ M}$.⁵⁷

These results demonstrate that, after removal of the quenching effect of the experimentally necessary contaminants O_2 and sensitizer, extremely long lifetimes are obtained, which should be limited only by e–v deactivation to the solvent, and therefore should be the correct basis for calculation of k_{XY}^Δ . The reduction of $^{16}\tau_\Delta$ in air-saturated solution by O_2 quenching decreases when $^{16}\tau_\Delta$ becomes smaller, as is shown by the results in Table 5, which lists lifetimes for strongly deactivating solvents. A comprehensive compilation of lifetimes τ_Δ was published by Wilkinson et al.^{17,18}

Table 4. Lifetimes of $^{16}\text{O}_2(^1\Delta_g)$ and $^{18}\text{O}_2(^1\Delta_g)$ in Weakly Deactivating Solvents^a

solvent	$^{16}\tau_{\Delta}$, ms ^b	$^{16}\tau_{\Delta}$, ms ^c	$^{18}\tau_{\Delta}$, ms ^c	$^{18}\tau_{\Delta}/^{16}\tau_{\Delta}$
CDCl_3	7.0	8.9	12.2	1.4
C_6F_6	21	30	45	1.5
$\text{C}_6\text{F}_{13}\text{I}$	25	53		
CS_2	45	79	119	1.5
$\text{C}_2\text{Br}_2\text{F}_4$	31	111	174	1.6
CCl_4	59	128	180	1.4
$\text{C}_2\text{Cl}_3\text{F}_3$	72	133	207	1.6
C_6F_{14}	68	214	271	1.3
$\text{C}_{10}\text{F}_{18}$	59	309	463	1.5

^a Data from Schmidt and Afshari.^{57,126} ^b Air-saturated. ^c $[\text{O}_2] \leq 10^{-5}$ M; sensitizer phenalene $\leq 10^{-5}$ M.

Table 5. Lifetimes of $^{16}\text{O}_2(^1\Delta_g)$ and $^{18}\text{O}_2(^1\Delta_g)$ in Strongly Deactivating Solvents^a

solvent	$^{16}\tau_{\Delta}$, μs ^b	$^{18}\tau_{\Delta}$, μs ^c	$^{18}\tau_{\Delta}/^{16}\tau_{\Delta}$
H_2O	3.1 ^d	3.1 ^e	1.00
CH_3OH	9.5	9.5	1.00
C_6H_{14}	23.4	26.4	1.13
C_6H_6	30.0	38.3	1.28
C_5H_{12}	34.7	40.3	1.16
$(\text{CH}_3)_2\text{CO}$	51.2	60.8	1.19
D_2O	68	68	1.00
CH_3CN	77.1	92.9	1.20
CH_2Cl_2	99	128	1.29
CHCl_3	229	294	1.28
C_2HCl_3	247	347	1.40
C_6D_6	681	795	1.17
$(\text{CD}_3)_2\text{CO}$	992	994	1.00

^a Data from Schmidt and Afshari.⁵⁷ ^b Air-saturated. ^c Partial pressure of $^{18}\text{O}_2 \approx 0.5$ bar. ^d Reference 119. ^e Value calculated with experimentally determined isotope effect 1.00 and $^{16}\tau_{\Delta} = 3.1 \mu\text{s}$.

The data in Tables 4 and 5 reveal the tremendous variation of the singlet oxygen lifetime which has been discovered stepwise over two decades, from the early work of Merkel and Kearns^{109,110} to the more recent results,^{57,124,126} and which covers 5 orders of magnitude. Tables 4 and 5 also list the isotope effects on the $\text{O}_2(^1\Delta_g)$ lifetimes which were determined by Schmidt and Afshari with the intention of finding out whether overtone excitations of accepting modes are important for the e–v deactivation of $\text{O}_2(^1\Delta_g)$ by polyatomic molecules.⁵⁷

Figure 10 illustrates their idea by means of the potential energy curves of the $^3\Sigma_g^-$ and $^1\Delta_g$ states of O_2 and the ground-state potential curve of C–H as deactivating bond X–Y. The corresponding vibrational levels are also shown and are split into halves for O_2 : the left one corresponds to $^{16}\text{O}_2$ and the right one to $^{18}\text{O}_2$. Since only very weak temperature effects have been determined for e–v deactivation,^{118,120,127,128} only exothermic deactivation paths should be relevant. Two different possible coupled transitions of $\text{O}_2(^1\Delta_g)$ and C–H are shown for the two isotopomers. With respect to overtone $n = 2$ excitation of C–H with transition energy $E_{XY,n}$ only the vibronic transitions of $\text{O}_2(^1\Delta_g)$, with transition energies $E_{O_2,m}$ leading to the $m = 0$ or 1 levels, are exothermic. Due to its larger mass, a closer vibrational spacing results for $^{18}\text{O}_2$. Therefore, the transition energies $E_{O_2,m}$ are always larger for $^{18}\text{O}_2$ than for $^{16}\text{O}_2$, and correspondingly larger off-resonance energies $E_{mn} = E_{O_2,m} - E_{XY,n}$ result for $^{18}\text{O}_2$. Figure 10 displays the $0 \rightarrow 1$

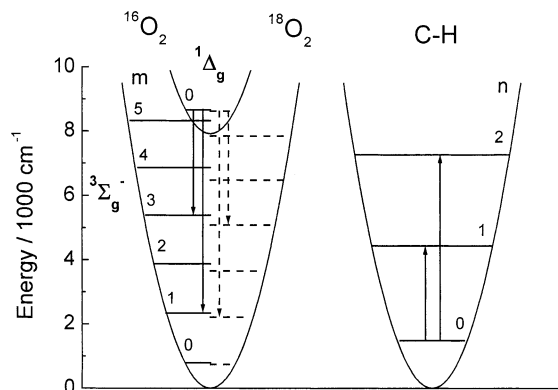
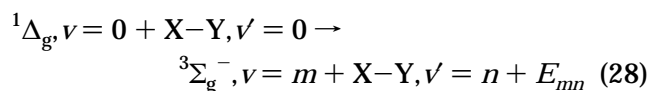


Figure 10. O_2 isotope effect on the e–v deactivation of $\text{O}_2(^1\Delta_g)$ by C–H. Coupled transitions to $m = 3$, $n = 1$ and to $m = 1$, $n = 2$ for $^{16}\text{O}_2$ and $^{18}\text{O}_2$ (broken lines). Lengths of arrows correspond to transition energies $E_{O_2,m}$ and $E_{XY,n}$, respectively. Reprinted with permission from ref 57. Copyright 1992 Deutsche Bunsen-Gesellschaft.

vibronic transition, which has a smaller off-resonance energy for overtone excitation of C–H. Here, E_{mn} is 90 cm^{-1} larger for $^{18}\text{O}_2$ than for $^{16}\text{O}_2$. With respect to the fundamental excitation of C–H, four vibronic transitions, $0 \leq m \leq 3$, are exothermic. The smallest off-resonance energy shown in Figure 10 is associated with the transition to $m = 3$, for which the transition energy $E_{O_2,m}$, and thus also the value of E_{mn} , is 308 cm^{-1} larger for $^{18}\text{O}_2$ than for $^{16}\text{O}_2$. Thus, the e–v deactivation of $^{18}\text{O}_2(^1\Delta_g)$ by C–H should be distinctly slower, and a distinct isotope effect $^{18}\tau_{\Delta}/^{16}\tau_{\Delta}$ should exist, if only the fundamental transition of C–H is excited. However, only a small isotope effect can be expected if the overtone of C–H is excited. Inspection of the data in Tables 4 and 5 reveals a significant but small isotope effect for solvents with C–H and O–H bonds. Therefore, it was concluded that overtone excitations of energy-accepting modes are important in the e–v deactivation of $\text{O}_2(^1\Delta_g)$.⁵⁷

b. Mechanism of e–v Deactivation of $\text{O}_2(^1\Delta_g)$. Hurst and Schuster showed that the solvent dependence of the $\text{O}_2(^1\Delta_g)$ lifetime could be explained qualitatively on the basis of an e–v energy transfer.¹²⁰ A model describing quantitatively the experimental rate constants and such essential findings as (i) the $^{18}\tau_{\Delta}/^{16}\tau_{\Delta}$ isotope effect, (ii) the heavy-atom effect with carbon–halogen bonds, and (iii) the negligible temperature effect was developed by Schmidt and Afshari.⁵⁷ They adopted Schuster's basic idea that e–v deactivation occurs competitively via different coupled transitions, according to eq 28. It should be noted that only terminal bonds X–Y are considered, since only these interact in collisions with O_2 . Furthermore, only stretching vibrations of X–Y were taken into account.^{57,121}



The rate constant $k_{XY}^{\Delta, mn}$ of a single coupled transition was assumed to be the product of the term C_{Δ} , which is proportional to the normalized collision frequency Z and to the matrix element of electronic coupling of the $^1\Delta_g$ and $^3\Sigma_g^-$ states, of the

Franck–Condon factors F_m and F'_n of the vibronic and vibrational transitions of O_2 and bond X–Y, and the off-resonance factor R_{mn} (see eq 29).

$$k_{XY}^{\Delta, mn} = C_{\Delta} F_m F'_n R_{mn} \quad (29)$$

The overall rate constant k_{XY}^{Δ} of deactivation of $O_2(^1\Delta_g)$ by a single terminal bond X–Y is given by eq 30, with n_{\max} being the vibrational quantum number of the highest overtone of X–Y, which can be excited.

$$k_{XY}^{\Delta} = \sum_{m=0}^5 \sum_{n=1}^{n_{\max}} k_{XY}^{\Delta, mn} \quad (30)$$

It was proposed that R_{mn} decreases exponentially with E_{mn} , as shown in eqs 31 and 32, where the constant α is a measure of the ability of the entire quenching molecule to accept the off-resonance energy by low-energy modes. Slightly endothermic transitions were considered by factoring with the Boltzmann term (see eqs 31 and 32).

$$E_{mn} > 0, \text{ exothermic: } R_{mn} = \exp(-\alpha E_{mn}) \quad (31)$$

$E_{mn} < 0$, endothermic:

$$R_{mn} = \exp(\alpha E_{mn} + E_{mn}/(RT)) \quad (32)$$

All data necessary for calculation of the rate constants $k_{XY}^{\Delta, mn}$ of a single channel, characterized by numbers m and n , by using eq 29 have been derived from experimental quantities: F_m for $^{16}O_2$ as well as $^{18}O_2$ from the ratios I_{00}/I_{01} of the $(0 \rightarrow 0)$ and $(0 \rightarrow 1)$ $a \rightarrow X$ emission intensities; $E_{O_2, m}$ from the data reported by Herzberg and the reduced masses of $^{16}O_2$ and $^{18}O_2$; F'_n and the respective transition energies $E_{XY, n}$ from bond dissociation energies D_{XY} and energies $E_{XY, 1}$ of the X–Y fundamental stretching modes.⁵⁷ With these data and eq 30, it is possible to fit calculated rate constants $k_{XY}^{\Delta, C}$ to the experimental values of k_{XY}^{Δ} by variation of only two parameters, the O_2 -specific constant C_{Δ} and the O_2 -independent constant α . The experimental values of k_{XY}^{Δ} for $^{16}O_2$ could quantitatively be described with $C_{\Delta} = 5.5 \times 10^5 \text{ M}^{-1} \text{ s}^{-1}$ and $\alpha = 0.0032 \text{ cm}$, as illustrated in Figure 11.

The value of k_{OH}^{Δ} was changed from 2.2×10^3 to $2.9 \times 10^3 \text{ M}^{-1} \text{ s}^{-1}$ in Figure 11, considering the revised lifetime in H_2O of $\tau_{\Delta} = 3.1 \mu\text{s}$.¹²⁴ The straight line with intercept $i = 0$ and slope $s = 1$ represents identity of experimental and calculated rate constants and describes the variation of the data over 5 orders of magnitude. The linear fit results in $i = -0.08 \pm 0.28$ and $s = 1.05 \pm 0.06$. Since the values of $k_{XY}^{\Delta, C}$ are well described by k_{XY}^{Δ} , of course the strong correlation of $\log(k_{XY}^{\Delta, C})$ with E_{XY} is also reproduced. It was further shown that the heavy-atom effect with carbon–halogen bonds and the isotope effect, which varies from $^{16}k_{OH}^{\Delta}/^{18}k_{OH}^{\Delta} = 1.0$ to $^{16}k_{CBr}^{\Delta}/^{18}k_{CBr}^{\Delta} = 1.9$, are quantitatively reproduced. A detailed inspection of the model demonstrated that overtone excitation of bonds X–Y is generally important. Low isotope effects result for X–Y bonds with large E_{XY} , due to the preference of vibronic transitions of $O_2(^1\Delta_g)$ to m

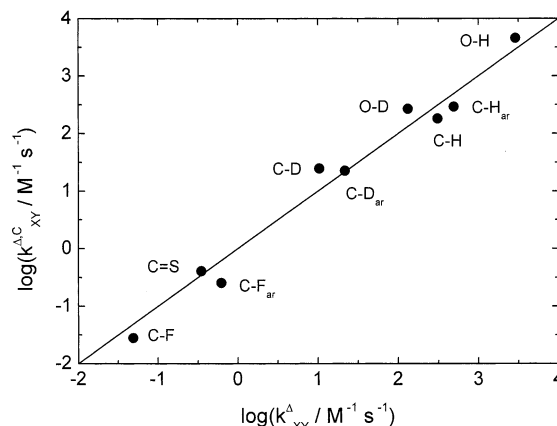


Figure 11. Double-logarithmic plot of calculated rate constants $k_{XY}^{\Delta, C}$ of $^{16}O_2(^1\Delta_g)$ deactivation versus experimental data k_{XY}^{Δ} . Subscript indicates terminal atoms connected with aromatic carbon atoms. Reprinted with permission from ref 57. Copyright 1992 Deutsche Bunsen-Gesellschaft.

$= 0, 1$ when most of the excitation energy is accepted by X–Y. Isotope effects ≥ 1.5 and a distribution over the vibronic transitions $0 \leq m \leq 4$ are calculated for weakly deactivating bonds of small E_{XY} , which take only the smaller part of the $O_2(^1\Delta_g)$ excitation energy in the deactivating collision. Since contributions of endothermic coupled transitions proved to be very small, it was concluded that the very weak temperature effect on k_Q^{Δ} should be caused by the temperature dependence of the collision frequency $Z \sim T^{0.5}$, which leads to an activation energy of $0.5(RT)$, in agreement with the experimental observations.^{118,120,127,128} Thus, a quantitative model of e–v energy transfer was derived to describe the unusual solvent dependence of the singlet oxygen lifetime.⁵⁷

c. Quenching of $O_2(^1\Sigma_g^+)$. The quenching of $O_2(^1\Sigma_g^+)$ is very fast. This is the main reason the deactivation of $O_2(^1\Sigma_g^+)$ could be investigated, for a long time, only in the gas phase. The experimental methods, results, and interpretations are discussed in the review by Wayne.¹⁰² The deactivation of $O_2(^1\Sigma_g^+)$ is 5–6 orders of magnitude faster than the e–v deactivation of $O_2(^1\Delta_g)$. According to Ogryzlo, this difference clearly indicates $O_2(^1\Sigma_g^+) \rightarrow O_2(^1\Delta_g)$ deactivation, since this process has a small energy gap and is spin-allowed.¹²⁹ Actually, Wildt et al. determined an efficiency of ≥ 0.90 for $O_2(^1\Delta_g)$ formation in the deactivation of $O_2(^1\Sigma_g^+)$ in the gas phase.¹³⁰ Second-order rate constants k_Q^{Σ} of quenching of $O_2(^1\Sigma_g^+)$ were determined in the gas phase for a large number of colliders, and deactivation by diatomic molecules was studied in great detail. It was found that k_Q^{Σ} increases from O_2 to H_2 by more than 4 orders of magnitude and correlates reasonably well with E_{XY} , thus pointing to an e–v energy transfer. This process could be induced by long-range interactions (LRIs) between the transition quadrupole of the $O_2(^1\Sigma_g^+) \rightarrow O_2(^1\Delta_g)$ transition and the transition dipole or transition quadrupole of the quencher^{131,132} or, alternatively, by short-range (repulsive) interactions (SRIs).¹³³ In the case of H_2 and HBr , for which complete calculations were carried out, it was shown that both LRIs and SRIs contribute to the quenching

Table 6. Rate Constants k_Q^Σ of Quenching of $O_2(^1\Sigma_g^+)$ Determined in the Gas Phase^a

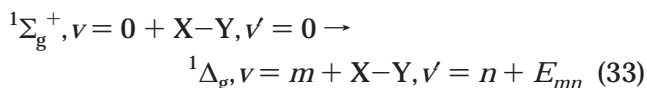
quencher	$k_Q^\Sigma, M^{-1} s^{-1}$	quencher	$k_Q^\Sigma, M^{-1} s^{-1}$
H ₂ O	2.9×10^9	CH ₄	5.0×10^7
NH ₃	8.3×10^8	C ₂ H ₆	2.3×10^8
D ₂ O	3.7×10^8	C ₃ H ₈	2.7×10^8 ^d
H ₂ S	2.6×10^8	C ₄ H ₁₀	3.8×10^8 ^d
CO ₂	1.7×10^8	C ₅ H ₁₂	4.5×10^8 ^d
ND ₃	8.4×10^7 ^b	C ₆ H ₁₄	5.5×10^8 ^d
NO ₂	1.5×10^7	C ₇ H ₁₆	6.0×10^8 ^d
CS ₂	1.7×10^6 ^c	C ₆ H ₆	3.9×10^8 ^e
SO ₂	1.1×10^6	CD ₄	4.0×10^7 ^b
SF ₆	9.0×10^5 ^c	C ₂ D ₆	1.0×10^8 ^c
CCl ₄	2.7×10^5 ^c	CF ₄	1.6×10^6 ^c
		C ₂ F ₆	1.9×10^6 ^c

^a Numbers without citation are average values evaluated in ref 149. ^b Reference 147. ^c Reference 143. ^d Reference 148. ^e Reference 139.

process, which leads, for H₂ and HBr, to excitation of the first and second vibrational levels, respectively.¹³² These are the dominant processes because they are almost resonant, i.e., all the electronic energy can be taken up in a combination of easily excited vibrational modes and allowed rotational transitions. The poor quenchers, such as N₂ and especially O₂, have vibrational levels which do not match the more favorable vibronic O₂(¹Σ_g⁺) → O₂(¹Δ_g) transitions. No calculations on the quenching of O₂(¹Σ_g⁺) by polyatomic molecules have been published; however, the experimental findings were interpreted qualitatively to indicate spin-allowed e−v deactivation.¹²⁹ Table 6 lists average values of k_Q^Σ for polyatomic quenchers which were evaluated from literature data.^{134–149}

The values of k_Q^Σ show an enormous variation, ranging from 2.7×10^5 (CCl₄) to 2.9×10^9 M^{−1} s^{−1} (H₂O). They decrease in the series C_nH_{2n+2}, C_nD_{2n+2}, C_nF_{2n+2}, and in each series with decreasing number *n*. These graduations strongly indicate that the same e−v energy-transfer mechanism takes place in deactivation of O₂(¹Δ_g) and O₂(¹Σ_g⁺).¹⁴⁹

d. Mechanism of e−v Deactivation of O₂(¹Σ_g⁺). The gas-phase data set of Table 6 was analyzed by Schmidt, as done previously with the data for the e−v deactivation of O₂(¹Δ_g).^{57,149} Rate constants k_{XY}^Σ were calculated to increase exponentially with E_{XY} . Equation 33 holds for the coupled transitions of O₂(¹Σ_g⁺) and deactivating bond X−Y.



The rate constant $k_{XY}^{\Sigma, mn}$ of a single coupled transition could be calculated by using eq 29 after substituting C_Δ by C_Σ , which is proportional to *Z* and to the matrix elements of the electronic coupling of the ¹Σ_g⁺ and ¹Δ_g states. Deactivation of O₂(¹Σ_g⁺) leads to only the vibrational levels 0 ≤ *m* ≤ 3 of O₂(¹Δ_g), due to the smaller energy gap. Using eq 30 with the corresponding changes, along with eqs 31 and 32, and the values of F_m , F'_m , and the O₂-independent constant $\alpha = 0.0032$ cm (derived earlier for the e−v deactivation of O₂(¹Δ_g)),⁵⁷ rate constants $k_{XY}^{\Delta, C}$ could

be fitted to experimental values of k_{XY}^Σ by variation of only *one* parameter, the constant C_Σ . A very good fit was obtained with $C_\Sigma = 8.8 \times 10^9$ M^{−1} s^{−1}, proving that the same e−v energy transfer operates for O₂(¹Δ_g) and O₂(¹Σ_g⁺). Hence, for the first time, a consistent model could be established for the gas-phase deactivation of O₂(¹Σ_g⁺).¹⁴⁹ It should be noted that, in contrast to deactivation of O₂(¹Δ_g), no heavy-atom effect was found for O₂(¹Σ_g⁺) deactivation, in accordance with the spin-allowed character of the latter process.

The first quantitative investigations of the O₂(¹Σ_g⁺) deactivation in solution were performed by Wang and Ogilby, who monitored the intensity of the *b* → *a* fluorescence without time resolution in CCl₄ at 1935 nm.¹⁵⁰ O₂(¹Σ_g⁺) was produced by photosensitization. Stern–Volmer constants K_{SV} of O₂(¹Σ_g⁺) quenching by CH₃OH, C₅H₁₂, toluene, C₆H₆, acetone, C₆D₆, and acetone-*d*₆ were found to decrease in this series by a factor of 15. The H–D isotope effect $K_{SV,H}/K_{SV,D}$ was determined to be 3 for benzene and 4.5 for acetone, which is much smaller than that for e−v deactivation of O₂(¹Δ_g). An estimate of the O₂(¹Σ_g⁺) lifetime in CCl₄ of $\tau_\Sigma \approx 3.2$ ns was also given. The variation of K_{SV} was discussed qualitatively in terms of the e−v deactivation model proposed by Schuster.^{120,150}

On the basis of $k_Q^\Sigma = 2.7 \times 10^5$ M^{−1} s^{−1} determined for CCl₄ as gas-phase quencher,¹³⁹ $\tau_\Sigma \approx 360$ ns was estimated by Schmidt for liquid CCl₄.¹⁴⁹ The first time-resolved experiments with O₂(¹Σ_g⁺) were performed by Schmidt and Bodesheim,⁹¹ who used a photomultiplier to detect the very weak *b* → *X* phosphorescence in CCl₄ at 765 nm. O₂(¹Σ_g⁺) was photosensitized by the triplet sensitizer phenalenone. Because of strong perturbations by very fast decaying emissions, a difference technique, allowing for lifetimes $\tau_\Sigma \geq 30$ ns, was applied. The evaluation of the biexponential rise and decay curves with time constants τ_T and τ_Σ yielded $\tau_\Sigma = 130$ ns in pure CCl₄, which was confirmed by Chou et al.⁹² With increasing [O₂], a proportional increase of 1/τ_T was found. Hereby, the O₂(¹Σ_g⁺) signals became shorter but also higher, as a consequence of the reduction of the lifetime τ_T at constant lifetime τ_Σ and quantum yield of O₂(¹Σ_g⁺) formation. When O₂(¹Σ_g⁺) quenching experiments were carried out in air-saturated solution, the second time constant τ_Σ varied at constant lifetime τ_T , proving that actually O₂(¹Σ_g⁺) was monitored. Rate constants k_Q^Σ were determined for CH₃OH, CHCl₃, CH₃CN, acetone, C₆H₆, and C₆H₁₂. A maximum value of $k_Q^\Sigma = 2.2 \times 10^9$ M^{−1} s^{−1} was reported for CH₃OH. For the rest of the quenchers, it was found that k_Q^Σ varies in proportion to the number of C–H bonds, in accordance with the e−v deactivation model derived above.⁹¹

Losev et al. performed time-resolved measurements of the *b* → *a* fluorescence at 1935 nm in CCl₄ solution by means of a fast GaInAsSb diode.⁸⁷ They determined $\tau_\Sigma = 105$ ns and rate constants k_Q^Σ for some quenchers, in accordance with the earlier results.^{91,92} They also quoted $\tau_\Sigma = 140$ ns in CS₂, which is a surprisingly long time, if one considers the 6-fold larger gas-phase k_Q^Σ value for CS₂ compared

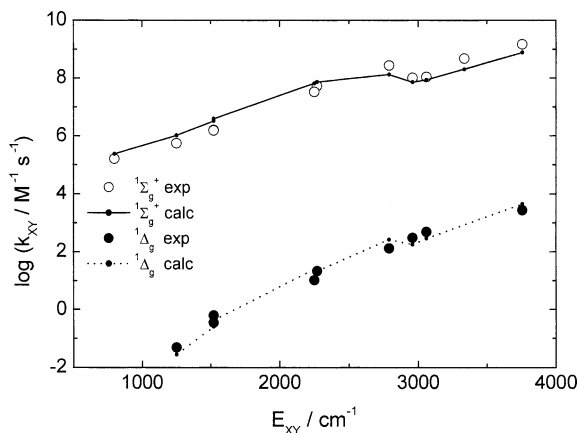


Figure 12. Logarithmic plot of experimental and calculated rate constants of e–v deactivation of $O_2(^1\Sigma_g^+)$ and $O_2(^1\Delta_g)$ by terminal bonds X–Y versus the corresponding energy E_{XY} . Reprinted with permission from ref 153. Copyright 1998 American Chemical Society.

with that for CCl_4 (see Table 6). Keszthelyi et al. used a step-scan FTIR spectrometer for time-resolved measurement of the $b \rightarrow a$ fluorescence in CS_2 and determined $\tau_\Sigma = 30$ ns.¹⁵¹

The studies on the quenching of $O_2(^1\Sigma_g^+)$ in CCl_4 were extended by Schmidt and Bodesheim,^{152,153} who evaluated the value of $0.97_5 \pm 0.02_5$ for the efficiency of $O_2(^1\Delta_g)$ formation in the deactivation of $O_2(^1\Sigma_g^+)$ by CCl_4 , CH_3OH , C_6H_6 , C_6H_{12} , and C_8H_{18} .¹⁵² The investigation of 22 quenchers with a variety of deactivating X–Y bonds yielded a large data set, which is suited for comparison of the collisional deactivation of $O_2(^1\Sigma_g^+)$ and $O_2(^1\Delta_g)$ in solution.¹⁵³ Rate constants k_Q^Σ were found to be larger, by a factor of ~ 2 , in solution than in the gas phase. From $k_Q^\Sigma = 3.2 \times 10^6$ $M^{-1} s^{-1}$ obtained with CS_2 , one calculates $\tau_\Sigma = 19$ ns for pure CS_2 , in agreement with the result of Keszthelyi et al.¹⁵¹ Values of k_{XY}^Σ for 11 different bonds were obtained using the e–v energy-transfer model developed earlier.¹⁴⁹ These experimental liquid-phase data could be well described with $\alpha = 0.0032$ cm, by a one-parameter fit yielding $C_\Sigma = 2.0 \times 10^{10}$ $M^{-1} s^{-1}$.¹⁵³ C_Σ was interpreted as the product of the normalized collision frequency in the liquid phase Z_l , the electronic factor f_Σ of the $^1\Sigma_g^+ \rightarrow ^1\Delta_g$ transition of O_2 , and a steric factor s . The differences between liquid- and gas-phase data could be qualitatively explained by assuming that Z_l exceeds the gas-phase frequency Z_g by the value of the pair distribution function $g(\sigma)$ at contact distance σ .¹⁵⁴ Z_l further depends on the size and mass of the quencher. s describes the accessibility of O_2 to the deactivating bond in collinear collisions and depends on the molecular structure of the quencher. Therefore, the use of a general value of C_Σ represents, of course, a significant simplification. Still, the experimental results are well described by the calculated data, as illustrated in Figure 12, with the correlations of $\log(k_{XY}^\Sigma)$ and $\log(k_{XY}^\Delta)$ with E_{XY} . $\log(k_{XY}^\Sigma)$ increases much more with E_{XY} than $\log(k_{XY}^\Delta)$, as a consequence of the larger energy gap for the corresponding deactivation process (7882 versus 5239 cm^{-1}). This is the actual reason the H–D isotope effect is much stronger in the e–v deactivation of $O_2(^1\Delta_g)$.¹⁵³

Figure 12 also reveals systematic deviations of the calculated values of $\log(k_{XY}^\Sigma)$ which are not observed with $\log(k_{XY}^\Delta)$. This deviation was shown to be caused by the neglect of bending vibrations and combinational modes, which also could couple to vibronic transitions of O_2 and induce deactivation of singlet oxygen. The neglect is less important in the calculation of $\log(k_{XY}^\Delta)$ because of its stronger E_{XY} dependence, resulting from the larger $^1\Delta_g - ^3\Sigma_g^-$ energy gap of 7882 cm^{-1} . The successful description of the $O_2(^1\Sigma_g^+) \rightarrow O_2(^1\Delta_g)$ and $O_2(^1\Delta_g) \rightarrow O_2(^3\Sigma_g^-)$ e–v deactivation processes also stimulated the calculation of the rate constants for the spin-forbidden $O_2(^1\Sigma_g^+) \rightarrow O_2(^3\Sigma_g^-)$ e–v deactivation with energy gap 13 121 cm^{-1} . Rate constants that are several orders of magnitude smaller and that depend much more on E_{XY} than the experimental $O_2(^1\Delta_g) \rightarrow O_2(^3\Sigma_g^-)$ deactivation data were obtained, even when the electronic factor was assumed to be identical to that for the spin-allowed $O_2(^1\Sigma_g^+) \rightarrow O_2(^1\Delta_g)$ deactivation. Thus, without referring to spin-forbiddenness, already the large energy gap causes the inefficiency of $O_2(^3\Sigma_g^-)$ formation in the e–v deactivation of $O_2(^1\Sigma_g^+)$.¹⁵³ This is the main reason why $O_2(^1\Delta_g)$ is the only product of the e–v deactivation of $O_2(^1\Sigma_g^+)$ and why e–v energy transfer is probably very slow for deactivation of electronically excited diatomic molecules with large energy gaps.

e. e–v Deactivation of $^1\Sigma^+$ States of Isoelectronic Molecules. The molecules NF, SO, and SeO are isoelectronic to O_2 . They have, like O_2 , a $^3\Sigma^-$ ground state and two low-lying $^1\Delta$ and $^1\Sigma^+$ excited states. To test whether the e–v energy-transfer model could generally describe the e–v deactivation of low-energy electronically excited diatomic molecules, Schmidt analyzed literature values of k_Q^Σ for the gas-phase deactivation of $^1\Sigma^+$ -excited NF,¹⁵⁵ SO,¹⁵⁶ and SeO.¹⁵⁶ By applying the model outlined above, it was shown that experimental values of k_{XY}^Σ could be reproduced for the three different molecules with the same constant $\alpha = 0.0032$ cm, determined with $O_2(^1\Delta_g)$ and $O_2(^1\Sigma_g^+)$, and a common constant $C_\Sigma = 1.3 \times 10^{10}$ $M^{-1} s^{-1}$, which is only 50% larger than $C_\Sigma = 8.8 \times 10^9$ $M^{-1} s^{-1}$, derived for the gas-phase deactivation of $O_2(^1\Sigma_g^+)$. Thus, the separation of a quencher into single deactivating bonds and the interpretation of the corresponding rate constants by the model of coupled transitions should be generally useful.¹⁵⁶

This model was also used by Setser and co-workers for the interpretation of gas-phase rate constants of deactivation of the $^1\Sigma^+$ states of NF and PF,¹⁵⁷ and NCl and PCl.^{158,159} The overall agreement between calculated and experimental rate constants was encouraging. The same values of C_Σ and α could be used. However, it was also reported that the model fails for individual reactions that are significantly off-resonance or for processes requiring large ($n \geq 3$) changes in vibrational quantum number. But this is certainly also a consequence of the neglect of deactivation by bending modes of bonds X–Y, since for NF, PF, NCl, and PCl the $^3\Sigma_g^- - ^1\Delta_g$ energy gap is even smaller than for O_2 .¹⁵³

f. High-Pressure Investigations of the e–v Deactivation of $O_2(^1\Delta_g)$. The e–v deactivation of $O_2(^1\Delta_g)$ reflects, in some way, the solvent structure. The structure of a liquid is described by the radial distribution function $g(d)$, which gives the local density of molecules as a function of their distance d to a central molecule, normalized to the average density value. $g(d)$ has its maximum value $g(\sigma) > 1$ at the collisional distance σ . For the simple model of a hard-sphere liquid, $g(d)$ falls off rapidly with increasing d , similarly to a damped oscillation, to reach finally the value of unity. $g(\sigma)$ increases with the particle density of the molecules, and thus with the packing fraction η' of the system. According to Einwohner and Alder, the normalized collision frequency Z_1 in liquids is given by eq 34, where k_B is Boltzmann's constant, μ is the reduced mass of the colliding pair, and N_A is Avogadro's number.¹⁵⁴

$$Z_1 = \sigma^2 g(\sigma) N_A (8\pi k_B T \mu)^{0.5} \quad (34)$$

The quenching of $O_2(^1\Delta_g)$ by $O_2(^3\Sigma_g^-)$ can be used as a probe for the determination of the value of the radial distribution function $g(\sigma_{OO})$ at the O_2 – O_2 collision distance σ_{OO} . The second-order rate constant k_Q^Δ is given by the product of Z_1 and the deactivation probability P_Q per collision, which is constant for a given temperature. As was shown by Maier and co-workers in a high-pressure investigation of the quenching of $O_2(^1\Delta_g)$ in pure gaseous and liquid O_2 , k_Q^Δ is directly proportional to $g(\sigma_{OO})$, which increases from $g(\sigma_{OO}) = 1$ in the low-density O_2 to $g(\sigma_{OO}) \approx 3$ in compressed O_2 at 2 kbar.¹⁶⁰ Maier and co-workers further extended their studies to the relaxation of the $^1\Sigma_g^+$ and $^1\Delta_g$ states of $^{16}O_2$ and $^{18}O_2$ in the gas, liquid, and solid phases at low temperatures.^{160,162} The temperature dependences of the rate constants of deactivation in the gas and liquid states as well as in the solid state have been discussed by applying the model of isolated binary interactions. The abrupt changes in the relaxation rates at the different solid-phase transitions were interpreted to be caused by the change in orientation of neighboring O_2 molecules, affecting the relaxation probability. It was concluded that the optimum orientation of the O_2 molecules for e–v deactivation is head-on.¹⁶² This result is in accordance with the conclusion, derived from the discussion of steric factors, that collinear collisions of O_2 and the bond X–Y are particularly effective in the deactivation of singlet oxygen.^{155,156}

The first high-pressure investigation of the e–v deactivation of $O_2(^1\Delta_g)$ in an ordinary solvent was carried out by Okamoto et al., who measured rate constants k_Q^Δ in the neat solvents hexane, methylcyclohexane, CH_3OH , and CH_3CN at 298 K.¹⁶³ From the pressure dependence of k_Q^Δ , they derived activation volumes $\Delta V_{obs}^\#$ that varied from -4 (CH_3OH) to -9 (hexane) $mL\ mol^{-1}$, via eq 35, where κ_T is the isothermal compressibility of the solvent.

$$\Delta V_{obs}^\# = -RT \left(\frac{d \ln(k_Q^\Delta)}{dP} \right)_T - \kappa_T RT \quad (35)$$

These results are, at first sight, surprising, since no intermediate bond formation should occur in the deactivation. $k_Q^\Delta = Z_1 P_Q$ was assumed, leading to proportionality between k_Q^Δ and $g(\sigma_{OS})$, where σ_{OS} is the collisional distance between O_2 and the solvent molecule. The application of pressure causes an increase of the packing fraction η' of the solvent. For the interpretation of $\Delta V_{obs}^\#$ data, a theory proposed by Yoshimura and Nakahara was applied.¹⁶⁴ These authors had demonstrated that, even in the complete absence of any attractive interaction, the formation of a contact complex is accompanied by a negative volume of contact complex formation, ΔV_C , which can be calculated by using eq 36.

$$\Delta V_C = -\kappa_T RT \eta' \frac{d \ln g(\sigma_{OS})}{d \eta'} - \kappa_T RT \quad (36)$$

Okamoto et al. used eq 36 to obtain values for ΔV_C which were in agreement with $\Delta V_{obs}^\#$.¹⁶³

The pressure dependence of τ_Δ was also investigated independently by Brauer and co-workers in 12 solvents; they determined -4.1 (formamide) $\geq \Delta V_{obs}^\# \geq -11.9$ $mL\ mol^{-1}$ (C_5H_{12}).¹²⁸ It was assumed that $O_2(^1\Delta_g)$ and the solvent molecule reversibly form a singlet-excited collision complex 1C , which forms by isc via e–v energy transfer (with rate constant k_{isc}) the triplet ground-state collision complex 3C , which finally dissociates to yield $O_2(^3\Sigma_g^-)$. This kinetic scheme results in $k_Q^\Delta = K_C k_{isc}$, where K_C is the equilibrium constant of contact complex formation and $\Delta V_{obs}^\# = \Delta V_C + \Delta V_{isc}^\#$. Using eq 36, they calculated -3.2 (formamide) $\geq \Delta V_C \geq -10.0$ $mL\ mol^{-1}$ (C_5H_{12}), and thus an average $\Delta V_{isc}^\# = -1.6$ $mL\ mol^{-1}$, which indicates a slight overlap of electron clouds of $O_2(^1\Delta_g)$ and the terminal atom of bond X–Y in the deactivating collision, in agreement with the conclusions concerning the heavy-atom effect with carbon–halogen bonds.¹²³ Further analysis revealed that the e–v deactivation of $O_2(^1\Delta_g)$ depends neither on the polarity of the solvent nor on the polarity of the collider or the deactivating bond.¹²⁸ Therefore, the investigation of the quenching of $O_2(^1\Delta_g)$ by $O_2(^3\Sigma_g^-)$ in ordinary solvents at atmospheric pressure can also yield information about $g(\sigma_{OO})$ in polyatomic solvents.¹⁶⁵ When the rate constants determined at 295 K and 1 bar— C_6F_{14} , 2600; $C_2Cl_3F_3$, 3200; CCl_4 , 3900; and $C_{10}F_{16}$, 4100 (solvent, $^{16}k_Q^\Delta$ in $M^{-1}\ s^{-1}$)¹²⁶—are divided by the corresponding gas-phase value $^{16}k_Q^\Delta = 1020\ M^{-1}\ s^{-1}$,¹²⁵ for which $g(\sigma_{OO}) = 1$ holds true, one obtains via $^{16}k_Q^\Delta \sim g(\sigma_{OO})$ experimental values of $g(\sigma_{OO}) = 2.5$ (C_6F_{14}), 3.1 ($C_2Cl_3F_3$), 3.8 (CCl_4), and 4.0 ($C_{10}F_{16}$). These numbers seem to be realistic, since the corresponding packing fractions η' increase just in this series.¹⁶⁵

Two further high-pressure studies were performed on the e–v deactivation of $O_2(^1\Delta_g)$.^{166,167} Hild and Brauer determined k_Q^Δ and $\Delta V_{obs}^\#$ for the quencher toluene in the neat liquid and as solute in several fluids. Using eq 36, it was shown that ΔV_C is the main part of $\Delta V_{obs}^\#$. Furthermore, the quenching by toluene, benzene, and cyclohexane was measured in the neat solvents and dissolved in CCl_4 , $C_2Cl_3F_3$, and

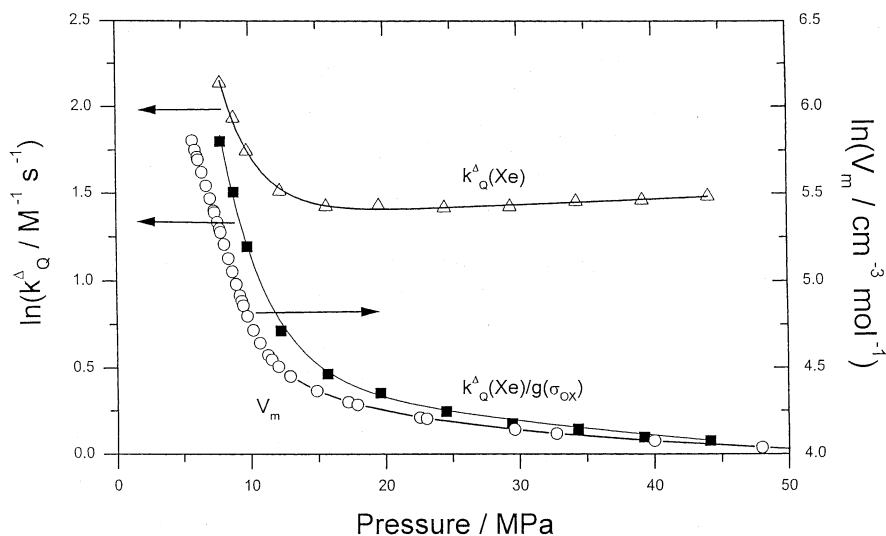


Figure 13. Plots showing the dependence of $\ln(k_Q^\Delta)$ (Δ), $\ln(V_m)$ (\circ), and $\ln(k_Q^\Delta/g(\sigma_{OX}))$ (\blacksquare) on the pressure in SCF-Xe at 325 K. Reprinted with permission from Abdel-Shafi, A. A.; Wilkinson, F.; Worrall, D. R. *Chem. Phys. Lett.* **2001**, *343*, 273–280. Copyright 2001 Elsevier Science.

C_2Cl_4 , and the correlation $k_Q^\Delta \sim g(\sigma_{OQ})$ was shown to hold true.¹⁶⁶ Okamoto and Tanaka determined k_Q^Δ and ΔV_{obs}^\ddagger for a series of neat *n*-alkanes (C_5 – C_8 , C_{12}).¹⁶⁷ ΔV_{obs}^\ddagger was split into contributions from CH_3 (–14.4 to –12.5 mL mol^{–1}) and CH_2 (–9.2 to –7.3 mL mol^{–1}). The results were successfully described by the model proposed by Yoshimura and Nakahara. In addition, the activation energy of k_Q^Δ was determined for methylcyclohexane to be $E_a = 1.6$ kJ mol^{–1}, in agreement with other studies on the temperature dependence of the e–v deactivation of $O_2(^1\Delta_g)$ in the liquid phase.^{118,120,127,128}

Recently, the first studies of e–v deactivation in supercritical fluids (SCFs) were published.^{168–171} Okamoto et al. produced $O_2(^1\Delta_g)$ by photosensitization with 9-acetylanthracene and determined τ_Δ in liquid and SCF CO_2 .¹⁶⁸ In both systems, τ_Δ decreased significantly with increasing pressure. Very large activation volumes, $\Delta V_{obs}^\ddagger = -170$ and -360 mL mol^{–1}, were calculated by using eq 35 for liquid CO_2 and SCF CO_2 , respectively. It was shown that, in both cases, the dominating part of ΔV_{obs}^\ddagger is the translational contribution $-\kappa_T RT$ of -140 and -340 mL mol^{–1}, respectively. The interpretation of ΔV_{obs}^\ddagger values by using eq 36 results in reaction volumes of contact complex formation $\Delta V_C = -190$ and -360 mL mol^{–1} for liquid CO_2 and SCF CO_2 . It is interesting to note that, under these conditions, a very large $-\kappa_T RT$ term is present in both equations for ΔV_{obs}^\ddagger and ΔV_C .¹⁶⁸

Worrall and co-workers also studied the lifetime τ_Δ in liquid and SCF CO_2 .¹⁶⁹ Rate constants k_Q^Δ were determined in the supercritical region for quenching of $O_2(^1\Delta_g)$ by CO_2 (16 M^{–1} s^{–1}), by O_2 (1.9×10^4 M^{–1} s^{–1}), and by *N,N,N,N*-tetraphenyl-1,4-phenylenediamine (7×10^7 M^{–1} s^{–1}). These results deviate in part significantly from the respective values in conventional solvents. Possible reasons for the differences were discussed. In a second study, Worrall et al. used SCF Xe as solvent.¹⁷⁰ One question was of particular interest: How does the lack of receiving vibrational modes and the increase in heavy-atom interactions,

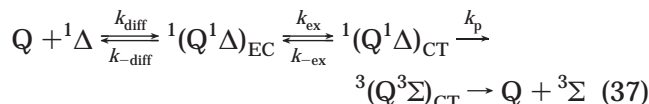
compared with SCF CO_2 , affect the rate constants for quenching of $O_2(^1\Delta_g)$ by Xe and O_2 ? At 325 K and 440 bar, values of $k_Q^\Delta = 4.4$ and 1.3×10^3 M^{–1} s^{–1} were measured for the spin-forbidden deactivation by Xe and the spin-allowed quenching by O_2 , respectively. The latter value is comparable with the corresponding constants determined at 1 bar in perhalogenated solvents (vide supra).¹²⁶ The e–v energy-transfer model developed by Schmidt and Afshari was used to interpret both rate constants.^{57,153} Hereby, it was concluded that, due to the very strong heavy-atom effect of Xe, the value of k_Q^Δ almost reaches the limiting value expected for a spin-allowed process.¹⁷⁰ The analysis of the pressure dependence of k_Q^Δ for the quenching of $O_2(^1\Delta_g)$ by Xe in SCF Xe led to the conclusion that the pressure dependence of k_Q^Δ arises from the pressure dependence of the molar volume V_m of Xe, which dominates at low pressures, and from the variation of $g(\sigma_{OX})$ with pressure, which explains the positive slope of $\ln(k_Q^\Delta)$ versus P at higher pressures. This finding, illustrated in Figure 13, is in agreement with Okamoto's results, since $\kappa_T = -d \ln(V_m)/dP$.

Very recently, Okamoto et al. investigated the e–v deactivation of $O_2(^1\Delta_g)$ by ethane in liquid and SCF ethane.¹⁷¹ Lifetimes τ_Δ decreased in the low-pressure range in SCF ethane much more than in the liquid. In the high-pressure range, the dependence generally leveled off. The apparent activation volume of k_Q^Δ varied from -120 (SCF) and -32 mL mol^{–1} (liquid) in the lower pressure region to -24 (SCF) and -15 mL mol^{–1} (liquid) at higher pressures. In liquid solution, the pressure dependence of k_Q^Δ could be interpreted by assuming reversible formation of encounter complexes of $O_2(^1\Delta_g)$ and quencher followed by isc, applying the model of contact complex formation. In SCF ethane, the failure of this model was attributed to the contribution of the local density augmentation around the solute molecules. The degree of the local density augmentation was defined as the ratio of the effective density around the solute

to bulk density, $\rho_{\text{eff}}/\rho_{\text{bulk}}$. The ratio $\rho_{\text{eff}}/\rho_{\text{bulk}}$ for O_2 was evaluated from the deviation of low-pressure rate constants from data extrapolated from the pressure dependence of rate constants in the high-pressure region. For the sensitizer 9-acetylanthracene, $\rho_{\text{eff}}/\rho_{\text{bulk}}$ could be obtained from the peak shift of the absorption maximum, with pressure differing strongly between SCF and liquid ethane. It is interesting to note that the pressure dependences of the ratios $\rho_{\text{eff}}/\rho_{\text{bulk}}$ for O_2 and 9-acetylanthracene agreed, indicating very similar density augmentations around both solutes in SCF ethane in the lower pressure region.

4. Radiationless Deactivation: Charge-Transfer Deactivation

a. Observation of Charge-Transfer-Induced Quenching of $\text{O}_2(^1\Delta_g)$. Molecules with high triplet energies ($E_T > 94 \text{ kJ mol}^{-1}$) and low oxidation potentials ($E_{\text{ox}} \lesssim 1.9 \text{ V vs SCE}$) quench $\text{O}_2(^1\Delta_g)$ with rate constants exceeding the values expected for an e-v process by up to 7 orders of magnitude. On the basis of correlations with the ease of ionization of the quencher, these events have been explained by a CT-induced process, where the deactivation of the initially formed singlet encounter complex $^1(\text{Q}^1\Delta)_{\text{EC}}$ is enhanced by the formation of a singlet $^1(\text{Q}^1\Delta)_{\text{CT}}$ exciplex, which is stabilized by the transfer of electric charge from the quencher to the oxygen molecule. This species decays mainly by isc to a triplet CT ground-state complex, $^3(\text{Q}^3\Sigma)_{\text{CT}}$, which finally dissociates to the products Q and $\text{O}_2(^3\Sigma_g^-)$, without charge separation in most cases.



However, a chemical reaction may also occur from $^1(\text{Q}^1\Delta)_{\text{CT}}$ exciplexes to some extent. Therefore, the overall quenching rate constant k_{Q}^{Δ} can be additively composed of a physical and a chemical component, i.e., $k_{\text{Q}}^{\Delta} = k_p + k_c$ (see section III.B.4.b).

A CT-induced mechanism was first suggested by Ouannès and Wilson¹⁷² to account for the quenching of $\text{O}_2(^1\Delta_g)$ by tertiary aliphatic amines, and especially diazabicyclo[2.2.2]octane (DABCO). These compounds were shown to inhibit $\text{O}_2(^1\Delta_g)$ -mediated oxidations and to suppress singlet-oxygen-sensitized fluorescence in both liquid and gas phases. On the basis of these observations, the authors suggested that interactions of $\text{O}_2(^1\Delta_g)$ with the lone electron pair of the amine are responsible for a CT-mediated physical deactivation process. Numerous systematic studies have been carried out since then, and it has been suggested that CT-induced physical quenching represents the main pathway of $\text{O}_2(^1\Delta_g)$ deactivation by aliphatic and aromatic amines,^{127,172–188} hydrazines,¹⁸⁹ aliphatic and aromatic mono-, di-, and trisulfides,^{190–195} phenols,^{196,197} electron-rich naphthalene,^{198,199} biphenyl,²⁰⁰ benzophenone,²⁰¹ and benzene^{188,202,203} derivatives; organic complexes of nickel^{204,205} and cobalt^{206,207} and other heavy-atom-containing aromatics;^{208,209} inorganic anions such as azide,^{210–212} iodide,²¹³ bromide²¹⁴ or superoxide;²¹⁵ and numerous biological

compounds, including derivatives of guanosine²¹⁶ and vitamin B12,²⁰⁷ vitamin E,^{197,217} chlorophylls,²¹⁸ porphyrins,²¹⁸ hydroxycinnamic acids,²¹⁹ ascorbate,²²⁰ and amino acids.²²⁰ It was also suggested that CT effects might play a role in the deactivation of $\text{O}_2(^1\Delta_g)$ by radicals with excited-state energies higher than 94 kJ mol^{-1} .²²¹

Several methods have been employed to study the CT nature of these interactions. The first and most straightforward one involved the use of correlations of the experimental overall second-order quenching rate constants k_{Q}^{Δ} with the electrochemical properties of the quencher. Correlations with Hammett σ , σ^+ , and σ^- values were reported for several series of compounds, and slopes were mostly found to be within -1.1 and -1.8 , thus showing a systematic decrease of k_{Q}^{Δ} upon introduction of electron-withdrawing groups.^{178,181,191,192,194,196,218} Most of these studies were carried out in the 1970s and have been thoroughly reviewed.^{8,9} More recent studies have obtained additional information from correlations of k_{Q}^{Δ} with the free energy change ΔG_{CET} of complete electron transfer, which is calculated by the Rehm–Weller equation,^{222,223}

$$\Delta G_{\text{CET}} = F(E_{\text{ox}} - E_{\text{red}}) - E_{\text{exc}} + C \quad (38)$$

where F is the Faraday constant, E_{red} is the reduction potential of molecular oxygen (-0.78 V vs SCE in acetonitrile),²²⁴ and $E_{\text{exc}} = 94 \text{ kJ mol}^{-1}$ is the state energy of $\text{O}_2(^1\Delta_g)$. Comparison of data from different solvents requires the introduction of the Coulomb term C ,²²³

$$C = \frac{e^2}{2} \left(\frac{1}{r^+} + \frac{1}{r^-} \right) \left(\frac{1}{\epsilon_s} - \frac{1}{37} \right) - \frac{e^2}{\epsilon_s(r^+ + r^-)} \quad (39)$$

where ϵ_s is the static dielectric constant of the solvent, e is the elementary charge ($e^2 = 14.43 \text{ eV \AA}$), and r^+ is the molecular radius of the quencher. r^- of the electron acceptor O_2 is 1.73 \AA . The major advantage over using Hammett plots is that these studies are not limited to a series of structurally equivalent quenchers, and effects other than CT (e.g., structural and steric effects) can be addressed. However, the error limits are often larger because oxidation potentials of organic quenchers are sometimes difficult to determine. An example of recent work¹⁸⁸ on aromatic amines and methyl- or methoxy-substituted benzenes is given in Figure 14. The increase of k_{Q}^{Δ} by 6 orders of magnitude corresponds to a decrease in E_{ox} from 1.76 to 0.16 V vs SCE .

A very similar dependence of $\log(k_{\text{Q}}^{\Delta})$ on ΔG_{CET} (respectively E_{ox} or the gas-phase ionization potential, IP) was observed for $\text{O}_2(^1\Delta_g)$ quenching by aromatic and aliphatic amines,^{177,178,180,181} phenols,¹⁹⁶ methoxybenzenes,¹⁹⁶ sulfides,¹⁹² disulfides,¹⁹⁵ hydrazines,¹⁸⁹ naphthalenes,^{198,199} biphenyls,²⁰⁰ benzophenones,²⁰¹ guanosines,²¹⁶ hydroxycinnamic acids,²¹⁹ and other biological compounds²¹⁸ in polar and nonpolar solvents. Gas-phase data for a series of sulfides¹⁸⁹ and aliphatic amines¹⁷⁵ are in good agreement with the respective liquid-phase data. All observations are clearly in support of a generally similar CT mecha-

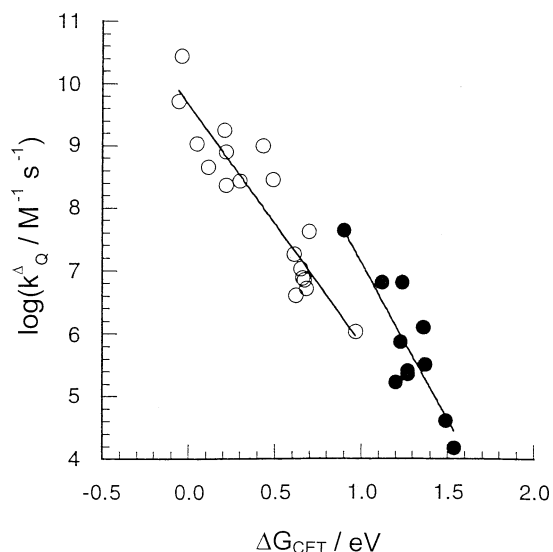


Figure 14. Charge-transfer-induced deactivation of singlet oxygen in acetonitrile, as demonstrated by a dependence of $O_2(^1\Delta_g)$ quenching rate constants (k_Q^Δ) on free energy of complete electron transfer from quencher to $O_2(^1\Delta_g)$. Open symbols correspond to a series of amines, solid symbols to methyl- or methoxy-substituted benzene derivatives. Reprinted with permission from ref 188. Copyright 1998 American Chemical Society.

nism for $O_2(^1\Delta_g)$ deactivation by electron-rich molecules. Because of the rather limited ΔG_{CET} range generally available in these experiments, the data do not allow the actual form of the relationship between $\log(k_Q^\Delta)$ and ΔG_{CET} to be ascertained; all observations are consistent with both linear and parabolic Marcus-type behavior. In early work on a series of hydrazines, Clennan et al.¹⁸⁹ ruled out the latter hypothesis on the basis of experimental reorganization energies $> 80 \text{ kJ mol}^{-1}$, resulting from a Marcus-type interpretation of the data, which were believed to be unreasonably high. More recent studies^{225,226} have shown that reorganization energies of this order do not disagree with Marcus theory. Regardless of the model used, the driving-force dependence for CT-induced $O_2(^1\Delta_g)$ deactivation is generally much weaker than expected for a complete electron transfer, and the authors largely agreed that the rate-limiting step involves exciplexes bearing partial CT character.

Significant deviations from correlations between $\log(k_Q^\Delta)$ and ΔG_{CET} are generally explained by structural and/or steric effects. Several authors observed different correlations for aliphatic and aromatic amines,¹⁷⁷ and also for aliphatic and aromatic sulfides,¹⁹² indicating that the molecular structure of the quencher plays a non-negligible role. However, not all studies are in agreement with this conclusion.¹⁷⁸ Steric interactions were first suggested by Monroe,¹⁸⁰ who correlated $\log(k_Q^\Delta)$ for a series of aliphatic amines with IP and observed systematic deviations to lower rate constants for sterically hindered nitrogen atoms. The same author found a significant decrease of k_Q^Δ when methyl substituents were introduced at the α -position of piperidines, and concluded that this CT process requires a close proximity between the nitrogen atom and the excited O_2 molecule. A quantitative demonstration of this

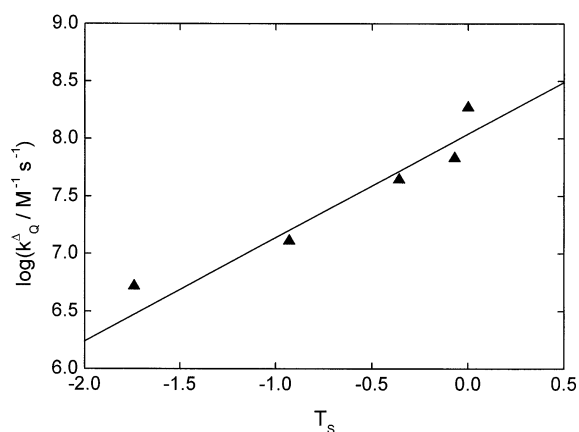


Figure 15. Steric effects on charge-transfer-induced deactivation of $O_2(^1\Delta_g)$, as evidenced by a correlation of quenching rate constants (k_Q^Δ) with the Taft steric parameter, T_s , for a series of hydrazines with $E_{ox} = (0.32 \pm 0.01) \text{ V vs SCE}$. Reprinted with permission from ref 195. Copyright 1997 American Chemical Society.

behavior was recently given by Clennan et al.¹⁹⁵ with a series of hydrazines with very low and identical oxidation potential, where a nearly 40-fold decrease of k_Q^Δ was obtained on going from methyl to neopentyl substituents. $\log(k_Q^\Delta)$ was shown to correlate with the Taft steric parameter T_s , which is a measure of the bulk introduced by a given substituent²²⁷ (see Figure 15).

Very similar behavior was observed with a series of sulfides and sulfenamides. Kacher and Foote¹⁹² reported a decrease of k_Q^Δ by more than 2 orders of magnitude on going from diethyl sulfide to di-*tert*-butyl sulfide, which both have the same oxidation potential. Clennan and Greer¹⁹⁴ obtained a slope of 1.47 in a Taft plot for $O_2(^1\Delta_g)$ quenching by a series of sulfenamides.

Disulfides exhibit a somewhat different dependence on steric factors. These compounds are generally less efficient quenchers than monosulfides but more efficient than trisulfides.¹⁹⁵ Clennan et al.¹⁹⁵ found that the k_Q^Δ values of disulfides bearing differently bulky substituents correlate with IP rather than with the Taft parameter. Moreover, these k_Q^Δ values were found to fall on a common line with the IP dependence of several cyclic disulfides. Significant deviations from this correlation were observed with Me_2S_2 (+1 order of magnitude) and 1,2-dithiolanes (+2 orders of magnitude). These deviations reflect the ability of the compound to form the corresponding persulfoxide, which could be explained by the particularly small steric demands on Me_2S_2 and the constrained $>\text{CSSC}$ dihedral angle of only 30° in the 1,2-dithiolanes, compared with the angles of $>85^\circ$ for the less efficient quenchers.

Several authors have also reported on the effect of heavy atoms on the deactivation of singlet oxygen. Carlsson et al.²⁰⁴ first noted that metal complexes can be very efficient quenchers of $O_2(^1\Delta_g)$, with rate constants approaching the diffusion-controlled limit. Farmilo and Wilkinson²²⁸ first suggested a heavy-atom mechanism for the deactivation of $O_2(^1\Delta_g)$ by aromatic complexes of Pd and Fe, where k_Q^Δ values are significantly below the diffusion-controlled limit.

Monroe and Mrowca²²⁹ explained large variations in k_Q^Δ for several complexes on the basis of steric interactions, since complexes possessing a square-planar geometry were found to be much more efficient quenchers than those possessing tetrahedral or octahedral geometries. This indicates that the quenching process occurs mainly by interactions with the metal center. Shiozaki et al.²³⁰ measured the overall rate constants for physical $O_2(^1\Delta_g)$ deactivation by nickel complexes to be close to the diffusion-controlled limit but noted a correlation of the chemical reaction with the reduction potential of these complexes.

Corey et al.²⁰⁸ observed rate constants on the order of $10^7 \text{ M}^{-1} \text{ s}^{-1}$ for $O_2(^1\Delta_g)$ deactivation by a gold(I) compound of the type $RSAuPEt_3$. Their investigation of a series of phenyl ether compounds $PhXCH_3$ revealed a systematic increase of k_Q^Δ by more than 4 orders of magnitude in the order $k_Q^\Delta(PhOCH_3) < k_Q^\Delta(PhSCH_3) < k_Q^\Delta(PhSeCH_3) < k_Q^\Delta(PhTeCH_3)$.²⁰⁹ $\log(k_Q^\Delta)$ could be correlated both with the ionization potential of the quencher and with $\log(Z^4)$, where Z is the atomic number of the X atom. Additionally, the value $k_Q^\Delta = 3.8 \times 10^9 \text{ M}^{-1} \text{ s}^{-1}$ observed for $PhTeCH_3$ is significantly higher than the rate constant for $O_2(^1\Delta_g)$ quenching by amines of the same IP. Since no heavy-atom effect was observed in the non-nucleophilic series PhH, PhF, PhCl, PhBr, PhI, the authors concluded that $O_2(^1\Delta_g)$ quenching by RTeR derivatives occurs by a combination of CT and heavy-atom mechanisms.

Oliveros and Braun and co-workers²⁰⁶ studied physical quenching of $O_2(^1\Delta_g)$ by metal complexes of ethylenediaminetetraacetic acid (EDTA). They observed rate constants significantly below the diffusion-controlled limit and an increase in the order $k_Q^\Delta(\text{EDTA}) \approx k_Q^\Delta(\text{Mn}^{2+}/\text{EDTA}) < k_Q^\Delta(\text{Al}^{3+}/\text{EDTA}) < k_Q^\Delta(\text{Cu}^{2+}/\text{EDTA}) < k_Q^\Delta(\text{Fe}^{3+}/\text{EDTA})$, which is similar to the order observed for the stability constants of these complexes. It was concluded that the d electrons of the metal play an important role in the enhancement of the CT process. CT interactions between $O_2(^1\Delta_g)$ and the Co^{2+} metal center of vitamin B12 derivatives were also suggested by the same group.²⁰⁷

Baranyai and Vidóczy²³¹ recently provided evidence for diffusion-controlled quenching of $O_2(^1\Delta_g)$ by cobalt complexes, on the basis of correlations of solvent-dependent data with the Smoluchowski equation,

$$k_{\text{diff}} = 4\pi N_A(D_O + D_Q)(r_O + r_Q) \quad (40)$$

where D_O and D_Q and r_O and r_Q are the diffusion coefficients and radii of O_2 and quencher, respectively. Their fit value of $r_O + r_Q = 0.33 \text{ nm}$ demonstrates the necessity of a close proximity between $O_2(^1\Delta_g)$ and the Co metal center. In agreement with previous literature data, the authors proposed that at least one open coordination site around the metal center, which allows for metal- O_2 orbital overlap, leads to diffusion-controlled quenching, whereas coordinatively saturated complexes, such as those studied by Oliveros et al.,²⁰⁷ exhibit significantly lower k_Q^Δ values.

Evidence for an electron-transfer mechanism was recently obtained by Fukuzumi et al.²³² for singlet oxygen deactivation by decamethylferrocene in acetonitrile. These authors observed that, in this case, $O_2(^1\Delta_g)$ decay is accompanied by the formation of both a decamethylferrocene cation and a superoxide anion; additionally, they suggested that complexes of Cr may also undergo electron transfer.

Diffusion-controlled quenching is clearly also in agreement with an electron-exchange energy-transfer mechanism. Especially in the case of nickel complexes, several authors have proposed that $O_2(^1\Delta_g)$ quenching occurs by electronic energy transfer^{228–230,233} or a combination of CT and electronic energy transfer.²⁰⁵ However, for most complexes, the triplet-state energies are unknown, and no triplet-triplet absorption measurements have been performed. Hence, the actual quenching mechanism remains unknown. A clear demonstration of an electronic energy-transfer mechanism could be given in only a few cases, including metal complexes of several phthalocyanines and naphthalocyanines. This is discussed in section III.B.5.

b. Competition between e–v, Charge-Transfer, and Chemical Deactivation Processes. It is important to note that, in most of the recent studies of the CT-induced deactivation of $O_2(^1\Delta_g)$, quenching rate constants were determined by monitoring the $O_2(^1\Delta_g \rightarrow ^3\Sigma_g^-)$ phosphorescence, which means that contributions from deactivation processes other than CT could not be explicitly separated. Collision-induced radiative deactivation is negligible compared with radiationless deactivation. However, e–v energy transfer, which is a general and non-CT-assisted process, is the most important quenching pathway for molecules with high oxidation potential, including many aromatic hydrocarbons with electron-withdrawing substituents.^{126,199,200} If the value of E_{ox} decreases below ca. 1.9 V vs SCE,^{199,200} CT deactivation surpasses e–v energy transfer even in nonpolar solvents, and in many cases, CT quenching additionally competes with chemical reactions, which are often far from being negligible. For example, chemical reactions with aromatic hydrocarbons, sulfides, and amines are well-documented.^{8–11} Hence, the observed CT quenching rate constant is additively composed of a physical and a chemical component, i.e., $k_Q^\Delta = k_p + k_c$. On the basis of parallel correlations of k_p and k_c with the ionization energy of amine quenchers, Gollnick and Lindner¹⁷⁹ suggested that the chemical and physical pathways may proceed via a common intermediate. Also, in the case of sulfides, a common intermediate has been suggested on both experimental¹⁹³ and theoretical²³⁴ grounds. Aubry et al.¹²² specifically addressed this issue in a recent study on the chemical deactivation of $O_2(^1\Delta_g)$ by 1,4-dimethylnaphthalene in 11 solvents. The authors observed an excellent linear correlation between $\log(k_c)$ and $\log(k_Q^\Delta)$, with a slope of unity (see Figure 16). From the intercept, the ratio $k_c/k_Q^\Delta = 0.29$ was calculated, which means that ~30% of quenching leads to photooxygenation of 1,4-dimethylnaphthalene, independent of solvent.

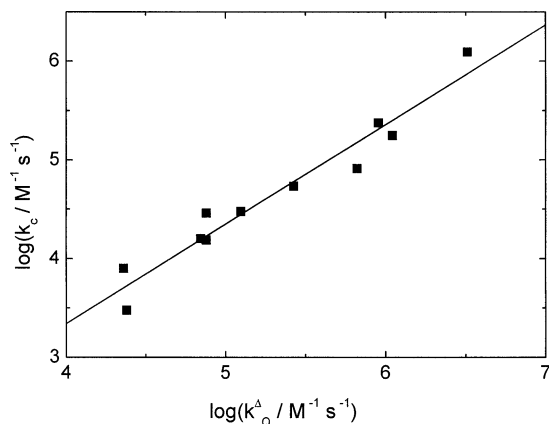


Figure 16. Evidence for a common intermediate in charge-transfer-induced physical and chemical deactivation of singlet oxygen, obtained by comparison of the chemical rate constants k_c with the overall quenching rate constants $k_Q^\Delta = (k_p + k_c)$, for $O_2(^1\Delta_g)$ quenching by 1,4-dimethylnaphthalene in 11 solvents. Reprinted with permission from ref 122. Copyright 1995 American Chemical Society.

This is also explained by a common intermediate in the physical and chemical CT process. However, Lemp et al.²³⁵ recently reported significant differences in the solvent dependence for chemical and physical deactivation of $O_2(^1\Delta_g)$ by 3-methylindole. The contribution of chemical reactions was found to increase from 1–2% in aprotic polar solvents to 30–40% in protic polar solvents.

Saito et al.¹⁸¹ noted chemical reactions following electron transfer during $O_2(^1\Delta_g)$ quenching by electron-rich amines in water. This was also confirmed by Manring and Foote,²³⁶ Peters and Rodgers,^{237,238} and Darmanyan et al.¹⁸⁸ Since the quantum yield of formation of superoxide appeared to correlate with the oxidation potential of the amines, and additionally, all values of $\log(k_Q^\Delta)$ fall on a common correlation with previously obtained $\log(k_Q^\Delta)$ CT quenching data, if plotted versus ΔG_{CET} , it was concluded that a common CT intermediate is associated with the rate-limiting step, and the decay of this exciplex competes with the dissociation of free ions.¹⁸¹ Hence, most observations reported to date are consistent with a mechanism in which the formation of an exciplex bearing partial CT character is followed by isc to the ground-state CT complex, by chemical reaction, or by separation of free ions. Many processes in which the chemical reaction is largely dominant over physical mechanisms are also in agreement with this mechanism.⁹

c. Influence of Temperature: Pre-equilibrium and Diffusion Control. Particularly interesting information on the kinetics of the quenching process has come from variable-temperature studies. Gorman and co-workers^{127,197} clearly identified two distinct regions in the Arrhenius plots for several quenchers of $O_2(^1\Delta_g)$. In the low-temperature region, a linear evolution of $\ln(k_Q^\Delta)$ with $1/T$ is observed, with a negative and identical slope for all quenchers investigated, including those operating by chemical reaction (CR) or electronic energy transfer (EET).¹²⁷ The common activation energy was found to be 7 kJ mol⁻¹. This behavior is in agreement with a diffusion-

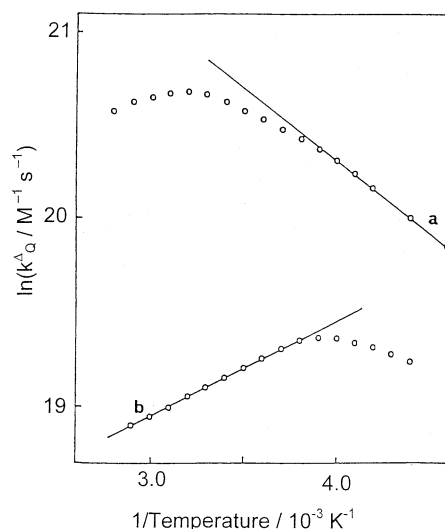


Figure 17. Arrhenius plots for the rate constants k_Q^Δ for quenching of $O_2(^1\Delta_g)$ in toluene by strychnine (a) and DABCO (b). Reprinted with permission from ref 127. Copyright 1988 American Chemical Society.

controlled process, where $k_{-diff} \ll k_p + k_c$. However, significant differences were found in the pre-exponential factors A (in $M^{-1} s^{-1}$): e.g., $A = 1.3 \times 10^{10}$ (strychnine, CT quenching), $A = 2.9 \times 10^{10}$ (1,3-diphenylisobenzofurane, CR), and $A = 3.1 \times 10^{11}$ (β -carotene, EET). These differences were explained by different steric factors for the different deactivation processes. Arrhenius plots for strychnine and DABCO exhibit a turnover point in the region corresponding to -20 to $+40$ °C, and in the high-temperature region, a positive slope, corresponding to an activation energy of -4.2 kJ mol⁻¹ (or $\Delta H^\ddagger = -6.7$ kJ mol⁻¹ and $\Delta S^\ddagger = -126$ J K⁻¹ mol⁻¹) was observed in the case of DABCO¹²⁷ (see Figure 17).

A very similar high-temperature behavior was reported for physical $O_2(^1\Delta_g)$ quenching by several phenol derivatives in a range of solvents of very different polarity.¹⁹⁷ Significantly negative activation energies were associated with rapid and reversible exciplex formation at the pre-equilibrium limit, where the subsequent isc to the ground-state CT complex is the rate-limiting step, i.e., $k_{-diff} \gg k_p + k_c$. Strongly negative activation entropies are explained by high steric demands.

d. High-Pressure Investigations. Microscopic information on the structural changes associated with the CT-induced quenching process could be gained from pressure-dependent studies.^{166,184,185,202,203} Variations over pressure ranges from 1 to 1200 bar showed that, for most quenchers, the rate constant k_Q^Δ for $O_2(^1\Delta_g)$ deactivation increases significantly with increasing pressure (see Figure 18).

From the linear portion of plots of $\ln(k_Q^\Delta)$ versus P , one can calculate, by using eq 35, the activation volume ΔV_{obs}^\ddagger , which describes the volume changes occurring on the way to the transition state. In the case of CT quenching, this volume is given by the sum of the volume change ΔV_C due to the formation of the $^1(Q^1\Delta)_{EC}$ encounter complex, the volume change ΔV_{CT} due to the formation of the $^1(Q^1\Delta)_{CT}$ exciplex from the encounter complex, and the activation

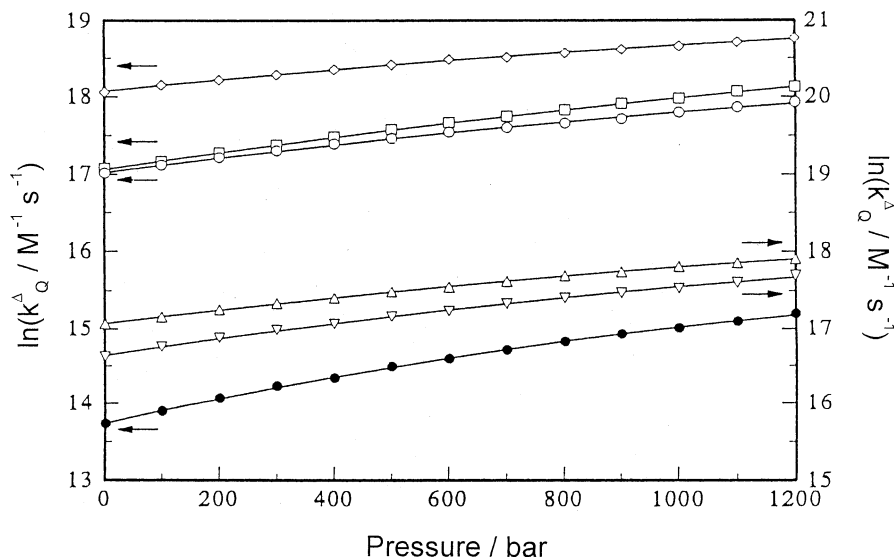


Figure 18. Pressure dependence of $\ln(k_Q^\Delta)$ for $O_2(^1\Delta_g)$ quenching by piperazine in *n*-hexane (●), toluene (□), dichloromethane (▽), chlorobenzene (○), *o*-dichlorobenzene (△), and benzonitrile (◇). Reprinted with permission from ref 185. Copyright 1996 Deutsche Bunsen-Gesellschaft.

volume ΔV_p^\ddagger associated with the isc from $^1(Q^1\Delta)_{CT}$ to the $^3(Q^3\Sigma)_{CT}$ exciplex: $\Delta V_{obs}^\ddagger = \Delta V_C + \Delta V_{CT} + \Delta V_p^\ddagger$. Using the hard-sphere model proposed by Yoshimura and Nakahara,¹⁶⁴ ΔV_C can be calculated by using eq 36, via the dependence of the value of radial distribution function $g(\sigma_{QO})$ at the closest approach distance σ_{QO} of O_2 and quencher on the packing fraction η' :

$$g(\sigma_{QO}) = \frac{1}{1 - \eta'} + \frac{3\eta'\sigma}{2(1 - \eta')^2\sigma_S} + \frac{\eta'^2\sigma^2}{2(1 - \eta')^3\sigma_S^2} \quad (41)$$

σ_O , σ_Q , and σ_S are the hard-sphere diameters of O_2 , the quencher, and the solvent molecule, and $\sigma = \sigma_Q(\sigma_O/\sigma_{QO})$. Different procedures for the estimation of η' to fit real liquids into the framework of the hard-spheres model were discussed by Schmidt et al.¹²⁸ Most realistic results are obtained when η' is calculated from the solvent molar volume V_m and compressibility κ_T via eq 42.

$$\kappa_T = \frac{V_m(1 - \eta')^4}{RT(1 + 4\eta' + 4\eta'^2 - 4\eta'^3 + \eta'^4)} \quad (42)$$

The activation volume, $\Delta V_{CT}^\ddagger = \Delta V_{obs}^\ddagger - \Delta V_C = \Delta V_{CT} + \Delta V_p^\ddagger$, for the reaction from the encounter complex to the transition state of isc from $^1(Q^1\Delta)_{CT}$ to $^3(Q^3\Sigma)_{CT}$ exciplexes can thus be easily calculated from the data shown in Figure 18. For several substituted benzenes, Okamoto and Tanaka²⁰² found a correlation between ΔV_{CT}^\ddagger and the ionization potential of the quencher which is in accordance with a CT-induced process. Brauer and co-workers^{184,185} described the solvent dependence of ΔV_{CT}^\ddagger for $O_2(^1\Delta_g)$ quenching by several amines by a linear relationship,

$$\Delta V_{CT} = (\Delta V_{CT})^0 - N_A \left(\frac{(\mu^\ddagger)^2}{(r^\ddagger)^3} - \frac{\mu_Q^2}{r_Q^3} - \frac{\mu_O^2}{r_O^3} \right) q_P \quad (43)$$

where μ^\ddagger , μ_Q , and μ_O and r^\ddagger , r_Q , and r_O are the dipole moments and radii of the transition state, the quencher,

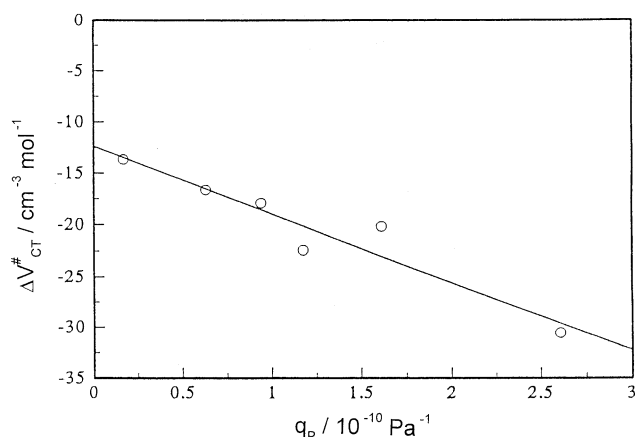


Figure 19. Evidence for charge-transfer-induced deactivation of $O_2(^1\Delta_g)$ by piperazine, from a plot of solvent-polarity-dependent activation volumes ΔV_{CT}^\ddagger versus the Kirkwood parameter q_P . Reprinted with permission from ref 185. Copyright 1996 Deutsche Bunsen-Gesellschaft.

er, and O_2 , respectively, and $q_P = (dq/dP)_T$, where $q = (\epsilon_s - 1)/(2\epsilon_s + 1)$ is the Kirkwood parameter (see Figure 19).

Reasonably linear correlations of ΔV_{CT}^\ddagger with q_P are found for aliphatic and aromatic amine quenchers, which yield a clear negative slope.^{184,185} This is in agreement with a CT process, and the slope can be used to estimate the CT character of the exciplexes (vide infra). The intercept $(\Delta V_{CT}^\ddagger)^0 = (\Delta V_{CT})^0 + (\Delta V_p^\ddagger)^0$ represents the activation volume in the absence of electrostriction effects. With the reasonable assumption that $(\Delta V_p^\ddagger)^0 = 0$, the intercept $(\Delta V_{CT}^\ddagger)^0$ can be interpreted as the overlapping volume of the electron clouds of O_2 and the quencher. Brauer and co-workers reported clearly negative $(\Delta V_{CT}^\ddagger)^0$ values ranging from -2.2 (*N,N,N,N*-tetramethylphenylene-1,4-diamine) to -12.4 $\text{cm}^3 \text{mol}^{-1}$ (piperazine),¹⁸⁵ which are in agreement with the formation of a relatively compact exciplex, as suggested previously by the negative activation entropies found by Gorman et al.¹²⁷ The relatively large differences

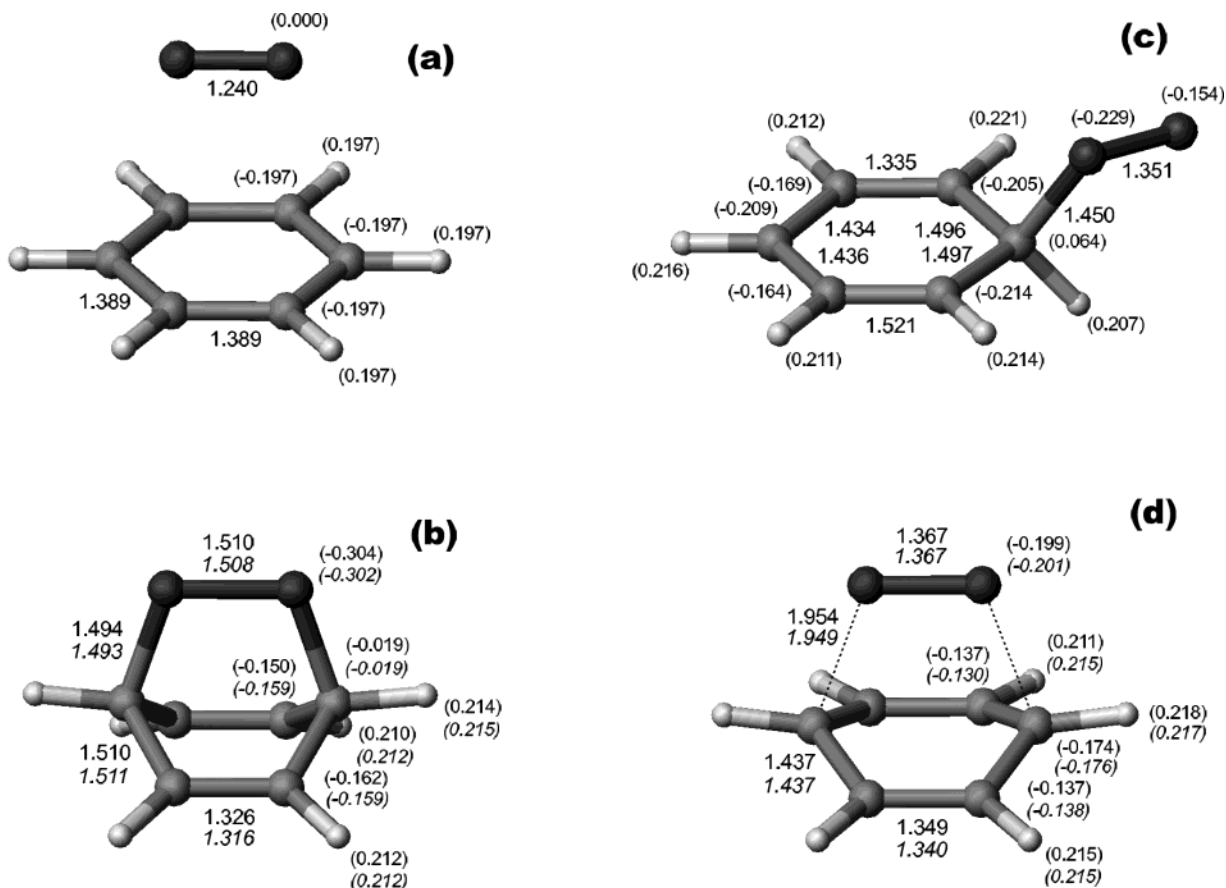


Figure 20. Stationary points on the benzene singlet oxygen surface: (a) the reactants, (b) the product, (c) the linear intermediate, and (d) the supra-supra transition structure from the reactants to the product. The lengths of selected bonds and interatomic distances are given in angstroms. Normal and italic fonts refer to different active spaces used in the calculations. Numbers in parantheses correspond to electric charge of atoms. Reprinted with permission from ref 239. Copyright 2000 American Chemical Society.

between the $(\Delta V_{CT}^\ddagger)^0$ values of differently substituted amines underscores the importance of steric interactions. Interestingly, no solvent dependence of ΔV_{CT}^\ddagger was found for $O_2(^1\Delta_g)$ quenching by toluene¹⁶⁶ and hexamethylbenzene.²⁰³ In the case of toluene, Hild and Brauer¹⁶⁶ explained this behavior by negligible CT interactions, i.e., a purely $e-v$ mechanism. In the case of hexamethylbenzene,²⁰³ this explanation is not possible, since a correlation of $\log(k_q^A)$ with q is observed at any pressure, indicating stronger CT interactions due to the lower E_{ox} value of hexamethylbenzene.

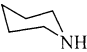
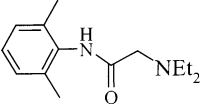
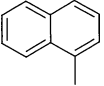
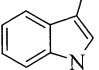
e. Results from Theoretical Studies: The Structure of CT Intermediates. Further information on the structure of CT complexes has come from recent theoretical studies. Martin et al.¹⁸⁶ performed semiempirical calculations on the physical deactivation of singlet oxygen by aliphatic amines. For the interaction of $O_2(^1\Delta_g)$ with the nitrogen atom of propylamine, they found a structure of minimum energy at a nitrogen–oxygen separation distance of 1.54 Å, with a nitrogen–oxygen bond angle of 119° and a carbon–nitrogen–oxygen–oxygen dihedral angle of 179°. A less distinct enthalpy minimum was found at the same separation distance in the case of secondary amines, and only an inflection point was found between 1.5 and 1.6 Å in the case of tertiary amines. For several simple aliphatic amines, the authors reported a linear correlation between logarithmic

experimental $O_2(^1\Delta_g)$ quenching rate constants and calculated values of the enthalpy of activation of isc of the excited amine– O_2 singlet complexes.

Bobrowski et al.²³⁹ performed ab initio calculations on the hypothetical addition of $O_2(^1\Delta_g)$ to benzene. The calculated structures are shown in Figure 20. Chemical reactions are not observed experimentally; these interactions lead to physical quenching only. The interaction of the π_g orbital with one of the two degenerate HOMO orbitals of benzene allows the formation of a supra-supra CT structure (Figure 20d) that preserves the C_{2v} symmetry. This complex should be the only intermediate in the CT quenching process, since no transition structure was found from the reactants to the linear intermediate (c). The formation of the 1,4-endoperoxide (b) is observed only when the benzene ring bears strongly electron-donating substituents.

Physical quenching is also the main pathway of $O_2(^1\Delta_g)$ deactivation by sulfides in aprotic solvents.¹⁹³ On the basis of ab initio calculations, electron transfer from the sulfur atom into the empty π_g orbital of $O_2(^1\Delta_g)$, leading to formation of peroxysulfoxide $R_2S^+-O_2^-$, has been suggested as the initial step. Jensen et al.²³⁴ calculated the sulfur–oxygen bond lengths to be 1.705 Å in the transition state and 1.651 Å in peroxysulfoxide. It is believed that physical (and chemical) quenching of $O_2(^1\Delta_g)$ proceeds via these intermediates. An excellent review of physical and

Table 7. Fit Parameters Describing the Solvent Dependence of the Rate Constant for O₂(¹Δ_g) Deactivation by Different Quenchers by Eq 44, and the Number, n_s, of Solvents Used in These Studies

entry	quencher	log(k _Q ^Δ) ₀	a	b	s	h	d	n _s	ref
1		8.10	-2.87					6	183
2	Et ₃ N	7.72	-2.18	1.82	0.36			7	15, 182
3	Et ₃ N	7.924	-1.305	0.362	0.321			28	187
4		5.946	-0.813	1.318	0.425			28	187
5		2.62			1.18	0.07		28	122
6		6.359			2.065		-0.526	19	235

chemical deactivation of O₂(¹Δ_g) by sulfides was published very recently.¹¹

f. Influence of Solvent. Numerous studies have reported solvent effects on the CT-induced deactivation of O₂(¹Δ_g), and rate constants were generally observed to increase in media where CT interactions are favored, i.e., in polar solvents. However, despite the large amount of qualitative information available, only a few systematic studies have been undertaken.^{122,182,183,187,235} These reports have described the solvent dependence of rate constants of O₂(¹Δ_g) quenching by linear complexation energy relationships,

$$\log(k_Q^\Delta) = \log(k_Q^\Delta)_0 + s\pi' + d\delta + a\alpha + b\beta + h\delta_H \quad (44)$$

where log(k_Q^Δ)₀ is a constant and π', δ, α, β, and δ_H are the empirical solvatochromic parameters given by Kamlet et al.²⁴⁰ These parameters are indicators for several physical properties of the solvent, and their relative contribution to the solvent dependence of log(k_Q^Δ) is expressed by the factors s, d, a, b, and h, which are obtained by multiple linear regression analysis. The π' scale is an index of solvent dipolarity/polarizability, which measures the ability of the solvent to stabilize a charge or a dipole by virtue of its dielectric effect and can be expressed as a function of its bulk dielectric constant and refractive index. δ is a correction term for polarizability. The α and β scales describe the ability of the solvent to donate and accept, respectively, a proton in a solute-solvent hydrogen bond. The Hildebrand solubility parameter δ_H = (-E/V)^{1/2} is defined as the square root of the cohesive energy density, where -E is the molal heat of vaporization to a gas at zero pressure and V is the molal volume. δ_H is a measure of the solvent-solvent interactions that are interrupted in creating a suitably sized cavity for the solute in the solvent. The results of these systematic studies are listed in Table 7.

Encinas et al.¹⁸² first investigated the solvent dependence of O₂(¹Δ_g) quenching by aliphatic amines and one hydroxylamine. These authors noted an increase of k_Q^Δ with increasing π' and decreasing α,

in agreement with a CT interaction of O₂(¹Δ_g) with the amine nitrogen atom that can be hindered by solute-to-solvent N-H hydrogen bonds. In the case of *N,N*-diethylhydroxylamine, no dependence of k_Q^Δ on π' was observed. This was explained by a free-radical-like mechanism, leading to a rupture of the O-H bond.

Clennan et al.¹⁸³ studied the evolution of k_Q^Δ with α in solvents with high π' values and found a clear negative one-parameter dependence on α for piperidine (1), which demonstrates that solvent-to-solute hydrogen bonding plays a major role in the deactivation of O₂(¹Δ_g) by aliphatic amines. Systematically lower k_Q^Δ values for *N,N*-dimethyl-*N*-(3-hydroxypropyl)amine compared with *N,N*-dimethyl-*N*-butylamine were explained by the possibility of intramolecular hydrogen bonding.

Later, Lissi et al.¹⁵ explained the solvent dependence of O₂(¹Δ_g) quenching by triethylamine on the basis of eq 44, using the parameters given in Table 7. These results indicate that an additional stabilization of O₂-amine CT complexes is achieved in hydrogen-bond-accepting solvents. Corroborative results were recently obtained by Zanocco et al.¹⁸⁷ for the same amine in 28 solvents. However, the relative importance of α and β has been strongly corrected (see Table 7). These authors also studied O₂(¹Δ_g) quenching by lidocaine (4) in the same solvents and found a somewhat different behavior, which was attributed to intramolecular interactions between the amido NH and the tertiary amino group. Semi-empirical quantum mechanical calculations showed that the electron density on the aminic nitrogen of lidocaine is lower than that on the nitrogen of triethylamine, which explains both the generally lower k_Q^Δ values and the lower importance of hydrogen bonding in the case of lidocaine.

Aubry et al.¹²² reported an extensive study of O₂(¹Δ_g) quenching by 1,4-dimethylnaphthalene (5) in 28 solvents. Interestingly, these authors found a significant dependence of k_Q^Δ on both π' and δ_H, but not on α and β. This shows that, in contrast to aliphatic amines, quenching by aromatic hydrocarbons is not influenced by hydrogen bonds. The

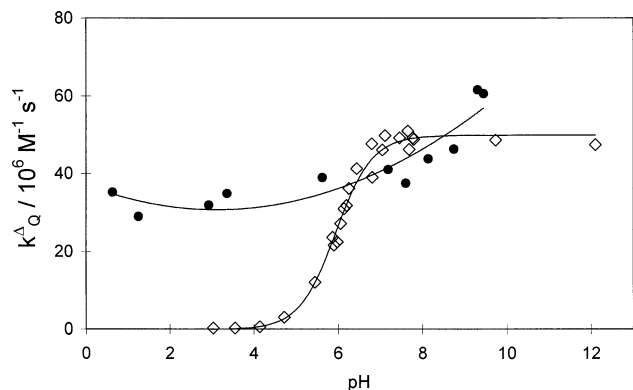


Figure 21. Effect of pH on the second-order rate constant (k_Q^Δ) for quenching of $O_2(^1\Delta_g)$ by histidine (\diamond) and tryptophan (\bullet). The rate constants were determined in D_2O /acetonitrile buffered with 40 mM phosphate, with the addition of NaOH or DCl as required. Reprinted with permission from ref 220. Copyright 1999 American Chemical Society.

positive dependence on δ_H demonstrates that exciplex formation is accompanied by the release of free solvent molecules, which means that this exciplex must be relatively compact, compared with the initially formed encounter complex. This conclusion is also in agreement with the negative activation entropies and activation volumes reported by Gorman et al.,¹⁹⁷ respectively Okamoto et al.²⁰² and Brauer et al.¹⁶⁶ However, even more negative ΔS^\ddagger and ΔV_{CT}^\ddagger values were found for $O_2(^1\Delta_g)$ quenching by aliphatic amines,^{127,184,185} where no dependence on δ_H was seen.¹⁸⁷ It should be noted that this insensitivity cannot be explained by the solvent range used in these studies. It is important to know that, for most solvents, δ_H correlates linearly with π' , and hence a dependence on δ_H can be revealed only when the data set includes solvents that are out of line in the δ_H versus π' correlation.²⁴⁰ However, since the study reported by Zanocco et al.,¹⁸⁷ which contained several of these solvents, did not reveal any statistically relevant dependence on δ_H , it appears that release of free solvent molecules is less significant during $O_2(^1\Delta_g)$ quenching by amines. Recently, Lemp et al.²³⁵ reported that also $O_2(^1\Delta_g)$ quenching by an aromatic amine, 3-methylindole (**6**), depends on π' but not on α or β . However, instead of the Hildebrand parameter δ_H , these authors used the polarizability correction term δ to describe their data.

In aqueous solutions (and hence in biological media), very important effects can be caused by variations in the pH. Scurlock et al.²⁴¹ showed that the state of protonation of several quenchers, such as phenols or thiols, has a dramatic impact on the rate constant of $O_2(^1\Delta_g)$ deactivation. Bisby et al.²²⁰ specifically addressed the effect of pH on the deactivation of $O_2(^1\Delta_g)$ by biological compounds in a recent study. Typical curves showing the evolution of k_Q^Δ with pH in a D_2O /acetonitrile solvent mixture are displayed in Figure 21.

For histidine and several other compounds possessing protons that are ionized in the investigated pH range, it was shown that deprotonation enhances the quenching process by more than 1 order of magnitude. The evolution of k_Q^Δ follows a sigmoidal

curve, which is characteristic of the pK_a value of the quencher (corrected for the influence of the addition of acetonitrile, in the case of Figure 21). Figure 21 also shows the pH dependence of k_Q^Δ for $O_2(^1\Delta_g)$ quenching by tryptophan, where no acid–base reaction takes place in this pH range. The insensitivity toward pH changes is consistent with the lack of ionizable protons. Similar results were obtained with several quenchers, indicating that quenching by $R-O^-$ anions is dominant over the interaction with aromatic rings.²²⁰

g. Charge-Transfer-Induced Quenching of $O_2(^1\Sigma_g^+)$. Two studies were concerned with the possibility of chemical reactions of $O_2(^1\Sigma_g^+)$.^{242,243} $O_2(^1\Sigma_g^+)$ and $O_2(^1\Delta_g)$ were generated during O_2 quenching of triplet states with excitation energies higher than 157 kJ mol^{-1} . Interestingly, no significant effect of quenchers on the efficiency of formation of $O_2(^1\Delta_g)$ from $O_2(^1\Sigma_g^+)$ has been observed. This indicates that all nonradiative $O_2(^1\Sigma_g^+)$ deactivation processes lead to formation of $O_2(^1\Delta_g)$; i.e., neither chemical reactions of $O_2(^1\Sigma_g^+)$ nor physical processes bypassing $O_2(^1\Delta_g)$ are significant. Scurlock et al.²⁴² found that $O_2(^1\Sigma_g^+)$ deactivation by DABCO is mainly an e–v process, since the experimental quenching rate constant is very similar to both the calculated e–v value and the value measured for $O_2(^1\Sigma_g^+)$ quenching by cyclohexane, a classical e–v quencher. In contrast, the deactivation of $O_2(^1\Sigma_g^+)$ by electron-rich and very fast chemical $O_2(^1\Delta_g)$ quenchers (such as furans and pyrroles) revealed small but significant positive differences between experimental rate constants of $O_2(^1\Sigma_g^+)$ deactivation and the values calculated for the respective e–v process. This suggests the existence of an additional $O_2(^1\Sigma_g^+)$ deactivation path, leading to formation of $O_2(^1\Delta_g)$.²⁴³ Since the differences between experimental and e–v rate constants were found to be identical to the rate constants for deactivation of $O_2(^1\Delta_g)$ by the same compounds, Schmidt and Bodesheim²⁴³ concluded that deactivation of $O_2(^1\Sigma_g^+)$ via the additional deactivation path, and quenching of $O_2(^1\Delta_g)$ by pyrroles, occur via a common transition state. On the basis of previous observations of $O_2(^1\Delta_g)$ with pyrroles, it was suggested that the most likely structure for this transition state is a CT complex.

h. Mechanism of Charge-Transfer Deactivation of $O_2(^1\Delta_g)$. As we have seen above, all experimental studies carried out on the dependence on temperature, pressure, solvent, and quencher redox properties, and also computational studies, agree that deactivation of $O_2(^1\Delta_g)$ by electron-rich quenchers generally proceeds via exciplexes bearing a partial CT character. An exciplex is generally considered as an intermediate whose wave function Ψ is described by the mixture of the wave functions of a locally excited ${}^1(Q^1\Delta)_{EC}$ encounter complex without CT interactions and an ion-radical pair ${}^1(Q^+{}^1\Delta^-)$, with α' and β' being the respective coefficients:

$$\Psi[{}^1(Q^1\Delta)_{CT}] = \alpha'\Psi[{}^1(Q^1\Delta)_{EC}] + \beta'\Psi[{}^1(Q^+{}^1\Delta^-)] \quad (45)$$

Numerous efforts have been made to estimate the relative importance of these two contributions, i.e.,

the charge-transfer character of the exciplex. In a linear correlation of $\log(k_{\text{Q}}^{\Delta})$ versus ΔG_{CET} , one expects in the endergonic range a slope of $-(2.3RT)^{-1} = -0.175 \text{ kJ mol}^{-1}$ if one electron is transferred at 25 °C. Several authors proposed estimating the CT character of the quencher–O₂ complexes by dividing the experimental slope by the limiting slope expected for a complete electron transfer. This led to a CT character of 44% for a series of phenols in methanol,¹⁹⁶ 60% for a series of *N,N*-dimethylanilines in water,¹⁸¹ 40% for a series of porphyrin-based compounds in benzene,²¹⁸ and 22% for a series of amines in acetonitrile.¹⁸⁸

Darmanyan et al.¹⁸⁸ used such estimates to calculate the free energy ΔG_{CT} for the charge-transfer step and interpreted their data in terms of Marcus theory, which describes the experimental free energy of activation as a function of ΔG_{CT} and the reorganization energy, λ . Using an estimated value of $\lambda = 0.104 \text{ eV}$, the authors computed a semiempirical relationship for calculation of the rate constant for the $\text{isc } {}^1(\text{Q}^1\Delta)_{\text{CT}} \rightarrow {}^3(\text{Q}^3\Sigma)_{\text{CT}}$ of CT complexes as a function of quencher redox properties, and they arrived at a very weak decrease from ca. 6×10^9 to $4.5 \times 10^9 \text{ s}^{-1}$ when augmenting quencher E_{ox} from 1 to 1.2 V vs SCE. Obviously, these estimates are valid only if isc is the rate-determining step, an assumption that was challenged in later investigations.

Two recent studies^{199,200} on naphthalene and biphenyl derivatives showed that the rate constants for the CT-induced deactivation of O₂(¹Δ_g) and the rate constants for the CT-induced deactivation of ππ*-excited triplet states by O₂, leading to formation of O₂(³Σ_g⁻), can be described by a common Marcus-type dependence on ΔG_{CET} . These observations were interpreted in terms of a common deactivation channel for both processes. In the case of the naphthalenes,¹⁹⁹ dipole moments of the transition state toward exciplex formation were estimated from correlations of quenching rate constants with the Kirkwood parameter q to be $6.2 \pm 0.8 \text{ D}$ for O₂(¹Δ_g) deactivation by the naphthalenes and $6.1 \pm 1.3 \text{ D}$ for quenching of the naphthalenes' T₁ states by O₂. These almost identical values also support a common deactivation channel and lead to a CT character of $25 \pm 5\%$ for both transition states, if they are divided by the product of elementary charge and separation distance. For both naphthalenes and biphenyls,²⁰⁰ the CT character of the exciplexes was estimated from the common fits of quenching rate constants to the Marcus equation, where ΔG_{CT} was envisioned as the product of ΔG_{CET} and the square of the CT character. This treatment leads to a similar CT character for the naphthalenes and biphenyls, which increases with increasing solvent polarity (from 43% in carbon tetrachloride to 59% in acetonitrile) and is significantly larger than the corresponding estimates in a linear model. The Marcus-type interpretation also yields the reorganization energy λ for the CT step. This parameter was reported to increase with increasing solvent polarity and to be somewhat larger for the naphthalenes than for the biphenyls (λ values were found to be in the range from 27.4 (33.6) kJ mol⁻¹ for biphenyls (naphthalenes) in CCl₄ to 86.0

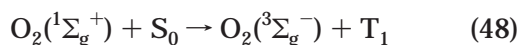
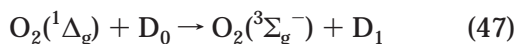
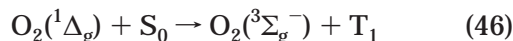
(91.7) kJ mol⁻¹ for biphenyls (naphthalenes) in CH₃CN). Reorganization energies are generally considered to be the sum of a solvent-dependent contribution λ_0 , depending directly on the square of the CT character and an intramolecular contribution λ_i , which is independent of the amount of CT. Since the CT character was estimated to be almost identical for both sensitizer series, the differences in λ should be due mainly to differences in λ_i . In ref 200, these differences are attributed to a mechanism where delocalization of electrons from the adjacent phenyl ring of naphthalenes leads to larger λ_i values compared with those of the biphenyls, where delocalization is less favorable due to rotation around the central bond. If both CT-induced quenching of O₂(¹Δ_g) and CT-induced quenching of T₁ by O₂ proceed via a common deactivation channel, all conclusions obviously apply to both processes. Since exciplex formation is rate-limiting in the case of O₂ quenching of triplet states (see section IV.A.2), it was suggested that, also for CT-induced quenching of O₂(¹Δ_g), the formation of the exciplex is the rate-determining step. However, this disagrees with the previous assumption made by Darmanyan et al.,¹⁸⁸ and also with the interpretation of previous temperature-dependent results, where negative activation energies appear to indicate that exciplex decay is rate-determining.¹²⁷ Note also that, for a series of benzophenones, no common deactivation channel was found.²⁰¹ However, this is not unexpected and does not contradict the previous observations, since the nπ* T₁ state of benzophenone derivatives is locally excited at the carbonyl bond. It was suggested that this leads to a locally excited sensitizer–oxygen complex structure (see also section IV.A.3), while O₂(¹Δ_g) deactivation by the benzophenones leads to a supra-supra complex structure, similar to that suggested for the naphthalenes or biphenyls.²⁰¹

Brauer and co-workers^{184,185} estimated the CT character of the exciplexes formed during O₂(¹Δ_g) quenching by amines from the pressure-dependent studies, using eq 43. Assuming that the van der Waals volume of the transition state is given by the sum of the van der Waals volume of the contact complex and the activation volume ($\Delta V_{\text{CT}}^{\ddagger}$)⁰ without solvent electrostriction, they calculated the radius r^{\ddagger} of the transition state;¹⁸⁴ hence, they obtained the dipole moment μ^{\ddagger} of the transition state from the slope of the plot of Figure 19. An estimate of the CT character is obtained by dividing μ^{\ddagger} by the dipole moment expected for a complete electron transfer. Using this method, values for the CT character of a series of amines were found to be between 30% and 84%.¹⁸⁵

Hence, the estimates of the CT character obtained by different methods seem to provide a consistent picture for several quenchers in several solvents. However, none of the proposed values claimed to describe the coefficients of eq 45 in a quantitative way, since the correlations with ΔG_{CET} neglect the changes related to E_{ox} or molecular structure, and the correlations with q or q_P neglect the solvent polarity dependence of the CT character.

5. Radiationless Deactivation: Electronic Energy Transfer

Molecules possessing an excited state with a state energy lower than that of $O_2(^1\Delta_g)$ or $O_2(^1\Sigma_g^+)$ deactivate these species by electronic energy-transfer (EET) mechanisms, leading to formation of an excited state of the quencher. Rate constants are generally found to be close to the diffusion-controlled limit k_{diff} , independent of the redox properties of the quencher. Three spin-allowed processes have been reported (eqs 46–48).



Equation 46 refers to quenchers possessing a singlet ground-state S_0 and a low-energy T_1 state ($E_T \leq 94 \text{ kJ mol}^{-1}$), such as carotenoids,^{228,244–260} naphthalocyanines,^{261,262} phthalocyanines,^{262–265} azomethine dyes²⁶⁶ and possibly also several metal complexes,^{228–231,233} and iodine.²⁶⁷ Equation 47 refers to free radicals possessing a doublet ground-state D_0 and a low-lying excited doublet state D_1 ,^{221,268} and eq 48 refers to molecules possessing a singlet ground-state S_0 and a triplet-state energy lower than 157 kJ mol^{-1} , such as fullerenes.²⁶⁹

Because of their importance as natural antioxidants,^{256,270} carotenoids are the best-investigated class of EET quenchers of $O_2(^1\Delta_g)$. Foote and Denny²⁴⁴ first observed physical quenching of $O_2(^1\Delta_g)$ by β -carotene, suggesting an EET mechanism for this process. These authors also found that *cis*- β -carotene isomers are efficiently isomerized to *all-trans*- β -carotene during the quenching process.²⁷¹ Wilkinson and co-workers^{228,247} and Rodgers and co-workers^{248,249} demonstrated that $O_2(^1\Delta_g)$ quenching by β -carotene and several other carotenoids leads to formation of the carotenoid T_1 state, with rate constants k_Q^Δ approaching the diffusion-controlled limit k_{diff} , as expected for an EET process. However, k_Q^Δ values significantly below k_{diff} (by up to 2 orders of magnitude) have been reported for several carotenoids.^{245,248,249,251,253–256} Correlations of the $O_2(^1\Delta_g)$ quenching activity were found with (i) the number N of conjugated C=C double bonds,^{245,253,256,259,272} (ii) the effective chain length N_{eff} ,²⁵⁷ as defined by Hirayama,²⁷³ (iii) the wavenumber of the lowest energy ground-state absorption maximum,^{254,256,257,260} and (iv) estimated values of the T_1 -state energy.^{246,253,257} No relationship was found between k_Q^Δ and the nature of the end group.^{254,255} Since the EET process of eq 46 has been clearly established,^{228,247–249,271} correlations with E_T are definitely the most meaningful ones. However, the extremely low triplet quantum yields (0.2–3%)²⁷⁴ of most carotenoids make E_T determinations difficult, and to date only the triplet energies, $E_T = 85 \text{ kJ mol}^{-1}$ for β -carotene (mean value from phosphorescence measurements in the zeolite ZSM-5²⁷⁵ and in C_6D_6 ,²⁷⁶ and photoacoustic calorimetry experiments in benzene)²⁷⁷ and $E_T = 73 \text{ kJ mol}^{-1}$ for decapreno- β -

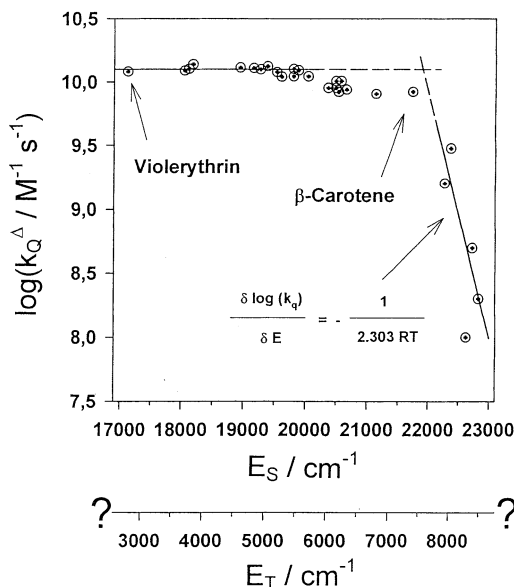


Figure 22. Electronic energy transfer from singlet oxygen to molecules with low triplet-state energies, represented by $\log(k_Q^\Delta)$ for $O_2(^1\Delta_g)$ quenching by carotenoids as a function of the $S_1(\pi\pi^*)$ excitation energy E_S . A tentative abscissa (in question marks) is given for the predominantly unknown triplet energies E_T ; the value $E_T = 85 \text{ kJ mol}^{-1}$ of β -carotene was used for adjustment. Reprinted with permission from ref 257. Copyright 1997 Wiley-VCH.

carotene (phosphorescence in the zeolite ZSM-5),²⁷⁵ have been reported. These data correspond to relaxed triplet states. A significantly higher triplet-state energy of $E_T = 95 \text{ kJ mol}^{-1}$ was determined by Gorman and co-workers in variable-temperature experiments on the quenching of $O_2(^1\Delta_g)$ by β -carotene in toluene,¹²⁷ which placed the spectroscopic triplet energy level 1.5 kJ mol^{-1} above the $O_2(^1\Delta_g)$ energy, which amounts to $E_\Delta = 93.8 \text{ kJ mol}^{-1}$ in toluene.⁹⁶

Several physical properties of carotenoids have been shown to correlate with each other; empirical relationships have been found between (i) the singlet–singlet and triplet–triplet excitation energies,^{246,274,278,279} (ii) the triplet–triplet maximum extinction coefficients and N ,²⁷⁹ (iii) the wavelength of the triplet–triplet absorption maxima and N ,²⁷⁹ and (iv) the singlet–singlet absorption maxima and N_{eff} .²⁵⁷ Hence, it is suggested that the triplet-state energy of carotenoids can be expressed as a function of any of these properties.

Baltschun et al.²⁵⁷ recently studied $O_2(^1\Delta_g)$ quenching by a large set of structurally different natural and synthetic carotenoids. These authors correlated $\log(k_Q^\Delta)$ with the lowest singlet–singlet $\pi\pi^*$ excitation energy E_S , as shown in Figure 22.

Assuming that the triplet-state energy E_T of these compounds is given by $E_T = E_S - 172 \text{ kJ mol}^{-1}$, as found for β -carotene, the slope of $-(2.3RT)^{-1}$ observed for $\log(k_Q^\Delta)$ versus E_S in the region of $E_S > 260 \text{ kJ mol}^{-1}$ ($> 22\,000 \text{ cm}^{-1}$) is in agreement with a thermally activated EET process. The evolution of $\log(k_Q^\Delta)$ with E_S exhibits a strong curvature in the region corresponding to 11 conjugated double bonds, where E_T approaches the state energy of $O_2(^1\Delta_g)$, and rate constants appear to be diffusion-

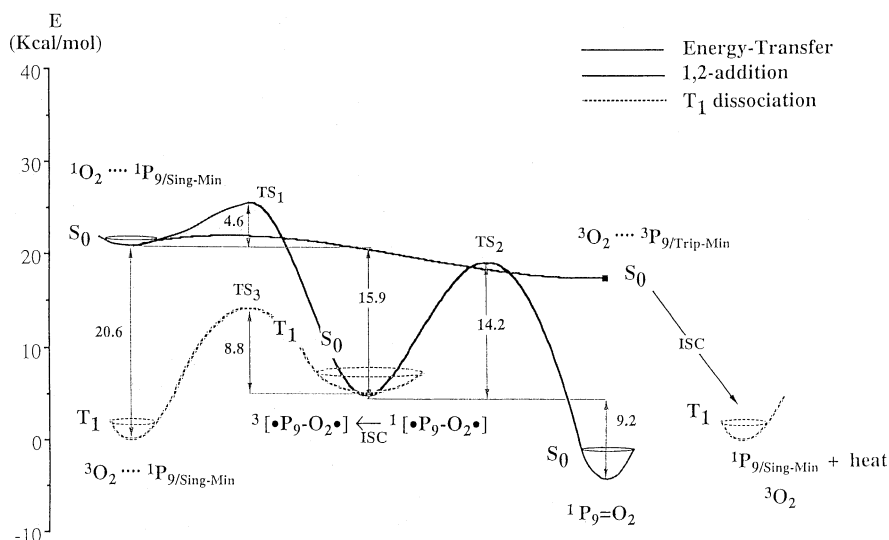


Figure 23. DFT energy profiles (spin-projected values in kilocalories per mole) of the main reaction paths computed for the interaction of $O_2(^1\Delta_g)$ with the carotenoid model *all-trans*-decaoctanonaene (P_9). The relative positions of the triplet (T_1) and singlet (S_0) states of reactants, intermediates, products, and transition states (TS_1 , TS_2 , and TS_3) are shown. Reprinted with permission from ref 258. Copyright 1998 American Chemical Society.

controlled in the range of the deeply colored magenta and blue carotenoids ($E_S < 240 \text{ kJ mol}^{-1}$ or $< 20\,000 \text{ cm}^{-1}$), where no thermal activation is required for the EET process.

Some additional information has come from solvent- and temperature-dependent studies. Conn et al.²⁵³ found a very small effect of solvent viscosity on k_Q^Δ , indicating that the process is not only diffusion-controlled, but other effects may also be important. Gorman et al.¹²⁷ reported a slight change in the Arrhenius behavior for $O_2(^1\Delta_g)$ quenching by β -carotene in toluene, indicating a progression from the diffusion limit to the pre-equilibrium limit, i.e., from a diffusion-controlled to an activation-controlled process. Oliveros et al.^{251,255} related unexpectedly low k_Q^Δ values in several solvents to the poor solubility of certain carotenoids in certain media, suggesting that aggregation can strongly diminish the $O_2(^1\Delta_g)$ quenching activity of carotenoids.

Although physical EET quenching is clearly the dominant pathway for $O_2(^1\Delta_g)$ deactivation by carotenoids, several studies showed that other processes can contribute significantly to the overall process.^{249,250,252,256,258,260,280} Chemical reactions leading to formation of epoxides and carotenoid bleaching have been reported in several cases.^{249,250,252,256,260,280} The efficiency of these reactions was shown to be strongly dependent on the nature of both the carotenoid²⁵⁶ and the solvent.^{250,251} Manitto et al.²⁵⁰ found a dependence of the rate constant for chemical reaction of $O_2(^1\Delta_g)$ with crocin derivatives on E_{ox} , suggesting that electron transfer is involved in the bleaching of these carotenoids. Garavelli et al.²⁵⁸ recently provided computational evidence for a free-radical pathway leading to both physical and chemical $O_2(^1\Delta_g)$ quenching by carotenoids. Their density functional theory study of the carotenoid model *all-trans*-decaoctanonaene (P_9) suggests that the two pathways depicted below do generally compete with the EET process.

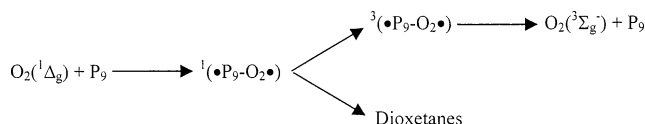


Figure 23 shows the energy profiles computed for $O_2(^1\Delta_g)$ deactivation by P_9 . The almost barrierless EET process competes with a pathway leading, via the transition state TS_1 , to a singlet diradical, ${}^1(\bullet P_9-O_2\bullet)$. The lowest activation energy, $4.6 \text{ kcal mol}^{-1}$, was found for the attack to the external double bond, but the energetic requirements for the attack to the central double bond are only slightly ($0.6 \text{ kcal mol}^{-1}$) higher, suggesting that any carotenoid double bond may be oxidized. Moreover, the optimized triplet diradical ${}^3(\bullet P_9-O_2\bullet)$ minimum was found to be virtually identical to the singlet one; hence, isc leading to formation of ${}^3(\bullet P_9-O_2\bullet)$ should be very fast. Therefore, the chemical 1,2-addition on the singlet potential energy surface, via the transition state TS_2 (activation energy $14.2 \text{ kcal mol}^{-1}$), is disfavored with respect to the triplet dissociation pathway, leading, via TS_3 (activation energy $8.8 \text{ kcal mol}^{-1}$), to physical $O_2(^1\Delta_g)$ quenching. Nonetheless, the most important deactivation process is EET, which proceeds almost barrierless on the S_0 surface from the ${}^1(O_2-{}^1P_9)$ to the ${}^1({}^3O_2-{}^3P_9)$ complex, followed by isc and dissociation, yielding ground-state carotenoid 1P_9 and $O_2(^3\Sigma_g^-)$ (see Figure 23).²⁵⁸

A second class of compounds with triplet energies close to 94 kJ mol^{-1} includes large polyheterocyclic aromatics such as naphthalocyanines^{261,281} and phthalocyanines.²⁸² Phosphorescence spectroscopy experiments yielded $E_T = 89 \text{ kJ mol}^{-1}$ for silicon naphthalocyanine,²⁶¹ $E_T = 88.7 \text{ kJ mol}^{-1}$ for silicon octabutoxybenzophthalocyanine,²⁶³ and $E_T = 108 \text{ kJ mol}^{-1}$ for palladium octabutoxyphthalocyanine,²⁸² and indirect measurements showed that several other naphthalocyanines have triplet-state energies lower than the state energy of $O_2(^1\Delta_g)$.²⁸¹ Rodgers and co-workers²⁶¹ observed the formation of triplet silicon

naphthalocyanine during $O_2(^1\Delta_g)$ quenching experiments in benzene and found that reversible energy transfer (i.e., $T_1 + O_2(^3\Sigma_g^-) \leftrightarrow S_0 + O_2(^1\Delta_g)$) takes place, with forward and backward rate constants of 1.6×10^8 and $1.14 \times 10^{10} \text{ M}^{-1} \text{ s}^{-1}$, respectively. Very similar results were obtained for several other metallophthalocyanines, for which measured or estimated E_T values below 94 kJ mol^{-1} were given.^{263–265,282} Krasnovsky et al.²⁶² measured k_Q^Δ values on the order of $10^9 \text{ M}^{-1} \text{ s}^{-1}$ for $O_2(^1\Delta_g)$ deactivation by several naphthalocyanines and phthalocyanines and showed that the EET mechanism can fully determine $O_2(^1\Delta_g)$ quenching by silicon naphthalocyanine.

Very recently, Berry et al.²⁶⁶ demonstrated that two photographic cyan azomethine dyes with triplet-state energies of 94 and 87 kJ mol^{-1} quench $O_2(^1\Delta_g)$ with rate constants of $7 \times 10^9 \text{ M}^{-1} \text{ s}^{-1}$, i.e., close to the diffusion-controlled limit. Iodine may also be a candidate for reversible energy-transfer processes with O_2 . This was suggested in a work by Wilkinson and Farmilo,²⁶⁷ who found $k_Q^\Delta \approx 10^9 \text{ M}^{-1} \text{ s}^{-1}$ in diluted benzene solutions of I_2 ($E_T \approx 102 \text{ kJ mol}^{-1}$) and significantly lower k_Q^Δ values at high I_2 concentrations.

The triplet states of several metal complexes were also estimated to be lower than 94 kJ mol^{-1} .²³³ However, experimental E_T values have not been reported so far. $O_2(^1\Delta_g)$ quenching rate constants close to the diffusion-controlled limit have been reported for many organic complexes of Ni, Co, or Zn and may be due to EET or CT mechanisms, or a combination of both. This is discussed in section III.B.3.

Few studies have been concerned with the interactions of $O_2(^1\Delta_g)$ with free radicals.^{221,268,283,284} In early gas-phase experiments, Becker et al.²⁶⁸ observed the $HO_2(^2A') \rightarrow HO_2(^2A'')$ emission in the presence of singlet oxygen, suggesting that the low-energy $^2A'$ state of HO_2^* (83 kJ mol^{-1}) is generated during EET quenching of $O_2(^1\Delta_g)$ by ground-state $HO_2(^2A'')$. Darmanyan et al.²²¹ recently measured quenching rate constants approaching the diffusion-controlled limit (i.e., $10^9 \text{ M}^{-1} \text{ s}^{-1} < k_Q^\Delta < 10^{10} \text{ M}^{-1} \text{ s}^{-1}$) for $O_2(^1\Delta_g)$ deactivation by peroxy radicals in solution. In agreement with the EET process of eq 47, the first excited doublet-state energies of several RO_2^* radicals were measured and/or calculated to be below the state energy of $O_2(^1\Delta_g)$. Rate constants on the order of $10^{10} \text{ M}^{-1} \text{ s}^{-1}$ were previously reported for $O_2(^1\Delta_g)$ quenching by peroxy and acylperoxy radicals,²⁸³ but significantly lower k_Q^Δ values (10^5 – $10^6 \text{ M}^{-1} \text{ s}^{-1}$) were found for nitroxy radicals²⁸⁴ and sulfur-centered radicals,²²¹ where no low-lying excited doublet or quartet state exists. Darmanyan et al.^{221,283,284} explained the latter deactivation process by an enhanced isc mechanism. Variations in the k_Q^Δ values and activation energies in a series of nitroxy radicals were attributed to steric effects.²⁸⁴ However, this suggestion contrasts with a recent work by Vidóczy and Baranyai,²⁸⁵ who measured rate constants for quenching of triplet hematoporphyrin and singlet oxygen by 13 nitroxide radicals. In the former case, a good correlation of k_Q^Δ was

found with calculated values for the accessibility of the nitroxide group, whereas no such correlation was observed for quenching of $O_2(^1\Delta_g)$ by the radicals.

Very little is known about EET quenching of $O_2(^1\Sigma_g^+)$ (eq 48). Scurlock and Ogilby²⁶⁹ determined a Stern–Volmer constant of $1.3 \times 10^4 \text{ M}^{-1}$ for $O_2(^1\Sigma_g^+)$ deactivation by C_{60} ($E_T = 155 \text{ kJ mol}^{-1}$) in CS_2 . Considering the $O_2(^1\Sigma_g^+)$ lifetime of 30 ns in this solvent,¹⁵¹ this value is indicative of diffusion-controlled EET to C_{60} . Since the state energy of the so-generated C_{60} triplet is higher than 94 kJ mol^{-1} , such an EET process should be followed by $O_2(^1\Delta_g)$ sensitization via oxygen quenching of triplet C_{60} , as described in section IV.

IV. Photosensitized Production of Singlet Oxygen

The most common means of singlet oxygen generation is photosensitization or, more precisely, energy transfer to $O_2(^3\Sigma_g^-)$ from an excited state of a sensitizer, which is formed by the absorption of light in a specific wavelength region. Singlet oxygen photosensitization is highly favored in nature, because (i) due to the very special electronic configuration of molecular O_2 , energy-transfer quenching of both excited singlet and triplet states is spin-allowed, in contrast to many competing deactivation processes; (ii) the excitation energies of both $O_2(^1\Sigma_g^+)$ and $O_2(^1\Delta_g)$ are lower than the state energy of many organic triplets, and in most cases, the energy difference is small enough to make the process fast and large enough to make it irreversible; and (iii) the very small size of the O_2 molecule allows for particularly rapid diffusion in many media, and due to the high atmospheric oxygen concentration, hardly any intermolecular process is able to compete with oxygen quenching.

Hence, any excited state that is sufficiently long-lived to allow for intermolecular interactions is likely to be quenched by $O_2(^3\Sigma_g^-)$, and singlet oxygen photosensitization is observed in virtually any chemical system where light is absorbed in the presence of molecular oxygen. In many cases, energy transfer results in the formation of both $O_2(^1\Sigma_g^+)$ and $O_2(^1\Delta_g)$. However, the spin-allowed $^1\Sigma_g^+ \rightarrow ^1\Delta_g$ deactivation occurs with extremely high rate constants in the condensed phase, and with unit efficiency in any medium; thus, all $O_2(^1\Sigma_g^+)$ will be recovered as $O_2(^1\Delta_g)$ (see sections III.B.3.c and III.B.4.g).

In the early 1930s, Kautsky and co-workers^{286–289} first attributed the photochemical modification of an acceptor by a spatially separated sensitizer to chemical reactions of singlet oxygen, formed by photosensitization following quenching by O_2 of luminescence of dyes. However, their clear and far-sighted concept was not generally accepted until 30 years later, when further evidence came from the works of Foote and Wexler^{290,291} and Corey and Taylor,²⁹² who observed the same products for self-sensitized and sodium hypochlorite-based oxidations of several compounds,²⁹⁰ and also for the oxidation of anthracene derivatives following irradiation and excitation of molecular O_2 by electrical discharge.²⁹²

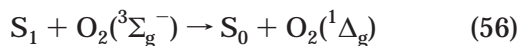
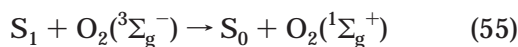
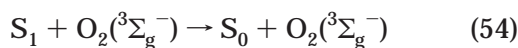
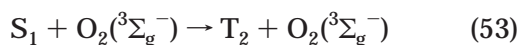
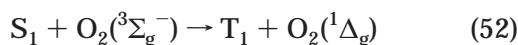
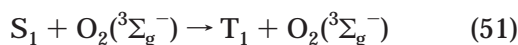
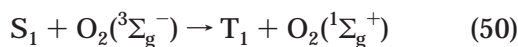
Kinetic studies on the deactivation of excited singlet (S_1) and triplet (T_1) states by O_2 have been

performed since the early 1950s.^{293–303} These investigations made it clear that O₂ quenches excited states of both multiplicities, with variable rate constants close to the diffusion-controlled limit. Later studies showed that both quenching processes can lead to energy transfer, which means that the overall quantum yield of singlet oxygen formation, Q_{Δ} ,

$$Q_{\Delta} = p_{S^{\text{O}_2}}^{\text{O}_2} f_{S^{\Delta}}^{\text{O}_2} + Q_{T^{\text{O}_2}} p_{T^{\text{O}_2}}^{\text{O}_2} S_{\Delta} \quad (49)$$

may vary between 0 and 2. In eq 49, $p_{S^{\text{O}_2}}^{\text{O}_2}$ and $p_{T^{\text{O}_2}}^{\text{O}_2}$ are the fractions of S₁ and T₁ states quenched by oxygen, $f_{S^{\Delta}}^{\text{O}_2}$ is the efficiency of singlet oxygen production during O₂ quenching of S₁, and $Q_{T^{\text{O}_2}}$ is the triplet quantum yield. The overall efficiency S_{Δ} of singlet oxygen generation during O₂ quenching of T₁ is the sum of the efficiencies a of formation of O₂(¹Σ_g⁺) and b of directly formed O₂(¹Δ_g).

In the case of O₂ quenching of S₁ states, five spin-allowed (eqs 50–54) and two spin-forbidden processes (eqs 55 and 56) have to be considered.



The four enhanced isc pathways (eqs 50–53) lead to formation of the first (T₁) or second (T₂) excited sensitizer triplet state and either of the three lowest O₂ states. The three enhanced internal conversion (ic) processes (eqs 54–56) generate the sensitizer ground state (S₀) and O₂(³Σ_g⁻), O₂(¹Σ_g⁺), or O₂(¹Δ_g). With the exception of a few compounds with high oxidation potentials and low excited-state energies, the experimental overall S₁ quenching rate constants $k_S^{\text{O}_2}$ are found to be nearly collision-controlled in the gas phase^{294,299,304,305} or diffusion-controlled in the liquid phase.^{226,297,298,306–309} However, all quenching pathways compete with relatively efficient intramolecular deactivation processes, and $p_{S^{\text{O}_2}}^{\text{O}_2}$ values distinctly smaller than unity are commonly found under air-saturated conditions in solution. The first experimental studies were concerned with the multiplicity of the sensitizer product state, and it was shown that isc (eqs 50–53) is dominant over ic (eqs 54–56); i.e., oxygen quenching of S₁ states leads mainly to formation of a triplet state.^{302,310–316} Brauer and Wagener^{317,318} first provided clear evidence for overall singlet oxygen yields larger than unity, thus showing that the energy-transfer process 52 can significantly contribute to the deactivation of S₁. These observations are obviously limited to molecules having a S₁–

T₁ energy gap larger than 94 kJ mol⁻¹, such as rubrene,^{308,317,319–324} heteroacridanthrone,^{318,319} tetracene,^{308,319,324,325} perylene,^{308,321,325,326} pyrene,^{308,321,325–328} chrysene,^{308,325–327} 1,3-diphenylisobenzofuran,³²² 1,6-diphenylhexatriene,³²¹ fluoranthene,^{325,326} a large series of anthracene derivatives,^{308,319,321,322,327–334} and several organic cations.³³⁵ No evidence has been obtained for process 50. This pathway would require a S₁–T₁ energy gap larger than 157 kJ mol⁻¹, which is normally not observed. Thus, enhanced isc, leading to formation of T₁ and O₂(³Σ_g⁻), is probably the dominant pathway for the deactivation of S₁ by O₂ in most cases.

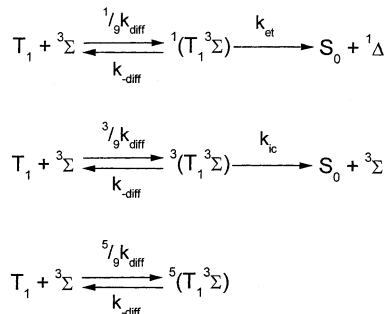
However, other observations have also been reported. Stevens and Mills³³⁶ first suggested that formation of the second excited triplet state, T₂ (process 53), could contribute to the overall process. Systematic studies by Wilkinson et al.³³³ showed that the efficiency of singlet oxygen formation during oxygen quenching of singlet states is a function of the relative importance of process 53.

Darmanyan suggested that the enhanced ic process 54 is also possible³²⁹ but is far from being general.³²³ This finding, made in triplet–triplet absorption experiments with 9,10-diphenylanthracene in toluene, was corroborated by Brauer's group in photo-oxygenation experiments.³³⁰ It was concluded that the O₂-enhanced ic could be promoted for few *meso*-diphenyl-substituted acenes by the formation of sterically hindered conformers.^{323,324} Triplet–triplet absorption experiments conducted by Potashnik et al.³¹⁵ demonstrated that the efficiency of T₁-state formation in the fluorescence quenching by O₂ decreases with solvent polarity for several condensed aromatic hydrocarbons and amounts to only 0.55 for pyrene in acetonitrile. It was suggested that CT interactions enhance the O₂-induced ic. Later works by the groups of Ogilby,³³⁷ Kikuchi,^{226,307,338} Wilkinson,^{325,326,333,334} and Brauer^{309,335} made it clear that the CT-induced, O₂-enhanced ic process 54 is of little importance in nonpolar solvents, whereas it becomes competitive with processes 51–53 in polar solvents.

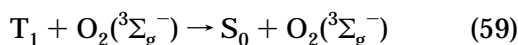
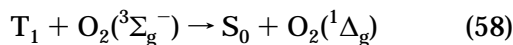
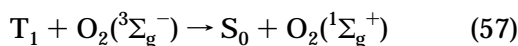
On the basis of measurements of oxygen consumption kinetics with 1,3-diphenylisobenzofuran in benzene, Stevens and Small³³⁹ ruled out the spin-forbidden processes 55 and 56. Thus, it appears that, in the absence of strong CT interactions, enhanced ic cannot compete efficiently with spin-allowed enhanced isc, either due to the large energy gap (process 54) or due to spin-forbiddenness (processes 55 and 56).

Hence, for most sensitizers, the role of O₂ quenching of S₁ is limited to enhancement of the triplet quantum yield, and the main pathway of singlet oxygen generation is O₂ quenching of the first excited triplet state, T₁. Because the intramolecular T₁ → S₀ transition is spin-forbidden, T₁ states generally have long lifetimes, allowing mostly for complete quenching by O₂ (i.e., $p_{T^{\text{O}_2}}^{\text{O}_2} \approx 1$) in air-saturated solution. Incomplete quenching is observed only with triplet states possessing a short lifetime due to high chemical reactivity or fast isc (i.e., $n\pi^*$ triplets), or in the presence of very high concentrations of other quench-

Scheme 2. Mechanism of Singlet Oxygen ($^1\Delta$) Sensitization during Quenching of Triplet States (T_1) by Ground-State Oxygen ($^3\Sigma$), As Proposed by Gijzeman et al. in the First Mechanistic Study of This Process



ers. If the T_1 -state energy is higher than 157 kJ mol⁻¹, then three possible spin-allowed processes,



are commonly observed, with overall rate constant k_T^Q significantly below the diffusion-controlled limit. In contrast to the interaction of excited singlet states with $O_2({}^3\Sigma_g^-)$, where only encounter complexes of triplet multiplicity can be formed, the deactivation of excited triplet states by ground-state O_2 is somewhat more complicated. This is expressed in Scheme 2, which was originally proposed by Gijzeman et al.³⁴⁰ in 1973, and served as a basis for the discussion of the deactivation of T_1 states by O_2 in many later studies.

Scheme 2 implies that the diffusion-controlled encounter of excited triplet sensitizer and triplet ground-state O_2 leads to reversible formation of excited ${}^{1,3,5}(T_1 {}^3\Sigma)$ complexes, whereby nine spin configurations are possible. Statistically, one of them will have singlet multiplicity, three will be triplets, and five will be quintets. Energy transfer occurs only within the singlet channel, whereas enhanced ic in the triplet channel yields S_0 and ground-state $O_2({}^3\Sigma_g^-)$. Since the quintet complex has no spin- and energy-allowed product, the rate constant for O_2 quenching of triplet states is expressed by eq 60, where k_{diff} and

$$k_T^Q = \frac{1}{9} \frac{k_{\text{diff}} k_{\text{et}}}{k_{\text{diff}} + k_{\text{et}}} + \frac{1}{3} \frac{k_{\text{diff}} k_{\text{ic}}}{k_{\text{diff}} + k_{\text{ic}}} \quad (60)$$

k_{diff} are the rate constants for formation and separation of encounter complexes, respectively, and k_{et} and k_{ic} are the rate constants for energy transfer and ic, respectively. Thus, if only the singlet channel contributes to the deactivation of T_1 by O_2 (i.e., $k_{\text{ic}} \ll k_{\text{diff}}$), we would expect $k_T^Q \leq 1/9 k_{\text{diff}}$ and, of course, S_Δ values of unity. If, in contrast, quenching proceeds via both the singlet and triplet channels, we expect $k_T^Q \leq 4/9 k_{\text{diff}}$ and $0.25 \leq S_\Delta \leq 1$. Since all k_T^Q values reported by Gijzeman et al.³⁴⁰ were clearly below

$1/9 k_{\text{diff}}$, it was originally concluded that oxygen quenching of T_1 states results exclusively in energy transfer.

However, also in 1973, Truscott et al.²⁷⁸ measured rate constants for oxygen quenching of triplet states of carotenoids on the order of $10^9 \text{ M}^{-1} \text{ s}^{-1}$. In these cases, only formation of $O_2({}^3\Sigma_g^-)$ is possible (since $E_T < 94 \text{ kJ mol}^{-1}$); hence, it is strongly indicated that process 59 may be far from negligible. However, the corresponding T_1 -state energies were unknown at that time, and only later studies demonstrated the importance of process 59, by providing evidence for k_T^Q values in excess of $1/9 k_{\text{diff}}$,³⁴¹⁻³⁵⁰ and even in excess of $4/9 k_{\text{diff}}$.³⁵¹⁻³⁵³ These results show clearly that that the triplet complex, and in some cases also the quintet complex, may contribute significantly to the quenching process.

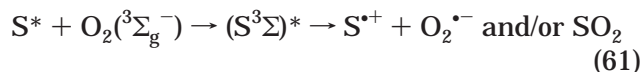
Since the late 1970s, several techniques (including pulse radiolysis,³⁵⁴ thermal lensing,³⁵⁵ photoacoustic calorimetry,^{83,356,357} and time-resolved ${}^1\Delta_g \rightarrow {}^3\Sigma_g^-$ phosphorescence measurements)³⁵⁸⁻³⁶⁰ have been proposed to quantify the overall quantum yield Q_Δ and efficiency S_Δ of singlet oxygen formation during oxygen quenching of T_1 states. It has rapidly become clear that, for most compounds, S_Δ is smaller than unity and varies significantly with sensitizer properties and environment. This confirms, once again, the importance of process 59.

In 1993, Wang and Ogilby³⁶¹ used the ${}^1\Sigma_g^+ \rightarrow {}^1\Delta_g$ fluorescence to make the first quantitative determinations of the fraction of $O_2({}^1\Sigma_g^+)$ formed in photosensitization experiments, and Schmidt and Bodesheim¹⁵² combined time-resolved ${}^1\Sigma_g^+ \rightarrow {}^3\Sigma_g^-$ and ${}^1\Delta_g \rightarrow {}^3\Sigma_g^-$ phosphorescence measurements to obtain absolute values for the efficiencies a and b of $O_2({}^1\Sigma_g^+)$ and $O_2({}^1\Delta_g)$, directly formed during O_2 quenching of T_1 states, allowing the calculation of the rate constants $k_T^{1\Sigma}$, $k_T^{1\Delta}$, and $k_T^{3\Sigma}$ for formation of $O_2({}^1\Sigma_g^+)$, $O_2({}^1\Delta_g)$, and $O_2({}^3\Sigma_g^-)$, respectively. Surprisingly, the ratio $k_T^{1\Sigma}/k_T^{1\Delta}$ was significantly smaller than expected for an electron-exchange energy-transfer mechanism according to Dexter.³⁶² Indeed, the integrals for spectral overlap of the $O_2({}^1\Sigma_g^+) \leftarrow O_2({}^3\Sigma_g^-) 0 \leftarrow 0$ absorption spectrum with common sensitizer T_1 emission spectra were calculated to be 2.5 orders of magnitude larger than those for overlap with the $O_2({}^1\Delta_g) \leftarrow O_2({}^3\Sigma_g^-) 0 \leftarrow 0$ transition.³⁶² Hence, a $k_T^{1\Sigma}/k_T^{1\Delta}$ ratio on the order of 500 would be expected, instead of the experimentally found $k_T^{1\Sigma}/k_T^{1\Delta} \leq 10$.³⁶³ This means that singlet oxygen formation during oxygen quenching of excited triplet states cannot be rationalized by common Dexter-type electron-exchange energy transfer.

While many S_Δ determinations have been made, the most important experimental problem in many systematic studies has been the incomplete nature of the T_1 quantum yield of many compounds. Many efforts have been made to overcome this problem. Gorman et al.⁶³ and Wilkinson et al.³⁶⁴⁻³⁶⁷ proposed populating T_1 states by energy transfer from a higher-lying T_1 state, being formed with high and known efficiency. Triplet benzophenone was shown to be an ideal sensitizer to generate the T_1 states of naphthalene and biphenyl derivatives with unit efficiency. Recently, Shafii and Schmidt³⁶⁸ adapted

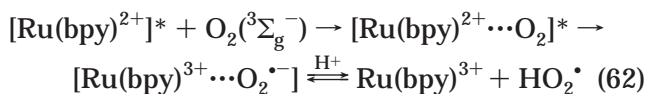
the methodology to $O_2(^1\Sigma_g^+)$ efficiency determinations, where fast $e-v$ deactivation allows for only low concentrations of aromatic hydrocarbons in the medium. This leads to incomplete quenching of triplet benzophenone by the sensitizer under investigation; hence, singlet oxygen formation from triplet benzophenone also needs to be accounted for.³⁶⁸

Another problem may arise from the fact that, in competition with energy transfer and enhanced isc (processes 50–59), formation of ions and/or chemical reactions may occur within the complexes of O_2 with excited sensitizer states. In eq 61, S^* represents an excited singlet or triplet state of the sensitizer molecule S .



Sato et al.²²⁶ studied the possibility of formation of ions during oxygen quenching of excited singlet states in acetonitrile. Among several investigated aromatic hydrocarbons, only one compound, 2,6-dimethoxynaphthalene, induced noticeable formation of ions. However, the ionization quantum yield was found to be as low as 0.003.

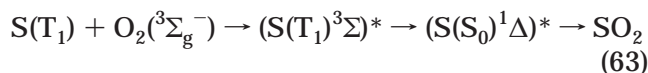
More investigations have been concerned with the possibility of process 61 during O_2 quenching of T_1 states. For example, Winterle et al.³⁶⁹ observed the formation of Ru^{3+} complexes upon O_2 quenching of excited tris(2,2'-bipyridyl)ruthenium(II) complexes ($Ru(bpy)^{2+}$) in acidic aqueous solutions. However, the process was found to be extremely inefficient: the authors reported a quantum yield as low as 0.035 for chemical bleaching of Ru^{2+} complexes. More recently, Zhang and Rodgers³⁷⁰ found an increase of the quantum yield for this process from 0 to 0.297, when the acid (D_2SO_4) concentration was increased from 0 to 5.0 M. However, the singlet oxygen yields were not affected by the acid concentration. The authors proposed that the mechanism displayed in eq 62 competes with processes 57–59 in this case.



Several chemical processes have also been suggested in the case of porphyrins and metalloporphyrins. Spin-trapping experiments conducted by Cox et al.³⁷¹ revealed the formation of "appreciable" quantities of superoxide during oxygen quenching of porphyrins and metalloporphyrins in several solvents. However, no quantum yields were determined, and the authors estimated that the process is significantly less efficient than energy transfer. A very puzzling effect was reported by Tanielian and Wolff³⁷² for O_2 quenching of the T_1 states of tetraphenylporphyrin and its Zn and Mg complexes. While identical values were found for near-infrared-emission- and oxygen-consumption-based determinations of Q_Δ for several compounds, the porphyrins showed significant differences between the two techniques. Since the value from $^1\Delta_g \rightarrow ^3\Sigma_g^-$ luminescence measurements ($Q_\Delta = 0.60$) was lower than that from O_2 consumption measurements ($Q_\Delta = 0.80$), it was argued that a long-

lived nonemissive complex may be formed between $O_2(^1\Delta_g)$ and the ground-state sensitizer. However, a recent redetermination of Q_Δ , using time-resolved $^1\Delta_g$ luminescence under conditions similar to those used in O_2 consumption experiments, yielded a value of 0.78, identical within experimental error to Tanielian and Wolff's previous O_2 consumption determination.³⁷³ Hence, the formation of long-lived nonemissive complexes between $O_2(^1\Delta_g)$ and the ground-state sensitizer has been ruled out.

Brauer et al.³⁷⁴ investigated the possibility of the geminate reaction,



during self-sensitized photo-oxygenations of helianthrene derivatives (S) in several solvents. Their treatment of oxygenation data led to quantum yields Q_{PO} up to 0.19 for this process in the case of helianthrene in high-viscosity solvents. However, the reaction was found to be less important in the case of *meso*-diphenylhelianthrene ($Q_{PO} < 0.13$) and largely negligible for *meso*-diphenylbenzhelianthrene ($Q_{PO} < 0.0035$).

In an early study, Gorman and Rodgers³⁷⁵ reported low singlet oxygen yields and multiexponential $^1\Delta_g$ phosphorescence decay signals in the presence of aromatic ketones, which they attributed to a rather complicated chemical mechanism. It was proposed that the generation of singlet oxygen competes with the successive formation of biradicals and trioxetane, whereupon quenching of $O_2(^1\Delta_g)$ by trioxetane would regenerate the ketone and two molecules of ground-state oxygen. However, this mechanism implies the possibility of exchange of an oxygen atom between the ketone and the O_2 molecule, which was ruled out some years later. Indeed, Bendig et al.³⁷⁶ showed that excitation of *N*-methylacridone (NMA, $S_\Delta = 0.29$) in $^{18}O_2$ -saturated solutions changes neither the mass of NMA nor the $^{18}O_2$ content of the dissolved O_2 molecules, which means that no exchange takes place between the ketone ^{16}O atom and $^{18}O_2$. The formation of trioxetane is thus excluded in this case. However, very recently, Cosa and Scaiano³⁷⁷ provided spectroscopic evidence for formation of a T_1 state– O_2 adduct during O_2 quenching of an excited diketone.

Finally, it is also important to know that several other pathways of singlet oxygen formation may be observed in addition to the energy-transfer quenching of S_1 and T_1 states. In the early 1950s, Evans³⁷⁸ and Munck and Scott³⁷⁹ reported that numerous organic molecules S (including alcohols, amines, aromatic hydrocarbons, and thus many common solvents) form ground-state complexes with $O_2(^3\Sigma_g^-)$, which are characterized by an absorption band that disappears when O_2 is removed from the solution. Tsubomura and Mulliken³⁸⁰ found a strong linear correlation between the maximum wavenumber of this band and the ionization potential of $S(S_0)$. Thus, these ground-state complexes possess a certain charge-transfer character and may be characterized as $^3(S^{\delta+}O_2^{\delta-})$. Irradiation of the band leads to formation of an excited CT complex $^3(S^{\delta+}O_2^{\delta-})^*$, which was shown by Scurlock and Ogilby to be a precursor of $O_2(^1\Delta_g)$.^{381,382}

Quantum yields Q_{Δ}^{CT} of $\text{O}_2(^1\Delta_{\text{g}})$ formation upon CT band excitation are rather high, even for alkanes, e.g., 0.12 for decalin and 0.22 for cyclohexane.³⁸² Since in the case of alkanes no low-lying excited states exist, which could sensitize $\text{O}_2(^1\Delta_{\text{g}})$, it was assumed that the reaction sequence $^3(\text{S}^{\delta+}\text{O}_2^{\delta-})^* \rightarrow ^1(\text{S}^{\delta+}\text{O}_2^{\delta-})^* \rightarrow ^1(\text{S}(\text{S}_0)^1\Delta) \rightarrow \text{S}(\text{S}_0) + \text{O}_2(^1\Delta_{\text{g}})$ is operative. Kristiansen et al.³³⁷ demonstrated that, for the excited CT complex of $\text{O}_2(^3\Sigma_{\text{g}}^-)$ with 1-methylnaphthalene (MN), dissociation forming radicals cannot compete with fast deactivation to $^{1,3}(\text{S}(\text{T}_1)^3\Sigma)$, which was suggested to be the only precursor of $\text{O}_2(^1\Delta_{\text{g}})$ in that system in cyclohexane. However, in acetonitrile, a significant decrease in the efficiency of $\text{O}_2(^1\Delta_{\text{g}})$ formation was observed, and it was proposed that, in a polar solvent, direct coupling of the excited CT state to the ground-state surface of $^3(\text{S}(\text{S}_0)^3\Sigma)$ may increase, providing a deactivation channel that will compete with $\text{O}_2(^1\Delta_{\text{g}})$ formation.³³⁷

Picosecond laser flash experiments on MN by Logunov and Rodgers yielded results which are consistent with the findings of Kristiansen et al. in cyclohexane.³⁸³ It was concluded that, in the deactivation of the $^3(\text{S}^{\delta+}\text{O}_2^{\delta-})^*$ complex, formation of T_1 -excited MN and $\text{O}_2(^3\Sigma_{\text{g}}^-)$ competes with ic to the ground-state $^3(\text{S}^{\delta+}\text{O}_2^{\delta-})$ complex. The first reaction should dominate in cyclohexane, whereas both deactivation paths contribute in equal amounts in acetonitrile, thus explaining the reduced quantum yield of $\text{O}_2(^1\Delta_{\text{g}})$ formation.³⁸³

Quantum yields of $\text{O}_2(^1\Delta_{\text{g}})$ formation of upon excitation of the CT band of 1-ethylnaphthalene (EN) were determined by McGarvey et al.³⁸⁴ in picosecond absorption experiments. Q_{Δ}^{CT} values of 0.78 (cyclohexane) and 0.36 (acetonitrile) were obtained, which are significantly larger than the quantum yields $Q_{\Delta} = Q_{\text{T}}S_{\Delta}$ of $\text{O}_2(^1\Delta_{\text{g}})$ production, 0.69 (cyclohexane) and 0.20 (acetonitrile), which are expected on the basis of the known values of S_{Δ} and the measured triplet quantum yields Q_{T} upon $^3(\text{S}^{\delta+}\text{O}_2^{\delta-})^*$ excitation. Thus, at least in acetonitrile, more $\text{O}_2(^1\Delta_{\text{g}})$ is produced from the $^3(\text{S}^{\delta+}\text{O}_2^{\delta-})^*$ state than can be accounted for from the amount of EN triplet state produced. To explain this result, it was suggested that the energy of the $^3(\text{S}^{\delta+}\text{O}_2^{\delta-})^*$ excited CT state should be high enough to deactivate partially via a doubly excited $^3(\text{S}(\text{T}_1)^1\Delta)$ complex, which dissociates under formation of T_1 -excited EN and $\text{O}_2(^1\Delta_{\text{g}})$.³⁸⁴ These studies consistently demonstrate that irradiation of the O_2 CT bands of saturated or unsaturated organic molecules also produces $\text{O}_2(^1\Delta_{\text{g}})$ in considerable yields.^{337,381–384}

A. Oxygen Quenching of Excited Triplet States

1. Parameters Influencing the Generation of Singlet Oxygen

a. Influence of the Triplet-State Energy. When photosensitized formation of singlet oxygen occurs upon energy transfer from an excited triplet state of energy E_{T} , theory predicts a dependence of quenching rate constants on the excess energy ΔE and thus on E_{T} . In the first theoretical work on this subject, Kawaoka et al.³⁸⁵ proposed eq 64, where k_{ic} repre-

$$k_{\text{ic}} = (4\pi^2/h)\rho(\Delta E)F(\Delta E)\beta^2 \quad (64)$$

sents the rate constants for the ic from the initially formed, electronically excited sensitizer–oxygen complexes $^{1,3}(\text{T}_1^3\Sigma)$ with excitation energy E_{T} to complexes $^1(\text{S}_0^1\Sigma)$, $^1(\text{S}_0^1\Delta)$, and $^3(\text{S}_0^3\Sigma)$, with excitation energies E_{Σ} , E_{Δ} , and zero, respectively, which dissociate finally to form the ground-state sensitizer S_0 and $\text{O}_2(^1\Sigma_{\text{g}}^+)$, $\text{O}_2(^1\Delta_{\text{g}})$, and $\text{O}_2(^3\Sigma_{\text{g}}^-)$, respectively. The corresponding excess energies which have to be dissipated are $\Delta E = E_{\text{T}} - E_{\Sigma}$, $E_{\text{T}} - E_{\Delta}$, and E_{T} . k_{ic} is expressed as a function of the electronic coupling matrix element between initial and final states, β , and of the Franck–Condon factors, $F(\Delta E)$, and the density of final states, $\rho(\Delta E)$ which both depend on ΔE . Because the Franck–Condon factor for O_2 becomes exceedingly small if the initial and final vibrational states of the O_2 molecule differ by more than a few quanta, it can be assumed that most of the vibrational energy goes into the organic molecule.³⁸⁵ This means that variations in k_{ic} will be principally determined by variations in the Franck–Condon weighted density of states factor, $F(\Delta E) = \rho(\Delta E)F(\Delta E)$, of the sensitizer, which, as shown by Siebrand, decreases strongly with increasing excess energy for aromatic hydrocarbons.^{386–388} Hence, the T_1 -state quenching rate constants should decrease with increasing E_{T} .³⁸⁵ Corroborative experimental results came only a few years later, from the works of Patterson et al.³⁸⁹ and Gijzeman et al.,³⁴⁰ who observed inverse correlations of k_{T}^{O} with E_{T} during investigations of a large number of aromatic hydrocarbons. Twenty years later, Bodesheim et al.³⁶³ presented the first systematic study of the excess energy dependence of the rate constants $k_{\text{T}}^{1\Sigma}$, $k_{\text{T}}^{1\Delta}$, and $k_{\text{T}}^{3\Sigma}$ for formation of $\text{O}_2(^1\Sigma_{\text{g}}^+)$, $\text{O}_2(^1\Delta_{\text{g}})$, and $\text{O}_2(^3\Sigma_{\text{g}}^-)$ during O_2 quenching of the T_1 states of aromatic compounds. These workers correlated multiplicity-normalized values of $\log(k_{\text{T}}^{\text{P}}/m)$ (i.e., using $k_{\text{T}}^{1\Sigma}$, $k_{\text{T}}^{1\Delta}$, and $k_{\text{T}}^{3\Sigma}/3$) with ΔE . Figure 24 shows the corresponding plot for the 11 $\pi\pi^*$ triplet sensitizers investigated.

From the common dependence of all $\log(k_{\text{T}}^{\text{P}}/m)$ values in the $\Delta E \leq 220$ kJ mol⁻¹ region, it was concluded that (i) the matrix elements (β) for ic of excited singlet and triplet $^{1,3}(\text{T}_1^3\Sigma)$ complexes of all compounds are the same, and (ii) there must be a fully established equilibrium between the singlet and triplet complexes. The empirical curve of Figure 24, describing the experimental data, should then directly reflect the excess energy dependence of the rate constants of ic of $^{1,3}(\text{T}_1^3\Sigma)$ complexes.³⁶² This curve is given by the polynomial depicted in eq 65, which

$$\log(k_{\Delta E}^{\text{P}}/m) = 9.05 + (9 \times 10^{-3})\Delta E - (1.15 \times 10^{-4})\Delta E^2 + (1.15 \times 10^{-7})\Delta E^3 + (9.1 \times 10^{-11})\Delta E^4 \quad (65)$$

applies to binary complexes of $\text{O}_2(^3\Sigma_{\text{g}}^-)$ and $\text{T}_1(\pi\pi^*)$ -excited aromatic molecules with high oxidation potentials in CCl_4 solution, where CT-assisted quenching of T_1 by O_2 is negligible if E_{ox} exceeds ca. 1.8 V vs SCE³⁶² (see section IV.A.1.b for a discussion of charge-transfer interactions). Figure 24 also displays

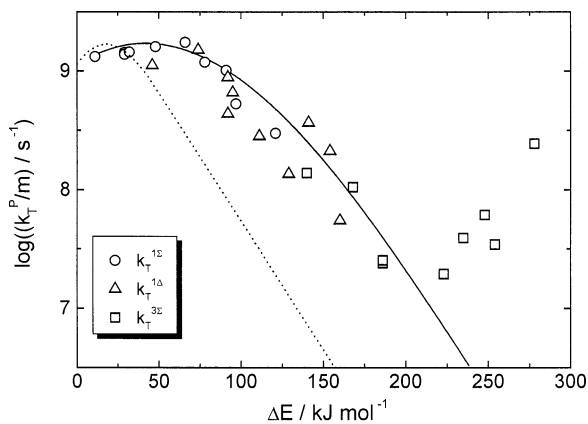


Figure 24. Dependence of multiplicity-normalized rate constants k_T^P/m for photosensitized formation of O_2 product state P [i.e., $O_2(^1\Sigma_g^+)$, $O_2(^1\Delta_g)$, or $O_2(^3\Sigma_g^-)$] on the corresponding excess energy, ΔE , for a series aromatic compounds in CCl_4 . The solid line is given by eq 65,³⁶² and the dotted line corresponds to Siebrand's energy gap law.³⁸⁶ Reprinted with permission from Bodesheim, M.; Schütz, M.; Schmidt, R. *Chem. Phys. Lett.* **1994**, *221*, 7–14. Copyright 1994 Elsevier Science.

the function $\log(F'(\Delta E))$ evaluated by Siebrand.³⁸⁶ This function strongly declines with ΔE , since it corresponds to the ic between deep potential minima of strongly bound aromatic molecules, in contrast to the broad experimental curve, which is related to ic occurring from shallow minima of very weakly bound $^{1,3}(T_1^3\Sigma)$ complexes.³⁶³

Recently, Abdel-Shafi et al.³⁹⁰ also correlated $\log(k_T^P/m)$ data for a series of Ru complexes with ΔE . Values for $\log(k_T^{1\Sigma})$ and $\log(k_T^{1\Delta})$ were estimated to fall on a curve similar to eq 65, while values of $\log(k_T^{3\Sigma}/3)$ were measured to be significantly larger. The same authors also measured $k_T^{3\Sigma}$ and the sum $(k_T^{1\Sigma} + k_T^{1\Delta})$ for a large number of aromatic hydrocarbons in solvents where distinction between $O_2(^1\Sigma_g^+)$ and $O_2(^1\Delta_g)$ is currently not possible (due to extremely fast deactivation of $O_2(^1\Sigma_g^+)$; see section III.B.3.c). Similarly to the previous works, they also proposed correlations of k_T^Q with E_T , and of $(k_T^{1\Sigma} + k_T^{1\Delta})$ with $\Delta E = E_T - 157 \text{ kJ mol}^{-1}$ in those cases where $O_2(^1\Sigma_g^+)$ formation is possible.^{326,391} The lowest $(k_T^{1\Sigma} + k_T^{1\Delta})$ values determined for aromatic hydrocarbons in cyclohexane solution were correlated with the empirical curve of eq 66, with $F = 2.5$ or 4.3 s^{-1} ,

$$(k_T^{1\Sigma} + k_T^{1\Delta}) = F \times 10^{11} (10^{-0.014(E_T-157)} + 10^{-0.014(E_T-94)}) \quad (66)$$

respectively,^{326,391} representing the excess energy relation for rate constants of singlet oxygen formation without CT assistance. This energy dependence is also less steep than expected from Siebrand's theory.

b. Influence of the Oxidation Potential. When the sensitizer is an easily oxidizable molecule, CT interactions with O_2 strongly influence the rate and efficiency of singlet oxygen formation. The first experimental evidence for such behavior came from the 1977 study reported by Garner and Wilkinson,³⁴² who noted clear deviations from Gijzeman's inverse dependence of k_T^Q on E_T . Instead, they reported an

increase of k_T^Q with E_T for compounds with high triplet energies ($E_T > 240 \text{ kJ mol}^{-1}$) and attributed this behavior to an enhancement of the rate of quenching by the presence of triplet CT states lying nearby T_1 . Later studies correlated singlet oxygen formation parameters with sensitizer E_{ox} , or with the free energy ΔG_{CET} for formation of an ion pair, which is calculated by the Rehm–Weller equation, $\Delta G_{CET} = F(E_{ox} - E_{red}) - E_{exc} + C$, as introduced in section III.B.4.a. Here, the excitation energy is the sensitizer triplet energy ($E_{exc} = E_T$), and thus, an increase in E_T will also result in an increase of the oxidizability of the excited complexes; i.e., k_T^Q values are expected to increase with increasing E_T , in contrast to regular energy transfer, as described above. Cebul et al.³⁴⁴ first noted a dependence of gas-phase O_2 quenching rate constants for several ketone triplet states on redox properties, and Chattopadhyay et al.³⁹² first correlated liquid-phase k_T^Q data for a series of benzophenone derivatives with Hammett σ^+ parameters. Several authors also reported the dependence of $O_2(^1\Delta_g)$ formation efficiencies (S_Δ) on redox properties. Smith determined S_Δ for several aromatic hydrocarbons with strongly varying E_T and found values decreasing from 1.0 for anthracene to 0.25 for triphenylene.³⁹³ Consideration of the corresponding oxidation potentials demonstrated that S_Δ becomes distinctly smaller with decreasing ΔG_{CET} . It was concluded that this results from a deactivation pathway proceeding through CT complex states. Exactly the opposite behavior (i.e., a decrease of S_Δ with increasing E_{ox}) was reported a few years later by McLean and Truscott.³⁹⁴ However, molecules with strongly varying excited-state properties were investigated in this study, and other parameters besides E_{ox} may have influenced S_Δ . The results of Smith were clearly corroborated by a systematic investigation by McGarvey et al.,³⁶⁴ who used a series of naphthalene derivatives, where a change in substituent leads to strong variations in E_{ox} , while all other relevant parameters (including E_T) remain nearly constant. It was found that an increase in E_{ox} results in a systematic increase in S_Δ and in a decrease in k_T^Q ; i.e., singlet oxygen formation becomes faster but less efficient with decreasing ΔG_{CET} . Similar results were obtained with derivatives of biphenyl^{350,366,367} and fluorene,³⁹⁵ amines,³⁵³ Ru complexes,^{396,397} and benzophenone derivatives,³⁹⁸ where E_T also remains almost constant upon introduction of E_{ox} -modifying substituents. These results were confirmed in non-polar as well as in polar solvents, as is illustrated in Figure 25 by the inverse correlation of the overall efficiencies S_Δ with the relative overall quenching rate constants k_T^Q/k_{diff} , determined for a series of biphenyl derivatives in cyclohexane, benzene, and acetonitrile by Wilkinson and Abdel-Shafi.^{366,367} Additionally, these investigations demonstrated that the dependence of k_T^Q on ΔG_{CET} is much weaker than expected for a complete electron transfer; thus, it was concluded that the rate-determining step features complexes bearing partial CT character. However, the correlation for benzophenone derivatives differs strongly from that for other aromatic hydrocarbons³⁹⁸ (as a consequence of their $n\pi^*$ T_1 -state configuration;

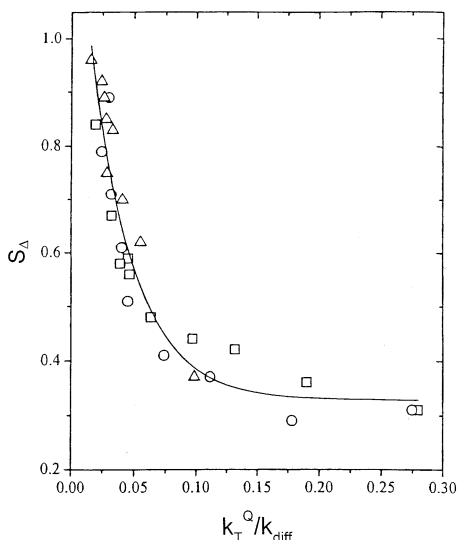


Figure 25. Dependence of the efficiency of $O_2(^1\Delta_g)$ production, S_Δ , on the relative rate constant for quenching of triplet state by oxygen, k_T^O/k_{diff} , for substituted biphenyls in acetonitrile (\square), benzene (\circ), and cyclohexane (\triangle). Reprinted with permission from ref 367. Copyright 1999 American Chemical Society.

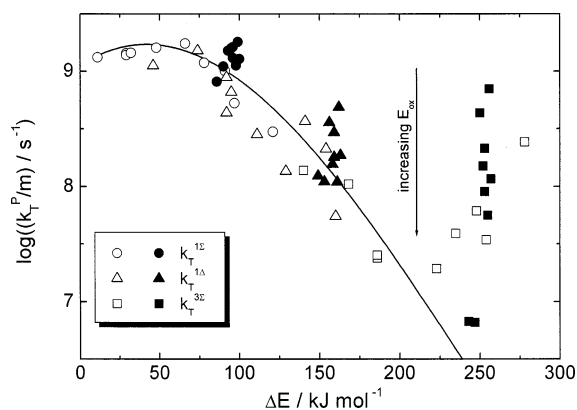


Figure 26. Dependence of $\log(k_T^P/m)$ for a series of $\pi\pi^*$ triplet-excited aromatic compounds on ΔE . The solid line is given by eq 65. Solid symbols correspond to a series of naphthalene derivatives, with strongly varying oxidation potentials. Reprinted with permission from ref 362. Copyright 2001 American Chemical Society.

see section IV.A.3), and Ru complexes also display a modified behavior.^{390,399}

Combining $O_2(^1\Delta_g)$ efficiency and k_T^O determinations, McGarvey et al.³⁶⁴ also showed that the oxidation potential has a stronger effect on the triplet channel than on the singlet channel. This was confirmed by Grewer and Brauer,⁴⁰⁰ who used a broader range of aromatic hydrocarbons, and more recently by Darmanyan et al.,³⁵³ who found an excellent common correlation for a large set of $\log(k_T^{3\Sigma})$ values with ΔG_{CET} but a less steep and also less accurate correlation for $\log(k_T^{1\Sigma} + k_T^{1\Delta})$ of the same compounds. Further confirmation of this behavior has also come from the recent $O_2(^1\Sigma_g^+)$ efficiency determinations. In Figure 26, the E_{ox} -dependent $\log(k_T^P/m)$ data for a series of naphthalene derivatives³⁶² are superimposed on the previously described ΔE -dependent $\log(k_T^P/m)$ data.³⁶³ At constant E_T , the multiplicity-normalized rate constants

for formation of each O_2 product state increase with decreasing E_{ox} , and the variation is clearly the most prominent in the triplet channel, while it is less important for $O_2(^1\Delta_g)$ formation and even smaller for formation of $O_2(^1\Sigma_g^+)$. This graduation was clearly reproduced with a series of biphenyl derivatives,³⁵⁰ and also a series of fluorene derivatives,³⁹⁵ but only a weak graduation was found with $n\pi^*$ -excited benzophenones.³⁹⁸

No E_{ox} dependence was observed for a series of anthracene derivatives in cyclohexane.³³³ In this case, $S_\Delta = 1$ and $k_T^O = 1/9 k_{diff}$ was found for all derivatives, despite a large variation in E_{ox} . This indicates that the particularly low triplet energies ($E_T \approx 172$ kJ mol⁻¹; values for all other investigated sensitizer series are at least 70 kJ mol⁻¹ higher) of these compounds suppress efficient CT-induced quenching in this nonpolar solvent. However, the sole indication for a CT mechanism with anthracenes was given in the very polar solvent acetonitrile, where $S_\Delta = 0.33$ was found for the most easily oxidizable compound in this series, 9-methoxyanthracene.³³⁴ These results may thus indicate that energy transfer and charge transfer can be simultaneously operative. This is also strongly suggested by the results displayed in Figure 26. The fact that the lowest $\log(k_T^P/m)$ values (i.e., for sensitizers with the highest oxidation potentials and negligible CT interactions) fall on the previously determined curve of the ΔE dependence for aromatic hydrocarbons was explained by a common dependence of k_T^P/m on both ΔE and ΔG_{CET} , i.e., all three k_T^P/m values can be considered as a sum of a ΔE -dependent contribution $k_{\Delta E}^P/m$ and a ΔG_{CET} -dependent contribution k_{CT}^P/m (eqs 67–69).³⁶²

$$k_T^{1\Sigma} = k_{\Delta E}^{1\Sigma} + k_{CT}^{1\Sigma} \quad (67)$$

$$k_T^{1\Delta} = k_{\Delta E}^{1\Delta} + k_{CT}^{1\Delta} \quad (68)$$

$$k_T^{3\Sigma} = k_{\Delta E}^{3\Sigma} + k_{CT}^{3\Sigma} \quad (69)$$

Abdel-Shafi et al.^{326,391} recently successfully applied this additivity assumption. Using the excess energy relation 66 for singlet oxygen formation without CT assistance, they calculated the corresponding CT contributions, named ${}^m k_T^m f_p / k_{diff}$, from the overall rate constants of singlet oxygen formation for 17 naphthalene derivatives of widely varying E_{ox} . Figure 27 shows plots of relative rate constants ${}^m k_T^m f_p / k_{diff}$ of CT-induced singlet ($m = 1$) and triplet oxygen ($m = 3$) formation versus ΔG_{CET} . Since the slopes obtained from the plots for both the singlet and triplet channels are about the same, it was concluded that the partial charge transfers of the singlet and triplet exciplexes are the same.

Schmidt et al.³⁶² used $k_{\Delta E}^P/m$ values, calculated by using eq 65, to estimate the ΔG_{CET} -dependent contribution k_{CT}^P/m for formation of each product state. Linear correlations of $\log(k_{CT}^P/m)$ with ΔG_{CET} resulted. It was found that, in each series of biphenyls,³⁵⁰ naphthalenes,³⁶² and fluorenes,³⁹⁵ the correlations of $\log(k_{CT}^{1\Sigma})$, $\log(k_{CT}^{1\Delta})$, and $\log(k_{CT}^{3\Sigma}/3)$ with ΔG_{CET} are parallels, differing by systematic con-

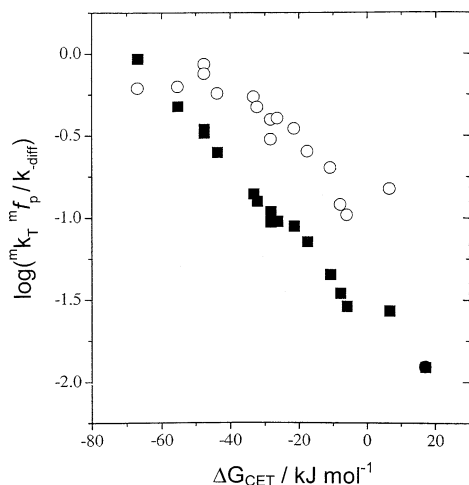


Figure 27. Plots showing the dependence on the free energy change ΔG_{CET} of $\log(^3k_{\text{T}}^m/{}^3k_{\text{P}}/k_{\text{-diff}})$ (■) and $\log(^1k_{\text{T}}^m/{}^1k_{\text{P}}/k_{\text{-diff}})$ (○) for charge-transfer-induced formation of ground-state and singlet oxygen, respectively, during O_2 quenching of 17 triplet-excited naphthalene derivatives in acetonitrile. From ref 391. Reproduced with permission from The Royal Society of Chemistry, on behalf of the PCCP Owner Societies.

stants, $\log(c^{\text{P}}/m)$ (with $c^{1\Sigma}/1 = 0.67$, $c^{1\Delta}/1 = 0.33$, and $c^{3\Sigma}/3 = 1.00$ for formation of $\text{O}_2(^1\Sigma_{\text{g}}^+)$, $\text{O}_2(^1\Sigma_{\text{g}}^+)$, and $\text{O}_2(^3\Sigma_{\text{g}}^-)$, respectively; see also section IV.A.2 for the physical meaning of these constants). However, for each series, small but significantly different intercepts c_1 and slopes c_2 were found. This behavior, described by eq 70, could be the consequence of the

$$\log(k_{\text{CT}}^{\text{P}}/m) = \log(c^{\text{P}}/m) + c_1 + c_2\Delta G_{\text{CET}} \quad (70)$$

different structure of the biphenyls, naphthalenes, and fluorenes. For example, it was suggested that interaction of biphenyl derivatives with O_2 occurs with only one of the aromatic rings, while in the case of naphthalenes, electronic delocalization occurs from the adjacent ring.²⁰⁰

However, for aromatic molecules, the dependence of $k_{\text{T}}^{\text{P}}/m$ on the molecular structure seems to be unimportant compared with the influence of triplet energy and oxidation potential.⁴⁰¹ This is demonstrated in Figure 28, where 127 multiplicity-normalized rate constants for formation of $\text{O}_2(^1\Sigma_{\text{g}}^+)$, $\text{O}_2(^1\Delta_{\text{g}})$, and $\text{O}_2(^3\Sigma_{\text{g}}^-)$ during O_2 quenching of T_1 of 45 sensitizers of very different structure, E_{T} and E_{ox} (including porphyrins and metalloporphyrins, fullerenes, naphthalenes, biphenyls, fluorenes, $\pi\pi^*$ ketones, and other homocyclic and heterocyclic aromatic hydrocarbons), are correlated with one common dependence on ΔE and ΔG_{CET} . The data are well described by the surface of Figure 28, which was calculated by eqs 38, 65, and 67–70 using $c_1 = 7.65$ and $c_2 = 0.23 \text{ mol kJ}^{-1}$. This demonstrates clearly that E_{T} and E_{ox} are by far the most important parameters determining $k_{\text{T}}^{1\Sigma}$, $k_{\text{T}}^{1\Delta}$, and $k_{\text{T}}^{3\Sigma}$. Note that for clarity reasons, eq 70 was approximated using $c^{\text{P}}/m = 1$ for formation of all three O_2 product states. Equation 70 leads to three distinct but closely lying surfaces and describes the data better than represented in Figure 28. It has been suggested that the equations given above can

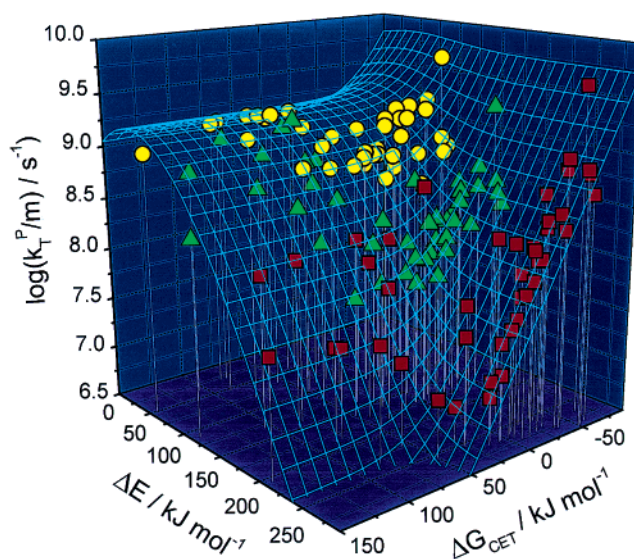


Figure 28. Singlet oxygen photosensitization from $\pi\pi^*$ triplet-excited aromatic compounds in CCl_4 can be generally described by a dependence of multiplicity-normalized rate constants $k_{\text{T}}^{\text{P}}/m$ for formation of $\text{O}_2(^1\Sigma_{\text{g}}^+)$ (yellow circles), $\text{O}_2(^1\Delta_{\text{g}})$ (green triangles), and $\text{O}_2(^3\Sigma_{\text{g}}^-)$ (red squares) on the excess energy ΔE for formation of the respective O_2 product state P and the free energy ΔG_{CET} for formation of an ion pair. The surface displayed in this figure is predicted by the model described in sections IV.A.1.b and IV.A.2, where the overall rate constant for formation of all three O_2 product states is considered as the sum of a non-charge-transfer contribution $k_{\Delta E}^{\text{P}}/m$ and a charge-transfer contribution $k_{\text{CT}}^{\text{P}}/m$, i.e., $k_{\text{T}}^{\text{P}}/m = k_{\Delta E}^{\text{P}}/m + k_{\text{CT}}^{\text{P}}/m$. The corresponding empirical relationships, $\log(k_{\Delta E}^{\text{P}}/m) = 9.05 + (9 \times 10^{-3})\Delta E - (1.15 \times 10^{-4})\Delta E^2 + (1.15 \times 10^{-7})\Delta E^3 + (9.1 \times 10^{-11})\Delta E^4$, and $\log(k_{\text{CT}}^{\text{P}}/m) = 7.65 - 0.23\Delta G_{\text{CET}}$, can be used to estimate the rate constants and efficiencies of formation of $\text{O}_2(^1\Sigma_{\text{g}}^+)$, $\text{O}_2(^1\Delta_{\text{g}})$, and $\text{O}_2(^3\Sigma_{\text{g}}^-)$ from a $\pi\pi^*$ -excited sensitizer in this medium. Reprinted with permission from ref 401. Copyright 2003 American Chemical Society.

be used to estimate $k_{\text{T}}^{1\Sigma}$, $k_{\text{T}}^{1\Delta}$, $k_{\text{T}}^{3\Sigma}$, and $S_{\Delta} [= (k_{\text{T}}^{1\Sigma} + k_{\text{T}}^{1\Delta}) / (k_{\text{T}}^{1\Sigma} + k_{\text{T}}^{1\Delta} + k_{\text{T}}^{3\Sigma})]$ values for any $\pi\pi^*$ sensitizer in CCl_4 .⁴⁰¹

c. Steric and Structural Effects. Few studies have been concerned with the influence of the molecular structure of a compound on its singlet oxygen photosensitization ability, and in most cases, only relatively minor effects have been noted.

Pfeil⁴⁰² first attributed differences in rate constants for oxygen quenching of triplet-excited Cr complexes to steric effects, and, a few years later, Demas et al.³⁴³ also discussed k_{T}^{Q} values for deactivation of several other excited metal complexes in this context. However, these authors found no changes in k_{T}^{Q} upon introduction of bulky substituents. Instead, they noted lower k_{T}^{Q} values for some Ir complexes compared with complexes of Ru and Os, a behavior which they attributed to the larger size of the Ir complexes, leading to greater separation of the charge center and the solvation sphere from each other.³⁴³ However, more recent studies also reported ligand effects for O_2 quenching of excited Ru complexes in water⁴⁰³ and acetonitrile.^{390,397,399} Abdel-Shafi et al.³⁹⁰ related a decrease in S_{Δ} on going from monosubstituted ligands to trisubstituted ligands to steric effects, and devia-

tions of k_T^Q from a ΔG_{CET} dependence were attributed to the structure of certain complexes.³⁹⁷ Xu et al.⁴⁰⁴ recently found that the rate constants for oxygen quenching of excited Ru complexes bound to polymeric cyclodextrins decrease when the bulk of the polymer increases, and they suggested that the complexes can be “shielded” from O_2 quenching. Steric effects were suggested by Darmanyan et al.³⁵³ for singlet oxygen formation from triplet-excited amines. However, this suggestion was based solely on the k_T^Q value for triphenylamine, which was found to be lower than those for several other amines of similar ΔG_{CET} .

Benson and Geacintov⁴⁰⁵ found deuteration effects on the O_2 quenching rate constants for the T_1 states of several aromatic hydrocarbons dissolved in a solid polystyrene matrix, and they explained the lower values found for the deuterated sensitizers by lower Franck–Condon factors. However, no deuteration effects were observed in fluid solution.⁴⁰⁶ Heavy atoms may also influence the interaction of O_2 with organic compounds. For example, Darmanyan and Foote⁴⁰⁷ correlated S_Δ values for a series of $n\pi^*$ -excited halogenated acetone derivatives with the square of the spin–orbit coupling factor of the halogen atom. However, no dependence on heavy atoms was found for $\pi\pi^*$ -excited compounds.⁴⁰⁷

Interesting observations have been made with fullerene derivatives. Anderson et al.⁴⁰⁸ first showed that functionalization of the fullerene core diminishes its singlet oxygen quantum yield, and Hamano et al.⁴⁰⁹ noted a decrease of Q_Δ with the number of addends. However, Prat et al.⁴¹⁰ recently demonstrated that this behavior is not the consequence of a modified interaction with O_2 , but rather it is due to a decrease in the fullerene’s triplet quantum yield. S_Δ values were found to be unity for a series of fullerene derivatives bearing one to six addends.

d. Influence of the Electronic Configuration.

The efficiencies of singlet oxygen generation from $\pi\pi^*$ -excited triplet states of aromatic hydrocarbons are generally close to unity ($S_\Delta \approx 0.8$ – 1.0), unless their triplet state is very high or oxidation potential is very low. This is also observed with $\pi\pi^*$ -excited aromatic ketones, which are commonly used as reference sensitizers because of their high singlet oxygen yields in many media.^{83,357} In sharp contrast to this behavior, however, S_Δ values for $n\pi^*$ -excited ketones are found to range from 0.3 to 0.5, despite their often very high oxidation potentials. The differences between $n\pi^*$ - and $\pi\pi^*$ -excited ketones are very marked and general, and also easy to observe, and Darmanyan and Foote⁴¹¹ even proposed using S_Δ as a criterion to define the nature of a T_1 state of an aromatic ketone. However, these differences seem to be limited to monoketones. Several studies showed that di- and particularly triketones can be highly efficient singlet oxygen sensitizers.^{377,412,413} Even larger values of S_Δ , 0.7 and 0.96, were recently reported for two structurally related azoalkanes with $n\pi^*$ triplet states.⁴¹⁴

In the very first study dedicated to $\text{O}_2(^1\Delta_g)$ efficiency determinations, Gorman et al.³⁵⁴ first noted that $n\pi^*$ -excited benzophenone is a less efficient

sensitizer than most aromatic hydrocarbons. Chattopadhyay et al.³⁹² also reported relatively inefficient singlet oxygen production from $n\pi^*$ -excited derivatives of benzophenone and acetophenone, and Redmond and Braslavsky⁴¹⁵ attributed low S_Δ values for a series of $n\pi^*$ ketones to the high polarizability of these compounds. Darmanyan and Foote compared the solvent dependence of singlet oxygen production from $n\pi^*$ and $\pi\pi^*$ triplets,⁴¹⁶ and they also noted that S_Δ values for a series of $n\pi^*$ triplets are influenced by the introduction of heavy atoms, while those for $\pi\pi^*$ triplets are not.⁴⁰⁷ It was suggested that both Franck–Condon factors and electronic matrix elements are more favorable for deactivation of $n\pi^*$ -excited ketones than for those involving $\pi\pi^*$ triplets.⁴⁰⁷ In the first study on the ΔE dependence of the multiplicity-normalized rate constants of formation of $\text{O}_2(^1\Sigma_g^+)$, $\text{O}_2(^1\Delta_g)$, and $\text{O}_2(^3\Sigma_g^-)$, Bodesheim et al.³⁶³ observed that $k_T^{1\Delta}$ values for formation of $\text{O}_2(^1\Delta_g)$ from $n\pi^*$ -excited ketones deviate significantly from the general dependence of $\log(k_T^P/m)$ on ΔE for $\pi\pi^*$ triplets. Wang and Ogilby⁴¹⁷ determined the efficiency ratios a/S_Δ for a series of acetophenone and benzophenone derivatives and noted that these are larger for $\pi\pi^*$ triplets than for $n\pi^*$ triplets. The largest values were found for those derivatives with the lowest triplet energies, and it was also noted that the influence of the sensitizer ionization potential (i.e., charge-transfer interactions) is only weak.⁴¹⁷ The reason for the different behavior of $n\pi^*$ triplets in the sensitization of singlet oxygen remained an open question until a systematic study performed by Mehrdad et al. appeared, in which rate constants $k_T^{1\Sigma}$, $k_T^{1\Delta}$, and $k_T^{3\Sigma}$ were determined as a function of E_{ox} for a series of $\text{T}_1(n\pi^*)$ benzophenone sensitizers of almost constant E_T .³⁹⁸ This is discussed in section IV.A.3.

e. Influence of Solvent Polarity. Many investigations on oxygen quenching of excited triplet states have been carried out in several solvents with varying solvatochromic properties, and it has been largely noted that solvent polarity has a major impact on all singlet oxygen formation parameters. Although no correlations with complexation energy relationships (such as eq 44) have been performed, it has been shown that, for most compounds, an increase in solvent polarity results in an increase of the T_1 -state quenching rate constant, and in a decrease in the quantum yield and efficiency S_Δ of singlet oxygen formation. For example, this behavior has been clearly established in the cases of chrysene,³⁴⁰ 1,3,5-triphenylbenzene,³⁹³ derivatives of naphthalene,^{199,365,393} biphenyl,^{200,367} and anthracene,^{334,418} ruthenium complexes,^{403,419,420} and tetraphenylporphyrin zinc.⁴²¹

However, the solvent dependence is less obvious for aromatic ketones. For both $n\pi^*$ -excited benzophenone and $\pi\pi^*$ -excited duroquinone, Darmanyan and Foote⁴¹⁶ did not find any noticeable dependence of k_T^Q or S_Δ on solvent polarity. Instead, they observed an increase of S_Δ in alcohols, which they attributed to the formation of hydrogen bonds.⁴¹⁶ Bendig et al.³⁷⁶ also reported a constant S_Δ value of 0.29 for singlet oxygen formation from *N*-methyl-

acridone in a range of solvents. However, in a more recent study on $O_2(^1\Delta_g)$ formation from a series of $n\pi^*$ -excited benzophenone derivatives, it was found that all S_Δ values decrease slightly, and all k_T^Q values increase on going from carbon tetrachloride to the more polar solvent dichloromethane.²⁰¹

Several authors have noted that singlet oxygen formation from aromatic carboxylic acids is influenced by the pH. It was shown that deprotonation leads to a decrease in the singlet oxygen yield,^{422,423} and in the case of hypericin,⁴²³ this decrease could be correlated with a sigmoidal curve, indicating a pK_a value of 9.9 for this compound. However, it was not specified whether this decrease is due to a decrease in Q_T or S_Δ . In the case of (tetra-*tert*-butylphthalocyaninato)zinc, Beeby et al.⁴²⁴ noted a significant decrease of S_Δ with increasing protonation. It was suggested that, in this specific case, protonation may lower the sensitizer triplet-state energy below the 94 $kJ\ mol^{-1}$ required for $O_2(^1\Delta_g)$ formation.

f. Influence of Oligomerization, Aggregation, and Excimer Formation. Singlet oxygen yields may be significantly diminished by the association of sensitizer molecules, either as excited dimers (excimers), ground-state complexes, or covalently bound oligomers. For example, Q_Δ values for naphthalene and pyrene, which form excimers upon excitation in concentrated solutions, reportedly decrease with increasing sensitizer concentration in methanol,⁴²⁵ hexane,⁴²⁵ and benzene,⁴²⁶ while they are constant for phenanthrene,⁴²⁵ which does not form excimers. Shold⁴²⁵ attributed this behavior to the formation of the monomer T_2 state by dissociation of the excimer T_1 state, and Marsh and Stevens⁴²⁶ proposed that the triplet state of the pyrene excimer does not sensitize the production of singlet oxygen at all. Darmanyan et al.⁴²⁷ found that S_Δ decreases with the degree of electron transfer in the exciplexes, and Levin et al.³⁴⁶ observed that oxygen-quenching rate constants of several excimers are higher than those of the corresponding monomers. Similar observations were also made by Darmanyan et al.,⁴²⁷ who attributed the higher rate constants to the lower triplet energies of the excimers.

Tanielian et al. reported sensitizer-concentration-independent Q_Δ values for hematoporphyrin⁴²⁸ and hematoporphyrin derivative⁴²⁹ in methanol, and a significant decrease of Q_Δ with increasing concentration of these compounds in water, which they attributed to the formation of ground-state dimers in this solvent.^{428,429} Similar results were recently reported by Borisov et al.⁴³⁰ and by Dairou et al.,⁴³¹ who determined dimerization constants and singlet oxygen yields for disulfonated deuterioporphyrin and its esters in D_2O and methanol. On the basis of Q_T estimations, Tanielian et al.⁴²⁸ suggested that the decrease of Q_Δ is at least partially due to a decrease in S_Δ . Aggregation of sensitizer ground states was also proposed to explain the solvent dependence of Q_Δ for (4-sulfonatophenyl)porphyrin, zinc coproporphyrin, and pheophorbides.⁴¹⁹

Maree and Nyokong⁴³² investigated singlet oxygen formation from covalently linked silicon octaphenoxypthalocyanines in dimethyl sulfoxide and found an

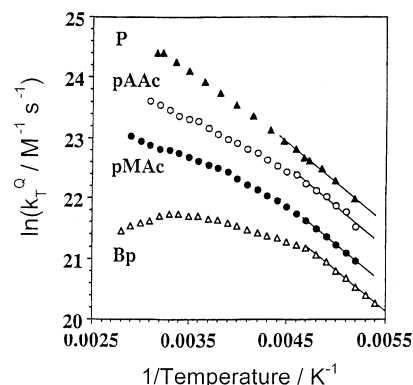


Figure 29. Arrhenius plots for bimolecular rate constants k_T^Q of O_2 quenching of triplet benzophenone (Bp, Δ), triplet *p*-aminoacetophenone (pAAc, \circ), triplet *p*-methoxyacetophenone (pMAc, \bullet), and singlet-excited pyrene (P, \blacktriangle) in toluene solution. Reprinted with permission from ref 351. Copyright 1993 American Chemical Society.

increase of Q_Δ on going from one to five phthalocyanine units but a strongly decreased efficiency for the oligomer containing nine rings. Pelliccioli et al.²⁶⁴ measured triplet-state and singlet oxygen yields for germanium and tin phthalocyanine monomers, and μ -oxo-bridged dimers thereof, in toluene. Interestingly, they found S_Δ values to be near unity for the monomers but significantly lower for the dimers. The authors explained this behavior by a lower triplet energy for the dimers, resulting in reversible energy transfer. This was also corroborated by biexponential transient absorbance decay signals for the excited dimers.²⁶⁴

g. Influence of Temperature and Pressure. Cebul et al.³⁴⁴ first measured the temperature dependence of the rate constant for oxygen quenching of the triplet states of several ketones in the gas phase. In the temperature region of 260–360 K, they found a linear increase of $\ln(k_T^Q)$ with $1/T$. The slopes of Arrhenius plots were found to be almost identical for several ketones, and an activation energy E_a of ca. $-7.5\ kJ\ mol^{-1}$ was obtained. Significant differences, however, were found for the pre-exponential factors. In toluene solution, McLean and Rodgers⁴³³ observed a similar behavior for O_2 quenching of triplet benzophenone in the high-temperature region. However, the corresponding Arrhenius plot exhibits a turnover point at $T = 300\ K$, and below this temperature, $\ln(k_T^Q)$ decreases with decreasing temperature. This behavior was discussed in terms of a switch from pre-equilibrium to diffusion control, in analogy to the interpretation of the temperature dependence of rate constants of $O_2(^1\Delta_g)$ deactivation by several strong CT quenchers (see Figure 17).¹²⁷ Their observations are represented in Figure 29, together with the respective data for two acetophenones and for O_2 quenching of the S_1 state of pyrene, which serves as a standard for diffusion control.³⁵¹ Note also that, in the low-temperature region, k_T^Q for *p*-aminoacetophenone becomes larger than $^{4/9}k_{diff}$.

Interesting observations were also made in temperature-dependent studies of O_2 quenching of triplet naphthalene in several solvents. For this compound,

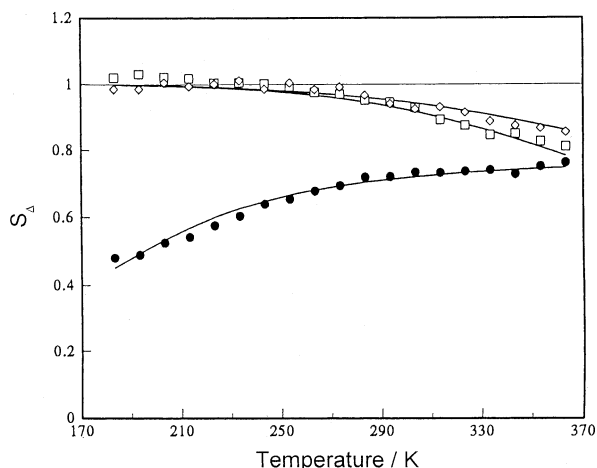


Figure 30. Temperature dependence of the efficiency S_{Δ} for singlet oxygen formation during oxygen quenching of the triplet states of chrysene (●), benzoylbiphenyl (□), and phenalene (◇) in air-saturated toluene. Reprinted with permission from ref 349. Copyright 1993 American Chemical Society.

E_a was found to be slightly positive in *n*-hexane and methylcyclohexane and negative in acetone, acetonitrile, and toluene.³⁴⁸ Similarly to the studies carried out on $O_2(^1\Delta_g)$ deactivation, negative activation energies were explained by the formation of exciplexes. Smith⁴³⁴ also noted that the activation energy for O_2 quenching of the T_1 states of several anthracenes in viscous 3-methylpentane solutions is lower than the activation energy for viscous flow, which means that the process is not diffusion-controlled.

Figure 30 shows the temperature dependence of singlet oxygen formation efficiencies, S_{Δ} , determined by Grewer and Brauer³⁴⁹ in toluene. Interestingly, a different behavior is found for chrysene and for two ketones. In the former case, S_{Δ} increases with increasing temperature, while the ketones' efficiencies decrease with increasing temperature.

Okamoto et al.^{347,435,436} investigated the pressure dependence of singlet oxygen formation from anthracene derivatives and pyrene in several solvents. These studies demonstrated that k_T^Q decreases with increasing pressure (see Figure 31b).

However, the dependence is much weaker than that found for the overall rate constant k_S^Q of S_1 -state quenching by O_2 , which is assumed to be diffusion-controlled (see Figure 31a). Whereas $\ln(k_S^Q)$ correlates linearly with $\ln(\eta)$ with slope -0.6 to -0.7 , as a consequence of increasing solvent viscosity, correlations of $\ln(k_T^Q)$ with $\ln(\eta)$ are non-linear, with a much smaller slope, -0.1 at 1 bar, in agreement with the nondiffusional character of T_1 -state quenching by O_2 at room temperature and atmospheric pressure. These observations are common to the quenching of anthracene derivatives.^{347,352} Finally, singlet oxygen yields for the anthracenes were also determined in several solvents, and it was found that Q_{Δ} and S_{Δ} are independent of pressure over the whole pressure range (0.1–400 MPa) in all investigated solvents.⁴³⁵ However, it remains unclear whether this behavior is general, since anthracene derivatives exhibit a rather uncommon insensitivity to variations in S_{Δ} due to their low triplet energies.

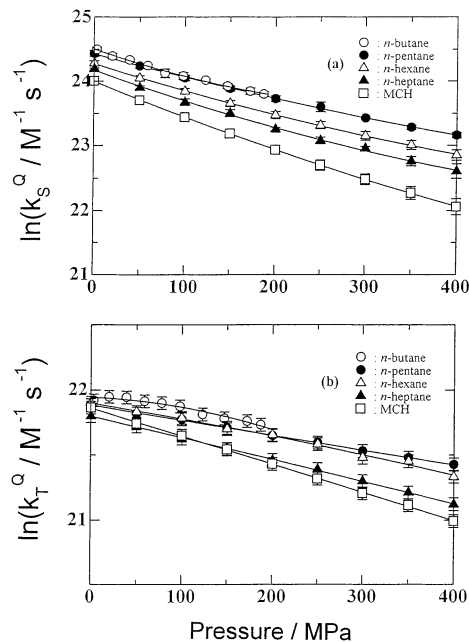


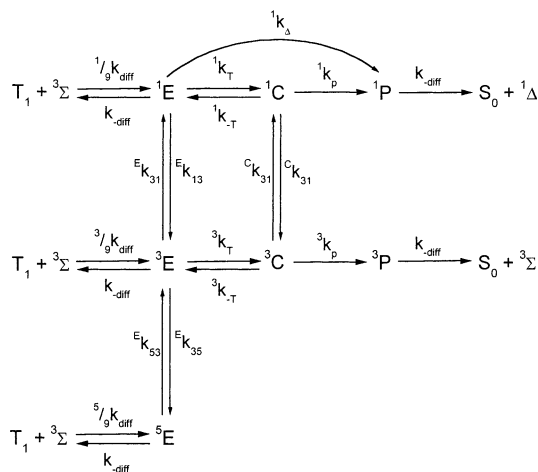
Figure 31. Pressure dependence of the rate constants k_T^Q and k_S^Q for oxygen quenching of the T_1 and S_1 states of 9-acetylanthracene in five solvents. Solid lines were drawn by assuming that $\ln(k_i^Q) = A + BP + CP^2$ ($i = S$ or T). Reprinted with permission from ref 435. Copyright 1998 American Chemical Society.

h. Influence of Magnetic Fields. Geacintov and Swenberg⁴³⁷ first investigated the possibility of magnetic field effects on the deactivation of triplet states of aromatic hydrocarbons by O_2 . On the basis of theoretical considerations, they predicted a negative effect of magnetic field on k_T^Q if the splitting among the singlet, triplet, and quintet complexes due to CT interactions is negligible compared to the spin–spin interaction, and no effect if the CT-induced splitting is large. Their own data, and also later experimental results, were in support of the latter hypothesis. Indeed, no magnetic field effect on the rate constants was observed for oxygen quenching of the T_1 states of chrysene, *a,h*-dibenzanthracene, and coronene absorbed on a polystyrene matrix,⁴³⁷ and also of chrysene and acridine in benzene, acetonitrile, and amorphous polystyrene.⁴³⁸ In contrast, however, Tachikawa and Bard⁴³⁹ found that magnetic field strength has a noticeable influence on the rate constant for oxygen quenching of delayed fluorescence of anthracene and pyrene in *N,N*-dimethylformamide but not in acetonitrile.

2. Mechanism of Oxygen Quenching of $\pi\pi^*$ Triplet States

It was shown in the previous paragraphs that the strongest effects on the quenching of T_1 states by O_2 and the corresponding efficiency of singlet oxygen formation are caused by variations of the oxidation potential and triplet-state energy of the sensitizer. Furthermore, the polarity of the solvent can also distinctly influence these processes. Thus, it is not surprising that the analysis of these dependences led to a quite detailed understanding of the events competing generally in the oxygen quenching of excited $\pi\pi^*$ triplet states.

Scheme 3. Mechanism of Singlet Oxygen ($^1\Delta$) Sensitization during Quenching of Triplet (T_1) States by Ground-State Oxygen ($^3\Sigma$), as Proposed by Wilkinson et al. after Examining Sensitizer Oxidation Potential and Solvent Dependence of Rate Constants and Efficiencies of $O_2(^1\Delta_g)$ Formation for Several Series of Organic Molecules at Constant Triplet Energy^a



^a This mechanism extends Scheme 2 by incorporating formation of charge-transfer (1C , 3C) and precursor (1P , 3P) complexes, in addition to encounter complexes (1E , 3E , 5E).

An important extension of the kinetic Scheme 2 originally proposed by Gijzeman et al.³⁴⁰ was formulated by Wilkinson and co-workers. It rests on the analysis of rate constants of overall singlet oxygen ($O_2(^1\Sigma_g^+) + O_2(^1\Delta_g)$) and of triplet oxygen formation, determined for numerous sensitizers of widely varying E_{ox} and E_T in solvents of different polarity.

Wilkinson's Scheme 3 modifies Scheme 2 by including precursor complexes and CT complexes, and the possibility of isc between the singlet and triplet quenching channels, as proposed initially by Garner and Wilkinson,³⁴² to account for k_T^Q values higher than $k_{diff}/9$ reported for several systems.^{200,333,342,349,366,367,391} In competition with the CT-assisted quenching with and without energy transfer, the formation of singlet oxygen via a non-charge-transfer (nCT) deactivation channel without CT-assisted energy transfer (i.e., including the step labeled 1k_A in Scheme 3) was assumed.^{366,367} 1E and 1C are used to represent the encounter complexes ${}^1(T_1^3\Sigma)$ and the charge-transfer complexes ${}^1,3(M^{\delta+}O_2^{\delta-})$, where M stands for the sensitizer molecule and 1,3P represent the precursor/encounter complexes ${}^1(S_0^1\Delta)$ and ${}^3(S_0^3\Sigma)$, respectively.³⁹¹ According to Scheme 3, the efficiency of singlet oxygen generation from the triplet state would be 1.0 if only the singlet channel were involved and 0.25 if the singlet and the triplet channels were both involved equally. In the absence of isc between the 1,3E complexes and/or the 1,3C complexes, rate constants of overall singlet oxygen and ground-state oxygen formation would be expected to be $\leq k_{diff}/9$ and $\leq k_{diff}/3$, respectively.

The importance of CT interactions during O_2 quenching of triplet states became most apparent from results in which an aromatic hydrocarbon and a range of its substituents were studied.^{362,364–367} In

these cases, changes in E_T are negligible, allowing any dependence on E_{ox} to be determined. For example, bimolecular rate constants k_T^Q of O_2 quenching and the efficiencies S_Δ of singlet oxygen formation were reported by Wilkinson et al.^{366,367} for a range of substituted biphenyl triplet states in acetonitrile, benzene, and cyclohexane, where only E_{ox} of the biphenyl derivatives varies while E_T is approximately constant. Values of k_T^Q increase as E_{ox} decreases and increase as the solvent polarity increases, whereas the values of S_Δ increase with E_{ox} and decrease with increasing solvent polarity. The inverse correlation of S_Δ with k_T^Q is shown in Figure 25.³⁶⁷

According to Wilkinson, these results, interpreted using Scheme 3, suggest that the triplet channel operates only when CT is favorable. Actually, very good linear correlations are found if the rate constants of ground-state oxygen formation are plotted on a logarithmic scale versus the change in free energy ΔG_{CET} for complete electron transfer from the T_1 -excited sensitizer to O_2 , for naphthalene and biphenyl sensitizers.^{365–367} Similar results in support of Scheme 3 were presented by Grever and Brauer, who investigated the T_1 -state quenching of aromatic hydrocarbons and ketones by O_2 .⁴⁰⁰ Further corroboration came also from the work of Darmanyan et al.,³⁵³ who obtained, on the basis of Scheme 3, an excellent correlation of the logarithms of the rate constants of ground-state oxygen formation with ΔG_{CET} for a much broader variation of $\pi\pi^*$ triplet sensitizers of widely varying E_{ox} and E_T . However, the corresponding correlations for the rate constant of overall singlet oxygen formation were much weaker and more scattered, and it was realized that this is the consequence of the important contribution of singlet oxygen formation via the nCT deactivation channel, labeled 1k_A in Scheme 3.^{353,366,367,400} Thus, formation of $O_2(^1\Delta_g)$ occurs with CT interactions via 1C and without CT interactions with rate constant 1k_A via the precursor complex ${}^1(S_0^1\Delta)$, circumventing 1C . Since the latter process was assumed to depend on the excess of electronic energy which needs to be dissipated, the energy gap relation 66 was derived by Wilkinson and co-workers for ${}^1k_A = k_T^{1\Sigma} + k_T^{1\Delta}$, i.e., for formation of $O_2(^1\Delta_g)$ in the nCT path.^{326,391} Using eq 66, Abdel-Shafi and Wilkinson calculated, from the rate constants of singlet and ground-state oxygen formation, corresponding multiplicity-normalized relative rate constants ${}^m k_T^m f_p / k_{diff}$ of singlet ($m = 1$) and triplet oxygen ($m = 3$) formation via the CT path for 17 naphthalene derivatives of widely varying E_{ox} and moderately differing E_T .³⁹¹ The plot of $\log({}^m k_T^m f_p / k_{diff})$ versus ΔG_{CET} is shown in Figure 27. Two almost parallel correlations with slope $-0.022 \text{ mol kJ}^{-1}$ were obtained, which can be compared with an expected slope of $-0.178 \text{ mol kJ}^{-1}$ for endergonic reactions involving complete electron transfer. The indications are that quenching is via singlet and triplet CT complexes with only partial charge-transfer character.

The ratio of experimental and expected slope was interpreted as representing the fraction of electron transfer which exists in the transition state, 12.5% and 17% for the naphthalenes in acetonitrile and

cyclohexane, respectively.³⁹¹ Interestingly, the same CT character of the transition state was estimated by the same procedure with a series of biphenyl derivatives, giving 12.5%, 14.5%, and 17% in acetonitrile, benzene, and cyclohexane.³⁶⁷ Since parallel correlations were found (see Figure 27), these CT estimates should be valid for CT-assisted formation of both $O_2(^1\Delta_g)$ and $O_2(^3\Sigma_g^-)$. Thus, it has been shown that the inclusion of the nCT path, leading directly to $O_2(^1\Delta_g)$, to both CT paths of Scheme 3 allows the quantitative reproduction of the experimental results with respect to the ΔG_{CET} dependence of the $O_2(^1\Delta_g)$ and $O_2(^3\Sigma_g^-)$ formation in the quenching of $T_1(\pi\pi^*)$ states by O_2 .^{325,326,366,367}

Abdel-Shafi and Wilkinson suggested that the unexpected shift of the multiplicity-normalized data for formation of $O_2(^1\Delta_g)$ in Figure 27 to larger values, compared with the corresponding data for $O_2(^3\Sigma_g^-)$ formation, could point to the occurrence of some isc from the triplet to the singlet channel.³⁹¹ In fact, the extent of isc between the singlet and triplet channels of Scheme 3 via $^{1,3}E$ complexes and/or $^{1,3}C$ complexes is still an open question. Using a simpler kinetic scheme without participation of $^{1,3}E$ complexes, it was previously reported that any rate constants of forward and backward isc between $^{1,3}C$ complexes of $\leq 10^{11} \text{ s}^{-1}$ (acetonitrile) and even of $\leq 10^{13} \text{ s}^{-1}$ (cyclohexane) gives good fits to the data,^{366,367} and in deriving the kinetic equations corresponding to the complete Scheme 3, it was argued that isc between $^{1,3}E$ complexes could be neglected.^{325,326,391}

It has to be noted that the wide range of experimental data on the quenching of $\pi\pi^*$ triplet states by O_2 , elaborated by numerous scientists in the past three decades, is successfully described by the kinetic scheme developed by Wilkinson and co-workers. The kinetic equations corresponding to Scheme 3 clearly demonstrate the principles of the mechanism, i.e., the competition of non-charge-transfer (nCT) and partial charge-transfer (pCT) deactivation paths.

The introduction of new techniques, allowing the separate determination of the rate constants of $O_2(^1\Sigma_g^+)$, $O_2(^1\Delta_g)$, and $O_2(^3\Sigma_g^-)$ formation in T_1 -state quenching by O_2 , opened the door to additional valuable information. On the basis of Wilkinson's Scheme 3, and the analysis of the E_T and E_{ox} dependences of the rate constants $k_T^{1\Sigma}$, $k_T^{1\Delta}$, and $k_T^{3\Sigma}$ determined for a large number of sensitizers with a broad variation of E_{ox} and E_T in the nonpolar solvent CCl_4 , Schmidt and co-workers recently developed the modified kinetic Scheme 4.^{350,362,363,395,401} The first step in Scheme 4 describes the formation of encounter complexes $^{1,3,5}(T_1^3\Sigma)$, with rate constant k_{diff} , which either dissociate back to T_1 and $O_2(^3\Sigma_g^-)$, with rate constant k_{-diff} , or deactivate to yield S_0 and $O_2(^1\Sigma_g^+)$, $O_2(^1\Delta_g)$, or $O_2(^3\Sigma_g^-)$, with overall rate constant k_D . Thus, $k_D = k_T^{1\Sigma} + k_T^{1\Delta} + k_T^{3\Sigma}$ holds true. Formation of $O_2(^1\Sigma_g^+)$, $O_2(^1\Delta_g)$, and $O_2(^3\Sigma_g^-)$ occurs via two different deactivation channels. The primarily formed encounter complexes $^{1,3}(T_1^3\Sigma)$ are deactivated by ic to lower complex states of the same multiplicity, i.e., $^1(T_1^3\Sigma) \rightarrow ^1(S_0^1\Sigma)$, $^1(T_1^3\Sigma) \rightarrow ^1(S_0^1\Delta)$, and $^3(T_1^3\Sigma) \rightarrow ^3(S_0^3\Sigma)$, which finally dissociate to the respective products. Since the excess energies ΔE have to be released as

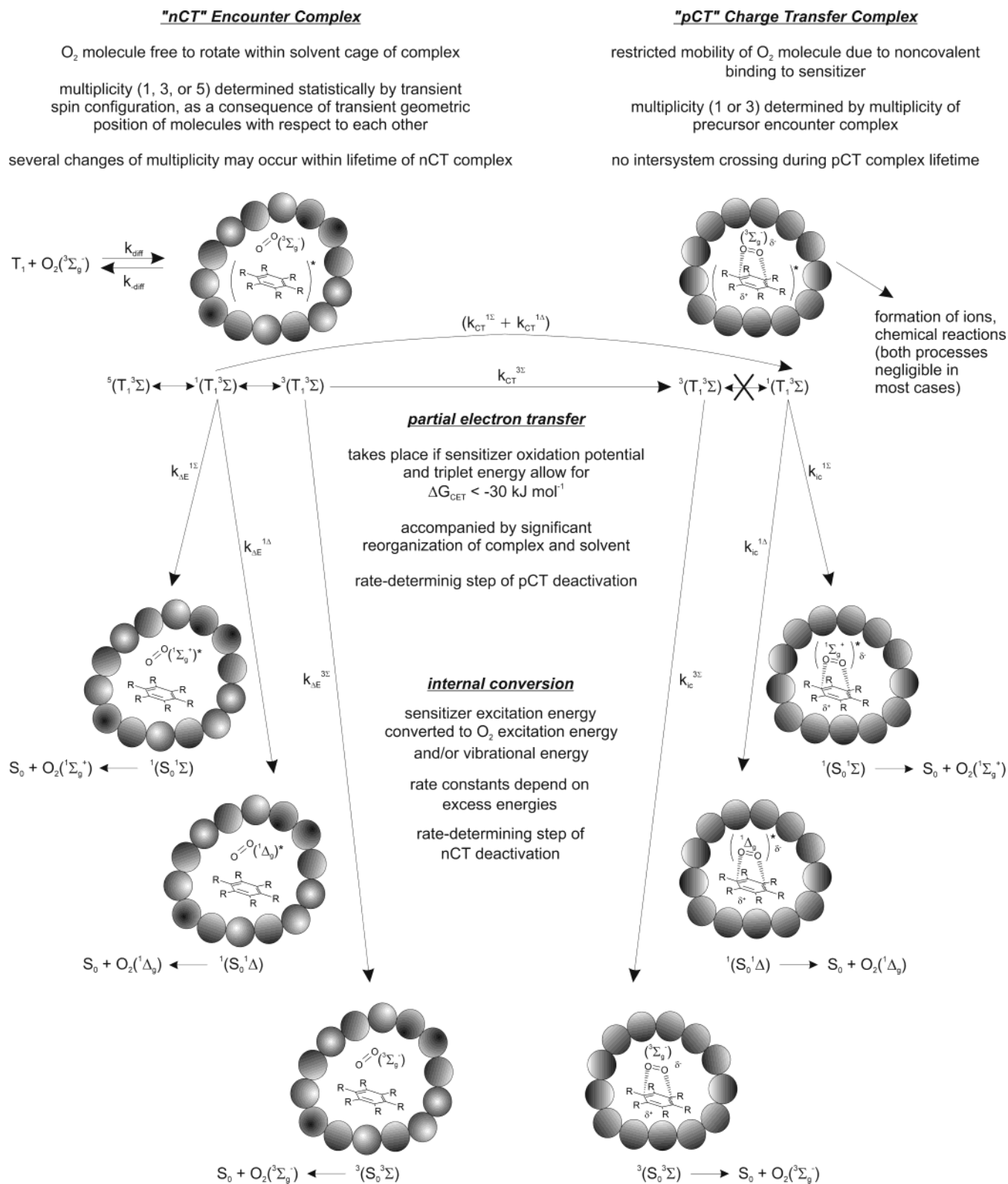
heat, the rate constants of ic should depend on ΔE via an energy gap relation. This was actually found in the investigation of a series of sensitizers with widely varying triplet energy E_T (see Figure 24), where multiplicity-normalized values $\log(k_T^P/m)$ (i.e., $k_T^{1\Sigma}$, $k_T^{1\Delta}$, and $k_T^{3\Sigma}/3$) are correlated with ΔE .³⁶³ The common excess energy dependence of $\log(k_T^P/m)$ for $\Delta E \leq 220 \text{ kJ mol}^{-1}$ was interpreted as a consequence of a fully established spin-statistical equilibrium between isoenergetic singlet- and triplet-excited complexes $^1(T_1^3\Sigma)$ and $^3(T_1^3\Sigma)$.

The empirical polynomial 65, describing the data shown in Figure 24, was considered to represent the energy gap law for the ic of $^{1,3}(T_1^3\Sigma)$ complexes without CT stabilization. This was concluded from the variation of $\log(k_T^P/m)$ data from a series of naphthalenes of widely varying E_{ox} but almost constant E_T ,³⁶² which is shown in Figure 26. The smallest values of $\log(k_T^P/m)$ of the naphthalenes correspond, in each case, to the derivatives with the largest values of E_{ox} , for which CT interactions are minimal. Since these data are in the range of the empirical curve, it is clear that this curve is a good approximation to the energy gap law for the ic in the absence of CT interactions, i.e., for nCT complexes.

The naphthalene $\log(k_T^P/m)$ data strongly increase with decreasing E_{ox} , indicating that increasing CT interactions lead to larger values of $k_T^{1\Sigma}$, $k_T^{1\Delta}$, and $k_T^{3\Sigma}/3$. Thus, Figure 26 impressively illustrates that two mechanisms operate in the quenching of $\pi\pi^*$ triplet states by O_2 , both leading to the formation of $O_2(^1\Sigma_g^+)$, $O_2(^1\Delta_g)$, and $O_2(^3\Sigma_g^-)$. The first is controlled via an energy gap law, and the second is controlled by the variation of CT interactions, which can be quantified by ΔG_{CET} . The first depends on the variation of ΔE and occurs with rate constants $k_{\Delta E}^{1\Sigma}$, $k_{\Delta E}^{1\Delta}$, and $k_{\Delta E}^{3\Sigma}$ via excited encounter complexes, the second depends on the strength of CT interactions and operates with rate constants $k_{CT}^{1\Sigma}$, $k_{CT}^{1\Delta}$, and $k_{CT}^{3\Sigma}$ via exciplexes with partial CT character (see Scheme 4).

Assuming that $k_{\Delta E}^P$ and k_{CT}^P add up to k_T^P , and that the excess energy dependence of $k_{\Delta E}^P$ can be calculated from the energy gap relation, rate constants k_{CT}^P could be calculated for each sensitizer from values of E_T and eqs 65 and 67–69.³⁶² These conclusions were confirmed in further investigations that included homologous series of biphenyls and fluorenes.^{350,395,401} Figure 32 displays the rate constants of the pCT channel obtained for a series of biphenyls in a plot of $\log(k_{CT}^P/m)$ versus ΔG_{CET} .³⁵⁰ Strong linear correlations were obtained. The fit function $\log(k_{CT}^P/3) = c_1 + c_2\Delta G_{CET}$, with $c_1 = 7.45$ and slope $c_2 = -0.033 \text{ mol kJ}^{-1}$, describes the experimental data. Although scattering, the values of $\log(k_{CT}^{1\Sigma})$ and $\log(k_{CT}^{1\Delta})$ are not very far from the straight line in Figure 32. Actually, it was shown that the linear fit of $\log(k_{CT}^{1\Sigma} + k_{CT}^{1\Delta})$ to $\log(k_{CT}^{3\Sigma}/3)$ results in the slope 1.0 ± 0.15 and intercept 0.1 ± 0.4 , indicating the ratio 3:1 between the triplet and singlet pCT deactivation channels, which exactly matches the spin-statistical ratio. Furthermore, it was found that

Scheme 4. Mechanism of Formation of $O_2(^1\Sigma_g^+)$, $O_2(^1\Delta_g)$, and $O_2(^3\Sigma_g^-)$ during Oxygen Quenching of Triplet States, as Proposed by Schmidt et al. after Investigating Sensitizer Triplet Energy and Oxidation Potential Dependence of Rate Constants and Efficiencies of $O_2(^1\Sigma_g^+)$, $O_2(^1\Delta_g)$, and $O_2(^3\Sigma_g^-)$ Formation for Several Series of Organic Compounds in CCl_4 ^a



^a The scheme shows the different non-charge-transfer and partial charge-transfer complexes in their solvent cage. This mechanism is based on Scheme 3, but includes formation of ground-state oxygen from encounter complexes and excludes intersystem crossing in charge-transfer complexes, which were both demonstrated by the additional data on $O_2(^1\Sigma_g^+)$ generation. Quantitative $O_2(^1\Sigma_g^+)$ efficiency determinations have thus far been possible only in CCl_4 , due to its extremely short lifetime in most other solvents.

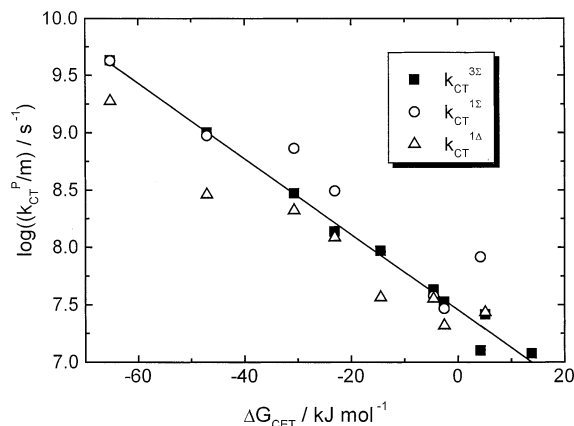


Figure 32. Plot showing the dependence of $\log(k_{CT}^P/m)$ of multiplicity-normalized rate constants for charge-transfer-induced formation of O_2 product state P on the change in free energy ΔG_{CET} for complete electron transfer from T_1 -excited biphenyls to O_2 . Straight line with slope $-0.033 \text{ kJ}^{-1} \text{ mol}$ and intercept 7.45 results from the linear fit to the $\log(k_{CT}^{3\Sigma}/3)$ data. Reprinted with permission from ref 350. Copyright 2001 American Chemical Society.

the values of $k_{CT}^{1\Sigma}$ are, on average, about 2-fold larger than $k_{CT}^{1\Delta}$.³⁵⁰

The results obtained with three homologous series of sensitizers agree in three important and partially new findings:^{350,362,395} (i) a common energy gap law exists for the ic of nCT complexes, which is given in good approximation by eq 65; (ii) the strength of CT interactions is the same in the singlet and triplet pCT deactivation channel, a conclusion which was also derived by Abdel-Shafi and Wilkinson in the analysis of their results, on which Scheme 3 is based;³⁹¹ and (iii) the statistical weights of formation of $O_2(^1\Sigma_g^+)$, $O_2(^1\Delta_g)$, and $O_2(^3\Sigma_g^-)$ in the pCT deactivation channel are $c^{1\Sigma} = 0.67$, $c^{1\Delta} = 0.33$, and $c^{3\Sigma} = 3$, in agreement with the graduation $k_{CT}^{3\Sigma}/3 > k_{CT}^{1\Sigma} > k_{CT}^{1\Delta}$ for a given sensitizer.

This experimentally found graduation has important implications. Considering the corresponding excess energies, the different graduation $k_{CT}^{1\Sigma} > k_{CT}^{1\Delta} > k_{CT}^{3\Sigma}/3$ was expected if the ic of pCT exciplexes $^1(T_1^3\Sigma)$ to pCT complexes $^1(S_0^1\Sigma)$, $^1(S_0^1\Delta)$, and $^3(S_0^3\Sigma)$ would be rate-determining, as is the case with the nCT complexes. Since the graduation according to the excess energies is not valid, it was concluded that ic of pCT complexes $^1(T_1^3\Sigma)$ and $^3(T_1^3\Sigma)$ must be much faster than isc between $^1,3(T_1^3\Sigma)$ pCT complexes and that formation of $^1,3(T_1^3\Sigma)$ pCT complexes from $^1,3(T_1^3\Sigma)$ nCT complexes should be the slowest and thus the rate-determining process.

The rate-determining reaction from encounter complexes to exciplexes also explains very easily the ratio $(k_{CT}^{1\Sigma} + k_{CT}^{1\Delta})/k_{CT}^{3\Sigma} = 1/3$. Since the $^1(T_1^3\Sigma)$ and $^3(T_1^3\Sigma)$ pCT exciplexes are formed in a parallel way from $^1,3(T_1^3\Sigma)$ nCT complexes, which are in a fully established fast isc equilibrium, the spin-statistical weight ratio of 1/3 is simply transferred. It was actually unexpected that a fast isc equilibrium should exist for $^1,3(T_1^3\Sigma)$ nCT complexes but not for $^1,3(T_1^3\Sigma)$ exciplexes. However, on the basis of the assumptions that the vector of the magnetic moment of the triplet O_2 molecule is rigidly coupled to the molecular axis,

and that spin flips in $^1,3(T_1^3\Sigma)$ complexes are brought about by rotation of the small O_2 molecule with respect to the large triplet sensitizer, Mehrdad et al.³⁹⁵ suggested that a fast isc equilibrium could well be established for $^1,3(T_1^3\Sigma)$ encounter complexes, since the rotational time is more than 1 order of magnitude smaller than the estimated lifetime of the encounter complex, $\tau_e \geq 2 \times 10^{-11} \text{ s}$. Such an isc mechanism would be slower for $^1,3(T_1^3\Sigma)$ pCT complexes because non-negligible binding interactions reduce the mobility of the O_2 moiety in the exciplex.

Thus, the analysis of the data from three series of $\pi\pi^*$ triplet sensitizers resulted in a consistent picture, which is described by the kinetic Scheme 4. It has to be noted that, in the papers by Schmidt and co-workers,^{350,362,395,398,401} values of ΔG_{CET} were calculated by using eq 38 with $C = 0$, which is not realistic for absolute data in the nonpolar solvent CCl_4 but is justified if results determined in only one solvent are compared on a relative ΔG_{CET} scale. The additional information obtained in the analysis of a large $k_T^{1\Sigma}$, $k_T^{1\Delta}$, and $k_T^{3\Sigma}$ data set led to the evolution from Scheme 3 to Scheme 4. Hereby, two principal extensions have been made:^{363,395,401} (i) a common energy gap law describing the excess energy dependence of $O_2(^1\Sigma_g^+)$, $O_2(^1\Delta_g)$, and $O_2(^3\Sigma_g^-)$ formation in the nCT deactivation channel was found for aromatic $\pi\pi^*$ triplet sensitizers, and (ii) the question concerning the isc between singlet and triplet deactivation channels seems to be answered, at least for the solvent CCl_4 . A fast isc equilibrium exists for $^1,3(T_1^3\Sigma)$ encounter complexes ($= ^1,3E$) but not for $^1,3(T_1^3\Sigma)$ exciplexes ($= ^1,3C$).

Scheme 4 appears to give a realistic picture of the processes competing in T_1 -state quenching by O_2 . For the first time, rate constants of $O_2(^1\Sigma_g^+)$, $O_2(^1\Delta_g)$, and $O_2(^3\Sigma_g^-)$ formation in CCl_4 could be described as a function of both ΔE and ΔG_{CET} (see Figure 28).⁴⁰¹ The simulation of the experimental data by the surface calculated by eqs 39, 65, and 67–70 is surprisingly good if the broad structural variety of sensitizers is taken into account. It is true that the deviations of experimental from calculated data are in part larger than the experimental uncertainties, but Schweitzer et al. attributed these differences to the general neglect of the electrostatic interaction energy C in eq 38, which depends on the molecular structure of the sensitizer (see eq 39). Thus, Figure 28 demonstrates clearly that E_T and E_{ox} are, by far, the most important parameters determining $k_T^{1\Sigma}$, $k_T^{1\Delta}$, and $k_T^{3\Sigma}$. The nCT path dominates for sensitizers with $\Delta G_{CET} \geq 50 \text{ kJ mol}^{-1}$, i.e., on the left-hand side of the surface of Figure 28. These sensitizers are characterized by rather small overall rate constants $k_T^Q \leq 3 \times 10^9 \text{ M}^{-1} \text{ s}^{-1}$ and values of $S_\Delta \geq 0.9$ if $E_T \geq 165 \text{ kJ mol}^{-1}$. The additional quenching via the pCT channel becomes important only in the exergonic range and dominates for sensitizers with $\Delta G_{CET} \leq -25 \text{ kJ mol}^{-1}$, i.e., on the right border of the calculated surface. As soon as the pCT channel participates, rate constants k_T^Q strongly increase and values of S_Δ decrease, whereby $S_\Delta \geq 0.25$ should hold true as long as the sensitizer is still photochemically stable.

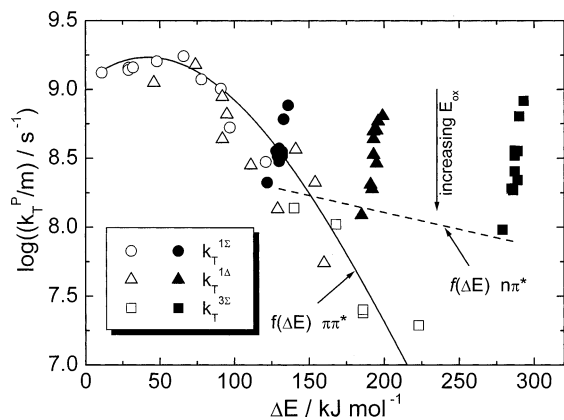


Figure 33. Dependence of $\log(k_T^P/m)$ on ΔE and E_{ox} . Open symbols correspond to $\pi\pi^*$ -excited triplets, solid symbols to $n\pi^*$ -excited benzophenone derivatives. Reprinted with permission from ref 398. Copyright 2002 American Chemical Society.

3. Mechanism of Oxygen Quenching of $n\pi^*$ Triplet States

A deeper insight into this puzzling problem was achieved in a systematic study conducted by Mehrdad et al. on a series of $T_1(n\pi^*)$ benzophenone sensitizers of almost constant E_T by determining rate constants $k_T^{1\Sigma}$, $k_T^{1\Delta}$, and $k_T^{3\Sigma}$ as a function of E_{ox} .³⁹⁸ These data were analyzed by considering data determined previously for $T_1(\pi\pi^*)$ sensitizers of very different E_T and E_{ox} , including the structurally related biphenyls. It was found that quenching proceeds for both $T_1(n\pi^*)$ and $T_1(\pi\pi^*)$ sensitizers via nCT and pCT deactivation channels, each capable of producing $O_2(^1\Sigma_g^+)$, $O_2(^1\Delta_g)$, and $O_2(^3\Sigma_g^-)$. However, very different energy gap relations determine the deactivation of $T_1(\pi\pi^*)$ and $T_1(n\pi^*)$ sensitizers in the nCT channel, whereby the ΔE dependence of the corresponding rate constants is much weaker for the $T_1(n\pi^*)$ ketones. This is demonstrated in Figure 33, which displays the benzophenone data in addition to the results obtained previously by Schmidt et al. for a series of $T_1(\pi\pi^*)$ sensitizers of widely varying E_T in the $\Delta E \leq 220$ kJ mol⁻¹ range.

The $\log(k_T^P/m)$ data for the benzophenones increase with decreasing oxidation potential at almost constant excess energy, as was already observed with $T_1(\pi\pi^*)$ sensitizers; however, there are several significant differences: (i) despite the large variation of E_{ox} by 0.87 V for the benzophenones, compared with only 0.71 V for the biphenyls (not shown in Figure 33), much smaller variations of $\log(k_T^{1\Sigma})$, $\log(k_T^{1\Delta})$, and $\log(k_T^{3\Sigma}/3)$ with E_{ox} of, at maximum, 1 order of magnitude were noted with the benzophenones when compared with the 2.5 orders of magnitude with the biphenyls; (ii) $\log(k_T^{1\Sigma})$, $\log(k_T^{1\Delta})$, and $\log(k_T^{3\Sigma}/3)$ are of similar magnitude for each BP sensitizer; (iii) the $\log(k_T^P/m)$ data for the benzophenones with the highest E_{ox} , for which only very small CT interactions can take place (i.e., the smallest values in each series), are far from the empirical curve $f(\Delta E)$ found for $T_1(\pi\pi^*)$ sensitizers.

These surprisingly different results were explained by the different electronic and, in consequence, steric structure of the intermediate $^{1,3}(T_1^3\Sigma)$ com-

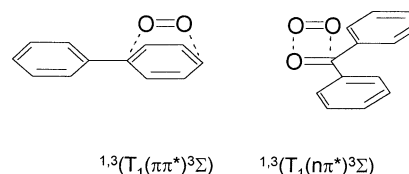


Figure 34. Structures of $^{1,3}(T_1(\pi\pi^*)^3\Sigma)$ and $^{1,3}(T_1(n\pi^*)^3\Sigma)$ complexes for biphenyl and benzophenone, respectively. Reprinted with permission from ref 398. Copyright 2002 American Chemical Society.

plexes (see Figure 34). It was shown that there is sufficient evidence that supra-supra structures, where the oxygen atoms of O_2 interact with two opposite carbon atoms of an aromatic ring, correspond to $(T_1(\pi\pi^*)^3\Sigma)$ and $(S_0(\pi^2)^1\Delta)$ complexes of biphenyls. Since the O–O bond distance varies only slightly between 1.207 ($^3\Sigma$), 1.216 ($^1\Delta$), and 1.227 Å ($^1\Sigma$), and since only small changes in bond lengths take place in the $\pi\pi^* \rightarrow \pi^2$ deactivation of the aromatic moiety, correspondingly small structural changes could be expected for the ic of supra-supra $^{1,3}(T_1(\pi\pi^*)^3\Sigma)$ complexes. This should explain why the empirical energy gap law (eq 65) found for $T_1(\pi\pi^*)$ sensitizers is still comparatively steep.

However, the situation is quite different for $(T_1(n\pi^*)^3\Sigma)$ complexes. The excitation energy of $T_1(n\pi^*)$ -excited benzophenones is localized on the carbonyl group. Therefore, a four-center structure, where O_2 is in parallel arrangement with the CO group, is much more probable for $(T_1(n\pi^*)^3\Sigma)$ complexes than a supra-supra structure, as was shown by Schweitzer et al.²⁰¹ Large structural changes could be expected for the ic of four-center $^{1,3}(T_1(n\pi^*)^3\Sigma)$ complexes, since it is known that significant changes in the lengths of all three bonds of the carbonyl carbon atom of benzophenone occur during $n\pi^* \rightarrow n^2$ de-excitation. Therefore, the deactivation of $^{1,3}(T_1(n\pi^*)^3\Sigma)$ complexes was assumed to be qualitatively best described by displaced potential energy curves of upper and lower states, which correspond to a weaker excess energy dependence of rate constants of ic.^{201,398}

The dependence of $\log(k_T^P/m)$ on ΔE observed for 4-cyanobenzophenone, for which minimal CT interactions take place, has been taken as an approach to the energy gap law for the ic of $^{1,3}(T_1(n\pi^*)^3\Sigma)$ complexes. This function is drawn as a straight line in Figure 33, and displays the much weaker excess energy dependence expected. Rate constants k_{CT}^P have been estimated which are much less dependent on ΔG_{CET} than was found for $T_1(\pi\pi^*)$ sensitizers, pointing to significantly weaker CT interactions in $^{1,3}(T_1(n\pi^*)^3\Sigma)$ pCT complexes.³⁹⁸

Thus, the different electronic configuration $n\pi^*$ versus $\pi\pi^*$ leads to different steric structures of $^{1,3}(T_1^3\Sigma)$ complexes: a reduced four-center structure of $^{1,3}(T_1(n\pi^*)^3\Sigma)$ complexes and an extended supra-supra structure of $^{1,3}(T_1(\pi\pi^*)^3\Sigma)$ complexes. It is suggested that these differences cause the complex deactivation to vary strongly in both the nCT and pCT channels. Because of the large structural changes accompanying the ic of $^{1,3}(T_1(n\pi^*)^3\Sigma)$ complexes, a weak ΔE dependence results for the energy gap law determining the deactivation of $^{1,3}(T_1(n\pi^*)^3\Sigma)$ nCT

complexes. Furthermore, since the substituents used to shift the oxidation potential of benzophenone are bound to the aromatic rings, but not to the excited carbonyl group, much weaker CT interactions may result for the deactivation of $^1,3(T_1(n\pi^*)^3\Sigma)$ pCT complexes due to this electronic decoupling.³⁹⁸

B. Oxygen Quenching of Excited Singlet States

In the 1930s, Kautsky observed the strong quenching by O_2 of the fluorescence and phosphorescence of many dyestuffs, and of biologically important compounds such as chlorophylls, porphyrins, and carotenoids.^{286–289} He showed that these processes yield a metastable excited form of O_2 , which he suggested to be $O_2(^1\Delta_g)$.²⁸⁹ This very important finding was made in qualitative studies which, however, did not allow more detailed investigation of the quenching mechanisms.

1. Rate Constants of S_1 -State Quenching

Quantitative studies of the fluorescence quenching have been performed only since the mid-1950s. It was realized that, besides O_2 , other paramagnetic gases, such as NO, are also very efficient quenchers of the fluorescence of aromatic molecules. The early investigations were performed in gas and solution phases by measuring the fluorescence intensities F^0 and F in the absence and in the presence of an added quencher Q in stationary experiments. The Stern–Volmer constant $K_{SV} = k_S^Q \tau_S$ was obtained by using eq 71 and was used as a relative measure of the quenching rate.

$$F^0/F = 1 + k_S^Q \tau_S [Q] \quad (71)$$

When the S_1 -state lifetime τ_S was known, either by direct measurement or by determination of the fluorescence quantum yield and calculation of the corresponding radiative rate constant of the emitting molecule from its absorption spectrum, the absolute quenching rate constants k_S^Q became accessible.

a. Collision- or Diffusion-Controlled Limit. Gas-phase fluorescence experiments conducted by Bowen with anthracene, 9-phenylanthracene, and 9,10-diphenylanthracene (DPA) resulted in very similar Stern–Volmer constants for self-quenching and for quenching by O_2 and NO.²⁹⁴ Using the gas kinetic rate constant for binary collisions from eq 34 and estimated values of τ_S , it was concluded that the magnitude of k_S^Q is consistent with a quenching probability of $p_Q \approx 1/3$ per collision.

Almost identical Stern–Volmer constants were obtained by Stevens for the self-quenching and the quenching by O_2 and NO of the fluorescence of anthracene, 9-phenylanthracene, and DPA in the gas phase.²⁹⁵ However, Stevens assumed the quenching process to be collision-controlled. He argued that if quenching by O_2 and NO is to be interpreted as a spin–orbit coupling due to the influence of their magnetic fields, then O_2 should be a more efficient quencher than NO, since its effective magnetic moment of $\mu_{\text{eff}} = 2.83 \mu_B$ is larger than $\mu_{\text{eff}} = 1.92 \mu_B$ of

NO, with μ_B being Bohr's magneton. Since both gases are, however, equally efficient quenchers, and also similar to the unexcited hydrocarbon in the self-quenching reaction, Stevens suggested that quenching takes place on every collision, i.e., $p_Q = 1$.²⁹⁵

Ware and Cunningham made the first time-resolved measurement of the fluorescence lifetime of anthracene in the gas phase more than 10 years later.²⁹⁹ With their result of $\tau_S = 5.7$ ns, they were able to remove the uncertainties of the previous interpretations with respect to the quenching probability p_Q . Using literature data on K_{SV} , they calculated $k_S^Q = 1.8 \times 10^{11} \text{ M}^{-1} \text{ s}^{-1}$ for O_2 at 570 K and $k_S^Q = 2.0 \times 10^{11} \text{ M}^{-1} \text{ s}^{-1}$ for NO at 550 K. The comparison with the gas kinetic rate constant from eq 34 resulted in $p_Q = 0.30$ for O_2 and $p_Q = 0.34$ for NO. Thus, fluorescence quenching occurs for both paramagnetic gases, on average, only on every third collision.²⁹⁹

In the liquid phase, the cage effect leads to repeated collisions between adjacent molecules. Therefore, if a bimolecular reaction between two solute molecules is efficient enough to require no more than a few collisions, then the rate will depend not on the total number of collisions, but on the number of encounters consisting of sets of repeated collisions.²⁹⁴ The limiting rate is then set by eq 72.

$$k_{\text{diff}} = 8RT/(3\eta) \quad (72)$$

Bowen investigated the fluorescence quenching by O_2 in solution to test this hypothesis. Experiments were carried out at room temperature with perylene, coronene, and several substituted anthracene derivatives and yielded rate constants for fluorescence quenching of $(2.7\text{--}4.0) \times 10^{10} \text{ M}^{-1} \text{ s}^{-1}$ in benzene, $(2.3\text{--}5.9) \times 10^{10} \text{ M}^{-1} \text{ s}^{-1}$ in CHCl_3 , and $(1.1\text{--}3.1) \times 10^{10} \text{ M}^{-1} \text{ s}^{-1}$ in kerosene.²⁹⁴ These values of k_S^Q are, on average, about 4-fold larger than k_{diff} calculated for the three solvents by using eq 72, whereas the likewise-determined self-quenching rate constants approximately agree with k_{diff} . This led Bowen to the conclusion that the O_2 molecule diffuses faster in liquids than estimated by using eq 72.²⁹⁴

Rate constants of the S_1 -state quenching by O_2 were determined by Ware in fluorescence lifetime measurements for anthracene, 9,10-dichloroanthracene, DPA, and perylene in 11 different solvents.²⁹⁷ Very similar results were obtained for the different hydrocarbons, and k_S^Q was found to decrease with increasing solvent viscosity. Only 9,10-dichloroanthracene gave rate constants that were a factor of ~ 0.6 smaller than the average value of the other hydrocarbons. It was suggested that this may be due to a lower probability of quenching once an encounter has taken place. Again, the experimental values of k_S^Q were much larger than the values of k_{diff} calculated by using the simple eq 72. Therefore, Ware also measured the diffusion coefficient D_O of O_2 in seven solvents of widely varying viscosity. Using literature diffusion coefficients D_H of hydrocarbons, and assuming the corresponding molecular radii to be $r_H = 4 \text{ \AA}$ and $r_O = 2 \text{ \AA}$, he calculated values of k_{diff} from eq 40 [$k_{\text{diff}} = 4\pi N_A (D_H + D_O)(r_H + r_O)$] which are in satisfactory agreement with the k_S^Q data. Thus, it

was shown that $3 \times 10^{10} \text{ M}^{-1} \text{ s}^{-1}$ is the diffusion-controlled limit for rate constants of reactions with O_2 in common organic solvents at room temperature and that the deviations from eq 72 are caused by the high mobility of the small O_2 molecule.²⁹⁷

Berlman and Walter measured lifetimes τ_S and ratios F^0/F for oxygen-free and air-saturated solutions of a variety of fluorescers in cyclohexane and found a good linear correlation of F^0/F with τ_S according to eq 71.²⁹⁸ From the slope $k_S^Q[\text{O}_2]$, they determined a general value of $k_S^Q = 2.3 \times 10^{10} \text{ M}^{-1} \text{ s}^{-1}$ in cyclohexane solution. Therefore, they suggested that S_1 -state quenching by O_2 in solution is generally diffusion-controlled; i.e., every encounter between an S_1 -excited molecule and O_2 leads to quenching. Actually, the results reported by Patterson et al. also seemed to confirm these conclusions.³⁸⁹

Much later, Okamoto and co-workers investigated the pressure dependence of k_S^Q for several aromatic hydrocarbons with nearly or completely diffusion-controlled S_1 -state quenching in alkane solvents.^{347,352,435,436} Interestingly, positive activation volumes $\Delta V_{\text{obs}}^\ddagger = 12\text{--}14 \text{ mL mol}^{-1}$ were obtained, which are only about half the values expected from the pressure dependence of the solvent viscosity according to eq 72. Plots of $\ln(k_S^Q)$ versus $\ln(\eta)$ were linear with a slope of -0.7 ± 0.1 , instead of the slope of -1 expected according to eq 72.^{352,436} It was noticed that these unusual effects for common diffusion-controlled reactions are often found in processes involving small molecules. Actually, it was previously found by Ware that the values of k_{diff} calculated according to eq 72 vary much stronger than the experimentally determined diffusion-controlled rate constants of the fluorescence quenching by O_2 .²⁹⁷ Equation 40 predicts a strong viscosity effect on k_{diff} . However, the deviation is less. Apparently, the decelerating effect of increasing viscosity is smaller for small molecules such as O_2 , which can slip easily through solvent molecules, than for solute molecules of ordinary size.

b. Rate Constants below Diffusion Control. Doubts about the general validity of the diffusion-controlled oxygen quenching were brought up early by several groups. Stevens and Algar determined rate constants of fluorescence quenching for a series of aromatic hydrocarbons in benzene. The values of k_S^Q decreased from 3.6×10^{10} (DPA) to $1.2 \times 10^{10} \text{ M}^{-1} \text{ s}^{-1}$ (rubrene). They interpreted this small but significant variation of k_S^Q in terms of a non-diffusion-limited quenching process.³⁰³

In the investigation of the fluorescence properties of fluoranthene and several of its derivatives, Berlman et al. noted an unusual immunity of these compounds to fluorescence quenching by O_2 . Rate constants k_S^Q up to 7-fold smaller than k_{diff} can be calculated from their results.³⁰⁰

In the following years, a large number of articles reported rate constants smaller than k_{diff} for oxygen quenching of $S_1(\pi\pi^*)$ -excited states in nonpolar as well as in polar solvents.^{226,306–309,325,326,333–335,337,347,352} For some acridinium cations, Kikuchi determined k_S^Q values which are 2 orders of magnitude smaller

than k_{diff} .³⁰⁷ Thus, k_S^Q may vary over a rather wide range. However, it has to be noted that, for the majority of investigated molecules with $\pi\pi^*$ configuration, fluorescence quenching is diffusion-controlled.

Very little has been published on O_2 quenching of $S_1(n\pi^*)$ states. Ware reported the very small value of $k_S^Q = 7.6 \times 10^7 \text{ M}^{-1} \text{ s}^{-1}$ for hexafluoroacetone in the gas phase.³⁰¹ Measurements made by Scaiano and Nau in nonpolar solvents yielded $k_S^Q = (1.7\text{--}2.7) \times 10^9 \text{ M}^{-1} \text{ s}^{-1}$ for several $S_1(n\pi^*)$ -excited alkanones⁴¹³ and $k_S^Q = 8 \times 10^9 \text{ M}^{-1} \text{ s}^{-1}$ for two $S_1(n\pi^*)$ -excited azoalkanes.⁴¹⁴ These solution rate constants are all much smaller than k_{diff} .

c. Influence of the Ionization Potential. Of course, it is interesting to know which parameters influence the rate constant k_S^Q . Since, in principle, the seven processes 50–56 could contribute to the quenching of S_1 by O_2 , the situation is much more complex than in the case of T_1 -state quenching by O_2 . Nonetheless, Brewer found already early that the ionization potential (IP) of the excited molecule can have an important effect on the magnitude of k_S^Q .³⁰⁴ He determined values of k_S^Q for a series of benzene derivatives with electron-donating or -withdrawing substituents in the gas phase and noted a decrease of k_S^Q from 2.5×10^{11} to $6.6 \times 10^{10} \text{ M}^{-1} \text{ s}^{-1}$ on going from *tert*-butylbenzene to difluorobenzene. $\log(k_S^Q)$ correlates linearly with IP. It was argued that the data tend to support a contact CT mechanism of fluorescence quenching by O_2 .

These results were corroborated by Brown and Phillips in an extensive gas-phase study on the fluorescence quenching by O_2 of 37 benzene derivatives.³⁰⁵ It was found that, for $\text{IP} \leq 9.0 \text{ eV}$, there is little variation in k_S^Q , with an average value of $2.2 \times 10^{11} \text{ M}^{-1} \text{ s}^{-1}$. Above this threshold, $\log(k_S^Q)$ begins to decrease with increasing IP. It was suggested that the deactivating step leads to formation of a CT-stabilized complex, ${}^3(\text{M}^{\delta+}\text{O}_2^{\delta-})$, which, for molecules of $\text{IP} \leq 9.0 \text{ eV}$, is sufficiently long-lived to undergo complete quenching. With increasing IP, the stabilization becomes weaker, and complex dissociation becomes more important than quenching.³⁰⁵

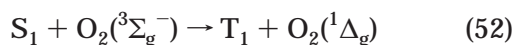
The strength of CT interactions is, of course, also important for the magnitude of k_S^Q in solution. This has been realized in experiments with S_1 -excited molecules with high oxidation potentials, which often result in particularly small quenching rate constants, such as those obtained in the investigations with series of cyanoanthracene derivatives by Schoof et al.³⁰⁶ and the groups of Kikuchi,³⁰⁷ Brauer,^{308,309} Wilkinson,^{333,334} and Ogilby,³³⁷ with acridinium cations by Kikuchi et al.,³⁰⁷ and with several heterocyclic aromatic cations by Brauer and co-workers.³³⁵

Okamoto's group investigated the pressure dependence of k_S^Q of anthracene derivatives bearing electron-withdrawing chlorine or cyano substituents in the 9- or 9,10-position.^{347,352} Very different pressure effects were observed, compared with those observed for the anthracene derivatives with electron-donating methyl or methoxy substituents. Zero or even nega-

tive values of ΔV_{obs} were obtained. Plots of $\ln(k_{\text{S}}^{\text{Q}})$ versus $\ln(\eta)$ were nonlinear with small slopes, or even convex curved in the low-viscosity range, which is in accordance with the nondiffusional character of the quenching of the anthracenes with high oxidation potentials at low pressures, approaching diffusion control only in the high-pressure region because of the strong increase of viscosity.

2. Products of S_1 -State Quenching

a. T_1 -State Formation by O_2 -Enhanced Inter-system Crossing. The early studies on fluorescence quenching did not provide much information on the electronic states involved in the S_1 -state quenching process.^{294,295,297–299,301} It was assumed that the sensitizer singlet ground-state S_0 should be the product state. However, while discussing the unusual immunity of the fluoranthene compounds to fluorescence quenching by O_2 , Berlman et al.³⁰⁰ first proposed the energy-transfer step 52,



as the principal path of effective S_1 -state quenching. This process cannot operate in the case of the fluoranthenes, for which the S_1 – T_1 energy gap ΔE_{ST} is smaller than the $O_2(^1\Delta_g)$ excitation energy of 94 kJ mol⁻¹, thus explaining the unusually small values of k_{S}^{Q} .

Quantitative kinetic investigations of the photo-oxygenation reaction of aromatic hydrocarbons can yield information on the product states of S_1 -state quenching. It was found that the quenching of electronically excited states of sensitizers by O_2 leads to formation of $O_2(^1\Delta_g)$, which reacts very rapidly with suitable substrates such as anthracene or tetracene derivatives in solution.⁴⁴⁰ By conducting a kinetic analysis of combined measurements of the dependence of the photo-oxygenation quantum yield Q_{PO} on substrate and O_2 concentration, and of the O_2 concentration dependence of the sensitizer fluorescence lifetime, Stevens and Algar first demonstrated that the T_1 state is formed in the fluorescence quenching of tetracene by O_2 .⁴⁴¹

Morikawa and Cvetanovic arrived at the same conclusion when they studied the quenching by O_2 of the fluorescence of benzene in the presence of varying amounts of *cis*-2-butene in the gas phase.³¹⁴ In this ternary system, *cis*-2-butene is photochemically transformed to *trans*-2-butene after being excited to T_1 by TT energy transfer from the benzene triplet state. This triplet-sensitized *cis*–*trans* isomerization was measured at different concentrations of O_2 and *cis*-2-butene. The fluorescence of benzene was strongly quenched by O_2 , with $k_{\text{S}}^{\text{Q}} = 1.3 \times 10^{11} \text{ M}^{-1} \text{ s}^{-1}$, without noticeably decreasing the concentration of the benzene triplet state, although the benzene S_1 state is the precursor of T_1 . Thus, it was concluded that the efficiency f_{S}^{T} of T_1 -state formation in the fluorescence quenching of benzene by O_2 is unity.³¹⁴

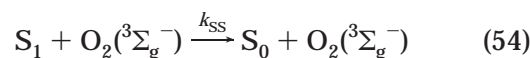
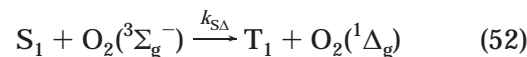
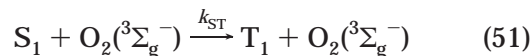
The finding that $f_{\text{S}}^{\text{T}} = 1$ seems to hold true in almost all cases of fluorescence quenching by O_2 in nonpolar solution. Unity efficiency of T_1 -state forma-

tion was determined by Darmanyan for rubrene in toluene,³²³ by Potashnik et al. for seven arenes in toluene,³¹⁵ by Kikuchi for pyrene and fluoranthene in cyclohexane,³³⁸ and by Wilkinson and co-workers for five anthracene derivatives and 11 aromatic hydrocarbons in cyclohexane.^{326,333} Very few exceptions have been reported (see section IV.B.2.c).

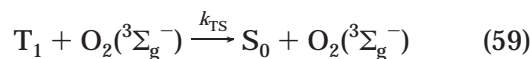
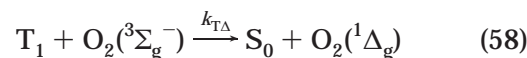
b. $O_2(^1\Delta_g)$ Formation by O_2 -Enhanced Inter-system Crossing. Livingston and Rao noted, in an early investigation of the photo-oxygenations of DPA and anthracene, that the fluorescent state as well as the triplet state of the hydrocarbon can react with O_2 to form an intermediate—later identified as $O_2(^1\Delta_g)$ —which leads to the formation of an endoperoxide.²⁹⁶ For strong fluorescers, such as DPA, it is S_1 -state quenching, for weak fluorescers, such as anthracene, it is T_1 -state quenching. However, this conclusion does not necessarily establish that quenching of the S_1 state of DPA is a direct source of $O_2(^1\Delta_g)$, since fluorescence quenching leads to formation of the T_1 state, which is subsequently quenched by O_2 under formation of $O_2(^1\Delta_g)$.

Stevens and Algar studied the kinetics of the photo-oxygenation of several aromatic compounds to elucidate which quenching processes actually yield $O_2(^1\Delta_g)$.^{302,303,311,312,441} Their kinetic analysis considered fluorescence, isc $S_1 \rightarrow T_1$, which occurs in the absence of O_2 with quantum yield Q_{T}^{D} , and ic $S_1 \rightarrow S_0$, which altogether contribute with overall rate constant k_{S}^{D} to monomolecular deactivation of S_1 , as well as the bimolecular steps 51 and 52.

Since it was later realized that, in some cases, process 54 may also be important,^{226,315,325,334} it is also repeated here. The overall rate constant of S_1 -state quenching by O_2 is $k_{\text{S}}^{\text{Q}} = k_{\text{ST}} + k_{\text{SA}} + k_{\text{SS}}$.



$p_{\text{S}}^{\text{O}_2}$, f_{S}^{Δ} , and f_{S}^{T} denote the fractions of S_1 quenched by O_2 , of S_1 quenched by O_2 leading to $O_2(^1\Delta_g)$, and of S_1 quenched by O_2 leading to T_1 , and are defined as $p_{\text{S}}^{\text{O}_2} = k_{\text{S}}^{\text{Q}}[O_2]/(k_{\text{S}}^{\text{D}} + k_{\text{S}}^{\text{Q}}[O_2])$, $f_{\text{S}}^{\Delta} = k_{\text{SA}}/k_{\text{S}}^{\text{Q}}$, and $f_{\text{S}}^{\text{T}} = (k_{\text{ST}} + k_{\text{SA}})/k_{\text{S}}^{\text{Q}}$. The triplet state is deactivated by isc $T_1 \rightarrow S_0$ with rate constant k_{T}^{D} and by the bimolecular processes 58 and 59,



with rate constant $k_{\text{T}}^{\text{Q}} = k_{\text{TA}} + k_{\text{TS}}$, where step 58 describes the overall $O_2(^1\Delta_g)$ formation in T_1 -state quenching by O_2 , which occurs with efficiency $S_{\Delta} = k_{\text{TA}}/k_{\text{T}}^{\text{Q}}$, and $p_{\text{T}}^{\text{O}_2} = k_{\text{T}}^{\text{Q}}[O_2]/(k_{\text{T}}^{\text{D}} + k_{\text{T}}^{\text{Q}}[O_2])$ denotes the fraction of T_1 quenched by O_2 . $p_{\text{T}}^{\text{O}_2} = 1$ is frequently assumed for ($\pi\pi^*$) triplet states in air-saturated solution. The overall quantum yield of $O_2(^1\Delta_g)$ forma-

tion is thus given by eq 73. The first term of eq 73

$$Q_{\Delta} = p_S^{O_2} f_S^{\Delta} + p_S^{O_2} f_S^T S_{\Delta} + Q_T^0 (1 - p_S^{O_2}) S_{\Delta} \quad (73)$$

represents the contribution to the quantum yield, which originates from S_1 -state quenching according to eq 52; the second and third terms represent the contributions resulting from T_1 -state quenching via processes 51 and 58. The fractions $p_S^{O_2} = (F^0 - F)/F^0$ and $(1 - p_S^{O_2}) = F/F^0$ are obtained from the ratio F^0/F of the fluorescence intensities in the absence and in the presence of O_2 via the Stern–Volmer relation 71. Thus, one can derive eq 74, which gives a deeper insight into the complex processes leading to $O_2(^1\Delta_g)$ sensitization. Since at that time no direct spectro-

$$Q_{\Delta}(F^0/F) = Q_T^0 S_{\Delta} + (f_S^{\Delta} + f_S^T S_{\Delta})[(F^0/F) - 1] \quad (74)$$

scopic measurements of singlet oxygen in solution were possible, Stevens and Algar measured photo-oxygenation quantum yields Q_{PO} , which are related to Q_{Δ} via the reaction efficiency $f_R = [A]/\{(k_c \tau_{\Delta})^{-1} + [A]\}$, where τ_{Δ} and k_c denote the singlet oxygen lifetime and the rate constant for its chemical reaction with the substrate A. They evaluated $Q_{PO}(F^0/F)$ data, which are relative values of $Q_{\Delta}(F^0/F)$ (see eqs 74 and 75).³⁰²

$$Q_{PO}(F^0/F) = f_R \{ Q_T^0 S_{\Delta} + (f_S^{\Delta} + f_S^T S_{\Delta})[(F^0/F) - 1] \} \quad (75)$$

Stevens and Algar investigated the self-sensitized (sensitizer = substrate) photo-oxygenation of 9,10-dimethylantracene, 9,10-dimethyl-1,2-benzanthracene, tetracene, and rubrene in benzene as a function of dissolved O_2 concentration. Plotting their results of $Q_{PO}(F^0/F)$ versus $(F^0/F) - 1$ resulted in linear correlations, as expected from eq 75. The intercept/slope ratios yielded values of $Q_T^0 S_{\Delta}/(f_S^{\Delta} + f_S^T S_{\Delta})$. Their discussion led to the conclusion that $O_2(^1\Delta_g)$ is produced solely by O_2 quenching of the aromatic hydrocarbon triplet state, i.e., reaction 58, which is a yield-limiting process at very low O_2 concentrations.³⁰² Further photo-oxygenation studies by Stevens and Algar, using other aromatic hydrocarbons as sensitizers, seemed to support these conclusions.^{311,312,441}

Parmenter and Rau estimated that smaller Franck–Condon factors, and hence smaller rate constants of fluorescence quenching, should result for molecules for which ΔE_{ST} is insufficient for $O_2(^1\Delta_g)$ excitation.⁴⁴² However, their measurements of k_S^Q values for a series of aromatic hydrocarbons in cyclohexane showed that $k_S^Q \approx k_{diff}$, irrespective of whether ΔE_{ST} is larger or smaller than the $O_2(^1\Delta_g)$ excitation energy. It was suggested that the energy-transfer process 52 could be excluded for fluorescence quenching of aromatic hydrocarbons, in agreement with the conclusions of Stevens and Algar.

Brauer und Wagener, however, arrived at very different conclusions in their 1975 investigation of the self-sensitized photo-oxygenation of rubrene in six different solvents.³¹⁷ Values of Q_{PO} were determined over a wide range of rubrene and O_2 concen-

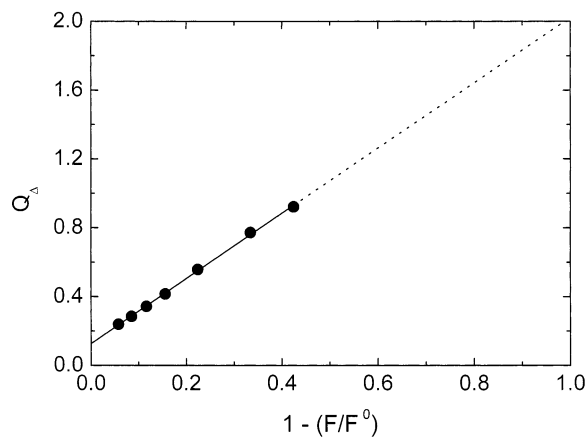


Figure 35. Dependence of Q_{Δ} on $1 - (F/F^0)$ for the sensitization of $O_2(^1\Delta_g)$ by rubrene in $CHCl_3$. Reprinted with permission from ref 317. Copyright 1975 Deutsche Bunsen-Gesellschaft.

trations. Their experiments allowed the separate determinations of $Q_{PO}(F^0/F)$ and f_R . Linear correlations of $Q_{PO}(F^0/F)$ versus $(F^0/F) - 1$ resulted for each solvent. The slopes $f_R(f_S^{\Delta} + f_S^T S_{\Delta})$ varied from 0.30 for benzene to 1.46 for CCl_4 as solvent. Division by the corresponding reaction efficiencies f_R yielded values of $f_S^{\Delta} + f_S^T S_{\Delta} = 1.6$ (toluene), 1.7 (benzene), 2.1 ($CHCl_3$), 1.7 ($C_6H_3Cl_3$), 1.9 (CCl_4), and 2.1 (CS_2). Since f_S^{Δ} , f_S^T , and S_{Δ} cannot be larger than 1, this result clearly indicates that, for rubrene, both processes 52 and 58 contribute to $O_2(^1\Delta_g)$ formation, with efficiencies near or equal to unity.³¹⁷

The fluorescence quantum yield of rubrene is very large and amounts to $Q_F^0 = 0.92$ in $CHCl_3$ in the absence of O_2 . By inserting $f_S^T = 1$ and the reasonable approximation $Q_T^0 = 1 - Q_F^0$ in eq 75, Brauer derived eq 76, which predicts a linear correlation between $Q_{\Delta} = Q_{PO}/f_R$ and $1 - (F/F^0)$ with the limiting value of $Q_{\Delta}^{\infty} = f_S^{\Delta} + S_{\Delta}$ for $F/F^0 = 0$, i.e., for $[O_2] \rightarrow \infty$.

$$Q_{\Delta} = Q_T^0 S_{\Delta} + (f_S^{\Delta} + Q_F^0 S_{\Delta})[1 - (F/F^0)] \quad (76)$$

Figure 35 shows the excellent linear plot obtained with the $CHCl_3$ data, with the intercept for $Q_{\Delta}^{\infty} = 2$ at $1 - (F/F^0) = 1$. Thus, Brauer and Wagner first demonstrated that both the T_1 state and $O_2(^1\Delta_g)$ may be formed during the fluorescence quenching by O_2 and that the maximum value of Q_{Δ} is 2.³¹⁷ This important result was confirmed by both authors in the subsequent investigation of the self-sensitized photo-oxygenation of heterocoerdianthrone.³¹⁸ For this likewise highly fluorescent compound, $f_S^{\Delta} + S_{\Delta} = 2$ was found.

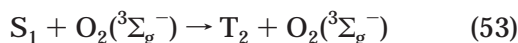
Interestingly, a little later, Stevens and Ors³¹⁹ used the Q_{PO} data reported by Stevens and Algar for 9,10-dimethylantracene, 9,10-dimethyl-1,2-benzanthracene, tetracene, and rubrene,³⁰² and newly determined reaction efficiencies f_R , to re-evaluate their previous data following the lines of Brauer and Wagener. This led to $f_S^{\Delta} + S_{\Delta} \approx 2$ for rubrene and 9,10-dimethylantracene in benzene, thus confirming the result of Brauer and Wagener.³¹⁹

Merkel and Herkstroeter studied the rubrene-sensitized photo-oxygenation of DPBF and obtained

$f_S^\Delta + S_\Delta = 1.2$ in benzene.⁴⁴³ However, Wu and Trozollo repeated this experiment and determined values of $f_S^\Delta + S_\Delta \approx 1.5$ in a series of solvents.³²⁰ The deviating result obtained by Merkel and Herkstroeter was explained by insufficient experimental conditions. Further photo-oxygenation studies by Wu and Trozollo yielded values of $Q_{PO} > 1$ for a larger number of aromatic hydrocarbons, indicating that $O_2(^1\Delta_g)$ can be directly produced in the fluorescence quenching by O_2 . The photo-oxygenation technique was also used by Brauer et al.³²⁴ and Usui et al.³²⁸ to determine, for a larger number of aromatic compounds, $1 \leq f_S^\Delta + S_\Delta \leq 2$.

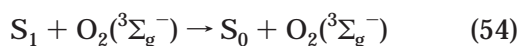
In a very fine work, Darmanyan demonstrated, by the combination of TT absorption and bleaching measurements, that for rubrene $f_S^\Delta + S_\Delta = 2$ in benzene.³²³ Spectroscopic techniques were used by Gurinovich and Salokhiddinov, who determined quantum yields of $O_2(^1\Delta_g)$ formation for aromatic molecules directly via the $a \rightarrow X$ emission at 1275 nm.³²⁷ They found values of $Q_\Delta \leq 1$ for $\Delta E_{ST} < 94 \text{ kJ mol}^{-1}$, and values of Q_Δ approaching the limit of 2 at high O_2 concentrations for $\Delta E_{ST} > 94 \text{ kJ mol}^{-1}$.³²⁷ Dobrowolski et al.,³³¹ Kanner and Foote,³³² and Ogilby et al.³³⁷ used chemical techniques and emission spectroscopy to determine the value of Q_Δ^∞ for 9,10-dicyanoanthracene and obtained values between 1.5 and 2 in benzene, cyclohexane, and acetonitrile. Thus, the results of the different investigations agree in the finding that $O_2(^1\Delta_g)$ formation in the fluorescence quenching by O_2 may be a very important process, particularly for highly fluorescent molecules.

The condition $\Delta E_{ST} > E_\Delta = 94 \text{ kJ mol}^{-1}$ is imperative but not sufficient for efficiencies $f_S^\Delta \approx 1$. This was first noted by Stevens and Ors, whose re-evaluation of previous Q_{PO} data led to $f_S^\Delta + S_\Delta = 1.0$ and 1.2 for 9,10-dimethyl-1,2-benzanthracene and tetracene in benzene, respectively.³¹⁹ For both compounds, $\Delta E_{ST} > 94 \text{ kJ mol}^{-1}$ holds true. However, their large isc quantum yields of 0.64 and 0.68 indicate that upper excited triplet states T_n ($n \geq 2$) lie below S_1 in both cases. Therefore, the deactivation process 53, leading to the triplet manifold, could take



place with subsequent very rapid ic $T_2 \rightarrow T_1$, without producing $O_2(^1\Delta_g)$. This assumption was confirmed by Brauer et al.,³²⁴ who found $f_S^\Delta + S_\Delta \leq 1$ for four aromatic compounds with $\Delta E_{ST} > E_\Delta$ and $S_1 > T_n$ in toluene, and by Usui et al., who determined $f_S^\Delta + S_\Delta \leq 1$ for five aromatic hydrocarbons with $\Delta E_{ST} > E_\Delta$ and $S_1 > T_n$ in cyclohexane.³²⁸ Thus, it appears that $f_S^\Delta \approx 0$, if $\Delta E_{ST} > E_\Delta$ and $S_1 > T_n$ hold true.

c. S_0 -State Formation by O_2 -Enhanced Internal Conversion. Process 54, O_2 -enhanced ic $S_1 \rightarrow S_0$, is spin-allowed but is expected to be negligible due to the large S_1-S_0 energy gap, which should lead to small corresponding rate constants. However,



Darmanyan first reported in 1982 that quenching of

the fluorescence of DPA by O_2 leads to formation of S_0 and $O_2(^3\Sigma_g^-)$ in toluene.³²⁹ Using TT absorption and fluorescence spectroscopy, he showed clearly that the sum $Q_F + Q_T$ of fluorescence and isc quantum yields decreases significantly below unity with increasing $[O_2]$. However, he also showed that $O_2(^1\Delta_g)$ is still formed by the energy-transfer process 52. This was verified by combined TT absorption and bleaching experiments with rubrene as substrate. The quantitative evaluation demonstrated that the ratio of bleached rubrene molecules to triplet-excited DPA molecules formed amounts to 2.1; i.e., each S_1 -excited DPA molecule which reacts with O_2 to yield T_1 generates two $O_2(^1\Delta_g)$ molecules.³²⁹ Temperature-dependent investigations led to the conclusion that the O_2 -enhanced ic of DPA occurs via a twist of the phenyl substituents under formation of sterically hindered conformers.³²⁹

Drews et al. investigated the peculiar behavior of DPA with respect to fluorescence quenching by self-sensitized photo-oxygenation techniques.³³⁰ They determined Q_{PO} as a function of the DPA and oxygen concentrations in toluene and modified the kinetic scheme by allowing for the enhanced ic process 54, which, according to Darmanyan, contributes with an efficiency of 0.67 to quenching of S_1 -excited DPA by O_2 .³²⁹ This evaluation confirmed the result reported by Darmanyan. If enhanced ic was neglected, the wrong result $f_S^\Delta + S_\Delta = 0.8$ would have been calculated, similar to the result $f_S^\Delta + S_\Delta = 1.0$ reported by Stevens and Mills, who did not consider enhanced ic.³³⁶ This example also demonstrates that photo-oxygenation measurements can easily lead to wrong conclusions if inappropriate kinetic models are used.

DPA is a rather peculiar case. Analogous O_2 -enhanced ic was reported by Brauer's group only for *meso*-diphenyl-substituted anthracenes, such as 1,4-dimethoxy-9,10-diphenylanthracene or *meso*-diphenyl-helanthrene.³²⁴ However, a more general mechanism of O_2 -enhanced ic, which is independent of twistable phenyl substituents, was discovered by Ottolenghi's group.^{315,316} Potashnik et al. measured triplet quantum yields by TT absorption in the absence and in the presence of O_2 for seven arenes in toluene and in acetonitrile.³¹⁵ The triplet yield f_S^T for the quenching of the S_1 state by O_2 was determined to be unity in the limits of uncertainty for all arenes investigated in toluene, whereas in acetonitrile all values of f_S^T were found to be significantly smaller, with the lowest values of 0.60 (pyrene) and 0.55 (phenanthrene). It was suggested that these observations indicate the involvement of CT interactions between S_1 -excited hydrocarbon and O_2 in the quenching process.³¹⁵

These conclusions were confirmed by studies reported by Sato et al., who determined values of f_S^T decreasing from 1.0 to 0.36 for nine aromatic compounds with strongly decreasing oxidation potential in acetonitrile,²²⁶ and by Wilkinson and co-workers, who measured values of f_S^T between 1.0 and 0.49 for nine anthracene derivatives and 12 aromatic hydrocarbons in acetonitrile.^{325,334}

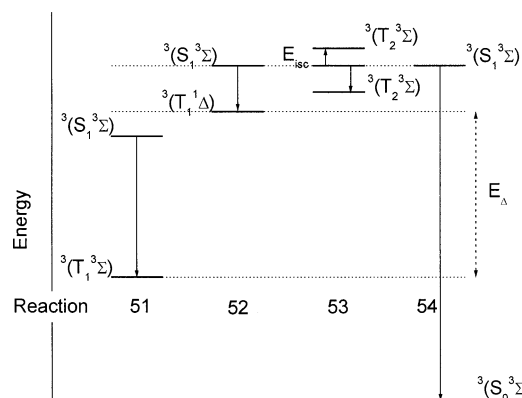
Fluorescence quenching by O₂ even may lead to electron transfer. Richards et al. observed the spectrum of pyrene cations after intense laser pulse excitation in alcoholic solutions of pyrene.³¹³ However, these ions were shown to be the product of a biphotonic process. Actually, the efficiency of free radical ion pair (RIP) generation is very low or zero in the fluorescence quenching, even if $\Delta G_{\text{CET}} \approx -100$ kJ mol⁻¹. Sato et al. first detected RIP generation in fluorescence quenching by O₂.²²⁶ They obtained corresponding signals only with 2,6-dimethoxynaphthalene in acetonitrile, and the quantum yield of monophotonic RIP formation amounted to only 0.003, although the process is extremely exergonic, with $\Delta G_{\text{CET}} = -140$ kJ mol⁻¹. Consequently, fluorescence quenching was still thought to be induced by exciplex formation or CT interactions, as long as $\Delta G_{\text{CET}} \geq -140$ kJ mol⁻¹.²²⁶ It was concluded that the small molecular size of O₂ leads to extremely high solvent reorganization energies for long-distance electron transfer from an aromatic molecule to O₂. For this reason, long-distance electron transfer cannot compete with exciplex formation in the fluorescence quenching by O₂.

3. Mechanism of Oxygen Quenching of Excited Singlet States

Since, below the S₁ state, at least one and often two excited triplet states exist, S₁-state quenching by O₂ is more complex than quenching of T₁. Furthermore, fluorescence quenching is, for most molecules, a diffusion-controlled process under ambient conditions, obscuring the variation of the actual deactivation rate constants and their dependences on molecular parameters. This is why quantitative analysis of the oxygen quenching of the S₁ state is much more complex than in the case of the T₁ state.

However, in the past decade, further significant progress has been made toward the understanding of the different competing deactivation processes by the works of the groups of Kikuchi,^{226,307} Brauer,^{308,309,335} and Wilkinson.^{325,326,333,334} Scheme 5 displays the four ic processes 51–54, which have been identified to be the most important. The different routes of ic lead from the initially formed excited

Scheme 5. The Most Important Deactivation Processes of the Excited Complex ³(S₁³Σ)^a



^aProcesses 51–54 lead by ic to the triplet complexes ³(T₁³Σ), ³(T₁¹Δ), ³(T₂³Σ), and ¹(S₀³Σ), which decay by fast dissociation to the respective components. For details, see text.

complex ³(S₁³Σ) to the product complexes ³(T₁³Σ), ³(T₁¹Δ), ³(T₂³Σ), and ³(S₀³Σ), which further dissociate to the respective components.

Kikuchi et al. investigated the fluorescence quenching by O₂ of five acridinium cations in acetonitrile, which all fulfill the energetic conditions T₂ ≫ S₁ and $\Delta E_{\text{ST}} < E_{\Delta}$.³⁰⁷ Therefore, the isolated reaction 51, enhanced isc without O₂(¹Δ_g) formation with rate constant k_{ST} , which occurs as spin-allowed ic from complex ³(S₁³Σ) to complex ³(T₁³Σ), could be studied separately. Values of $k_{\text{S}}^{\text{Q}} = (1.0\text{--}3.5) \times 10^8$ M⁻¹ s⁻¹ were determined for four of the ions, for which $\Delta E_{\text{ST}} \approx 85$ kJ mol⁻¹ and the change in free energy for full electron transfer to O₂ is $\Delta G_{\text{CET}} \approx 35$ kJ mol⁻¹. Therefore, only very small rate constants of $k_{\text{S}}^{\text{Q}} \approx 2 \times 10^8$ M⁻¹ s⁻¹ result in the absence of strong CT interactions and energy transfer. For the fifth acridinium cation, for which $\Delta G_{\text{CET}} = -75$ kJ mol⁻¹ was calculated, the much larger rate constant $k_{\text{S}}^{\text{Q}} = 2.2 \times 10^9$ M⁻¹ s⁻¹ was measured. Thus, the increase of CT interactions enhances the rate constant k_{ST} of ³(S₁³Σ) → ³(T₁³Σ) deactivation, similarly to the ic ³(T₁³Σ) → ³(S₀³Σ) in the T₁-state quenching by O₂.

Four anthracene derivatives with one to four cyano substituents were studied by Kikuchi et al.²²⁶ For these compounds, T₂ ≫ S₁ and $\Delta E_{\text{ST}} > E_{\Delta}$ hold true.³⁰⁷ Reaction 52, enhanced isc with O₂(¹Δ_g) formation, should be dominant, because of the small amount of excitation energy which has to be dissipated, although reaction 51 also may take place. In acetonitrile, the value of k_{S}^{Q} decreases from 1.6×10^{10} (9-cyanoanthracene) to 5.3×10^9 M⁻¹ s⁻¹ (2,6,9,10-tetracyanoanthracene, TCA), with ΔG_{CET} increasing from -51 to 24 kJ mol⁻¹. Again, an increase of the rate constant with increasing CT interaction has to be noted. Comparison of rate constants k_{S}^{Q} for acridinium cations and TCA of approximately the same value of ΔG_{CET} shows that the overall quenching rate constant of TCA is about 20-fold larger. Thus, it was clearly shown that, in the absence of strong CT interactions, the rate constant $k_{\text{S}\Delta}$ of process 52, ³(S₁³Σ) → ³(T₁¹Δ) with subsequent dissociation to T₁ and O₂(¹Δ_g), is about 1 order of magnitude larger than k_{ST} of process 51, ³(S₁³Σ) → ³(T₁³Σ), in accordance with the much smaller excess energy which has to be dissipated. The same series of cyanoanthracenes was studied by Kikuchi et al. in benzene. The values of k_{S}^{Q} decreased, on average, by a factor of 2. Thus, only a small solvent effect was found.³⁰⁷

Wirp et al. investigated the oxygen quenching of the fluorescence of eight 9-cyanoanthracene derivatives bearing different substituents in the 10-position and of several other anthracenes substituted with electron-donating groups in the 9,10-positions, for which T₂ ≫ S₁ and $\Delta E_{\text{ST}} > E_{\Delta}$ also hold true, in acetonitrile.³⁰⁹ With decreasing ΔG_{CET} , they found values of k_{S}^{Q} increasing from 4.3×10^9 M⁻¹ s⁻¹ (9,10-dicyanoanthracene, DCA) to almost diffusion-controlled values of 3.4×10^{10} M⁻¹ s⁻¹. Additional information was obtained from the efficiencies f_{S}^{Δ} of O₂(¹Δ_g) formation, which decrease in the same series from 1.0 (DCA) to 0.15 (9,10-diethoxyanthracene). It was noted that, to a first approximation, an inverse

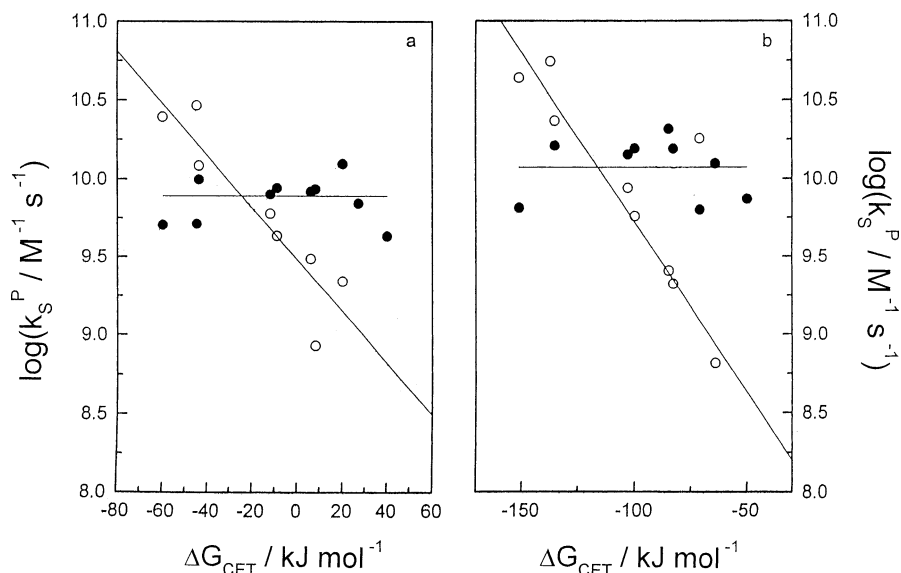


Figure 36. Dependence of $\log(k_S^P)$ [$= \log(k_S^{3\Sigma})$ (○) and $\log(k_S^{1\Delta})$ (●)] on the change in free energy ΔG_{CET} for complete electron transfer from S_1 -excited anthracenes to O_2 in a) toluene and b) acetonitrile. Straight line with slope $-0.022 \text{ kJ mol}^{-1}$ mol results from the linear fit to the $\log(k_S^{3\Sigma})$ data for acetonitrile. Reprinted with permission from ref 309. Copyright 1996 Deutsche Bunsen-Gesellschaft.

relationship exists between k_S^Q and f_S^Δ , similarly to the empirical inverse relation between k_T^Q and S_Δ found in the T_1 -state quenching by O_2 (see Figure 25). Since only reactions 51 and 52 can compete and only reaction 52 produces $O_2(^1\Delta_g)$, the separation of the corresponding rate constants by calculation of $k_S^{3\Sigma} = (1 - f_S^\Delta)k_S^Q$ and $k_S^{1\Delta} = f_S^\Delta k_S^Q$ was obvious. Figure 36 displays the dependences of $\log(k_S^{3\Sigma})$ (reaction 51, ○) and $\log(k_S^{1\Delta})$ (reaction 52, ●) on the change in free energy ΔG_{CET} . Only the $\log(k_S^{3\Sigma})$ data show a clear dependence on ΔG_{CET} . Thus, it appears that process 52 is not CT-assisted, whereas process 51 is, where the latter result is in qualitative agreement with the finding reported by Kikuchi (vide supra). However, the values of $k_S^{3\Sigma}$ obtained with the anthracenes are much larger than the value of k_{ST} determined with the acridinium cation in the highly exergonic region. Since the charge of the S_1 -excited species should have no influence on the quenching by the uncharged O_2 , either the comparison between both classes of compounds is impossible for some unknown reason, or both processes 51 and 52 have nCT and pCT contributions, as was found for processes $^3(T_1^3\Sigma) \rightarrow ^3(S_0^3\Sigma)$ and $^1(T_1^3\Sigma) \rightarrow ^1(S_0^1\Delta)$ competing in the T_1 -state quenching by O_2 . The simple separation of the rate constants, which rests on the assumption that the doubly excited complex $^3(T_1^1\Delta)$ formed in reaction 52 decays completely under formation of $O_2(^1\Delta_g)$ and T_1 -excited sensitizer, would then be misleading. Thus, the question of whether process 52 could also be CT-assisted still seems to be open. The rate constants of fluorescence quenching were also measured for these anthracene derivatives in acetonitrile. Only a very small increase of k_S^Q by a factor of ~ 2 was found.

Wilkinson et al. studied the fluorescence quenching by O_2 of a series of 9- and 9,10-substituted anthracene derivatives in cyclohexane.³³³ Rate constants k_S^Q varying from 4.7×10^9 (DCA) to diffusion-controlled values and values of f_S^Δ ranging from 1 to

0 were reported. Previously, Usui et al. had clearly demonstrated that the magnitude of f_S^Δ depends markedly on the position of T_2 relative to S_1 .³²⁸ For many 9- and 9,10-substituted anthracene derivatives, T_2 lies close above S_1 . This leads to temperature-dependent fluorescence quantum yields, which are explained by the activation-controlled isc $S_1 \rightarrow T_2$, leading to radiationless deactivation in the triplet manifold, where the activation energy E_{isc} is interpreted as the energy difference between T_2 and S_1 . Wilkinson et al. examined whether the strong variation of f_S^Δ could be explained by the competition of processes 52 and 53, i.e., ic $^3(S_1^3\Sigma) \rightarrow ^3(T_1^1\Delta)$ and a slightly endothermic ic $^3(S_1^3\Sigma) \rightarrow ^3(T_2^3\Sigma)$ (Scheme 5). Since $f_S^T = 1$ was found for all investigated derivatives, $f_S^\Delta = k_{S\Delta}/(k_{S\Delta} + k_{\text{ST}})$ holds true. Assuming $k_{\text{ST}} = A \exp(-E_{\text{isc}}/(RT))$, they derived eq 77.

$$f_S^\Delta = k_{S\Delta}/\{k_{S\Delta} + A \exp(-E_{\text{isc}}/(RT))\} \quad (77)$$

Figure 37 shows the dependence of f_S^Δ on E_{isc} . The calculated sigmoidal curve describing the experimental data is a fit using eq 77 and the known values of E_{isc} .³³³ The slightly endothermic ic $^3(S_1^3\Sigma) \rightarrow ^3(T_2^3\Sigma)$ appears to reduce f_S^Δ to values below 0.05 for $E_{\text{isc}} \lesssim 10 \text{ kJ mol}^{-1}$ for these systems in cyclohexane. The inset of Figure 37 displays the linear correlation of $\ln(1/f_S^\Delta - 1)$ with E_{isc} . This equivalent representation yields a slope of $-1/(RT) = -0.41 \text{ mol kJ}^{-1}$, as expected from eq 77 at room temperature. Wilkinson et al. concluded from these results that, once the complex $^3(T_2^3\Sigma)$ is formed, very fast subsequent dissociation occurs, yielding $O_2(^3\Sigma_g^-)$ and the T_2 state of the anthracene derivative, which then dissipates excess energy by ic $T_2 \rightarrow T_1$ without forming $O_2(^1\Delta_g)$. These important results indicate that the quenching process 53 via $^3(T_2^3\Sigma)$ becomes dominant for molecules for which T_2 lies below S_1 , i.e., when process 53 becomes exothermic.

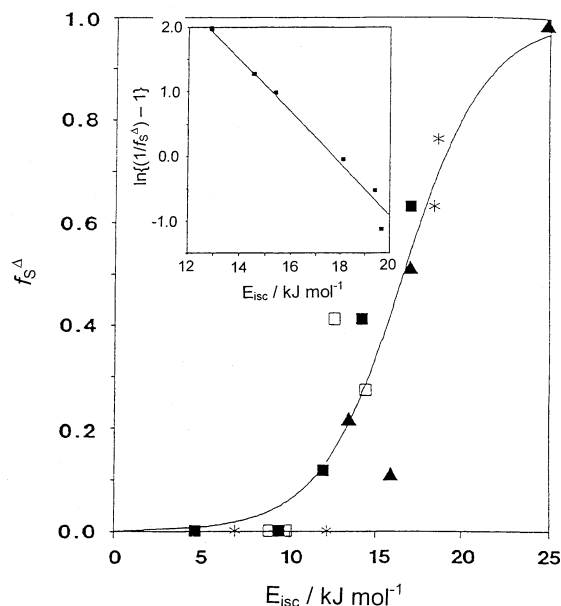


Figure 37. Plot of the fraction f_S^Δ of $O_2(^1\Delta_g)$ produced due to O_2 quenching of S_1 -excited anthracenes versus activation energy E_{isc} of $S_1 \rightarrow T_2$ isc. Different symbols indicate different data sources. Inset: Plot of $\ln\{(1/f_S^\Delta) - 1\}$ against E_{isc} . Reprinted with permission from ref 333. Copyright 1993 American Chemical Society.

The fluorescence quenching by O_2 of a series of aromatic compounds with strongly varying values of ΔG_{CET} was investigated by Sato et al. in acetonitrile. Only for 2,6-dimethoxynaphthalene ($\Delta G_{CET} = -140$ kJ mol $^{-1}$) was RIP formation observed.²²⁶ Comparing the fluorescence quenching of aromatic fluorophores by aromatic donors, by SCN^- , and by O_2 , Kikuchi's group found that the switchover in the mechanisms from exciplex quenching to electron-transfer quenching occurs for aromatic quenchers at $\Delta G_{CET} = -40$ kJ mol $^{-1}$, for SCN^- at $\Delta G_{CET} = -105$ kJ mol $^{-1}$, and for O_2 at $\Delta G_{CET} \leq -140$ kJ mol $^{-1}$.^{226,444} It was shown that this shift depends on the molecular size of the quencher, which tremendously influences the solvent reorganization energy, estimated to be about 60 kJ mol $^{-1}$ for SCN^- but as much as 260 kJ mol $^{-1}$ for O_2 .^{226,444} Thus, it is the small size of the O_2 molecule and the correspondingly extremely high solvent reorganization energy which prevents effective RIP formation in the oxygen quenching of the fluorescence of aromatic compounds, even in the highly exergonic range.

Sato et al. measured rate constants k_S^Q and efficiencies f_S^T of T_1 -state formation in the quenching of S_1 states by O_2 .²²⁶ They observed a strong decrease of f_S^T from 1.0 ($\Delta G_{CET} = -24$ kJ mol $^{-1}$) to a minimum value of 0.36 ($\Delta G_{CET} = -114$ kJ mol $^{-1}$). This decrease can be attributed to strong CT interactions in the intermediately formed exciplex, $^3(S_1^3\Sigma)$, which open the door to deactivation process 54, i.e. $^3(S_1^3\Sigma) \rightarrow ^3(S_0^3\Sigma)$, leading directly to the ground-state surface without $O_2(^1\Delta_g)$ formation, i.e., with $f_S^\Delta = 0$. Thus, in the exergonic range ($\Delta G_{CET} < -30$ kJ mol $^{-1}$ in acetonitrile), process 54 begins to compete with reaction 51–53, contributing to an increase of k_S^Q and a reduction of f_S^Δ .

The S_1-T_1 and S_1-T_2 energy gaps determine the possible competition of reactions 51–53. Together with the strength of CT interactions in the excited $^3(S_1^3\Sigma)$ complex, quantified by ΔG_{CET} , which also determines the contribution of process 54, they finally determine the values of k_S^Q , f_S^T , and f_S^Δ .

The following rough rules could be established. Reaction 51 takes place for every fluorophore, with $2 \times 10^8 \lesssim k_{ST} \lesssim 2 \times 10^9$ M $^{-1}$ s $^{-1}$, where the upper limit could be 1 order of magnitude higher according to the results of Wirp et al.³⁰⁹ The rate constant k_{ST} increases with decreasing ΔG_{CET} . Reaction 52 demands $\Delta E_{ST} > E_\Delta$ and contributes with $f_S^\Delta = 1$ and $5 \times 10^9 \lesssim k_{S\Delta} \lesssim 2 \times 10^{10}$ M $^{-1}$ s $^{-1}$ to k_S^Q , and it is still open whether $k_{S\Delta}$ also depends on ΔG_{CET} . Reaction 53 demands the T_2 state to be nearby or below S_1 and is rather fast, with $k_{ST} < k_{diff}$, without producing $O_2(^1\Delta_g)$. Reaction 54 becomes competitive for $\Delta G_{CET} < -30$ kJ mol $^{-1}$ and takes place with $f_S^\Delta = 0$ and rate constant k_{SO} approaching k_{diff} in the strongly exergonic range.

Further extended investigations of fluorescence quenching by O_2 were performed by the groups of Brauer^{308,335} and Wilkinson^{325,326,334} and can be successfully analyzed by applying the above-mentioned rules. Grewer et al. determined rate constants for 15 aromatic compounds in toluene and observed a decrease of k_S^Q with increasing ΔG_{CET} , from 3.5×10^{10} to 0.4×10^{10} M $^{-1}$ s $^{-1}$. The corresponding efficiencies f_S^Δ are substantially larger than zero only in those cases where $\Delta E_{ST} > E_\Delta$, where $\Delta G_{CET} \geq 0$, and where $T_2 \gg S_1$ holds true.³⁰⁸ From temperature-dependent measurements of k_S^Q , it could be shown that quenching of DCA fluorescence is activationless in the high-temperature region. Wirp et al. measured values of k_S^Q and f_S^Δ for seven protonated aromatic compounds and four acridinium cations in acetonitrile.³³⁵ Rate constants varied between 3.0×10^8 and 2.9×10^{10} M $^{-1}$ s $^{-1}$. The results indicated that fluorescence quenching could be described as a competition between processes 52 and 53. k_S^Q showed, to a first approximation, a correlation with the S_1-T_2 energy gap.

Olea and Wilkinson investigated the fluorescence quenching of nine anthracene derivatives in acetonitrile.³³⁴ With the exception of 9-cyanoanthracene and DCA, all values of k_S^Q were found to be almost or completely diffusion-controlled. Efficiencies f_S^Δ were found to be smaller than those in cyclohexane and varied between 0 and 0.5. Efficiencies f_S^T of T_1 -state formation in the S_1 -state quenching by O_2 were determined for four derivatives to be between 0.57 and 0.53. Thus, the contribution of process 54, which operates for these compounds in acetonitrile but not in cyclohexane, leads to an increase of k_S^Q and a decrease of f_S^Δ . Abdel-Shafi et al. studied the oxygen quenching of the fluorescence of a large number of aromatic hydrocarbons in acetonitrile and in cyclohexane.^{325,326} Since values of k_S^Q , f_S^Δ , and f_S^T had been determined, a detailed analysis could be performed. Quenching by energy transfer and by CT-assisted pathways was shown to operate.

Thus, an extensive database on the fluorescence quenching by O_2 has been elaborated, and can be well explained, although discrepancies between some of the data still exist. However, discrepancies are hard to avoid, particularly in the measurement of f_S^Δ , which is rather indirect. All these data are consistent with the finding that fluorescence quenching by O_2 is dominated by the competition of processes 51–54, whereby energy gap rules and CT interactions direct the different deactivation routes, similar to the case of T_1 -state quenching by oxygen.

V. Detection of Singlet Oxygen

The first time-resolved detection of $O_2(^1\Delta_g)$ singlet oxygen in solution was achieved by Krasnovsky in 1976,⁵⁴ using the $a \rightarrow X$ phosphorescence at 1270 nm. Since then, the method has become the standard technique for investigations of singlet oxygen photochemistry, and especially for determination of $O_2(^1\Delta_g)$ formation yields, lifetimes, and deactivation rate constants. Excellent introductions to these techniques can be found in a recent review by Krasnovsky⁴⁴⁵ and in a recent volume of *Methods in Enzymology*.⁴⁴⁶ Rate constants for $O_2(^1\Delta_g)$ formation are commonly determined from the decay of the sensitizer-excited state, but in a carefully built setup, these data can also be obtained from the rise of the $a \rightarrow X$ luminescence.^{152,447} Several methods for detection of $O_2(^1\Sigma_g^+)$ are also well established. These include time-resolved measurements of the $b \rightarrow X$ phosphorescence⁹¹ and $b \rightarrow a$ fluorescence of $O_2(^1\Sigma_g^+)$,^{87,151} and the $b \leftarrow a$ absorption of $O_2(^1\Delta_g)$.^{45–48} Ogilby and co-workers recently reviewed the techniques used in their laboratory for $O_2(^1\Sigma_g^+)$ detection.¹⁵¹

Due to the outstanding importance of singlet oxygen in numerous photobiological processes, it is expected that a great deal of future research will be devoted to $O_2(^1\Delta_g)$ detection in biological environments. However, the currently used technology has important limitations which need to be overcome in order to make quantitative studies in these complicated and strongly deactivating media. During the past 20 years, the 1270 nm singlet oxygen luminescence has been detected mainly with cryogenic germanium diodes, the sensitivity of which is often insufficient to provide quantitative information, even in aqueous media, where the $O_2(^1\Delta_g)$ lifetime is 3.1×10^{-6} s.

Difference techniques have recently been employed to improve the sensitivity with semiconductor detectors. For example, Kakinuma and co-workers used a dual charge-integrating amplifier coupled to two InGaAs/InP pin photodiodes for the investigation of enzyme-catalyzed production of $O_2(^1\Delta_g)$ in aqueous solution under physiological conditions. This setup enabled the simultaneous measurement of the emissions of sample and background, yielding the signal as the difference.⁴⁴⁸ Röder and co-workers used time-resolved emission experiments for the detection of singlet oxygen luminescence in red-cell ghost suspensions.⁴⁴⁹ Careful selection of the sensitizer, optimization of the detection system, use of D_2O as solvent and sodium azide as quencher, and variation of the O_2 concentration were necessary to separate from the

strong background emission a small signal which was interpreted to be emission of $O_2(^1\Delta_g)$ originating from within ghost membranes.

Probably one of the most important advances has been made with the recent introduction of near-infrared photomultipliers, whose sensitivity in the 1270 nm region was reported to be about an order of magnitude larger than that of Ge diodes.⁶ Using this device, Wilson and co-workers recently made the first determination of $O_2(^1\Delta_g)$ lifetime *in vivo*, during photodynamic therapy in the skin and liver of a rat.⁶ Values of about 40 ns were reported. This result was obtained in well-thought-out experiments comparing the findings with homogeneous H_2O solutions, with suspensions of leukemia cells in H_2O , and finally with the living animal. Bäumlér and co-workers measured, with this photomultiplier, the dynamics of the triplet-state deactivation of 8-methoxypsoralen in D_2O via singlet oxygen emission under particularly unfavorable conditions in air-saturated solution where $Q_\Delta \lesssim 0.02$.⁴⁵⁰ For the *in vivo* situation inside the skin, they obtained an estimate of $Q_\Delta \lesssim 0.005$. Using the same technique, Bäumlér and co-workers also studied very recently the chemically pure hydrophobic PDT sensitizer 9-acetoxy-2,7,12,17-tetrakis(methoxyethyl)porphycene in deuterated ethanol.⁴⁵¹

Obviously, biological media are highly heterogeneous, and the $O_2(^1\Delta_g)$ lifetime determined is probably an average over a multitude of very different deactivation processes. Therefore, more detailed insight into the photobiology of singlet oxygen would be expected from spatially resolved spectroscopy. The first step in this direction was recently taken by Andersen and Ogilby,⁵ who measured the lifetime of $O_2(^1\Delta_g)$ in polystyrene in a transmission microscope, using the $b \leftarrow a$ absorption of O_2 at 1930 nm. The time resolution of their first measurements was ~ 160 ns, which is still insufficient for biological samples, but the lifetime of 40 ns reported by Wilson and co-workers⁶ seems to be within reach. Unfortunately, the spatial resolution available with this tool was still limited to a spot size of $\sim 150 \mu m$.⁵ In a very recent separate effort, Ogilby and co-workers used the $a \rightarrow X$ phosphorescence at 1270 nm for $O_2(^1\Delta_g)$ detection. They reported that singlet oxygen can be detected upon irradiation of phase-separated toluene/water mixtures that contain a photosensitizer, and that singlet oxygen images of these heterogeneous samples can be constructed with $2.5 \mu m$ spatial resolution with the new setup (see Figure 38).⁴⁵² For the $a \rightarrow X$ transition at 1272 nm, a lateral resolution of $2.5 \mu m$ is close to the diffraction limit, which, depending on the numerical aperture of the optics used, is ~ 1.5 – $2.0 \mu m$. An even better spatial resolution should be possible with two-photon nonlinear excitation of a sensitizer.⁴⁵²

Although these new technologies look extremely promising, both time-resolved and spatially resolved methods suffer from weak signals, and quantitative detection of very small amounts of $O_2(^1\Delta_g)$ is currently not possible in any medium. Two different approaches have been proposed to make such observations. Both rely on the introduction of fluorescent probes, which are either (i) nonfluorescent molecules

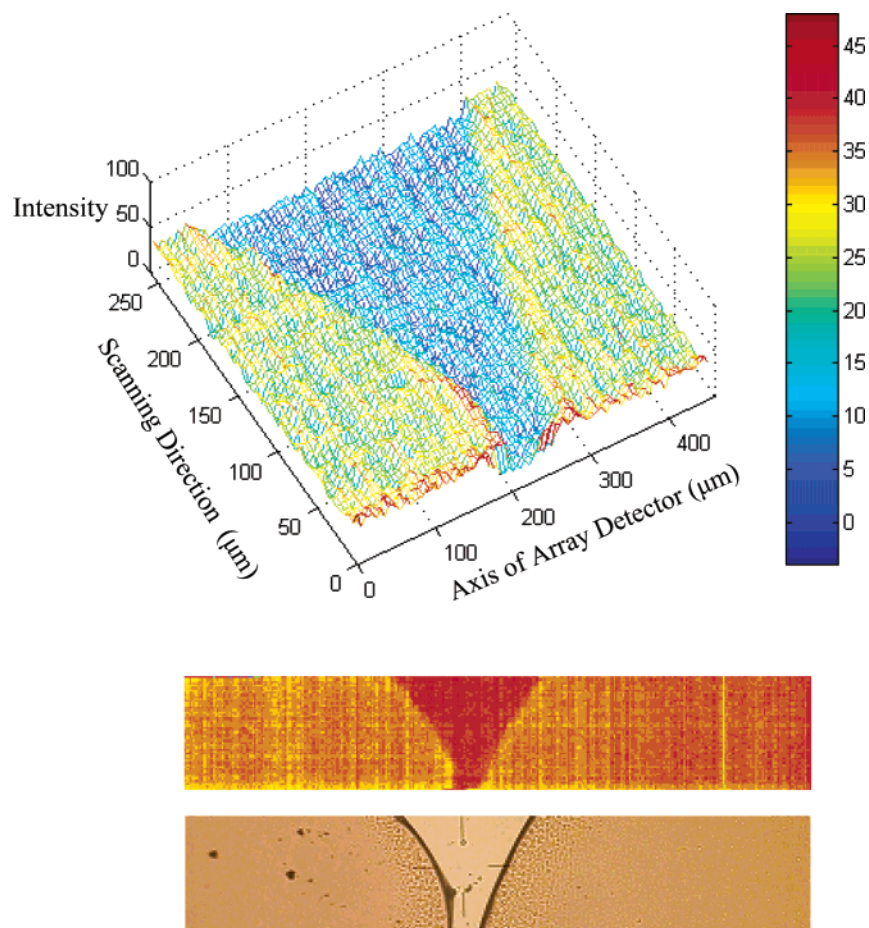


Figure 38. Images of a “V”-shaped water channel between two toluene domains. The bottom panel shows a transmission-based image of the sample recorded in the visible region of the spectrum. The middle and top panels show images of this same sample constructed using the $a \rightarrow X$ phosphorescence of singlet oxygen detected by the InGaAs array (only a portion of the data recorded by the array is shown). The singlet oxygen signal originates from continuous excitation of tetraphenylporphyrin in the toluene domains, whereas the “V”-shaped domain in the center is void of singlet oxygen. The colors chosen for the singlet oxygen images are arbitrary and reflect the intensity scale used. Reprinted with permission from ref 452. Copyright 2002 American Chemical Society.

that become fluorescent after reaction with singlet oxygen or (ii) molecules that fluoresce strongly upon energy transfer from singlet oxygen.

The first group of molecules are fluorescein derivatives in which the benzoic acid moiety is replaced by 9,10-diphenyl- or 9,10-dimethyl-substituted anthracene-2-carboxylic acid (ACA).^{1,2} This modification leads to a strong decrease of the fluorescence quantum yield to values below 0.01, caused by electron transfer from the ACA moiety to the xanthene fluorophore. However, the endoperoxide obtained upon addition of $O_2(^1\Delta_g)$ to the ACA moiety in the 9,10-position has a fluorescence yield on the order of 0.5–0.9 in many cases. The reaction with $O_2(^1\Delta_g)$ is relatively fast and highly selective, and leads to a stable product; thus, the method is ideal for quantitative investigations in aqueous and biological media. However, it cannot be used at low pH, where the peroxides are nonfluorescent, and it is obviously limited to steady-state investigations.

The second group of compounds are phthalocyanines, naphthalocyanines, and porphyrazines, which exhibit strong delayed fluorescence upon energy transfer from two $O_2(^1\Delta_g)$ molecules.^{3,4} The luminescence is emitted in the visible (~ 700 nm) region, and its quantum yield exceeds that of the a

$\rightarrow X$ phosphorescence of $O_2(^1\Delta_g)$ by 2–4 orders of magnitude. The signal is easily detected in laser-pulsed time-resolved studies; thus, the method may be very useful for singlet oxygen measurements in numerous systems. However, all of these molecules also sensitize the formation of $O_2(^1\Delta_g)$, which may be an advantage or a disadvantage.

VI. Applications

The large number of theoretical and experimental studies of the radiative and radiationless deactivation of $O_2(^1\Delta_g)$ and $O_2(^1\Sigma_g^+)$ and of the photosensitization of singlet oxygen discussed in this review has led to a detailed understanding of many of the complex processes constituting singlet oxygen photophysics. This knowledge is very valuable not only with respect to mechanistic interpretations, but also for many practical applications. In the following, the most important practical consequences of these findings will be discussed.

A. Estimation of the $a \rightarrow X$ Radiative Rate Constant in Different Environments

We have seen in section V that, in many systems, the observation of singlet oxygen is limited by poor

Table 8. Rate Constants of the $a \rightarrow X$ Radiative Transition^a

solvent	k_{a-X} , s ⁻¹	k_{a-X}^c , M ⁻¹ s ⁻¹	solvent	k_{a-X} , s ⁻¹	k_{a-X}^c , M ⁻¹ s ⁻¹
water	0.209	0.0038	2-ethylnaphthalene	2.03	0.319
water- <i>d</i> ₂	0.206	0.0038	diphenyl sulfide	2.66	0.442
methanol	0.390	0.0159	formic acid	0.25	0.0094
carbon disulfide	3.14	0.189	dibromomethane	0.80	0.056
1,1,1-trifluoroethanol	0.331	0.0241	propionic acid	0.79	0.059
acetone	0.543	0.040	1,2-dichloroethane	0.75	0.059
chloroform	0.962	0.077	acetic anhydride	0.53	0.050
benzene	1.50	0.133	<i>n</i> -pentane	0.47	0.054
carbon tetrachloride	1.17	0.113	toluene- <i>d</i> ₈	1.47	0.156
tetrachloroethylene	1.89	0.193	anisole	1.80	0.196
iodobenzene	2.61	0.291	<i>n</i> -hexane	0.60	0.078
perchlorobutadiene	1.85	0.290	<i>p</i> -xylene	1.70	0.208
acetonitrile	0.45	0.0234	<i>p</i> -chloroanisole	2.20	0.270
ethanol- <i>d</i>	0.35	0.0203	<i>p</i> -bromoanisole	1.90	0.238
dichloromethane	0.75	0.048	1,3-dimethoxybenzene	1.90	0.249
2-propanol	0.47	0.036	1,2,4-trimethylbenzene	2.00	0.270
tetrahydrofuran	0.62	0.050	mesitylene	1.72	0.239
1,4-dioxane	0.56	0.047	diphenyl ether	2.00	0.317
diiodomethane	3.04	0.245	benzene- <i>d</i> ₆	1.335	0.118
fluorobenzene	1.28	0.120	1,2-dibromotetrafluoroethane	1.395	0.168
1-iodopropane	1.44	0.140	bromobenzene- <i>d</i> ₅	2.07	0.218
chlorobenzene	1.68	0.171	perfluorobenzene	0.51	0.059
toluene	1.44	0.153	chloropentafluorobenzene	0.885	0.109
cyclohexane	0.66	0.071	bromopentafluorobenzene	1.245	0.155
benzonitrile	1.80	0.184	iodopentafluorobenzene	1.23	0.164
bromobenzene	1.97	0.206	perfluorohexyl iodide	1.41	0.305
trifluorotoluene	1.14	0.139	ethanol	0.55	0.032
1,3-dibromobenzene	2.72	0.328	1-propanol	0.53	0.040
<i>n</i> -heptane	0.66	0.097	<i>N,N</i> -dimethylformamide	0.63	0.049
1-methylnaphthalene	2.96	0.420	diethyl ether	0.615	0.064
1-bromonaphthalene	3.11	0.432	1-butanol	0.465	0.043
			2-butanol	0.57	0.053

^a Data compiled by Hild and Schmidt.⁸⁵

signals of O₂(¹Δ_g) phosphorescence. The quality of the time-resolved signal is directly related to the $a \rightarrow X$ radiative rate constant, which exhibits an unusually strong dependence on the medium. The mechanistic studies presented above have established these rate constants for many solvents and provide a very valuable tool for estimation of k_{a-X} data in a multitude of environments.

1. Liquid Phase

It is shown in section III.B.1.a that the probability of the $a \rightarrow X$ phosphorescence of O₂(¹Δ_g) is tremendously enhanced in binary collisions. The corresponding second-order rate constants k_{a-X}^c increase strongly with the molecular polarizability of the collision partner. For pure solvents, the first-order rate constant k_{a-X} is the product of k_{a-X}^c and the solvent molarity [S]. Reliable literature data for k_{a-X} for 63 pure liquids ranging from 0.21 (H₂O) to 3.1 s⁻¹ (CS₂) were compiled by Hild and Schmidt and are listed in Table 8.⁸⁵ This data set can also be used to calculate k_{a-X} for homogeneous solvent mixtures by using eq 78, where [*i*] represents the molar concentration of the component *i* of the system, and $k_{a-X,i}^c$ represents the respective second-order rate constant.

$$k_{a-X} = \sum_i k_{a-X,i}^c [i] \quad (78)$$

It was shown by Schmidt et al.⁸⁰ that eq 78 is valid for ideal mixtures as well as for strongly nonideal systems with large excess volumes Δ*V*_{exc}. However,

in the latter case, it is recommended to consider the values of Δ*V*_{exc} in the calculation of the actual concentrations of the mixture components to obtain accurate results. If this is not done, then small deviations have to be taken into account. For example, for the strongly nonideal system water/acetone, the maximum deviation of the calculated value of k_{a-X} amounts to only -3.7% if Δ*V*_{exc} is ignored.

2. Gas Phase

Badger et al. observed that the molecular absorption coefficient of the continuous $a \leftarrow X$ band increases linearly with pressure.²⁹ The second-order rate constant of $a \leftarrow X$ absorption with O₂ as collision partner was determined to be $k_{a-X}^c = 2.4 \times 10^{-2}$ M⁻¹ s⁻¹, which agrees in the limits of mutual uncertainty with $k_{a-X}^c = 2.0 \times 10^{-2}$ M⁻¹ s⁻¹ measured by Fink and co-workers in gas-phase $a \rightarrow X$ emission experiments.^{50,51} Since the same mechanism operates in gas and liquid phases, eq 78 can also be used to calculate radiative rate constants k_{a-X} of the $a \rightarrow X$ emission in gases or vapors consisting of one or more components.

3. Microheterogeneous Systems

Equation 78 fails for micellar systems since O₂(¹Δ_g) concentrations and radiative lifetimes differ in the different microphases. The O₂(¹Δ_g) concentration differences between the interior organic and the exterior aqueous phases can be quantified by the equilibrium constant $K_{\text{eq}} = [\text{O}_2(\text{}^1\Delta_g)]_{\text{int}} / [\text{O}_2(\text{}^1\Delta_g)]_{\text{ext}}$, which is equal to the ratio of the corresponding O₂

solubilities, as shown by Lee and Rodgers.⁸² Their pseudophase model also considers the volume fractions f_m and $1 - f_m$ of the micellar and the aqueous phases, in which deactivation occurs with rate constants $k_{d,int}$ and $k_{d,ext}$. The observable overall rate constant k_d is then given by eq 19.⁸²

$$k_d = \frac{K_{eq} f_m k_{d,int} + (1 - f_m) k_{d,ext}}{K_{eq} f_m + (1 - f_m)} \quad (19)$$

It was shown by Martinez et al.⁸¹ that eq 19, originally derived for the radiationless deactivation of $O_2(^1\Delta_g)$, quantitatively reproduces the experimental $k_{a-X,m}$ data measured in microheterogeneous systems if the values of k_d are replaced by the values of k_{a-X} corresponding to the respective microphases.

B. Estimation of the Contribution of e-v, CT, EET, and Chemical Pathways to $O_2(^1\Delta_g)$ and $O_2(^1\Sigma_g^+)$ Deactivation

Mechanistic studies of singlet oxygen photochemistry and photophysics require a clear distinction between the different pathways contributing to the deactivation of to $O_2(^1\Delta_g)$ and $O_2(^1\Sigma_g^+)$. We have seen in section III that, in the case of $O_2(^1\Delta_g)$, five main processes may compete in a given situation. These are, in the order of increasing rate constants, (i) radiative processes, (ii) electronic-to-vibrational deactivation (e-v), (iii) charge-transfer quenching (CT) and chemical reactions (CR) (both often of comparable magnitude), and (iv) electronic energy transfer (EET). The information presented in this review allows us to establish simple strategies for the evaluation of the quenching mechanism in a given situation, and for the estimation of the contributions of individual pathways, on the basis of simple experimental data such as quenching rate constants.

If we consider the magnitude of the rate constants for radiative deactivation presented above, it is clear that the efficiency of this process is largely negligible whenever nonradiative processes are observed (i.e., in solution, in the solid phase, and in the heterogeneous gas phase). The second mechanism, deactivation by e-v energy transfer, generally needs to be taken into account if rate constants of other moderately fast deactivation mechanisms are of interest. Thus, our starting point for the assessment of the mechanism of singlet oxygen deactivation will be the estimation of the bimolecular rate constant k_Q^Δ for e-v deactivation, which, according to eq 26 (introduced in section III.B.3.a), is simply given by the sum of the rate constants k_{XY}^Δ for e-v deactivation by each individual terminal X-Y bond of the quencher molecule (N_{XY} is the number of terminal X-Y bonds per quencher molecule). Table 9 lists all k_{XY}^Δ values determined to date.

$$k_Q^\Delta = \sum_{XY} N_{XY} k_{XY}^\Delta \quad (26)$$

In general, any experimental quenching rate constant exceeding the value estimated according to eq 26 can be attributed to an additional deactivation pathway competing with e-v quenching. Among the

Table 9. Rate Constants k_{XY}^Δ and k_{XY}^Σ of Quenching of $O_2(^1\Delta_g)$ and $O_2(^1\Sigma_g^+)$ by Bonds X-Y in the Liquid Phase^a

X-Y	$k_{XY}^\Delta, M^{-1} s^{-1}$	$k_{XY}^\Sigma, M^{-1} s^{-1}$
O-H	2900 ^b	1.5×10^9
N-H	1530 ^c	4.7×10^8
C-H _{ar} ^d	494 ^e	1.1×10^8
C-H	309 ^e	1.0×10^8
O-D	132 ^e	2.7×10^8
C-D _{ar} ^d	21.7 ^e	5.3×10^7
C-D	10.4 ^e	3.3×10^7
C=S	0.351 ^e	1.6×10^6
C-F _{ar} ^d	0.625 ^e	1.5×10^6
C-F	0.049 ^e	5.6×10^5
C-Cl	0.181 ^e	1.6×10^5

^a Numbers without citation are average values evaluated in ref 153. ^b k_{OH}^Δ considering $\tau_\Delta = 3.1 \mu s$ in H_2O .¹²⁴ ^c Reference 122. ^d Terminal atom bound to aromatic ring. ^e Reference 57.

three possible mechanisms, CT and CR may compete in any situation, whereas EET is possible only for quenchers with low triplet energies (i.e., $E_T \leq 94$ kJ mol⁻¹).

The following criteria can be used to distinguish among the three possibilities: (i) Experimental quenching rate constants $k_Q^\Delta > 5 \times 10^9 M^{-1} s^{-1}$ are indicative (but not demonstrative) of an EET mechanism, especially if the quencher has a high oxidation potential. To establish this mechanism in an unequivocal way, determination of the quencher triplet energy or time-resolved measurement of quencher triplet-triplet absorption is required. If EET takes place, then e-v, CT, and chemical processes are negligible in most cases. (ii) Chemical reactions of $O_2(^1\Delta_g)$ generally lead to formation of peroxides or hydroperoxides, which can be quantified by following product formation or by measuring O_2 consumption, if measurements are carried out in homogeneous systems, where competing free radical reactions can be excluded. In this case, it is important to consider that peroxides are often unstable and may decompose under experimental conditions. In general, chemical reactions of a quencher with $O_2(^1\Delta_g)$ can be qualitatively identified if the quencher consumption is efficiently reduced by the addition of strong quenchers of $O_2(^1\Delta_g)$, such as sodium azide ($k_Q^\Delta \approx 4 \times 10^8 M^{-1} s^{-1}$ in H_2O) or 2,3-dimethyl-2-butene ($k_Q^\Delta \approx 1 \times 10^6 M^{-1} s^{-1}$ in organic solvents). (iii) Any contribution in excess of the rate constant for e-v deactivation that cannot be explained by EET or CR is generally attributed to charge-transfer-induced physical quenching. This treatment was successfully applied to a series of benzene,¹⁸⁸ naphthalene,¹⁹⁹ biphenyl,²⁰⁰ and benzophenone derivatives.²⁰¹ A rough qualitative estimate of the rate constant for CT deactivation may also be obtained from Figure 14, where the free energy for electron transfer is obtained from the Rehm-Weller equation (see section III.B.4.a).

We may proceed analogously to evaluate the mechanism of $O_2(^1\Sigma_g^+)$ deactivation. Scurlock et al.²⁴² and Bodesheim and Schmidt²⁴³ showed that the rate constants k_{XY}^Σ for e-v deactivation of $O_2(^1\Sigma_g^+)$ by an individual X-Y bond (see Table 9) can be used analogously to estimate rate constant for the overall

e–v deactivation of $O_2(^1\Sigma_g^+)$ by a given quencher, according to eq 26. The chemistry of $O_2(^1\Sigma_g^+)$ has not yet been discovered, despite significant efforts.^{242,243} Thus, any experimental value exceeding the rate constant for e–v quenching can be attributed to charge transfer, unless the quencher E_T is lower than 157 kJ mol⁻¹. In the latter case, EET and diffusion-controlled quenching is expected. e–v and CT deactivation leads to quantitative formation of $O_2(^1\Delta_g)$ and the quencher ground state, whereas EET leads to formation of $O_2(^3\Sigma_g^-)$ and the quencher triplet state, which sensitizes $O_2(^1\Delta_g)$ again.²⁶⁹

C. Estimation of $O_2(^1\Delta_g)$ and $O_2(^1\Sigma_g^+)$ Lifetimes in Different Environments

1. Liquid Phase

From the investigations reported by Darmanyan et al. and Schweitzer et al., it can be concluded that molecules with ionization potential $IP \geq 8.8$ eV or oxidation potential $E_{ox} \geq 1.9$ V vs SCE in CH_3CN quench $O_2(^1\Delta_g)$ mainly by e–v energy transfer.^{188,199–201} For these molecules, k_Q^Δ can be calculated simply by using eq 26 and the k_{XY}^Δ data shown in Table 9. For mixtures of liquids consisting of such molecules i , the lifetime τ_Δ of $O_2(^1\Delta_g)$ can be estimated by using eq 79, where $[i]$ is the molar concentration of the component i .

$$\tau_\Delta = \left(\sum_i k_{Q,i}^\Delta [i] \right)^{-1} \quad (79)$$

This procedure works rather well for pure solvents and for homogeneous liquid mixtures of several components i . Limitations exist for CS_2 and perhalogenated solvents, in which τ_Δ is additionally reduced by quenching of $O_2(^1\Delta_g)$ by O_2 (see Table 4).^{57,126} Furthermore, it should be considered that the values of k_{XY}^Δ were derived for freely accessible X–Y bonds. Therefore, deviations to smaller values result for calculated τ_Δ data if a strongly deactivating X–Y bond such as O–H is sterically hindered. This is illustrated by the τ_Δ data (experimental, calculated) for butanol isomers: 1-butanol, 17.5, 16.1 μs ; 2-butanol, 19.7, 16.1 μs ; 2-methyl-1-propanol, 21.1, 16.2 μs ; and 2-methyl-2-propanol, 30.8, 16.8 μs . The lifetime of $O_2(^1\Sigma_g^+)$, τ_Σ , can be estimated analogously via rate constants k_Q^Σ , which are accessible from the k_{XY}^Σ data listed in Table 9. With the exception of perhalogenated solvents and CS_2 , very small values of $\tau_\Sigma \leq 1$ ns are generally obtained.

2. Polymers

Since the ubiquitous O_2 is also present in polymers, $O_2(^1\Delta_g)$ can be formed in this medium by photosensitization.⁴⁵³ Clough et al. demonstrated that values of τ_Δ in homogeneous polymers at temperatures above the glass temperature T_g are practically equal to values of τ_Δ in liquid solutions consisting of analogous molecular structures. In silicone rubber, $\tau_\Delta = 50$ μs was measured, and in a low-molecular-weight siloxane liquid, $\tau_\Delta = 51$ μs was obtained.⁴⁵⁴ For poly(methyl methacrylate) and polystyrene (PS), τ_Δ was found to be in agreement with the lifetimes

in liquid methyl propionate ($\tau_\Delta = 38$ μs) and ethyl benzene ($\tau_\Delta = 28$ μs) at $T \geq T_g$.⁴⁵⁵ Below the glass temperature, diffusion is strongly restricted, leading to a drastic increase of the triplet-state lifetime of the sensitizer. Since the triplet is the precursor of $O_2(^1\Delta_g)$, the apparent decay time of $O_2(^1\Delta_g)$ becomes equal to the triplet lifetime, τ_T . However, besides τ_T , deconvolution of the slowly decaying $O_2(^1\Delta_g)$ emission signal also yields the intrinsic lifetime τ_Δ , which was found to be in accordance with τ_Δ measured at $T \geq T_g$ and with τ_Δ measured in analogous liquid-phase systems. Furthermore, irradiating the polymer– O_2 CT band of PS instantaneously produces $O_2(^1\Delta_g)$, the lifetime of which was shown to be identical to that observed in ethyl benzene, even at $T < T_g$.⁴⁵⁶ Thus, the value of τ_Δ is limited by the e–v deactivation of $O_2(^1\Delta_g)$ by the directly neighboring polymer units. Therefore, lifetimes τ_Δ can also be estimated for polymers by the above-described procedure.⁴⁵⁷ These conclusions also hold true for $O_2(^1\Sigma_g^+)$. In this case, τ_Σ can be estimated from the k_{XY}^Σ data shown in Table 7. Generally, very small values of $\tau_\Sigma \leq 1$ ns result for common polymers.

3. Gas Phase

The major components of air are N_2 , O_2 , and Ar, with 78, 21, and 1 vol %, respectively. The corresponding rate constants k_Q^Δ are 84,¹⁰³ 1020,⁹³ and 5 $M^{-1} s^{-1}$.¹⁰³ $k_Q^\Delta = 5800 M^{-1} s^{-1}$ was determined for H_2O .⁹³ Thus, only N_2 and O_2 , and in case of humidity also H_2O , contribute to $O_2(^1\Delta_g)$ deactivation in air. The concentration of H_2O depends on its temperature-dependent vapor pressure, which amounts to 0.031 bar at 298 K. Using these numbers, τ_Δ is calculated to be 86 or 54 ms for air of 0% or 100% relative humidity, respectively, at 1 bar and 298 K. If further polyatomic molecules with $IP \geq 8.8$ eV or $E_{ox} \geq 1.9$ V vs SCE contribute to quenching in the gas phase, their rate constants k_Q^Δ can be estimated from the data shown in Table 9 and eq 26 to provide a basis for the estimation of τ_Δ by eq 79. The values of k_Q^Σ decrease strongly in the series of quenchers H_2O , N_2 , and O_2 from 2.9×10^9 to 1.3×10^6 and $2.4 \times 10^4 M^{-1} s^{-1}$.¹⁰² Since H_2O is the most important quencher of $O_2(^1\Sigma_g^+)$, τ_Σ strongly depends on the humidity. For absolutely dry air of 1 bar pressure at 298 K, τ_Σ is estimated to be 24 μs . τ_Σ decreases to 2.4 μs and to only 270 ns at 10% and 100% relative humidity, respectively. Rate constants k_Q^Σ for other polyatomic quenchers of $O_2(^1\Sigma_g^+)$ and corresponding gas-phase lifetimes τ_Σ can be evaluated from the data shown in Table 9 and eqs 26 and 79.

4. Microheterogeneous Systems

The above procedure fails in nonhomogeneous systems due to the different concentrations and lifetimes of $O_2(^1\Delta_g)$ in the different microphases. For this case, Lee and Rodgers derived eq 19, already mentioned in section VI.A.3.⁸² Equation 19 quantitatively reproduces the first-order rate constant of overall $O_2(^1\Delta_g)$ decay.^{81,82} The model was extended by Lee and Rodgers to include the effect of added quenchers of $O_2(^1\Delta_g)$.⁴⁵⁸ Aubry and Bouttemy modi-

fied and applied this model to quantitatively describe the decay of $O_2(^1\Delta_g)$, which was chemically generated in the aqueous phase of microemulsions consisting of dichloromethane, 1-butanol, sodium dodecyl sulfate, and H_2O .⁴⁵⁹ Montenegro et al.²⁶⁰ successfully used the modified model to study the influence of the medium's heterogeneity on the rate constants of physical and chemical quenching of $O_2(^1\Delta_g)$ by seven natural and three synthetic carotenoids in reverse micelle systems of hexane, sodium bis(2-ethylhexyl) sulfosuccinate, and H_2O , where singlet oxygen was generated by photosensitization inside the water pools of the reverse micelles. Thus, in microheterogeneous solutions, $O_2(^1\Delta_g)$ decays monoexponentially; however, the decay constant is not determined by the average composition of the liquid, but rather it is given as a weighted average of the single-phase decay constants $k_{d,int}$ and $k_{d,ext}$, according to eq 19. This model holds as long as the microdroplets are small enough to allow for the fast $O_2(^1\Delta_g)$ equilibrium. If the droplets become too large, a biexponential decay with rate constants $k_{d,int}$ and $k_{d,ext}$ will result if $O_2(^1\Delta_g)$ is produced in the interior of both phases. The limiting droplet diameters are estimated via the corresponding diffusion lengths (see section VI.G) to amount to ~ 0.5 and $0.2 \mu\text{m}$, respectively, for hydrocarbon and water droplets.

5. Zeolite Systems

Very recently, Pace and Clennan determined an upper limit of the $O_2(^1\Delta_g)$ lifetime in the interior of the supercages of zeolite Y suspended in organic liquids.⁴⁶⁰ By investigation of the photo-oxygenation kinetics of 2-methyl-2-heptene adsorbed into zeolite Y in either hexane or perfluorohexane, a zeolite-leveled upper limit of $\tau_\Delta \leq 7.5 \mu\text{s}$ was established. This very small value, which is only about twice the lifetime value in H_2O , was attributed to significant charge-transfer quenching of $O_2(^1\Delta_g)$ due to the aluminum tetrahedral AlO_4^- framework. Using a very conservative estimate of the intrazeolite O_2 diffusion coefficient, the authors estimated that $O_2(^1\Delta_g)$ could migrate approximately 370 \AA within its lifetime. This implies that $O_2(^1\Delta_g)$ can sample many of more than 5000 zeolite supercages surrounding the locus of its generation.⁴⁶⁰

D. Estimation of $a \rightarrow X$ Emission Quantum Yields

The emission quantum yield of $O_2(^1\Delta_g)$ in a given situation can easily be estimated by using eq 80,

$$Q_{a-X} = k_{a-X}\tau_\Delta \quad (80)$$

where the values of k_{a-X} and τ_Δ for the corresponding medium may be estimated according to the procedures described above. For example, the following values of Q_{a-X} were calculated for three neat liquids from the data given in Tables 4, 5, and 8 (solvent, k_{a-X} , τ_Δ): 6.5×10^{-7} (H_2O , 0.21 s^{-1} , $3.1 \mu\text{s}$), 4.5×10^{-5} (C_6H_6 , 1.5 s^{-1} , $30 \mu\text{s}$), and 7×10^{-2} (air-saturated CCl_4 , 1.2 s^{-1} , 59 ms). These data illustrate the tremendous variation, by about 5 orders of magnitude, and the smallness of Q_{a-X} in the liquid phase.

The presence of quenchers of $O_2(^1\Delta_g)$ further reduces τ_Δ and thus Q_{a-X} . This leads to particularly small values of the emission quantum yield in biological tissues. Very recently, Wilson and co-workers⁶ estimated values of τ_Δ to be between 0.03 and $0.18 \mu\text{s}$ in skin and liver of living rats. These results rest on measurements of the $a \rightarrow X$ emission intensity, and the large uncertainty in τ_Δ depends mainly on the assumed value of k_{a-X} . The upper limiting value was obtained by using the value of k_{a-X} for H_2O . $\tau_\Delta = 0.05 \mu\text{s}$ is obtained for both tissues, with an estimated value of $k_{a-X} = 0.65 \text{ s}^{-1}$.⁶ This estimate is close to $k_{a-X} = 0.8 \text{ s}^{-1}$, which was obtained experimentally and by calculation on the basis of eq 19 by Martinez et al. for microemulsions consisting of 69 wt % cyclohexane, 16% 1-butanol, 7% H_2O , and 8% surfactant (sodium dodecyl sulfate, cetyltrimethylammonium chloride, or Triton X-100).⁸¹ Assuming this number to be representative for the radiative rate of $O_2(^1\Delta_g)$ in cells, $\tau_\Delta = 0.04 \mu\text{s}$ is obtained for the investigated tissues. Hence, these considerations point rather to the lower limit of the results reported by Wilson. They also allow for calculation of $Q_{a-X} \approx 3 \times 10^{-8}$. This tiny number also explains why $O_2(^1\Delta_g)$ emission experiments in living tissue are so difficult.

E. e-v Deactivation of Isoelectronic Molecules

Diatomic molecules consisting of group VI–VII atoms, or group V–VII atoms, such as SO or NF, are isoelectronic with O_2 and have a $^3\Sigma^-$ ground state and two low-lying $^1\Delta$ and $^1\Sigma^+$ excited states. The bimolecular deactivation of the excited singlet states of such molecules was investigated in the gas phase.^{461–463} It was found that the lifetime of the metastable $^1\Delta_g$ state is limited mostly by the chemical process. However, the much shorter living $^1\Sigma^+$ excited states are deactivated by fast physical processes. It was shown by Schmidt^{155,156} and by Setzer's group^{157–159} that the e-v energy-transfer model originally developed for $O_2(^1\Sigma_g^+)$ and $O_2(^1\Delta_g)$ can be applied for the bimolecular quenching of the $^1\Sigma^+$ excited state of SO, SeO, NF, PF, NCl, and PCl, proving the more general validity of this semi-empirical model. This is discussed in detail in the context of e-v energy transfer in section III.B.3.d and III.B.3.e.

F. Optimization of Singlet Oxygen Sensitizers

We have seen in section IV that the highest singlet oxygen yields are obtained when $O_2(^1\Delta_g)$ can be formed during O_2 quenching of both S_1 and T_1 . In these cases, Q_Δ can be, under particular conditions, as high as 2; i.e., two molecules of $O_2(^1\Delta_g)$ are formed per photon absorbed. However, this ideal situation is rare, since both quenching processes compete with both intra- and intermolecular pathways.

The efficiency of $O_2(^1\Delta_g)$ formation during O_2 quenching of S_1 approaches 2 when five conditions are simultaneously met: (i) the energy gap between S_1 and T_1 exceeds 94 kJ mol^{-1} , (ii) no second triplet state lies below S_1 , (iii) the O_2 quenching process leads to quantitative formation of the T_1 state, (iv) the S_1 state is quantitatively quenched by O_2 , and (v) the subsequent quenching of T_1 leads to quantita-

tive formation of singlet oxygen. Unfortunately, conditions (iii) and (iv) almost exclude each other. Efficient fluorescence quenching with diffusion-controlled rate constant k_S^Q is obtained only for sensitizers with moderate to strong CT interactions, which reduce the efficiency of the T_1 -state population during quenching. However, sensitizers with negligible CT interactions are distinguished by values $k_S^Q \ll k_{\text{diff}}$. As a consequence, the limiting quantum yield of 2 is only obtained in nonpolar solvents at very high O_2 partial pressures. This is well illustrated in the case of 9,10-dicyanoanthracene (DCA), for which quantum yields of $O_2(^1\Delta_g)$ formation at extrapolated infinite oxygen concentration of $1.5 \leq Q_\Delta^\infty \leq 2.0$ were reported.^{309,331–334,337} Equation 76, derived by Brauer for strong fluorescers for which the approximation $Q_T^0 + Q_F^0 = 1$ holds true, allows the estimation of the O_2 concentration dependence of Q_Δ via the ratio $F^0/F = 1 + k_S^Q \tau_S [O_2]$ if values of Q_T^0 , f_S^Δ , and S_Δ are known.

$$Q_\Delta = Q_T^0 S_\Delta + (f_S^\Delta + Q_F^0 S_\Delta) [1 - (F/F^0)] \quad (76)$$

From data reported by Olea and Wilkinson for DCA in acetonitrile ($k_S^Q = 4.4 \times 10^9 \text{ M}^{-1} \text{ s}^{-1}$, $\tau_S = 15.2 \text{ ns}$, $[O_2] = 0.0019 \text{ M}$ (air saturation), $Q_T^0 = 0.003$, $f_S^\Delta = 0.53$, and $S_\Delta = 1$),³³⁴ values of $Q_\Delta = 0.17, 0.58$, and 1.41 result for air-saturated ($p = 1 \text{ bar}$), O_2 -saturated ($p = 1 \text{ bar}$), and O_2 -saturated ($p = 20 \text{ bar}$) solutions, respectively, and finally $Q_\Delta^\infty = 1.53$. The respective data in cyclohexane³³³ yield for Q_Δ the values $0.22, 0.72$, and 1.83 with the respective graduation in $[O_2]$, and $Q_\Delta^\infty = 2.0$. Thus, it is true that these compounds may be very efficient sensitizers of $O_2(^1\Delta_g)$, but it has to be noted that the advantage is obtained only at high O_2 partial pressures, where the danger of combustion increases with hydrocarbon solvents.

Under common conditions, i.e., in air-saturated solution, sensitization via triplet states is the most effective method of $O_2(^1\Delta_g)$ formation. The five necessary conditions listed here apply for optimum triplet sensitization approaching the maximum yield of unity: (i) The sensitizer triplet energy must be larger than 94 kJ mol^{-1} (optimally larger than 157 kJ mol^{-1} , to allow for competitive formation of $O_2(^1\Sigma_g^+)$). (ii) The triplet state is quantitatively formed, i.e., via intramolecular isc or, in particular cases, by energy transfer from a higher-lying triplet. (iii) The triplet state is quantitatively quenched by O_2 . This is commonly observed for most $\pi\pi^*$ -excited triplets, where almost complete quenching occurs at $[O_2] \approx 2 \times 10^{-4} \text{ M}$ (unless other quenchers are present at very high concentration), as opposed to $n\pi^*$ -excited triplets, which often react chemically. (iv) Franck–Condon factors are favorable for energy transfer and unfavorable for enhanced internal conversion. This is observed for all $\pi\pi^*$ -excited aromatic hydrocarbons, as opposed to $n\pi^*$ -excited ketones. (v) Charge-transfer interactions are negligible. This is favored in nonpolar solvents and by high sensitizer oxidation potentials and low triplet energies. For example, we have seen in section IV.A.1.b that, in CCl_4 solution, CT interactions are negligible if $\Delta G_{\text{CET}} = F(E_{\text{ox}} - E_{\text{red}}) - E_T$ exceeds 50 kJ mol^{-1} .

Relation 65 allows the calculation of the rate constants $k_{\Delta E}^{1\Delta}$, $k_{\Delta E}^{1\Sigma}$, and $k_{\Delta E}^{3\Sigma}$ for $O_2(^1\Sigma_g^+)$, $O_2(^1\Delta_g)$, and $O_2(^3\Sigma_g^-)$ formation in the quenching of $T_1(\pi\pi^*)$ states by O_2 in the absence of CT interactions. If the triplet-

$$\log(k_{\Delta E}^P/m) = 9.05 + (9 \times 10^{-3})\Delta E - (1.15 \times 10^{-4})\Delta E^2 + (1.15 \times 10^{-7})\Delta E^3 + (9.1 \times 10^{-11})\Delta E^4 \quad (65)$$

state energy exceeds the $O_2(^1\Sigma_g^+)$ excitation energy, there are two paths leading to singlet oxygen, resulting in high efficiencies $S_\Delta = (k_{\Delta E}^{1\Sigma} + k_{\Delta E}^{1\Delta}) / (k_{\Delta E}^{1\Sigma} + k_{\Delta E}^{1\Delta} + k_{\Delta E}^{3\Sigma})$ of singlet oxygen formation, which are calculated by using eq 65 to be in the range $0.91 \leq S_\Delta \leq 0.995$ for a $168 \leq E_T \leq 255 \text{ kJ mol}^{-1}$ variation.

It is interesting to note that, for the sensitizer phenalene ($Q_T = 1.0$, $E_T = 186 \text{ kJ mol}^{-1}$),^{83,464} $S_\Delta = 0.96$ is calculated, in agreement with the experimental result $S_\Delta = 0.97$.^{83,357} CT interactions are, indeed, very small for phenalene, as is indicated by the large positive value $\Delta G_{\text{CET}} = 78 \text{ kJ mol}^{-1}$ determined recently.⁴⁰¹ Actually, phenalene could be established as a universal singlet oxygen reference sensitizer, since no solvent dependence of Q_Δ was observed. Values $0.94 \leq Q_\Delta \leq 1$ were determined with high certainty in 13 solvents of very different physical properties, ranging from cyclohexane to H_2O .⁸³ The solubility of phenalene is only moderate in water. Therefore, Nonell et al. proposed the more soluble phenalene-2-sulfonic acid, with $Q_\Delta = 1.03 \pm 0.10$, as the reference in water.⁴⁶⁵

The solvent independence of S_Δ for phenalene indicates that changes in the polarity of the environment seem not to influence the deactivation in the absence of CT interactions. Thus, generally high efficiencies of $S_\Delta \geq 0.9$ could be expected for $\pi\pi^*$ triplet sensitizers with both $E_T \geq 165 \text{ kJ mol}^{-1}$ and $\Delta G_{\text{CET}} \geq 50 \text{ kJ mol}^{-1}$. These sensitizers are characterized by rather small overall rate constants $k_Q^T \leq 3 \times 10^9 \text{ M}^{-1} \text{ s}^{-1}$.

In addition to photophysical and electrochemical properties, it is also important that no aggregation of ground-state sensitizer molecules occurs, and that no formation of exciplexes occurs. We have seen in section IV.A.1.f that such interactions can reduce both the triplet yield and S_Δ . In these cases, the singlet oxygen yield decreases with increasing sensitizer concentration.

It is also interesting to note that all conditions which favor the formation of $O_2(^1\Delta_g)$ during O_2 quenching of T_1 also favor that of $O_2(^1\Sigma_g^+)$, if it is energetically feasible.

To obtain a maximum amount of observable or utilizable singlet oxygen, it is also important to minimize its deactivation by the sensitizer. Quenching of $O_2(^1\Sigma_g^+)$ is an entirely physical process, which leads to quantitative formation of $O_2(^1\Delta_g)$; thus, it can be disregarded in most cases. Deactivation of $O_2(^1\Delta_g)$ by the sensitizer, in contrast, can be both chemical (i.e., leading to modifications in the sensitizer, which, in most cases, reduce its $O_2(^1\Delta_g)$ sensitization ability) and physical (i.e., leading to formation of the sensitizer ground state and $O_2(^3\Sigma_g^-)$). Chemical reactions

occur mainly with electron-rich aromatic rings, dienes, or double bonds, and with amines and sulfides. Significant physical quenching can occur (i) via diffusion-controlled EET, if the sensitizer triplet energy is only a few kJ mol^{-1} higher than 94 kJ mol^{-1} , or (ii) via CT, if the sensitizer oxidation potential is sufficiently low. Thus, a high sensitizer oxidation potential favors singlet oxygen formation both by increasing its efficiency of production and by minimizing its physical and chemical deactivation.

In recent years, much emphasis has been put on the development of singlet oxygen sensitizers for biological and medical applications, and especially for the photodynamic therapy (PDT) of cancer. In addition to the requirements described above, PDT sensitizers need to fulfill several other demands: (i) absorption in the deep red region, preferably above 700 nm, where absorption by biological tissues is minimal, (ii) high extinction coefficients, (iii) fluorescence for tumor detection, (iv) negligible toxicity, and (v) selective retention in the tumor tissue.

The desired long wavelength of the absorption maximum corresponds with low-lying excited singlet and triplet states, which prevent sensitization of $\text{O}_2(^1\Delta_g)$ via fluorescence quenching and also triplet sensitization of $\text{O}_2(^1\Sigma_g^+)$. Since only $\text{O}_2(^1\Delta_g)$ can be produced besides ground-state oxygen, smaller efficiencies $S_\Delta = k_{\Delta E}^{1\Delta} / (k_{\Delta E}^{1\Delta} + k_{\Delta E}^{3\Sigma})$ of singlet oxygen formation result. For example, using eq 65, a variation of $0.43 \approx S_\Delta \approx 0.76$ is estimated when varying E_T from 110 to 150 kJ mol^{-1} for formation of $\text{O}_2(^1\Delta_g)$ in the absence of charge-transfer interactions. Interestingly, for sensitizers with triplet energies of 150 kJ mol^{-1} , the condition $\Delta G_{\text{CET}} \approx 50 \text{ kJ mol}^{-1}$, required to prevent CT during O_2 quenching of T_1 , is fulfilled as long as $E_{\text{ox}} > 1.1 \text{ V vs SCE}$. Oxidation potentials for commonly used PDT sensitizers such as porphyrins are often close to this value, and thus, many of them may be optimized by introducing electron-withdrawing substituents on their aromatic rings. Additionally, it should be noted that biological tissues are significantly more polar than CCl_4 (for which eq 65 was established), and thus, variations ensuing from CT interactions may be even more important than those obtained according to this estimation.

G. Estimation of Singlet Oxygen Diffusion Lengths

The average value of the square of distance d which an O_2 molecule travels during time t depends on its diffusion coefficient D_0 according to $d^2 = 6D_0t$.⁴⁶⁶ This expression could be used to estimate how far $\text{O}_2(^1\Delta_g)$ can move from the place of its creation until it is quenched or reacts. With $D_0 = 0.232 \text{ cm}^2 \text{ s}^{-1}$ for O_2 gas at 298 K,⁴⁶⁷ and $\tau_\Delta = 54 \text{ ms}$ for air of 100% relative humidity at 298 K and 1 bar, the diffusion length of $\text{O}_2(^1\Delta_g)$ is estimated to be 2.7 mm. The values of D_0 appear to vary not too much in organic solvents:⁴⁶⁸ 3.7×10^{-5} (CCl_4 , 299 K), 5.31×10^{-5} (cyclohexane, 303 K), and $2.64 \times 10^{-5} \text{ cm}^2 \text{ s}^{-1}$ ($\text{C}_2\text{H}_5\text{OH}$, 303 K). Since τ_Δ varies in this series of air-saturated solvents from 59 ms to $23 \mu\text{s}$ and $15.3 \mu\text{s}$ (Tables 4 and 5), the corresponding diffusion lengths of $\text{O}_2(^1\Delta_g)$ are estimated to be 36, 0.9, and $0.5 \mu\text{m}$.

Thus, on a molecular scale, $\text{O}_2(^1\Delta_g)$ can effect chemical reactions still far from the place of its creation. However, with $D_0 = 1.4 \times 10^{-5} \text{ cm}^2 \text{ s}^{-1}$ given by Moan for cells,⁴⁶⁹ and the very short lifetime $\tau_\Delta = 0.04 \mu\text{s}$, which was recently measured by Wilson's group⁶ in PDT experiments with skin and liver of living rats, inside cells only a rather small diffusion length of 20 nm results.

VII. Conclusion

Despite the very academic approach of the studies presented in this review, it is clear that the most important interest in singlet oxygen is due to the fact that its photochemistry and photophysics affect our lives in a continuous and rather significant way. Every photon of light absorbed in the presence of molecular oxygen may provoke $\text{O}_2(^1\Delta_g)$ -mediated alterations, leading to degradation or aging. To achieve efficient protection from the detrimental effects of singlet oxygen photochemistry, but also to maximize the effect of its numerous applications, it is essential to understand the mechanisms governing its formation and deactivation. The present review provides information allowing the comprehension and, in many cases, even the quantitative prediction of $\text{O}_2(^1\Delta_g)$ and $\text{O}_2(^1\Sigma_g^+)$ generation and deactivation parameters, especially during photophysical interactions with organic molecules.

However, while most processes in simple chemical or physical systems are well understood, the actual mechanisms of its biological activity remain to be entirely established. For example, the estimated diffusion length of 20 nm in vivo indicates that $\text{O}_2(^1\Delta_g)$ does not necessarily react with the biological unit that is responsible for its generation, and that many further studies will be required to completely understand singlet oxygen photochemistry in vivo. Several techniques were recently developed with the aim of observing $\text{O}_2(^1\Delta_g)$ in biological situations, and the perspective for mechanistic studies in vivo seems to be better than ever. New observations and new interpretations have to be expected, and most probably, new mechanistic approaches will be required. However, it is also clear that most observations will be understood on the basis of the mechanisms established using simple systems, and thus, any study of singlet oxygen in heterogeneous systems will require an excellent comprehension of the individual mechanisms of generation and deactivation of $\text{O}_2(^1\Delta_g)$ and $\text{O}_2(^1\Sigma_g^+)$.

VIII. Acknowledgment

Financial support by the Deutsche Forschungsgemeinschaft and the Adolf Messer Stiftung is greatly appreciated. C.S. thanks the Ministère de la Culture, de l'Enseignement Supérieur et de la Recherche of Luxembourg for a BFR scholarship.

IX. References

- Umehawa, N.; Tanaka, K.; Urano, Y.; Kikuchi, K.; Higuchi, T.; Nagano, T. *Angew. Chem., Int. Ed.* **1999**, *38*, 2899.
- Tanaka, K.; Miura, T.; Umehawa, N.; Urano, Y.; Kikuchi, K.; Higuchi, T.; Nagano, T. *J. Am. Chem. Soc.* **2001**, *123*, 2530.

- (3) Krasnovsky, A. A., Jr.; Schweitzer, C.; Leismann, H.; Tanielian, C.; Luk'yanets, E. A. *Quantum Electron.* **2000**, *30*, 445.
- (4) Krasnovsky, A. A., Jr.; Bashtanov, M. E.; Drozdova, N. N.; Yuzhakova, O. A.; Luk'yanets, E. A. *Quantum Electron.* **2002**, *32*, 83.
- (5) Andersen, L. K.; Ogilby, P. R. *Photochem. Photobiol.* **2001**, *73*, 489.
- (6) Niedre, M.; Patterson, M. S.; Wilson, B. C. *Photochem. Photobiol.* **2002**, *75*, 382.
- (7) Hübner, C. G.; Renn, A.; Renge, I.; Wild, U. P. *J. Chem. Phys.* **2001**, *115*, 9619.
- (8) Frimer, A. A., Ed. *Singlet oxygen*; CRC Press: Boca Raton, FL, 1985.
- (9) Gorman, A. A. *Adv. Photochem.* **1992**, *17*, 217.
- (10) Foote, C. S.; Valentine, J. S.; Greenberg, A.; Liebman, J. F., Eds. *Active oxygen in chemistry*; Chapman and Hall: London, 1995.
- (11) Clennan, E. L. *Acc. Chem. Res.* **2001**, *34*, 875.
- (12) Wentworth, P.; Jones, L. H.; Wentworth, A. D.; Zhu, X. Y.; Larsen, N. A.; Wilson, I. A.; Xu, X.; Goddard, W. A.; Janda, K. D.; Eschenmoser, A.; Lerner, R. A. *Science* **2001**, *293*, 1806.
- (13) Datta, D.; Vaidehi, N.; Xu, X.; Goddard, W. A. *Proc. Natl. Acad. Sci. U.S.A.* **2002**, *99*, 2636.
- (14) DeRosa, M. C.; Crutchley, R. J. *Coord. Chem. Rev.* **2002**, *233–234*, 351.
- (15) Lissi, E. A.; Encinas, M. V.; Lemp, E.; Rubio, M. A. *Chem. Rev.* **1993**, *93*, 699.
- (16) Wilkinson, F.; Helman, W. P.; Ross, A. B. *J. Phys. Chem. Ref. Data* **1993**, *22*, 113.
- (17) Wilkinson, F.; Helman, W. P.; Ross, A. B. *J. Phys. Chem. Ref. Data* **1995**, *24*, 663.
- (18) <http://www.rcdc.nd.edu>
- (19) Redmond, R. W.; Gamlin, J. N. *Photochem. Photobiol.* **1999**, *70*, 391.
- (20) Mullikan, R. S. *Phys. Rev.* **1928**, *32*, 186.
- (21) Childs, W. H. J.; Mecke, R. Z. *Phys.* **1931**, *68*, 344.
- (22) Mullikan, R. S. *Rev. Mod. Phys.* **1932**, *4*, 1.
- (23) Ellis, J. W.; Kneser, H. O. *Z. Phys.* **1933**, *86*, 583.
- (24) Herzberg, G. *Spectra of Diatomic Molecules*; Van Nostrand Reinhold: New York, 1950.
- (25) Pittner, P.; Carsky, P.; Hubac, I. *Int. J. Quantum Chem.* **2002**, *90*, 1031.
- (26) Ritter, K. J.; Wilkerson, T. D. *J. Mol. Spectrosc.* **1987**, *121*, 1.
- (27) Noxon, J. F. *Can. J. Phys.* **1961**, *39*, 1110.
- (28) Kasha, M. In ref 8, p 1.
- (29) Badger, R. M.; Wright, A. C.; Whitlock, R. F. *J. Chem. Phys.* **1965**, *43*, 4345.
- (30) Spalek, O.; Kodymova, J.; Stopka, P.; Micek, I. *J. Phys. B—At. Mol. Opt. Phys.* **1999**, *32*, 1885.
- (31) Miller, H. C.; McCord, J. E.; Choy, J.; Hager, G. D. *J. Quant. Spectrosc. Radiat. Transfer* **2001**, *69*, 305.
- (32) Newman, S. M.; Orr-Ewing, A. J.; Newnham, D. A.; Ballard, J. *J. Phys. Chem. A* **2000**, *104*, 9467.
- (33) Minaev, B. F.; Agren, H. *J. Chem. Soc., Faraday Trans.* **1997**, *93*, 2231.
- (34) Klotz, R.; Marian, C. M.; Peyerimhoff, S. D.; Hess, B. A.; Buenker, A. J. *Chem. Phys.* **1984**, *89*, 223.
- (35) Minaev, B. F. *Int. J. Quantum Chem.* **1980**, *17*, 367.
- (36) Tinkham, M.; Strandberg, M. V. *Phys. Rev.* **1955**, *97*, 951.
- (37) Minaev, B. F.; Lunell, S.; Kobzev, G. I. *J. Mol. Struct. (THEOCHEM)* **1993**, *284*, 1.
- (38) Long, C.; Kearns, D. R. *J. Chem. Phys.* **1973**, *59*, 5729.
- (39) Schmidt, R.; Bodesheim, M. *J. Phys. Chem.* **1995**, *99*, 15919.
- (40) Chou, P.-T.; Chen, Y.-C.; Wei, C.-Y.; Chen, S.-J.; Lu, H.-L.; Wei, T.-H. *J. Phys. Chem. A* **1997**, *101*, 8581.
- (41) Becker, A. C.; Schurath, U.; Dubost, H.; Galaup, J. P. *Chem. Phys.* **1988**, *125*, 321.
- (42) Becker, A. C.; Schurath, U. *Chem. Phys. Lett.* **1987**, *142*, 313.
- (43) Chou, P.-T.; Frei, H. *Chem. Phys. Lett.* **1985**, *122*, 87.
- (44) Fink, E. H.; Setzer, K. D.; Wildt, J.; Ramsay, D. A.; Vervloet, M. *Int. J. Quantum Chem.* **1991**, *39*, 287.
- (45) Weldon, D.; Ogilby, P. R. *J. Am. Chem. Soc.* **1998**, *120*, 12978.
- (46) Andersen, L. K.; Ogilby, P. R. *Rev. Sci. Instrum.* **2002**, *73*, 4313.
- (47) Dam, N.; Keszhelyi, T.; Andersen, L. K.; Mikkelsen, K. V.; Ogilby, P. R. *J. Phys. Chem. A* **2002**, *106*, 5263.
- (48) Andersen, L. K.; Ogilby, P. R. *J. Phys. Chem. A* **2002**, *106*, 11064.
- (49) Bachilo, S. M.; Nichiporovich, I. N.; Losev, A. P. *J. Appl. Spectrosc.* **1998**, *65*, 849.
- (50) Wildt, J.; Fink, E. H.; Biggs, P.; Wayne, R. P. *Chem. Phys.* **1989**, *139*, 401.
- (51) Wildt, J.; Fink, E. H.; Biggs, P.; Wayne, R. P. *Chem. Phys.* **1992**, *159*, 127.
- (52) Cho, C. W.; Allin, E. J.; Welsh, H. L. *J. Chem. Phys.* **1956**, *25*, 371.
- (53) McKellar, A. R. W.; Rich, N. H.; Welsh, H. L. *Can. J. Phys.* **1972**, *50*, 1.
- (54) Krasnovsky, A. A., Jr. *Biofizika* **1976**, *21*, 748.
- (55) Khan, A. U.; Kasha, M. *Proc. Natl. Acad. Sci. U.S.A.* **1979**, *76*, 6047.
- (56) Salokhiddinov, K. I.; Dzagharev, B. M.; Byteva, I. M.; Gurinovich, G. P. *Chem. Phys. Lett.* **1980**, *76*, 85.
- (57) Schmidt, R.; Afshari, E. *Ber. Bunsen-Ges. Phys. Chem.* **1992**, *96*, 788.
- (58) Macpherson, A. N.; Truscott, T. G.; Turner, P. H. *J. Chem. Soc., Faraday Trans.* **1994**, *90*, 1065.
- (59) Chou, P.-T.; Chen, Y.-C.; Wei, C.-Y.; Chen, S.-J.; Lu, H. L.; Lee, M. Z. *Chem. Phys. Lett.* **1997**, *280*, 134.
- (60) Krasnovsky, A. A., Jr. *Chem. Phys. Lett.* **1981**, *81*, 443.
- (61) Hurst, J. R.; McDonald, J. D.; Schuster, G. B. *J. Am. Chem. Soc.* **1982**, *104*, 2065.
- (62) Scurlock, R. D.; Ogilby, P. R. *J. Phys. Chem.* **1987**, *91*, 4599.
- (63) Gorman, A. A.; Hamblett, I.; Lambert, C.; Prescott, A. L.; Rodgers, M. A. J.; Spence, H. M. *J. Am. Chem. Soc.* **1987**, *109*, 3091.
- (64) Schmidt, R.; Seikel, K.; Brauer, H.-D. *J. Phys. Chem.* **1989**, *93*, 4507.
- (65) Schmidt, R.; Afshari, E. *J. Phys. Chem.* **1990**, *94*, 4377.
- (66) Losev, A. P.; Byteva, I. M.; Gurinovich, G. P. *Chem. Phys. Lett.* **1988**, *143*, 127.
- (67) Losev, A. P.; Nichiporovich, I. N.; Byteva, I. M.; Drozdov, N. N.; Al Jhngami, I. F. *Chem. Phys. Lett.* **1991**, *181*, 45; *Chem. Phys. Lett.* **1991**, *186*, 586 (Erratum).
- (68) Schmidt, R. *Chem. Phys. Lett.* **1988**, *151*, 369.
- (69) Shimizu, O.; Watanabe, J.; Imakubo, K.; Naito, S. *J. Phys. Soc. Jpn.* **1998**, *67*, 3664.
- (70) Scurlock, R. D.; Nonell, S.; Braslavsky, S. E.; Ogilby, P. R. *J. Phys. Chem.* **1995**, *99*, 3521.
- (71) Darmanyan, A. P. *Chem. Phys. Lett.* **1993**, *215*, 477.
- (72) Kuriyama, Y.; Ogilby, P. R.; Mikkelsen, K. V. *J. Phys. Chem.* **1994**, *98*, 11918.
- (73) Minaev, B. F. *J. Prikl. Spektrosk.* **1985**, *42*, 766.
- (74) Minaev, B. F. *J. Mol. Struct. (THEOCHEM)* **1989**, *183*, 207.
- (75) Minaev, B. F.; Lunell, S.; Kobzev, G. I. *Int. J. Quantum Chem.* **1994**, *50*, 279.
- (76) Darmanyan, A. P. *J. Phys. Chem. A* **1998**, *102*, 9833.
- (77) Poulsen, T. D.; Ogilby, P. R.; Mikkelsen, K. V. *J. Phys. Chem. A* **1998**, *102*, 9829.
- (78) Shimizu, O.; Watanabe, J.; Imakubo, K.; Naito, S. *Chem. Lett.* **1999**, *1*, 67.
- (79) Bilski, P.; Holt, R. N.; Chignell, C. F. *J. Photochem. Photobiol. A: Chem.* **1997**, *109*, 243.
- (80) Schmidt, R.; Shafii, F.; Hild, M. *J. Phys. Chem. A* **1999**, *103*, 2599.
- (81) Martinez, L. A.; Martinez, C. G.; Klopotek, B. B.; Lang, J.; Neuner, A.; Braun, A. M.; Oliveros, E. *J. Photochem. Photobiol. B: Biol.* **2000**, *58*, 94.
- (82) Lee, P. C.; Rodgers, M. A. J. *J. Phys. Chem.* **1983**, *87*, 4894.
- (83) Schmidt, R.; Tanielian, C.; Dunsbach, R.; Wolff, C. J. *Photochem. Photobiol. A: Chem.* **1994**, *79*, 11.
- (84) Hirayama, S.; Phillips, D. J. *Photochem.* **1980**, *12*, 139.
- (85) Hild, M.; Schmidt, R. *J. Phys. Chem. A* **1999**, *103*, 6091.
- (86) Tyczkowski, G.; Schurath, U.; Bodenbinde, M.; Willner, H. *Chem. Phys.* **1997**, *215*, 379.
- (87) Losev, A. P.; Bachilo, S. M.; Nichiporovich, I. N. *J. Appl. Spectrosc.* **1998**, *65*, 1.
- (88) Belford, R. E.; Seely, G.; Gust, D.; Moore, T. A.; Moore, A.; Cherepy, N. J.; Ekbundit, S.; Lewis, J. E.; Lin, S. H. *J. Photochem. Photobiol. A: Chem.* **1993**, *70*, 125.
- (89) Ogilby, P. R. *Acc. Chem. Res.* **1999**, *32*, 512.
- (90) Weldon, D.; Poulsen, T. D.; Mikkelsen, K. V.; Ogilby, P. R. *Photochem. Photobiol.* **1999**, *70*, 369.
- (91) Schmidt, R.; Bodesheim, M. *J. Phys. Chem.* **1994**, *98*, 2874.
- (92) Chou, P. T.; Wei, G. T.; Lin, C. H.; Wei, C. Y.; Chang, C. H. *J. Am. Chem. Soc.* **1996**, *118*, 3031.
- (93) Wild, E.; Klingshirn, H.; Maier, M. *J. Photochem.* **1984**, *25*, 131.
- (94) Bromberg, A.; Foote, C. S. *J. Phys. Chem.* **1989**, *93*, 3968.
- (95) Byteva, I. M.; Gurinovich, G. P.; Losev, A. P.; Mudryi, A. V. *Opt. Spektrosk.* **1990**, *68*, 317.
- (96) Wessels, J. M.; Rodgers, M. A. J. *J. Phys. Chem.* **1995**, *99*, 17586.
- (97) Schmidt, R. *J. Phys. Chem.* **1996**, *100*, 8049.
- (98) Weldon, D.; Wang, B.; Poulsen, T. D.; Mikkelsen, K. V.; Ogilby, P. R. *J. Phys. Chem. A* **1998**, *102*, 1498.
- (99) Keszhelyi, T.; Poulsen, T. D.; Ogilby, P. R.; Mikkelsen, K. V. *J. Phys. Chem. A* **2000**, *104*, 10550.
- (100) Poulsen, T. D.; Ogilby, P. R.; Mikkelsen, K. V. *J. Phys. Chem. A* **1998**, *102*, 8970.
- (101) Poulsen, T. D.; Ogilby, P. R.; Mikkelsen, K. V. *J. Phys. Chem. A* **1999**, *103*, 3418.
- (102) Wayne, R. P. In ref 8, p 81.
- (103) Collins, R. J.; Husain, D.; Donovan, R. J. *J. Chem. Soc., Faraday Trans. 2* **1973**, *69*, 145.
- (104) Wilkinson, F.; Brummer, J. G. *J. Phys. Chem. Ref. Data* **1981**, *10*, 809.
- (105) Young, R. H.; Wehrly, K.; Martin, R. L. *J. Am. Chem. Soc.* **1971**, *93*, 5774.
- (106) Foote, C. S.; Chang, Y. C.; Denny, R. W. *J. Am. Chem. Soc.* **1970**, *92*, 5216.

- (107) Adams, D. R.; Wilkinson, F. *J. Chem. Soc., Faraday Trans. 2* **1972**, *68*, 586.
- (108) Young, R. H.; Brewer, D.; Keller, R. A. *J. Am. Chem. Soc.* **1973**, *95*, 375.
- (109) Merkel, P. B.; Kearns, D. R. *Chem. Phys. Lett.* **1971**, *12*, 120.
- (110) Merkel, P. B.; Kearns, D. R. *J. Am. Chem. Soc.* **1972**, *94*, 7244.
- (111) Salokhiddinov, K. I.; Byteva, I. M.; Gurinovich, G. P. *Zh. Prikl. Spektrosk.* **1981**, *34*, 92.
- (112) Ogilby, P. R.; Foote, C. S. *J. Am. Chem. Soc.* **1981**, *103*, 1219.
- (113) Krasnovsky, A. A., Jr. *Photochem. Photobiol.* **1979**, *29*, 29.
- (114) Byteva, I. M.; Gurinovich, G. P.; Isbavitelev, S. P. *Zh. Prikl. Spektrosk.* **1978**, *23*, 285.
- (115) Parker, J. G.; Stanbro, W. D. *J. Am. Chem. Soc.* **1982**, *104*, 2067.
- (116) Ogilby, P. R.; Foote, C. S. *J. Am. Chem. Soc.* **1982**, *104*, 2069.
- (117) Jenny, T. A.; Turro, N. J. *Tetrahedron Lett.* **1982**, *23*, 2923.
- (118) Ogilby, P. R.; Foote, C. S. *J. Am. Chem. Soc.* **1983**, *105*, 3423.
- (119) Rodgers, M. A. J. *J. Am. Chem. Soc.* **1983**, *105*, 6201.
- (120) Hurst, J. R.; Schuster, G. B. *J. Am. Chem. Soc.* **1983**, *105*, 5756.
- (121) Schmidt, R.; Brauer, H.-D. *J. Am. Chem. Soc.* **1987**, *109*, 6976.
- (122) Aubry, J.-M.; Mandard-Cazin, B.; Rougee, M.; Bensasson, R. V. *J. Am. Chem. Soc.* **1995**, *117*, 9159.
- (123) Schmidt, R. *J. Am. Chem. Soc.* **1989**, *111*, 6983.
- (124) Egorov, S. Y.; Kamalov, V. F.; Koroteev, N. I.; Krasnovsky, A. A.; Toleutaev, B. N.; Zinukov, S. V. *Chem. Phys. Lett.* **1989**, *163*, 421.
- (125) Plötz, J.; Maier, M. *Chem. Phys. Lett.* **1987**, *138*, 419.
- (126) Afshari, E.; Schmidt, R. *Chem. Phys. Lett.* **1991**, *184*, 128.
- (127) Gorman, A. A.; Hamblett, I.; Lambert, C.; Spencer, B.; Standen, M. C. *J. Am. Chem. Soc.* **1988**, *110*, 8053.
- (128) Schmidt, R.; Seikel, K.; Brauer, H.-D. *Ber. Bunsen-Ges. Phys. Chem.* **1990**, *94*, 1100.
- (129) Ogryzlo, E. A. *Org. Chem.* **1979**, *40*, 35.
- (130) Wildt, J.; Bednarek, G.; Fink, E. H.; Wayne, R. P. *Chem. Phys.* **1988**, *122*, 463.
- (131) Braithwaite, M.; Davidson, J. A.; Ogryzlo, E. A. *J. Chem. Phys.* **1976**, *65*, 771.
- (132) Braithwaite, M.; Davidson, J. A.; Ogryzlo, E. A. *Ber. Bunsen-Ges. Phys. Chem.* **1977**, *81*, 179.
- (133) Kear, K.; Abrahamson, E. W. *J. Photochem.* **1975**, *3*, 409.
- (134) Aviles, R. G.; Muller, D. F.; Houston P. L. *Appl. Phys. Lett.* **1980**, *37*, 358.
- (135) Becker, K. H.; Groth, W.; Schurath, U. *Chem. Phys. Lett.* **1971**, *8*, 259.
- (136) Gauthier, M.; Snelling, D. R. *J. Photochem.* **1975**, *4*, 27.
- (137) Derwent, R. G.; Thrush B. A. *Trans. Faraday Soc.* **1971**, *67*, 2036.
- (138) Stuhl, F.; Niki, H. *Chem. Phys. Lett.* **1971**, *7*, 473.
- (139) O'Brien, R. J.; Myers, G. H. *J. Chem. Phys.* **1970**, *53*, 3832.
- (140) Filseth, S. V.; Zia, A.; Welge, K. H. *J. Chem. Phys.* **1970**, *52*, 5502.
- (141) Thomas, R. G. O.; Thrush, B. A. *Proc. R. Soc. London Ser. A* **1977**, *356*, 287.
- (142) Singh, J. P.; Setser, D. W. *J. Phys. Chem.* **1985**, *89*, 5353.
- (143) Davidson, J. A.; Kear, K. E.; Abrahamson, E. W. *J. Photochem.* **1973**, *1*, 307.
- (144) Boodaghians, R. B.; Borell, P. M.; Borell, P. *Chem. Phys. Lett.* **1983**, *97*, 193.
- (145) Borell, P. M.; Borell, P.; Grant, K. R. *J. Chem. Phys.* **1983**, *78*, 748.
- (146) Stuhl, F.; Welge, K. H. *Can. J. Chem.* **1969**, *47*, 1870.
- (147) Kohse-Höinghaus, K.; Stuhl, F. *J. Chem. Phys.* **1980**, *72*, 3720.
- (148) Davidson, J. A.; Ogryzlo, E. A. *Can. J. Chem.* **1974**, *52*, 240.
- (149) Schmidt, R. *Ber. Bunsen-Ges. Phys. Chem.* **1992**, *96*, 794.
- (150) Wang, B.; Ogilby, P. R. *J. Phys. Chem.* **1993**, *97*, 193.
- (151) Keszthelyi, T.; Weldon, D.; Andersen, T. N.; Poulsen, T. D.; Mikkelsen, K. V.; Ogilby, P. R. *Photochem. Photobiol.* **1999**, *70*, 531.
- (152) Schmidt, R.; Bodesheim, M. *Chem. Phys. Lett.* **1993**, *213*, 111.
- (153) Schmidt, R.; Bodesheim, M. *J. Phys. Chem. A* **1998**, *102*, 4769.
- (154) Einwohner, T.; Alder, B. *J. Chem. Phys.* **1968**, *49*, 1548.
- (155) Schmidt, R. *J. Phys. Chem.* **1993**, *97*, 3658.
- (156) Schmidt, R. *J. Photochem. Photobiol. A: Chem.* **1994**, *80*, 1.
- (157) Zhao, Y.; Setser, D. W. *J. Phys. Chem.* **1994**, *98*, 9723.
- (158) Zhao, Y.; Setser, D. W. *J. Chem. Soc., Faraday Trans.* **1995**, *91*, 2979.
- (159) Liu, C.; Zou, S.; Guo, J.; Gu, Y.; Cao, D.; Chu, Y.; Setser, D. W. *J. Phys. Chem.* **1997**, *101*, 7345.
- (160) Chatelet, M.; Tardieu, A.; Spreitzer, W.; Maier, M. *Chem. Phys.* **1986**, *102*, 387.
- (161) Seidl, M.; Kaa, J.; Maier, M. *Chem. Phys.* **1991**, *157*, 279.
- (162) Kaa, J.; Maier, M. *Chem. Phys.* **1993**, *177*, 309.
- (163) Okamoto, M.; Tanaka, F.; Teranishi, H. *J. Phys. Chem.* **1990**, *94*, 669.
- (164) Yoshimura, Y.; Nakahara, M. *J. Chem. Phys.* **1984**, *81*, 4080.
- (165) Schmidt, R. *J. Phys. Chem. A* **1998**, *102*, 9082.
- (166) Hild, M.; Brauer, H.-D. *Chem. Phys. Lett.* **1998**, *283*, 21.
- (167) Okamoto, M.; Tanaka, F.; Teranishi, H. *Phys. Chem. Chem. Phys.* **2000**, *2*, 5571.
- (168) Okamoto, M.; Takagi, T.; Tanaka, F. *Chem. Lett.* **2000**, 1396.
- (169) Worrall, D. R.; Abdel-Shafi, A. A.; Wilkinson, F. *J. Phys. Chem. A* **2001**, *105*, 1270.
- (170) Abdel-Shafi, A. A.; Wilkinson, F.; Worrall, D. R. *Chem. Phys. Lett.* **2001**, *343*, 273.
- (171) Okamoto, M.; Nagano, M.; Nagashima, H.; Tanaka, F. *Phys. Chem. Chem. Phys.* **2002**, *4*, 1866.
- (172) Ouannès, C.; Wilson, T. *J. Am. Chem. Soc.* **1968**, *90*, 6527.
- (173) Ogryzlo, E. A.; Tang, C. W. *J. Am. Chem. Soc.* **1970**, *92*, 5034.
- (174) Young, R. H.; Martin, R. L. *J. Am. Chem. Soc.* **1972**, *94*, 5183.
- (175) Furukawa, K.; Ogryzlo, E. A. *J. Photochem.* **1972/73**, *1*, 163.
- (176) Smith, W. F., Jr. *J. Am. Chem. Soc.* **1972**, *94*, 186.
- (177) Matheson, I. B. C.; Lee, J. *J. Am. Chem. Soc.* **1972**, *94*, 3310.
- (178) Young, R. H.; Martin, R. L.; Feriozi, D.; Brewer, D.; Kayser, R. *Photochem. Photobiol.* **1973**, *17*, 233.
- (179) Gollnick, K.; Lindner, J. H. E. *Tetrahedron Lett.* **1973**, *21*, 1903.
- (180) Monroe, B. M. *J. Phys. Chem.* **1977**, *81*, 1861.
- (181) Saito, I.; Matsuura, T.; Inoue, K. *J. Am. Chem. Soc.* **1983**, *105*, 3200.
- (182) Encinas, M. V.; Lemp, E.; Lissi, E. A. *J. Chem. Soc., Perkin Trans. 2* **1987**, 1125.
- (183) Clennan, E. L.; Noe, L. J.; Wen, T.; Szneler, E. *J. Org. Chem.* **1989**, *54*, 3581.
- (184) Seikel, K.; Brauer, H.-D. *Ber. Bunsen-Ges. Phys. Chem.* **1991**, *95*, 900.
- (185) Hild, M.; Brauer, H.-D. *Ber. Bunsen-Ges. Phys. Chem.* **1996**, *100*, 1210.
- (186) Martin, N. H.; Allen, N. W.; Cottle, C. A.; Marschke, C. K. *J. Photochem. Photobiol. A: Chem.* **1997**, *103*, 33.
- (187) Zanoce, A. L.; Lemp, E.; Pizarro, N.; de la Fuente, J. R.; Günther, G. *J. Photochem. Photobiol. A: Chem.* **2001**, *140*, 109.
- (188) Darmanyan, A. P.; Jenks, W. S.; Jardon, P. *J. Phys. Chem. A* **1998**, *102*, 7420.
- (189) Clennan, E. L.; Noe, L. J.; Szneler, E.; Wen, T. *J. Am. Chem. Soc.* **1990**, *112*, 5080.
- (190) Ackerman, R. A.; Rosenthal, I.; Pitts, J. N., Jr. *J. Chem. Phys.* **1971**, *54*, 4960.
- (191) Monroe, B. M. *Photochem. Photobiol.* **1979**, *29*, 761.
- (192) Kacher, M. L.; Foote, C. S. *Photochem. Photobiol.* **1979**, *29*, 765.
- (193) Liang, J.-J.; Gu, C.-L.; Kacher, M. L.; Foote, C. S. *J. Am. Chem. Soc.* **1983**, *105*, 4717.
- (194) Clennan, E. L.; Greer, A. *Tetrahedron Lett.* **1996**, *37*, 6093.
- (195) Clennan, E. L.; Wang, D.; Clifton, C.; Chem, M.-F. *J. Am. Chem. Soc.* **1997**, *119*, 9081.
- (196) Thomas, M. J.; Foote, C. S. *Photochem. Photobiol.* **1978**, *27*, 683.
- (197) Gorman, A. A.; Gould, I. R.; Hamblett, I.; Standen, M. C. *J. Am. Chem. Soc.* **1984**, *106*, 6959.
- (198) Soltermann, A. T.; Luiz, M.; Biasutti, M. A.; Carrascoso, M.; Amat-Guerri, F.; Garcia, N. A. *J. Photochem. Photobiol. A: Chem.* **1999**, *129*, 25.
- (199) Schweitzer, C.; Mehrdad, Z.; Shafii, F.; Schmidt, R. *J. Phys. Chem. A* **2001**, *105*, 5309.
- (200) Schweitzer, C.; Mehrdad, Z.; Shafii, F.; Schmidt, R. *Phys. Chem. Chem. Phys.* **2001**, *3*, 3095.
- (201) Schweitzer, C.; Mehrdad, Z.; Noll, A.; Grabner, E.-W.; Schmidt, R. *Helv. Chim. Acta* **2001**, *84*, 2493.
- (202) Okamoto, M.; Tanaka, F. *J. Phys. Chem.* **1993**, *97*, 177.
- (203) Okamoto, M. *J. Photochem. Photobiol. A: Chem.* **1999**, *124*, 113.
- (204) Carlsson, D. J.; Mendenhall, G. D.; Suprunchuk, T.; Wiles, D. M. *J. Am. Chem. Soc.* **1972**, *94*, 8960.
- (205) Rajadurai, S.; Das, P. K. *J. Photochem.* **1987**, *37*, 33.
- (206) Hessler, D. P.; Frimmel, F. H.; Oliveros, E.; Braun, A. M. *Helv. Chim. Acta* **1994**, *77*, 859.
- (207) Oliveros, E.; Besançon, F.; Boneva, M.; Kräutler, B.; Braun, A. M. *J. Photochem. Photobiol. B: Biol.* **1995**, *29*, 37.
- (208) Corey, E. J.; Mehrotra, M. M.; Khan, A. U. *Science* **1987**, *97*, 177.
- (209) Corey, E. J.; Khan, A. U.; Ha, D.-K. *Tetrahedron Lett.* **1990**, *31*, 1389.
- (210) Harbour, J. R.; Issler, S. L. *J. Am. Chem. Soc.* **1982**, *104*, 903.
- (211) Haag, W. R.; Mill, T. *Photochem. Photobiol.* **1987**, *45*, 317.
- (212) Rubio, M. A.; Mártire, D. O.; Braslavsky, S. E.; Lissi, E. A. *J. Photochem. Photobiol. A: Chem.* **1992**, *66*, 153.
- (213) Rosenthal, I.; Frimer, A. A. *Photochem. Photobiol.* **1976**, *23*, 209.
- (214) Bilski, P.; Szychlinski, J.; Oleksy, E. *J. Photochem. Photobiol. A: Chem.* **1988**, *45*, 269.
- (215) Guiraud, H. I.; Foote, C. S. *J. Am. Chem. Soc.* **1976**, *98*, 1984.
- (216) Sheu, C.; Foote, C. S. *J. Org. Chem.* **1995**, *60*, 4498.
- (217) Kaiser, S.; DiMascio, P.; Murphy, M. E.; Sies, H. *Arch. Biochem. Biophys.* **1990**, *227*, 101.
- (218) Tanielian, C.; Wolff, C. *Photochem. Photobiol.* **1988**, *48*, 277.
- (219) Foley, S.; Navaratnam, S.; McGarvey, D. J.; Land, E. J.; Truscott, G. T.; Rice-Evans, C. A. *Free Radical Biol. Med.* **1999**, *26*, 1202.
- (220) Bisby, R. H.; Morgan, C. G.; Hamblett, I.; Gorman, A. A. *J. Phys. Chem. A* **1999**, *103*, 7454.
- (221) Darmanyan, A. P.; Gregory, D. D.; Guo, Y.; Jenks, W. S.; Burel, L.; Eloy, D.; Jardon, P. *J. Am. Chem. Soc.* **1998**, *120*, 396.
- (222) Rehm, D.; Weller, A. *Isr. J. Chem.* **1970**, *8*, 259.
- (223) Weller, A. *Z. Phys. Chem. Neue Folge* **1982**, *133*, 93.

- (224) Mattes, S. L.; Farid, S. In *Organic Photochemistry*; Padwa, A., Ed.; Marcel Dekker: New York, 1983.
- (225) Gould, I. R.; Farid, S. *Acc. Chem. Res.* **1996**, *29*, 522.
- (226) Sato, C.; Kikuchi, K.; Okamura, K.; Takahashi, Y.; Miyashi, T. *J. Phys. Chem.* **1995**, *99*, 16925.
- (227) Charton, R. *J. Am. Chem. Soc.* **1969**, *91*, 615.
- (228) Farmilo, A.; Wilkinson, F. *Photochem. Photobiol.* **1973**, *18*, 447.
- (229) Monroe, B. M.; Mrowca, J. J. *J. Phys. Chem.* **1979**, *83*, 591.
- (230) Shiozaki, H.; Nakazumi, H.; Takamura, Y.; Kitao, T. *Bull. Chem. Soc. Jpn.* **1990**, *63*, 2653.
- (231) Baranyai, P.; Vidóczy, T. *J. Photochem. Photobiol. B: Biol.* **2000**, *58*, 143.
- (232) Fukuzumi, S.; Fujita, S.; Suenobu, T.; Yamada, H.; Imahori, H.; Araki, Y.; Ito, O. *J. Phys. Chem. A* **2002**, *106*, 1241.
- (233) Furue, H.; Russell, K. E. *Can. J. Chem.* **1978**, *56*, 1595.
- (234) Jensen, F.; Greer, A.; Clennan, E. L. *J. Am. Chem. Soc.* **1998**, *120*, 4439.
- (235) Lemp, E.; Pizarro, N.; Encinas, M. V.; Zanocho, A. L. *Phys. Chem. Chem. Phys.* **2001**, *3*, 5222.
- (236) Manring, L. E.; Foote, C. S. *J. Phys. Chem.* **1982**, *86*, 1257.
- (237) Peters, G.; Rodgers, M. A. J. *Biochem. Biophys. Res. Commun.* **1980**, *96*, 770.
- (238) Peters, G.; Rodgers, M. A. J. *Biochim. Biophys. Acta* **1981**, *637*, 43.
- (239) Bobrowski, M.; Liwo, A.; Oldziej, S.; Jeziorek, D.; Ossowski, T. *J. Am. Chem. Soc.* **2000**, *122*, 8112.
- (240) Kamlet, M. J.; Abboud, J.-L. M.; Abraham, M. H.; Taft, R. W. *J. Org. Chem.* **1983**, *48*, 2877.
- (241) Scurlock, R.; Rougeé, M.; Bensasson, R. V. *Free Radical Res. Commun.* **1990**, *8*, 251.
- (242) Scurlock, R. D.; Wang, B.; Ogilby, P. R. *J. Am. Chem. Soc.* **1996**, *118*, 388.
- (243) Bodesheim, M.; Schmidt, R. *J. Phys. Chem. A* **1997**, *101*, 5672.
- (244) Foote, C. S.; Denny, R. W. *J. Am. Chem. Soc.* **1968**, *90*, 6233.
- (245) Foote, C. S.; Chang, Y. C.; Denny, R. W. *J. Am. Chem. Soc.* **1970**, *92*, 5216.
- (246) Mathis, P.; Kleo, J. *Photochem. Photobiol.* **1973**, *18*, 343.
- (247) Wilkinson, F.; Ho, W.-T. *Spectrosc. Lett.* **1978**, *11*, 455.
- (248) Rodgers, M. A. J.; Bates, A. L. *Photochem. Photobiol.* **1980**, *31*, 533.
- (249) Matheson, I. B. C.; Rodgers, M. A. J. *Photochem. Photobiol.* **1982**, *36*, 1.
- (250) Manitto, P.; Speranza, G.; Monti, D.; Gramatica, P. *Tetrahedron Lett.* **1987**, *28*, 4221.
- (251) Murasecco-Suardi, P.; Oliveros, E.; Braun, A. M.; Hansen, H.-J. *Helv. Chim. Acta* **1988**, *71*, 1005.
- (252) Speranza, G.; Manitto, P.; Monti, D. *J. Photochem. Photobiol. B: Biol.* **1990**, *8*, 51.
- (253) Conn, P. F.; Schalch, W.; Truscott, T. G. *J. Photochem. Photobiol. B: Biol.* **1991**, *11*, 41.
- (254) Devasagayam, T. P. A.; Werner, T.; Ippendorf, H.; Marin, H.-D.; Sies, H. *Photochem. Photobiol.* **1992**, *55*, 511.
- (255) Oliveros, E.; Braun, A. M.; Aminian-Saghafi, T.; Sliwka, H.-R. *New J. Chem.* **1994**, *18*, 535.
- (256) Edge, R.; McGarvey, D. J.; Truscott, T. G. *J. Photochem. Photobiol. B: Biol.* **1997**, *41*, 189.
- (257) Baltschun, D.; Beutner, S.; Briviba, K.; Martin, H.-D.; Paust, J.; Peters, M.; Röver, S.; Sies, H.; Stahl, W.; Steigel, A.; Stenhorst, F. *Liebigs Ann./Recueil* **1997**, 1887.
- (258) Garavelli, M.; Bernardi, F.; Olivucci, M.; Robb, M. A. *J. Am. Chem. Soc.* **1998**, *120*, 10210.
- (259) Yamano, Y.; Sato, Y.; Watanabe, Y.; Namikawa, K.; Miki, W.; Ito, M. *J. Chem. Soc., Perkin Trans. 1* **2001**, 1862.
- (260) Montenegro, M. A.; Nazareno, M. A.; Durantini, E. N.; Borsarelli, C. D. *Photochem. Photobiol.* **2002**, *75*, 353.
- (261) Firey, P. A.; Ford, W. E.; Sounik, J. R.; Kenney, M. E.; Rodgers, M. A. J. *J. Am. Chem. Soc.* **1988**, *110*, 7626.
- (262) Krasnovsky, A. A., Jr.; Rodgers, M. A. J.; Galpern, M. G.; Rihter, B.; Kenney, M. E.; Lukjanetz, E. A. *Photochem. Photobiol.* **1992**, *55*, 691.
- (263) Aoudia, M.; Cheng, G.; Kennedy, V. O.; Kenney, M. E.; Rodgers, M. A. J. *J. Am. Chem. Soc.* **1997**, *119*, 6029.
- (264) Pelliccioli, A. P.; Henbest, K.; Kwag, G.; Carvagno, T. R.; Kenney, M. E.; Rodgers, M. A. J. *J. Phys. Chem. A* **2001**, *105*, 1757.
- (265) Nikolaitchik, A. V.; Korth, O.; Rodgers, M. A. J. *J. Phys. Chem. A* **1999**, *103*, 7587.
- (266) Berry, R. J.; Douglas, P.; Garley, M. S.; Jolly, T.; Clarke, D.; Moglestue, H.; Walker, H.; Winscom, C. J. *Photochem. Photobiol. A: Chem.* **1999**, *120*, 29.
- (267) Wilkinson, F.; Farmilo, A. J. *Photochem.* **1984**, *25*, 153.
- (268) Becker, K. H.; Fink, E. H.; Langen, P.; Schurath, U. *J. Chem. Phys.* **1974**, *60*, 4623.
- (269) Scurlock, R. D.; Ogilby, P. R. *J. Phys. Chem.* **1996**, *100*, 17226.
- (270) Stahl, W.; Sies, H. *Ann. N.Y. Acad. Sci.* **1993**, *691*, 10.
- (271) Foote, C. S.; Chang, Y. C.; Denny, R. W. *J. Am. Chem. Soc.* **1970**, *92*, 5218.
- (272) DiMascio, P.; Kaiser, S.; Sies, H. *Arch. Biochem. Biophys.* **1989**, *274*, 532.
- (273) Hirayama, K. *J. Am. Chem. Soc.* **1955**, *77*, 373.
- (274) Bensasson, R.; Land, E. J.; Maudinas, B. *Photochem. Photobiol.* **1976**, *23*, 189.
- (275) Haley, J. L.; Fitch, A. N.; Goyal, R.; Lambert, C.; Truscott, T. G.; Chacon, J. N.; Stirling, D.; Schalch, W. *J. Chem. Soc., Chem. Commun.* **1992**, 1175.
- (276) Marston, G.; Truscott, T. G.; Wayne, R. P. *J. Chem. Soc., Faraday Trans.* **1995**, *91*, 4059.
- (277) Lambert, C.; Redmond, R. W. *Chem. Phys. Lett.* **1994**, *228*, 495.
- (278) Truscott, T. G.; Land, E. J.; Sykes, A. *Photochem. Photobiol.* **1973**, *17*, 43.
- (279) Becker, R. S.; Bensasson, R. V.; Lafferty, J.; Truscott, T. G.; Land, E. J. *J. Chem. Soc., Faraday Trans. 2* **1978**, *74*, 2246.
- (280) Hasegawa, K.; Macmillan, J. D.; Maxwell, W. A.; Chichester, C. O. *Photochem. Photobiol.* **1969**, *9*, 165.
- (281) Ford, W. E.; Rihter, B. D.; Rodgers, M. A. J. *J. Am. Chem. Soc.* **1989**, *111*, 2362.
- (282) Ford, W. E.; Rihter, B. D.; Kenney, M. E.; Rodgers, M. A. J. *Photochem. Photobiol.* **1989**, *50*, 277.
- (283) Darmanyan, A. P.; Foote, C. S.; Jardon, P. *J. Phys. Chem.* **1995**, *99*, 11854.
- (284) Darmanyan, A. P.; Tatikolov, A. S. *J. Photochem.* **1986**, *32*, 157.
- (285) Vidóczy, T.; Baranyai, P. *Helv. Chim. Acta* **2001**, *84*, 2640.
- (286) Kautsky, H.; de Bruijn, H. *Naturwissenschaften* **1931**, *19*, 1043.
- (287) Kautsky, H.; Hirsch, A. *Chem. Ber.* **1931**, *64*, 2677.
- (288) Kautsky, H.; de Bruijn, H.; Neuwirth, R.; Baumeister, W. *Chem. Ber.* **1933**, *66*, 1588.
- (289) Kautsky, H. *Trans. Faraday Soc.* **1939**, *35*, 216.
- (290) Foote, C. S.; Wexler, S. *J. Am. Chem. Soc.* **1964**, *86*, 3879.
- (291) Foote, C. S.; Wexler, S. *J. Am. Chem. Soc.* **1964**, *86*, 3880.
- (292) Corey, E. J.; Taylor, W. C. *J. Am. Chem. Soc.* **1964**, *86*, 3881.
- (293) Groh, H. J., Jr.; Luckey, G. W.; Noyes, W. A., Jr. *J. Chem. Phys.* **1953**, *21*, 115.
- (294) Bowen, E. J. *Trans. Faraday Soc.* **1954**, *50*, 97.
- (295) Stevens, B. *Trans. Faraday Soc.* **1955**, *51*, 610.
- (296) Livingston, R.; Rao, V. S. *J. Phys. Chem.* **1959**, *63*, 794.
- (297) Ware, W. R. *J. Phys. Chem.* **1962**, *66*, 455.
- (298) Berlman, I. B.; Walter, T. A. *J. Chem. Phys.* **1962**, *37*, 1888.
- (299) Ware, W. R.; Cunningham, P. T. *J. Chem. Phys.* **1965**, *43*, 3826.
- (300) Berlman, I. B.; Wirth, H. O.; Steingraber, O. J. *J. Am. Chem. Soc.* **1968**, *90*, 566.
- (301) Ware, W. R.; Lee, J. K. *J. Chem. Phys.* **1968**, *49*, 217.
- (302) Stevens, B.; Algar, B. E. *J. Phys. Chem.* **1968**, *72*, 3468.
- (303) Stevens, B.; Algar, B. E. *J. Phys. Chem.* **1968**, *72*, 2582.
- (304) Brewer, T. *J. Am. Chem. Soc.* **1971**, *93*, 775.
- (305) Brown, R. G. Phillips, D. *J. Chem. Soc., Faraday Trans. 2* **1974**, *70*, 630.
- (306) Schoof, S.; Güsten, H.; von Sonntag, C. *Ber. Bunsen-Ges. Phys. Chem.* **1977**, *81*, 305.
- (307) Kikuchi, K.; Sato, C.; Watabe, M.; Ikeda, H.; Takahashi, Y.; Miyashi, T. *J. Am. Chem. Soc.* **1993**, *115*, 5180.
- (308) Grewer, C.; Wirp, C.; Neumann, M.; Brauer, H.-D. *Ber. Bunsen-Ges. Phys. Chem.* **1994**, *98*, 997.
- (309) Wirp, C.; Güsten, H.; Brauer, H.-D. *Ber. Bunsen-Ges. Phys. Chem.* **1996**, *100*, 1217.
- (310) Snelling, D. R. *Chem. Phys. Lett.* **1968**, *2*, 347.
- (311) Stevens, B.; Algar, B. E. *J. Phys. Chem.* **1969**, *73*, 1711.
- (312) Algar, B. E.; Stevens, B. *J. Phys. Chem.* **1970**, *74*, 3029.
- (313) Richards, J. T.; West, G.; Thomas, J. K. *J. Phys. Chem.* **1970**, *74*, 4137.
- (314) Morikawa, A.; Cvetanovic, R. J. *J. Chem. Phys.* **1970**, *52*, 3237.
- (315) Potashnik, R.; Goldschmidt, C. R.; Ottolenghi, M. *Chem. Phys. Lett.* **1971**, *9*, 424.
- (316) Goldschmidt, C. R.; Potashnik, R.; Ottolenghi, M. *J. Phys. Chem.* **1971**, *75*, 1025.
- (317) Brauer, H.-D.; Wagener, H. *Ber. Bunsen-Ges. Phys. Chem.* **1975**, *79*, 597.
- (318) Wagener, H.; Brauer, H.-D. *Mol. Photochem.* **1976**, *7*, 441.
- (319) Stevens, B.; Ors, J. A. *J. Phys. Chem.* **1976**, *80*, 2164.
- (320) Wu, K. C.; Trozzolo, A. M. *J. Phys. Chem.* **1979**, *83*, 2823.
- (321) Wu, K. C.; Trozzolo, A. M. *J. Phys. Chem.* **1979**, *83*, 3180.
- (322) Stevens, B.; Marsh, K. L.; Barltrop, J. A. *J. Phys. Chem.* **1981**, *85*, 3079.
- (323) Darmanyan, A. P. *Chem. Phys. Lett.* **1982**, *86*, 405.
- (324) Brauer, H.-D.; Acs, A.; Drews, W.; Gabriel, R.; Ghaeni, S.; Schmidt, R. *J. Photochem.* **1984**, *25*, 475.
- (325) Abdel-Shafi, A. A.; Wilkinson, F. *J. Phys. Chem. A* **2000**, *104*, 5747.
- (326) Abdel-Shafi, A. A.; Worrall, D. R.; Wilkinson, F. *J. Photochem. Photobiol. A: Chem.* **2001**, *142*, 133.
- (327) Gurinovich, G. P.; Salokhiddinov, K. I. *Chem. Phys. Lett.* **1982**, *85*, 9.
- (328) Usui, Y.; Shimizu, N.; Mori, S. *Bull. Chem. Soc. Jpn.* **1992**, *65*, 897.
- (329) Darmanyan, A. P. *Chem. Phys. Lett.* **1982**, *91*, 396.
- (330) Drews, W.; Schmidt, R.; Brauer, H.-D. *Chem. Phys. Lett.* **1983**, *100*, 466.
- (331) Dobrowolski, D. C.; Ogilby, P. R.; Foote, C. S. *J. Phys. Chem.* **1983**, *87*, 2261.
- (332) Kanner, R. C.; Foote, C. S. *J. Am. Chem. Soc.* **1992**, *114*, 678.

- (333) Wilkinson, F.; McGarvey, D. J.; Olea, A. F. *J. Am. Chem. Soc.* **1993**, *115*, 12144.
- (334) Olea, A. F.; Wilkinson, F. *J. Phys. Chem.* **1995**, *99*, 4518.
- (335) Wirp, C.; Bendig, J.; Brauer, H.-D. *Ber. Bunsen-Ges. Phys. Chem.* **1997**, *101*, 961.
- (336) Stevens, B.; Mills, L. E. *Chem. Phys. Lett.* **1972**, *15*, 381.
- (337) Kristiansen, M.; Scurlock, R. D.; Iu, K.-K.; Ogilby, P. R. *J. Phys. Chem.* **1991**, *95*, 5190.
- (338) Kikuchi, K. *Chem. Phys. Lett.* **1991**, *183*, 103.
- (339) Stevens, B.; Small, R. D., Jr. *Chem. Phys. Lett.* **1979**, *61*, 233.
- (340) Gijzeman, O. L. J.; Kaufman, F.; Porter, G. *J. Chem. Soc., Faraday Trans. 2* **1973**, *69*, 708.
- (341) Garner, A.; Wilkinson, F. *J. Chem. Soc., Faraday Trans. 2* **1976**, *72*, 1010.
- (342) Garner, A.; Wilkinson, F. *Chem. Phys. Lett.* **1977**, *45*, 432.
- (343) Demas, J. N.; Harris, E. W.; McBride, R. P. *J. Am. Chem. Soc.* **1977**, *99*, 3547.
- (344) Cebul, F. A.; Kirk, K. A.; Lupo, D. W.; Pittenger, L. M.; Schuh, M. D.; Williams, I. F.; Winston, G. C. *J. Am. Chem. Soc.* **1980**, *102*, 5656.
- (345) Wilson, T.; Halpern, A. M. *J. Am. Chem. Soc.* **1980**, *102*, 7279.
- (346) Levin, P. P.; Pluzhnikov, P. F.; Kuzmin, V. A. *Chem. Phys. Lett.* **1988**, *152*, 409.
- (347) Yasuda, H.; Scully, A. D.; Hirayama, S.; Okamoto, M.; Tanaka, F. *J. Am. Chem. Soc.* **1990**, *112*, 6847.
- (348) McLean, A. J.; Rodgers, M. A. J. *J. Am. Chem. Soc.* **1993**, *115*, 4786.
- (349) Grever, C.; Brauer, H.-D. *J. Phys. Chem.* **1993**, *97*, 5001.
- (350) Schmidt, R.; Shafii, F. *J. Phys. Chem. A* **2001**, *105*, 8871.
- (351) McLean, A. J.; Rodgers, M. A. J. *J. Am. Chem. Soc.* **1993**, *115*, 9874.
- (352) Hirayama, S.; Yasuda, H.; Scully, A. D.; Okamoto, M. *J. Phys. Chem.* **1994**, *98*, 4609.
- (353) Darmanyan, A. P.; Lee, W.; Jenks, W. S. *J. Phys. Chem. A* **1999**, *103*, 2705.
- (354) Gorman, A. A.; Lovering, G.; Rodgers, M. A. J. *J. Am. Chem. Soc.* **1978**, *100*, 4527.
- (355) Rossbroich, G.; Garcia, N. A.; Braslavsky, S. E. *J. Photochem.* **1985**, *31*, 37.
- (356) Heihoff, K.; Redmond, R. W.; Braslavsky, S. E.; Rougee, M.; Salet, C.; Favre, A.; Bensasson, R. V. *Photochem. Photobiol.* **1990**, *51*, 634.
- (357) Marti, C.; Jürgens, O.; Cuenca, O.; Casals, M.; Nonell, S. *J. Photochem. Photobiol. A: Chem.* **1996**, *97*, 11.
- (358) Gorman, A. A.; Hamblett, I.; Rodgers, M. A. J. *J. Am. Chem. Soc.* **1984**, *106*, 4679.
- (359) Gorman, A. A.; Hamblett, I.; Rodgers, M. A. J. *J. Photochem.* **1984**, *25*, 115.
- (360) Boch, R.; Mehta, B.; Conolly, T.; Durst, T.; Arnason, J. T.; Redmond, R. W.; Scaiano, J. C. *J. Photochem. Photobiol. A: Chem.* **1996**, *93*, 39.
- (361) Wang, B.; Ogilby, P. R. *J. Phys. Chem.* **1993**, *97*, 9593.
- (362) Schmidt, R.; Shafii, F.; Schweitzer, C.; Abdel-Shafi, A. A.; Wilkinson, F. *J. Phys. Chem. A* **2001**, *105*, 1811.
- (363) Bodesheim, M.; Schütz, M.; Schmidt, R. *Chem. Phys. Lett.* **1994**, *221*, 7.
- (364) McGarvey, D. J.; Szekeres, P. G.; Wilkinson, F. *Chem. Phys. Lett.* **1992**, *199*, 314.
- (365) Wilkinson, F.; McGarvey, D. J.; Olea, A. F. *J. Phys. Chem.* **1994**, *98*, 3762.
- (366) Wilkinson, F.; Abdel-Shafi, A. A. *J. Phys. Chem. A* **1997**, *101*, 5509.
- (367) Wilkinson, F.; Abdel-Shafi, A. A. *J. Phys. Chem. A* **1999**, *103*, 5425.
- (368) Shafii, F.; Schmidt, R. *J. Phys. Chem. A* **2001**, *105*, 1805.
- (369) Winterle, J. S.; Kliger, D. S.; Hammond, G. S. *J. Am. Chem. Soc.* **1976**, *98*, 3719.
- (370) Zhang, X.; Rodgers, M. A. J. *J. Phys. Chem.* **1995**, *99*, 12797.
- (371) Cox, G. S.; Whitten, D. G.; Giannotti, C. *Chem. Phys. Lett.* **1979**, *67*, 511.
- (372) Tanielian, C.; Wolff, C. *J. Phys. Chem.* **1995**, *99*, 9825.
- (373) Schmidt, R.; Tanielian, C. *J. Phys. Chem. A* **2000**, *104*, 3177.
- (374) Brauer, H.-D.; Acs, A.; Schmidt, R. *Ber. Bunsen-Ges. Phys. Chem.* **1987**, *91*, 1337.
- (375) Gorman, A. A.; Rodgers, M. A. J. *J. Am. Chem. Soc.* **1986**, *108*, 5074.
- (376) Bendig, J.; Schmidt, R.; Brauer, H.-D. *Chem. Phys. Lett.* **1993**, *202*, 535.
- (377) Cosa, G.; Scaiano, J. C., to be published. Cosa, G., Ph.D. Thesis, University of Ottawa, 2002.
- (378) Evans, D. F. *J. Chem. Soc.* **1953**, 345.
- (379) Munck, A. U.; Scott, J. F. *Nature* **1956**, *177*, 587.
- (380) Tsubomura, H.; Mulliken, R. S. *J. Am. Chem. Soc.* **1960**, *82*, 5966.
- (381) Scurlock, R. D.; Ogilby, P. R. *J. Am. Chem. Soc.* **1988**, *110*, 640.
- (382) Scurlock, R. D.; Ogilby, P. R. *J. Phys. Chem.* **1989**, *93*, 5493.
- (383) Logunov, S. L.; Rodgers, M. A. J. *J. Phys. Chem.* **1993**, *97*, 5643.
- (384) McGarvey, D. J.; Wilkinson, F.; Worrall, D. R.; Hobleby, J.; Shaikh, W. *Chem. Phys. Lett.* **1993**, *202*, 528.
- (385) Kawaoka, K.; Khan, A. U.; Kearns, D. R. *J. Chem. Phys.* **1967**, *46*, 1842.
- (386) Siebrand, W.; Williams, D. F. *J. Chem. Phys.* **1967**, *46*, 403.
- (387) Siebrand, W. *J. Chem. Phys.* **1967**, *47*, 2411.
- (388) Siebrand, W.; Williams, D. F. *J. Chem. Phys.* **1968**, *49*, 1860.
- (389) Patterson, L. K.; Porter, G.; Topp, M. R. *Chem. Phys. Lett.* **1970**, *7*, 612.
- (390) Abdel-Shafi, A. A.; Beer, P. D.; Mortimer, R. J.; Wilkinson, F. *J. Phys. Chem. A* **2000**, *104*, 192.
- (391) Abdel-Shafi, A. A.; Wilkinson, F. *Phys. Chem. Chem. Phys.* **2002**, *4*, 248.
- (392) Chattopadhyay, S. K.; Kumar, C. V.; Das, P. K. *J. Photochem.* **1985**, *30*, 81.
- (393) Smith, G. *J. Chem. Soc., Faraday Trans. 2* **1982**, *78*, 769.
- (394) McLean, A. J.; Truscott, T. G. *J. Chem. Soc., Faraday Trans. 2* **1990**, *86*, 2671.
- (395) Mehrdad, Z.; Noll, A.; Grabner, E.-W.; Schmidt, R. *Photochem. Photobiol. Sci.* **2002**, *1*, 263.
- (396) Tan-Sien-Hee, L.; Jacquet, L.; Kirsch-DeMesmaeker, A. *J. Photochem. Photobiol. A: Chem.* **1994**, *98*, 1145.
- (397) Abdel-Shafi, A. A.; Beer, P. D.; Mortimer, R. J.; Wilkinson, F. *Helv. Chim. Acta* **2001**, *84*, 2784.
- (398) Mehrdad, Z.; Schweitzer, C.; Schmidt, R. *J. Phys. Chem. A* **2002**, *106*, 228.
- (399) Abdel-Shafi, A. A.; Beer, P. D.; Mortimer, R. J.; Wilkinson, F. *Phys. Chem. Chem. Phys.* **2000**, *2*, 3137.
- (400) Grever, C.; Brauer, H.-D. *J. Phys. Chem.* **1994**, *98*, 4230.
- (401) Schweitzer, C.; Mehrdad, Z.; Noll, A.; Grabner, E.-W.; Schmidt, R. *J. Phys. Chem. A* **2003**, *107*, 2192.
- (402) Pfeil, A. *J. Am. Chem. Soc.* **1971**, *93*, 5395.
- (403) García-Fresnadillo, D.; Georgiadou, Y.; Orellana, G.; Braun, A. M.; Oliveros, E. *Helv. Chim. Acta* **1996**, *79*, 1222.
- (404) Xu, W.; Jain, A.; Betts, B. A.; Demas, J. N.; DeGraff, B. A. *J. Phys. Chem. A* **2002**, *106*, 251.
- (405) Benson, R.; Geacintov, N. E. *J. Chem. Phys.* **1974**, *60*, 3251.
- (406) Adamczyk, A.; Wilkinson, F. In *Organic Scintillators and Liquid Scintillation Counting*; Horrocks, O. L., Peng, C. T., Eds.; Academic: New York, 1971.
- (407) Darmanyan, A. P.; Foote, C. S. *J. Phys. Chem.* **1992**, *96*, 3723.
- (408) Anderson, J. L.; An, Y.-Z.; Rubin, Y.; Foote, C. S. *J. Am. Chem. Soc.* **1994**, *116*, 9763.
- (409) Hamano, T.; Okuda, K.; Mashino, T.; Hirobe, M.; Arakane, K.; Ryu, A.; Mashiko, S.; Nagano, T. *Chem. Commun.* **1997**, 21.
- (410) Prat, F.; Stackow, R.; Bernstein, R.; Qian, W.; Rubin, Y.; Foote, C. S. *J. Phys. Chem. A* **1999**, *103*, 7230.
- (411) Darmanyan, A. P.; Foote, C. S. *J. Phys. Chem.* **1993**, *97*, 4573.
- (412) Netto-Ferreira, J. C.; Scaiano, J. C. *Photochem. Photobiol.* **1991**, *54*, 17.
- (413) Nau, W. M.; Scaiano, J. C. *J. Phys. Chem.* **1996**, *100*, 11360.
- (414) Nau, W. M.; Adam, W.; Scaiano, J. C. *J. Am. Chem. Soc.* **1996**, *118*, 274.
- (415) Redmond, R. W.; Braslavsky, S. E. *Chem. Phys. Lett.* **1988**, *148*, 523.
- (416) Darmanyan, A. P.; Foote, C. S. *J. Phys. Chem.* **1993**, *97*, 5032.
- (417) Wang, B.; Ogilby, P. R. *J. Photochem. Photobiol. A: Chem.* **1995**, *90*, 85.
- (418) Darmanyan, A. P. *Chem. Phys. Lett.* **1983**, *96*, 383.
- (419) Tanielian, C.; Wolff, C.; Esch, M. *J. Phys. Chem.* **1996**, *100*, 6555.
- (420) Zahir, K. O.; Haim, A. J. *J. Photochem. Photobiol. A: Chem.* **1992**, *63*, 167.
- (421) Yeow, E. K. L.; Braslavsky, S. E. *Phys. Chem. Chem. Phys.* **2002**, *4*, 239.
- (422) de la Peña, D.; Martí, C.; Nonell, S.; Martínez, L. A.; Miranda, M. A. *Photochem. Photobiol.* **1997**, *65*, 828.
- (423) Ehrenberg, B.; Anderson, J. L.; Foote, C. S. *Photochem. Photobiol.* **1998**, *68*, 135.
- (424) Beeby, A.; FitzGerald, S.; Stanley, C. F. *J. Chem. Soc., Perkin Trans. 2* **2001**, 1978.
- (425) Shold, D. M. *J. Photochem.* **1978**, *8*, 39.
- (426) Marsh, K. L.; Stevens, B. *J. Phys. Chem.* **1983**, *87*, 1765.
- (427) Darmanyan, A. P.; Arbogast, J. W.; Foote, C. S. *J. Phys. Chem.* **1991**, *95*, 7308.
- (428) Tanielian, C.; Heinrich, G. *Photochem. Photobiol.* **1995**, *61*, 131.
- (429) Tanielian, C.; Schweitzer, C.; Mechin, R.; Wolff, C. *Free Radical Biol. Med.* **2001**, *30*, 208.
- (430) Borisov, S. M.; Blinova, I. A.; Vasil'ev, V. V. *High Energy Chem.* **2002**, *36*, 189.
- (431) Dairou, J.; Vever-Bizet, C.; Brault, D. *Photochem. Photobiol.* **2002**, *75*, 229.
- (432) Maree, M. D.; Nyokong, T. *J. Photochem. Photobiol. A: Chem.* **2001**, *142*, 39.
- (433) McLean, A. J.; Rodgers, M. A. J. *J. Am. Chem. Soc.* **1992**, *114*, 3145.
- (434) Smith, G. *J. Am. Chem. Soc.* **1994**, *116*, 5005.
- (435) Okamoto, M.; Tanaka, F.; Hirayama, S. *J. Phys. Chem. A* **1998**, *102*, 10703.
- (436) Okamoto, M.; Tanaka, F. *J. Phys. Chem. A* **2002**, *106*, 3982.
- (437) Geacintov, N. E.; Swenberg, C. E. *J. Chem. Phys.* **1972**, *57*, 378.
- (438) Ogilby, P. R.; Sanetra, J. *J. Phys. Chem.* **1993**, *97*, 4689.

- (439) Tachikawa, H.; Bard, A. J. *J. Am. Chem. Soc.* **1973**, *95*, 1672.
- (440) Gollnick, K. *Adv. Photochem.* **1968**, *6*, 1.
- (441) Stevens, B.; Algar, B. E. *Ann. N.Y. Acad. Sci.* **1970**, *171*, 50.
- (442) Parmenter, C. S.; Rau, J. D. *J. Chem. Phys.* **1969**, *51*, 2242.
- (443) Merkel, P. B.; Herkstroeter, W. G. *Chem. Phys. Lett.* **1978**, *53*, 350.
- (444) Sato, C.; Kikuchi, K.; Ishikawa, H.; Iwahashi, M.; Ikeda, H.; Takahashi, Y.; Miyashi, T. *Chem. Phys. Lett.* **1997**, *276*, 210.
- (445) Krasnovsky, A. A., Jr. *Membr. Cell. Biol.* **1998**, *12*, 665.
- (446) Nonell, S.; Braslavsky, S. E. *Methods Enzymol.* **2000**, *319*, 37.
- (447) Iu, K.-K.; Ogilby, P. R. *J. Phys. Chem.* **1987**, *91*, 1611.
- (448) Kiryu, C.; Makiuchi, M.; Miyazaki, J.; Fujinaga, T.; Kakinuma, K. *FEBS Lett.* **1999**, *443*, 154.
- (449) Oelckers, S.; Ziegler, T.; Michler, I.; Röder, B. *J. Photochem. Photobiol. B: Biol.* **1999**, *53*, 121.
- (450) Engl, R.; Kilger, R.; Maier, M.; Scherer, K.; Abels, C.; Bäumler, W. *J. Phys. Chem. B* **2002**, *106*, 5776.
- (451) Baumer, D.; Maier, M.; Engl, R.; Szeimies, R. M.; Bäumler, W. *Chem. Phys.* **2002**, *285*, 309.
- (452) Andersen, L. K.; Gao, Z.; Ogilby, P. R.; Poulsen, L.; Zebger, I. *J. Phys. Chem. A* **2002**, *106*, 8488.
- (453) Ogilby, P. R.; Iu, K.-K.; Clough, R. L. *J. Am. Chem. Soc.* **1987**, *109*, 4746.
- (454) Clough, R. L.; Iu, K.-K.; Dillon, M. P.; Ogilby, P. R. *Polym. Prepr. (Am. Chem. Soc., Div. Polym. Chem.)* **1988**, *29*, 550.
- (455) Clough, R. L.; Dillon, M. P.; Iu, K.-K.; Ogilby, P. R. *Macromolecules* **1989**, *22*, 3620.
- (456) Clough, R. L.; Kristiansen, M.; Ogilby, P. R. *Macromolecules* **1990**, *23*, 2698.
- (457) Schiller, K.; Müller, F. W. *Polym. Int.* **1991**, *25*, 19.
- (458) Rodgers, M. A. J.; Lee, P. C. *J. Phys. Chem.* **1984**, *88*, 3480.
- (459) Aubry, J.-M.; Bouttemy, S. *J. Am. Chem. Soc.* **1997**, *119*, 5286.
- (460) Pace, A.; Clennan, E.; L. *J. Am. Chem. Soc.* **2002**, *124*, 11236.
- (461) Cha, H.; Setser, D. W. *J. Phys. Chem.* **1989**, *93*, 235.
- (462) Liu, D.; Setser, D. W. *J. Phys. Chem.* **1985**, *89*, 1561.
- (463) Bao, X. Y.; Setser, D. W. *J. Phys. Chem.* **1989**, *93*, 8612.
- (464) Flors, C.; Nonell, S. *Helv. Chim. Acta* **2001**, *84*, 2533.
- (465) Nonell, S.; Gonzalez, M.; Trull, F. R. *Afinidad* **1993**, *50*, 445.
- (466) Moan, J. *J. Photochem. Photobiol. B: Biol.* **1990**, *6*, 343.
- (467) *D'Ans Lax Taschenbuch für Chemiker und Physiker*, 3rd ed.; Lax, E., Ed.; Springer-Verlag: Berlin, 1967; Vol. 1.
- (468) Weast, R. C., Ed. *Handbook of Chemistry and Physics*, 57th ed.; CRC Press: Boca Raton, FL, 1976–1977; p F-61.
- (469) Moan, J.; Boye, E. *Photobiochem. Photobiophys.* **1981**, *2*, 301.

CR010371D

